WETUMPKA IMPACT STRUCTURE MODELED AS THE EXPOSED REMAINS OF

A LARGE, SHALLOW-WATER, MARINE-TARGET IMPACT CRATER FOR

ANALYSIS AND INTERPRETATION OF TWO DRILL CORES TAKEN

FROM NEAR THE STRUCTURE'S GEOGRAPHIC CENTER

Except where reference is made to the work of others, the work described in this thesis is my own or was done in collaboration with my advisory committee. This thesis does not include proprietary or classified information.

_____

Reuben Carl Johnson

Certificate of Approval:

_____	_____
Robert B. Cook Professor Geology	David T. King, Jr., Chair Professor Geology
_____	_____
Willis E. Hames Professor Geology	Joe F. Pittman Interim Dean Graduate School

WETUMPKA IMPACT STRUCTURE MODELED AS THE EXPOSED REMAINS OF A LARGE, SHALLOW-WATER, MARINE-TARGET IMPACT CRATER FOR ANALYSIS AND INTERPRETATION OF TWO DRILL CORES TAKEN FROM NEAR THE STRUCTURE'S GEOGRAPHIC CENTER

Reuben Carl Johnson

A Thesis

Submitted to

the Graduate Faculty of

Auburn University

in Partial Fulfillment of the

Requirements for the

Degree of

Master of Science

Auburn, Alabama
May 10, 2007

WETUMPKA IMPACT STRUCTURE MODELED AS THE EXPOSED REMAINS OF A LARGE, SHALLOW-WATER, MARINE-TARGET IMPACT CRATER FOR ANALYSIS AND INTERPRETATION OF TWO DRILL CORES TAKEN FROM NEAR THE STRUCTURE'S GEOGRAPHIC CENTER

Reuben Carl Johnson

_____
Signature of Author

_____
Date of Graduation

VITA

Reuben Carl Johnson is the son of Vern L. Johnson and Karen M. (Williams) Fowles, and the stepson of Frank H. Fowles III. He was born December 8, 1969, in Bishop, California, and graduated from Bishop High School in 1988 in the top 15% of his class. After working as an Emergency Medical Technician for nearly three years, Reuben joined the U.S. Navy (active duty) to gain worldly experience, earn money for college, and serve his country. He served in the Persian Gulf War, and while serving in the Balkans conflict as a third-class petty officer, Reuben began attending college classes at sea via shipboard studies through Central Texas College headquartered in Killeen, Texas. After earning an honorable discharge, Reuben continued his education at Madison Area Technical College in Madison, Wisconsin. A short time later, Reuben transferred to the University of Wisconsin – Madison and graduated in 2003 with a Bachelor of Science degree in Geology and Geophysics having given emphasis to planetary geology and astronomy. Reuben entered Graduate School at Auburn University in January of 2004, and married Megan Lee Anderson on August 13, 2005, whom he met while a student at UW-Madison. During the course of researching and documenting this thesis project, Reuben endured a badly ruptured disk in his lower back, back surgery, chronic back pain, three bouts of kidney stones, one non-functioning kidney, and surgery on both kidneys. He defended this thesis on his 37th birthday.

THESIS ABSTRACT

WETUMPKA IMPACT STRUCTURE MODELED AS THE EXPOSED REMAINS OF A LARGE, SHALLOW-WATER, MARINE-TARGET IMPACT CRATER FOR ANALYSIS AND INTERPRETATION OF TWO DRILL CORES TAKEN FROM NEAR THE STRUCTURE'S GEOGRAPHIC CENTER

Reuben Carl Johnson

Master of Science, May 10, 2007
(B.S., University of Wisconsin – Madison, 2003)

345 Typed Pages

Directed by David T. King, Jr.

The early Campanian, Wetumpka impact structure has a raised 7.6-km-diameter crystalline rim of pre-impact metamorphic basement. Filling the region within the crystalline rim is a mélange of impact-related sedimentary megaclasts in a sandy matrix ~100 m thick overlying a fallback breccia of unknown thickness. Just outside the crystalline rim are two impact-related structurally disturbed regions. To date, all published works on Wetumpka depict the crystalline rim as the outermost rim. However, when compared to other marine impact structures, the above characteristics indicate Wetumpka is the deeply eroded remains of a larger impact structure.

The principle activity of this study was the description and analysis of two drill cores extracted from near Wetumpka's geographic center. Drill core was cleaned by abrasive blasting, digitally photographed in high resolution, reassembled according to lithologic characteristics, and described using drill-core-logging software. Ancillary investigations, such as clarifying structures and patterns in the drill cores, determining the positions of the drill cores relative to the impact structure's central peak, elucidating an apparent intra-crater paleosol, and investigating the age of shock metamorphism added supplementary quantitative data. Results were compared to other marine-target impact structures to model Wetumpka as a shallow-water, marine-target impact structure having a speculative 16.5-km-diameter outer rim in Upper Cretaceous target strata.

Structural and morphological features at Wetumpka collectively model very well as a large, deeply eroded marine-target impact structure, and crater-filling materials are consistent with those at other marine-target impact structures. *Washback*, *flowin*, and *fallout* units have been completely eroded away, but a *fallback* breccia and a mixed *surgeback*/*slumpback* breccia are preserved within Wetumpka's inner basin. No intra-crater paleosol divides these two main crater-filling units, but the *fallback* breccia shows evidence of reworking by *surgeback*. Within both drill cores, twelve recognizable facies comprise three correlative units, and several enigmatic structures and patterns were modeled and interpreted. Normal faults within disturbed Upper Cretaceous strata outside the crystalline rim do not cut into the regional metamorphic basement even though pre-impact target sediments were >170 m thick. The impact event was not hot enough to cause much loss of radiogenic ^{40}Ar from shocked muscovite, but it was able to vaporize and/or disintegrate Mooreville Chalk. Wetumpka's central peak is not exposed, but one drill core may have penetrated this feature's upper edge at depth.

ACKNOWLEDGEMENTS

The author would like to thank Dr. David T. King, Jr. for his interminable patience, sage guidance, and numerous free meals. Thank you, Dr. Robert B. Cook, and Dr. Willis E. Hames, for your enthusiasm while addressing my questions. Thanks go to the Wetumpka Impact Crater Fund (WICF) for funding various aspects of this work, and to the Alabama Geological Society as well for supporting this study through the John G. Newton Memorial Scholarship for 2005. Thanks are also due to the Auburn Geology faculty for their nomination to that scholarship. To Dr. Mark Steltenpohl and Dr. Lorraine Wolf, thank you for use of lab space for abrasive blasting of the drill core. Thank you too, Dr. Luke Marzen, for teaching me about GIS. To the graduate students with whom I worked, thank you all for the support, suggestions, and critical comments. Many thanks go to my wife, Megan, for her tireless assistance with abrasive blasting and sample preparation. And to my father, Vern, a very special thank you for taking me out time and again as a boy to look at hulking mountains, sprawling lava flows, upturned bedding, ancient fossils, tight folds in road cuts, dried river channels, dripping glaciers, mud-cracked lakebeds, meteor showers, satellites, the Moon, the planets, the stars, the galaxies… and for making me wonder where all these things came from.

Journal style used: Geology

Computer software used: Adobe® Acrobat® Professional 6.0
Adobe® Photoshop® CS2
ESRI® ArcGIS® 9.1 and Extensions
LogPlot 2005™
Microsoft® Office Excel 2003
Microsoft® Office PowerPoint® 2003
Microsoft® Office Word 2003
TOPO!® 2.7.4 (Alabama)
TurboCAD® Deluxe version 11.1
Unit Converter Pro© 1.0

TABLE OF CONTENTS

page

LIST OF FIGURES

page

LIST OF TABLES

page

INTRODUCTION

Statement of Purpose

The investigation of impact structures is a relatively new field of study which has expanded rapidly only in the last few decades (Melosh, 1989). As such, existing impact-related drill core that is available for study is relatively rare (C. Koeberl, pers. comm., 2004). Additionally, data and photographs from such drill core are commonly patchy because most researchers working with impact-related drill core published studies that either gave emphasis to specific portions only, or simply contained a brief summary of the drill core rather than a thorough data set. This new field can benefit by having thorough photographic and descriptive records of entire drill cores that are objective, detailed, easy to supplement, compact, and easily accessible.

To that end, the purpose of this study is to describe, analyze, and interpret two whole-round (not split) NX drill cores pulled from the nearshore marine-target Wetumpka impact structure in Elmore County, Alabama. In doing so, this study not only makes available a thorough record of impact-related drill core data, but also draws new conclusions about the structure, makes predictions about future findings there, and sheds light on marine-target impact processes and their outcomes.

Impacts in General

The formation of impact structures is a major geologic process that significantly affects the solid bodies of our solar system regardless of their size (King, 1976; Shoemaker, 1977). Myriad celestial objects ranging from sand-sized grains to planetary bodies show impact scars, in some instances to the point of saturation, and not even the cosmic projectiles themselves are immune (Figure 1). However, Earth is unlike most terrestrial worlds known because it currently exhibits only about 176 confirmed impact structures or astroblemes (Whitehead and Spray, 2005), and roughly 539 other known structures that may be considered possible astroblemes (Rajmon, 2006). This inequity owes itself to atmospheric braking, the deleterious effects of weathering, erosion, and plate tectonics, and concealment by sediment, seawater, ice caps, and dense vegetative cover. Moreover, other potential impact structures remain undiscovered or unconfirmed because of the effects of politics, war, and cultural differences.

Impact structures form during a bolide impact event wherein a hyper-velocity celestial object, such as a comet nucleus, asteroid, meteoroid, or fragment thereof, explodes on or close to a planet's surface, or within its shallow crust. These events cause instantaneous, catastrophic effects that can be regional and/or global in scope. Further, bolide impacts alter then-existing geological and biological systems by creating instantaneous sediment accommodation space, depositing a regional ejecta annulus, initiating intense seismic (and potentially, tsunami) activity, decimating floral and faunal populations, and causing local and global extinctions. Cockell and Lee (2002) report these alterations can be persistent, and temporally and regionally unique, even when compared to major volcanic eruptions.

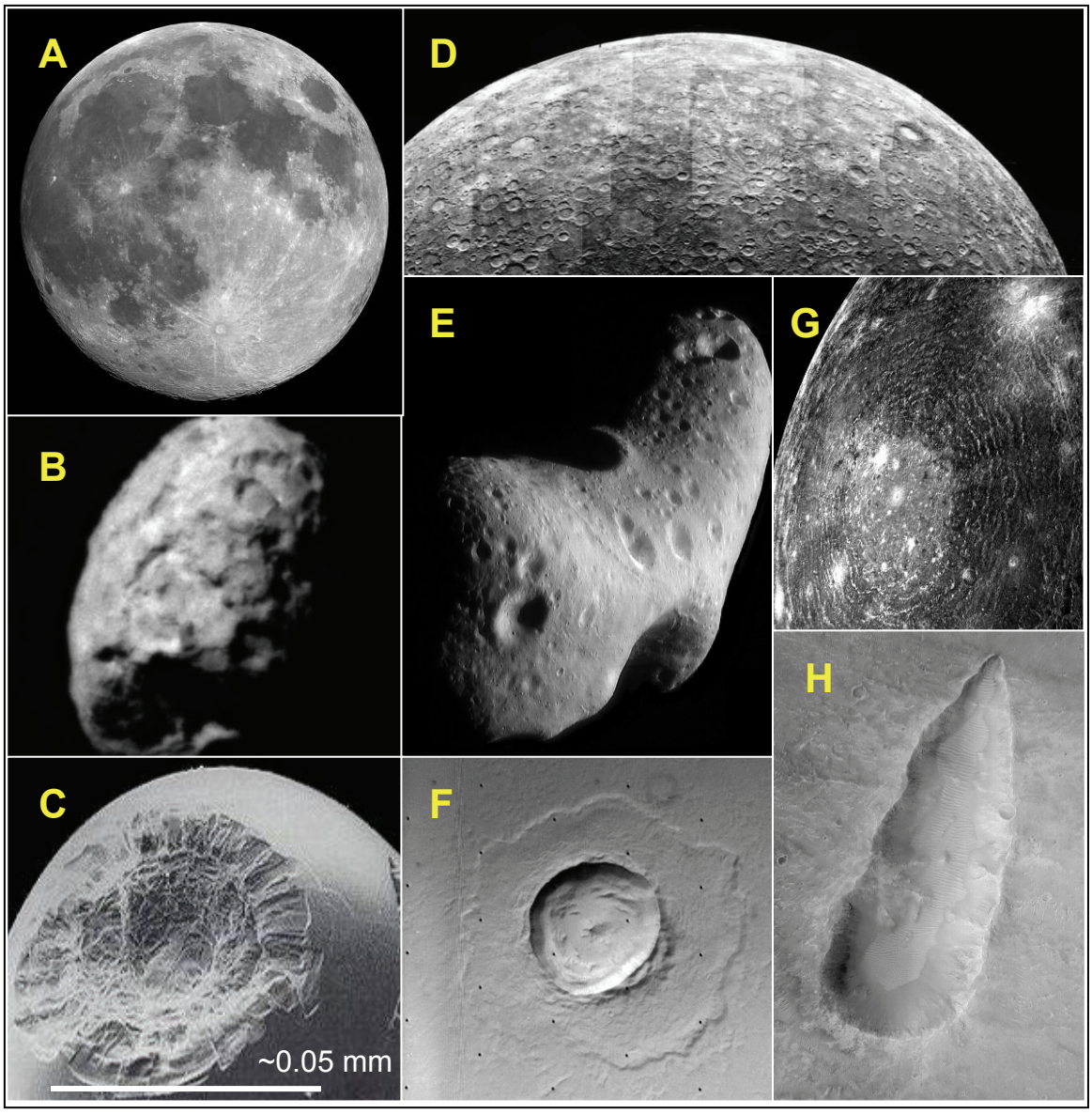

Figure 1. Impact structures on various celestial bodies. Note striking similarities and/or differences in morphology, and importantly, consequences of modification and digenesis such as slumping, burial, preservation, and erosion despite parallels and/or variations in age, host object, projectile, impact-event dynamics, etc. A: Earth's Moon displays fresh ray-craters (bright streaks emanating from bright craters) and basalt-filled impact basins (dark regions). B: Nucleus of comet Wilde 2 exhibits steep-walled, flat-floored craters in ice. C: A sand-sized glass spherule from the Moon exhibits a microcrater. D: Impact-saturated face of Mercury. E: Asteroid 433 Eros shows simple, bowl-shaped craters. F: Belz crater, Mars, exhibits fluidized ejecta, rim-wall slumping, and central peak. G: Valhalla impact basin, Callisto, shows relatively low relief and multiple rings. H: An unnamed elongated crater on Mars (MOC2-689) is an example of aberrant crater morphologies. All photos NASA/JPL/MSSS.

Types of Craters

Crater morphology is closely linked to crater diameter, and has thus far been divided into four main classes referred to as *micro*-, *simple*, *complex*, and *multiring* (Melosh, 1989; French, 1998). Before proceeding, the reader is advised to review the explanatory notes about impact-related nomenclature in Appendix 1.

Microcraters (Figure 1C) can be found on celestial bodies lacking sufficient atmosphere to filter the cosmic-velocity dust-size particles that create them. Melosh (1989) writes that these craters range up in size from 0.1μm, and show features not unlike their better-known, larger cousins. It is worth noting that the physics of microcrater excavation is nearly the same as in larger craters (Melosh, 1989).

Simple craters, like those typical of the asteroid 433 Eros (Figure 1E), and other bodies, are generally circular, bowl-shaped structures, with no particularly outstanding morphological features other than a raised rim with minor slumping around the inside of the rim-wall. The lower size limit for this crater type depends on the strength of the target body, whereas the upper size limit is an inverse function of the target's gravitational acceleration (Melosh, 1989).

In contrast, **complex craters** (Figure 1F) have a lower depth-to-diameter ratio probably owing to collapse of the overall structure, and exhibit numerous structural morphologies that include a central peak and/or peak ring, flat basin floor, and mass-wasting features of significant size within the structure (Melosh, 1989). Melosh (1989) also reports that the diameter of a complex crater is linked to an inverse relationship with the gravitational force of the host body thereby dictating crater diameter through collapse of the overall structure. Worthy of special attention is the subclass of complex craters

referred to as **peak-ring craters**, beautifully exemplified by King Crater, on the Moon, and Lowell Crater on Mars (Figure 2). Peak ring morphology is similar in appearance to the morphology of marine-target impact structures (Figure 3). Consequently, they are sometimes confused even though the processes of formation differ greatly between the two (Melosh, 1989; Ormö and Lindström, 2000; Poag et al., 2004). For a time, it was thought that the Wetumpka structure might be the peak ring within what would have been a larger impact structure (King, 1997; Nelson, 2000), but that idea was based on the confusion of morphologies just mentioned, and new ideas have taken its place. These new ideas will be detailed in coming sections.

Multiring basins (Figure 1G) are generally characterized as a very large central basin surrounded by a series of two or more concentric ridge and trough "ring graben" formations (Melosh, 1989; French, 1998). However, Melosh (1989) cautions there may be more at work than the gravity-related scaling that is responsible for the morphologies of these crater types, possibly because large-scale geological properties of the target body seem to have been significantly altered by the impact event associated with their excavation and modification.

As with any classification system, there are crater morphologies that do not precisely fit into the classes populated by the more typical forms observed. Melosh (1989) categorizes these morphologies as "**aberrant crater types**" (e.g., Figure 1H).

Melosh (1989) also hints that there are **effective subtypes** within the four main categories. For example, "central pit craters" on Jupiter's moon Ganymede are not aberrant, but they do stray from the above four morphologies nonetheless (Melosh, 1989). Additionally, several studies over at least the last three decades document that

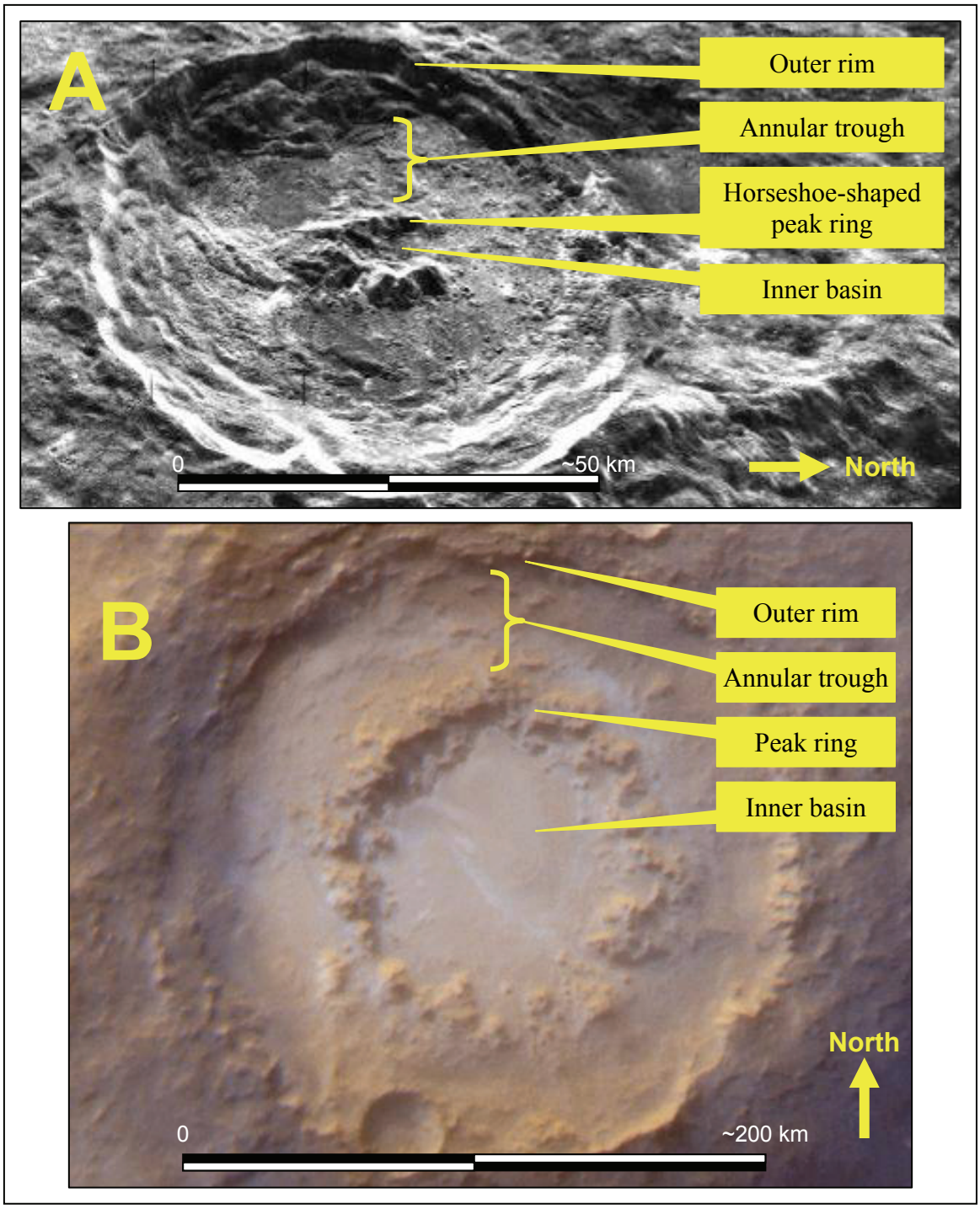

Figure 2. Examples of peak-ring craters, which are a subclass of the complex-impact-crater morphology. A: King Crater on the surface of Earth's moon shows an inner basin within a horseshoe-shaped peak ring surrounded by an annular trough and outer rim. Note rim-wall slumping. Photo credit NASA, Apollo 16. B: Lowell Crater on Mars is much larger, but shows a similar morphology. Photo credit NASA/JPL/Malin Space Science Systems.

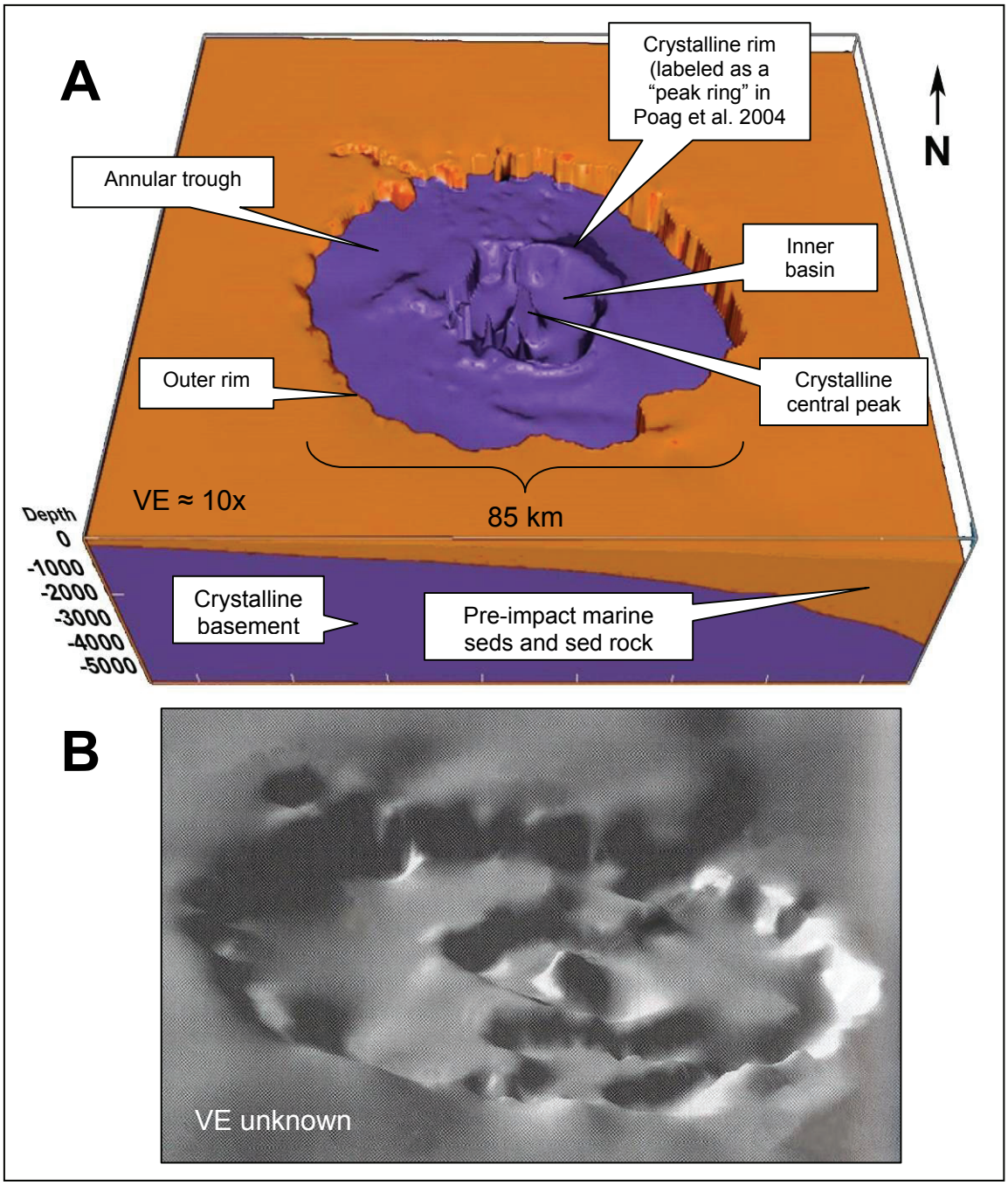

Figure 3. Structural and morphological features typical of marine-target impact structures as exemplified by 3-D maps of the Chesapeake Bay impact structure. A: All crater-filling deposits are removed to show the structure of the crystalline basement and undisturbed pre-impact marine sedimentary material. Note the incomplete crystalline rim surrounding the inner basin. This crystalline rim may be confused with a peak ring, and has been mislabeled as such by numerous authors. B: The morphological floor of the now breccia-filled impact structure exhibits the same various features, subdued, but still discernable. Modified from CD-ROM.4 and Figure 10.18 in Poag et al. (2004).

marine-target impact structures (Figure 3) deviate from the morphologies generalized above (Kieffer and Simonds, 1980; McKinnon and Goetz, 1981; Melosh, 1982; Ormö and Lindström, 2000; von Dalwigk and Ormö, 2001; Ormö et al., 2002; Dypvik and Jansa, 2003; Gisler et al., 2003; Poag et al., 2004). Although large craters forming in shallow water will exhibit many of the morphological features already outlined for their particular size (Ormö and Lindström, 2000), marine-target impact structures may also show evidence of powerful hydrodynamic erosional forces as well as hydraulic reworking and deposition of extant and/or impact-generated earth materials not found in dry-target impact structures (von Dalwigk and Ormö, 2001; Poag et al., 2004). Kieffer and Simonds (1980), Gault and Sonett (1982), and Ormö and Lindström (2000) also suggest that craters forming in targets covered by relatively deep water commonly will lack melt sheets, will have no rim wall, and that the impact event surely required more energy than that indicated by the diameter of its resultant deep-water crater. If the water is sufficiently deep, the impact will form only a temporary water crater, and projectile fragments will form a debris field on the sea floor (Melosh, 1989). The next two sections outline how these water-born structures diverge from the typical processes outlined for crater formation and modification.

Stages of Crater Formation – Generic Model

The process of crater formation by hyper-velocity projectiles begins during the precise moment the projectile (or blast-wave for air-burst events) strikes the target (French, 1998). The stages of crater formation are described by Melosh (1989) and French (1998) as orderly but complex, and are typically divided into the three stages of *contact/compression*, *excavation*, and *modification* (Figure 4), each summarized here.

In the **contact/compression stage**, tremendous kinetic energy is imparted to the target as the projectile makes initial contact with it and begins to penetrate. Intense pressures radiate into both the target and projectile from the point of impact as high-velocity shock waves. Once this compressive wave reaches the back of the projectile, it is reflected back through the projectile as a rarefaction causing the projectile to unload from compression and vaporize, thus ending this first stage.

The **excavation stage** begins as the above rarefaction wave enters the target material and other rarefaction waves are reflected from the target's surface causing the target to unload from compression. This unloading initiates an excavation flow that expels target material at subsonic velocities from the opening transient crater thereby forming the ejecta curtain. The excavation stage dies off when the forces driving the excavation flow can no longer expel target material from the transient crater.

As the developing crater transitions out of the excavation stage, the **modification stage** begins wherein the transient crater stops growing, and rim-wall collapse and rebound of the crater floor occur. It is in this stage that the central peak, inner basin, peak ring, annular trough, and outer rim develop and take on their "final" forms as constructed

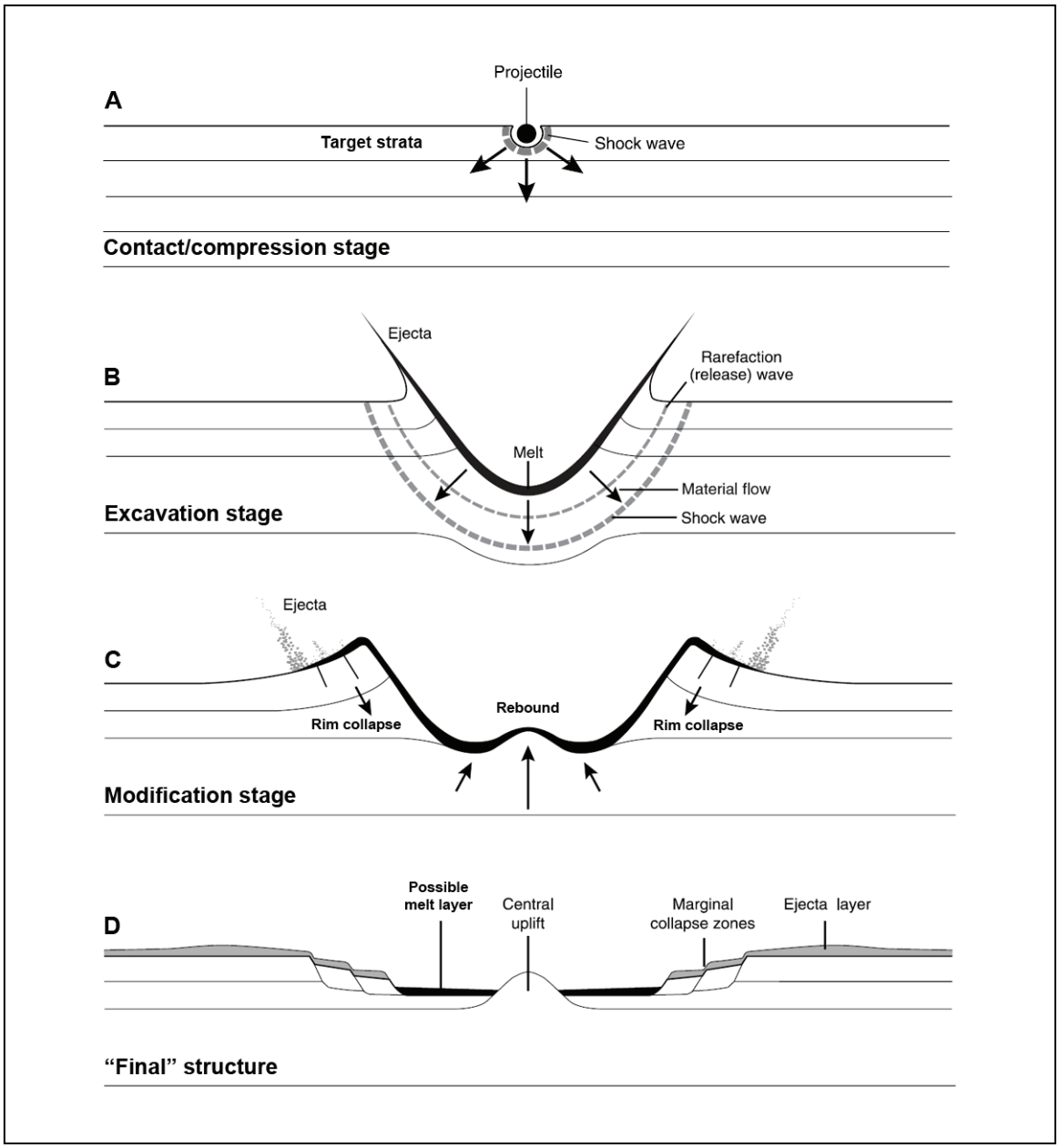

Figure 4. General stages of crater formation as exemplified by development of a generic complex impact structure. A: Contact and compression stage wherein the projectile strikes target causing intense compression. B: Excavation stage carves out transient cavity via excavation flow by rarefaction of target. C: Modification stage wherein central peak and/or peak ring rebounds, and rim-wall faulting, slumping, and sliding occur. D: "Final" structure formed during impact-related processes as illustrated by French (1998). Such is not the case in marine-target impact events as illustrated in the next section. Modified from Figures 3.3 and 3.10 in French (1998).

during the *typical* impact event. However, the process is slightly different for marine-target impact events, as detailed in the next section.

As a final note, it is worth bearing in mind that the modification stage will in fact persist, regardless of however slowly it may operate, until the structure no longer exists. This ever-continuing process depends on numerous factors that include the regional geography and geology of the crater's locale, as well as the chemical composition, orbital dynamics, and meteorology of the crater's host world. The numerous destructive processes at play will vary greatly with the advance of time, and will range in scope from the sluggish cycle of seasonal weathering to sudden and catastrophic structural failure. Such modifications not only change the impact structure itself, but the surrounding region too.

Stages of Crater Formation – Nearshore Marine-target Model

As indicated earlier, water-born impact structures forming in relatively shallow targets will diverge from the typical crater morphologies (outlined above), as well as from the processes typically associated with crater formation and modification. There are at least two types of process variation: 1) those affecting the paleoecosystem, and 2) those affecting the final morphology of the crater itself.

First, marine-target impacts produce a host of significant perturbations to extant ecosystems not otherwise found in association with impact events on dry targets. These perturbations include vaporization of large quantities of seawater leading to significant alteration of the atmosphere once injected there (Croft, 1982); development of an enormous hollow water column with subsequent basal surge, resurge, and waterspouts (Glasstone and Dolan, 1977; Gault and Sonett, 1982; Oberbeck et al., 1993); a shockwave transmitted through the water; and a possible tsunami wave train (Oberbeck et al., 1993; Melosh, 2003; Chesley and Ward, 2006).

Second, the structures that form during the impact event experience vigorous processes of hydraulic erosion, reworking, and deposition not experienced by dry targets. Additionally, Kieffer and Simonds (1980) found that melt sheets are largely absent from water-born impact structures because the melt is apparently carried away by expanding water vapor.

Poag et al. (2004) have built on the work of several published studies (particularly Oberbeck et al., 1993) to flesh out the processes inherent to a bolide impact in a shallow-water environment (Figure 5). Because the Wetumpka impact structure is thought to have formed in a shallow nearshore marine setting, these models are outlined below.

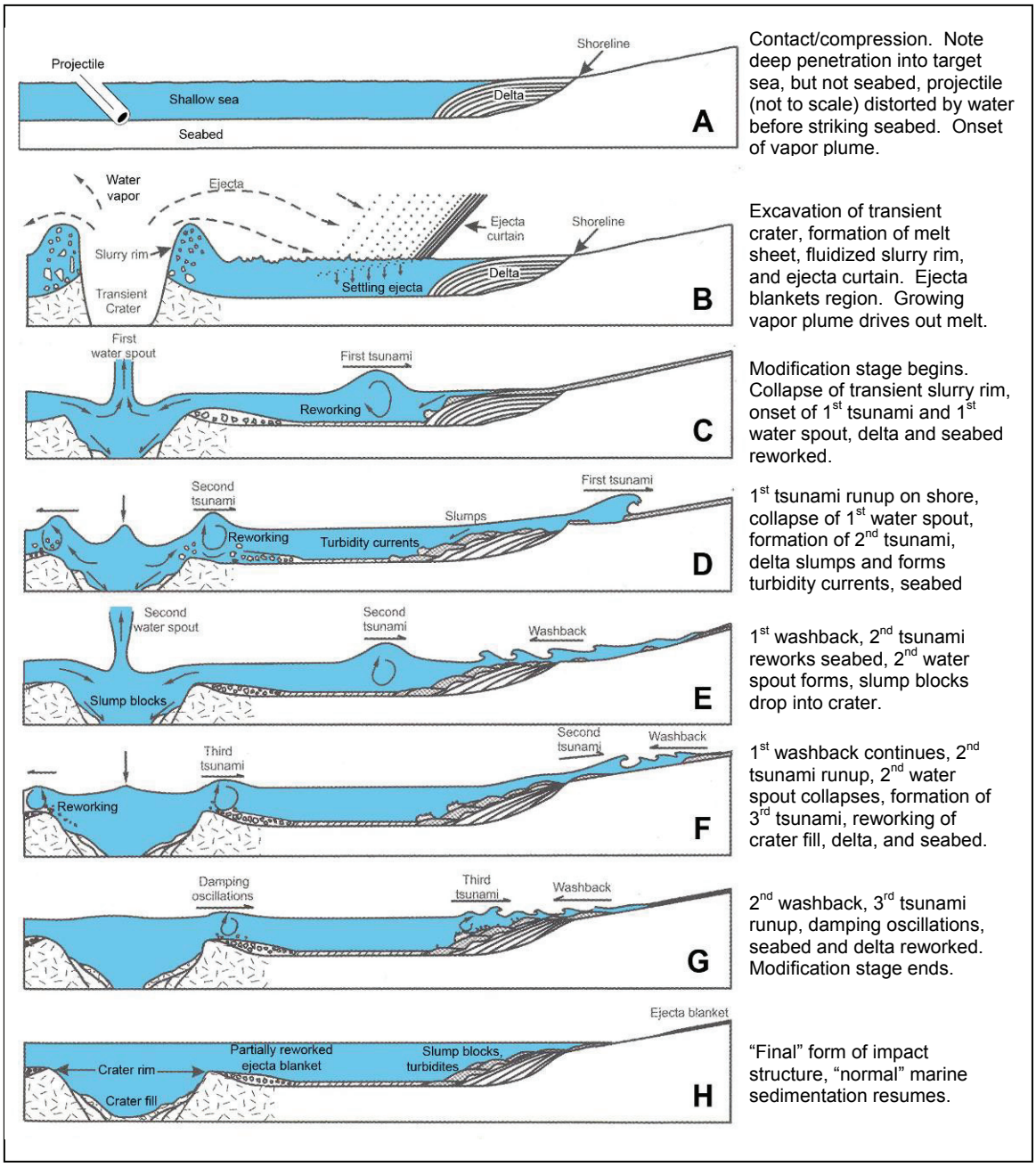

Figure 5. Schematic diagram showing conceptual stages of crater formation in a shallow, nearshore, marine-target setting. Angle of incidence depicted is the average 45° (Melosh, 1989). Note the difference in projectile behavior during the contact/compression stage in marine versus dry impact events (Melosh, 1982), and actions of the tsunami wave train that follow. Portion A modified from Ormö and Lindström (2000). Portions B–H originally developed by Oberbeck et al. (1993); modified by Poag et al. (2004); further modified for this study by author. Vertical scale exaggerated.

Marine-target Contact/Compression Stage

As the projectile makes initial contact with the shallow sea (Figure 5A), an intense compressive shockwave is communicated to the water as well as the projectile in a manner not unlike that in the same stage of an impact onto a dry target (Melosh, 1982). However, the liquid target is less dense than a solid target, so the projectile penetrates deeper into the target than it otherwise would (Ormö and Lindström, 2000). An expanding plume of vaporized seawater begins to form (Kieffer and Simonds, 1980), and before the projectile strikes the seabed, its hydraulic bow shock contacts the marine sediment and this shockwave is imparted to the strata (Croft, 1982). The expanding plume of water vapor may now be joined by expanding CO_2 derived from vaporization of carbonates (if available) in the seabed; this violent expansion of gasses begins to drive out shock-induced melt already forming in this stage, and will continue to drive it away in the excavation stage (Kieffer and Simonds, 1980). The contact/compression stage ends when the projectile is destroyed either in the water column, in the sediments of the seafloor, or in the underlying bedrock having conveyed all of its kinetic energy to the target.

Marine-target Excavation Stage

The excavation stage as depicted in Figure 5B also shows attributes of dry-target impact events, that include opening of the transient crater, formation of the ejecta curtain, and deposition of ejecta outside the crater. However, in this aqueous setting, a short-lived slurry rim develops inside the ejecta curtain at the rim of the transient crater, and the vapor plume continues to expand and drive out any melt (Kieffer and Simonds, 1980;

Oberbeck et al., 1993). Current studies are investigating the influence that shock-vaporization of pore water has on the impact structure at this stage in the cratering process (Ormö et al., 2006). As in the model of typical impact cratering, this stage also dies off when the forces driving the excavation flow can no longer expel target material from the transient crater.

Marine-target Modification Stage

The model of shallow nearshore marine-target cratering conceived by Oberbeck et al. (1993) shows that the crater modification stage (Figure 5C–H) is far more complex than that seen in the crating of dry targets. This model was built on by Poag et al. (2004) through the recognition of six depositional regimes, each having a specific genetic connotation as well as the ability to overlap, and in some instances, repeat. These regimes, listed in a generalized temporal/stratigraphic order are defined as follows: 1) *fallback* – deposition of coarse debris derived from the crystalline crater floor; 2) *slumpback* – deposition of coarse debris in megaslides/megaslumps; 3) *surgeback* – deposition of debris scoured from seafloor and crater walls/floor by collapsing water column; 4) *washback* – deposition of debris scoured from seafloor and coastal plain by onshore tsunami runup; 5) *flowin* – deposition of fine-grained multidirectional gravity flows; and 6) *fallout* – deposition of fine atmospheric debris and vapor condensates. Normal marine sedimentation (a long-term modification process) resumes once the crater-forming ends, and there is normally a transitional boundary layer between the fallout and the normal pelagic sediments. Additionally, other long-term modification

processes such as weathering and erosion may also begin if the crater is partly exposed above the sea, for example.

The above compilation of models describing a shallow nearshore marine-target impact event will be applied in this study to the interpretation of drill core pulled from the Wetumpka impact structure in 1998 by King et al. (1999a).

BACKGROUND AND GEOLOGIC SETTING

This section begins with specific descriptions of the Wetumpka region and the impact structure itself, as they presently exist. The broad region *surrounding* the impact structure is described separately to emphasize the significant differences between it and the structure itself. This opening section is followed by descriptions of the pre-impact paleoenvironmental setting, and the post-impact paleoenvironmental setting. In addition, the reader is advised again to read beforehand the explanatory notes about impact-related nomenclature in Appendix 1.

The Wetumpka Region Today

Today, the Wetumpka impact structure sits on the Coastal Plain at the southwestern edge of the *high-rank metamorphic belt* of the northern Piedmont as shown in Figure 6 (Neathery et al., 1976a). This is not to be confused with the southern edge of the physiographic region referred to as the southern Piedmont, which is an entirely different and distinct suite of rock in a nearby locale.

Figure 7 shows that the 7.6-km diameter Wetumpka impact structure is located in Elmore County, Alabama, adjacent to the city of Wetumpka, and is centered ~19.7 km northwest of the state Capitol building in Montgomery. The structure crops out as an eroded, crescent-shaped series of low hills composed of crystalline basement rock, and

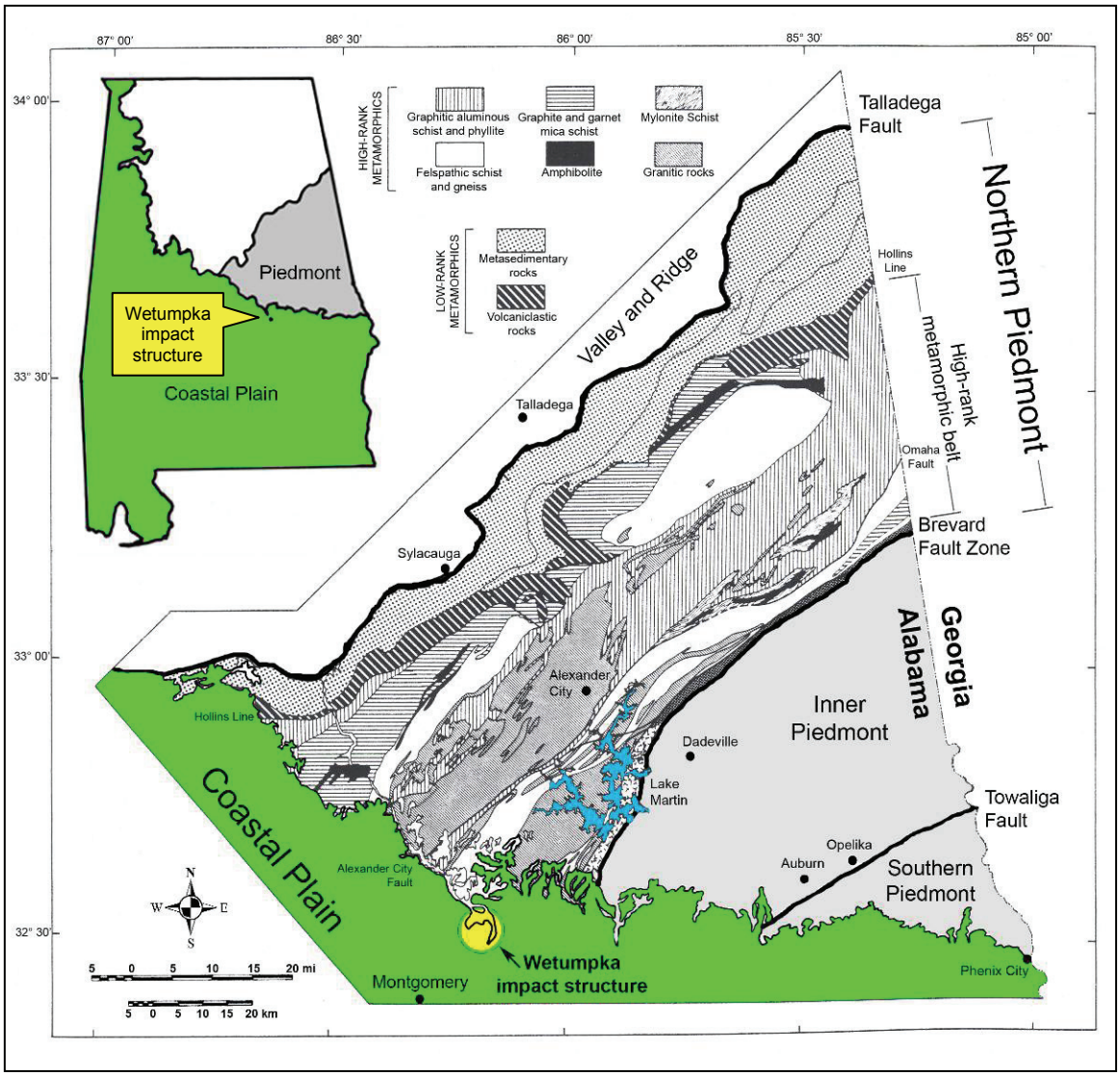

Figure 6. Regional map showing the geologic setting of the Wetumpka impact structure near the southwestern edge of the *high-rank metamorphic belt* of the northern Piedmont physiographic province. Details of relevant Coastal Plain stratigraphy given below. Adapted from Neathery et al. (1976b).

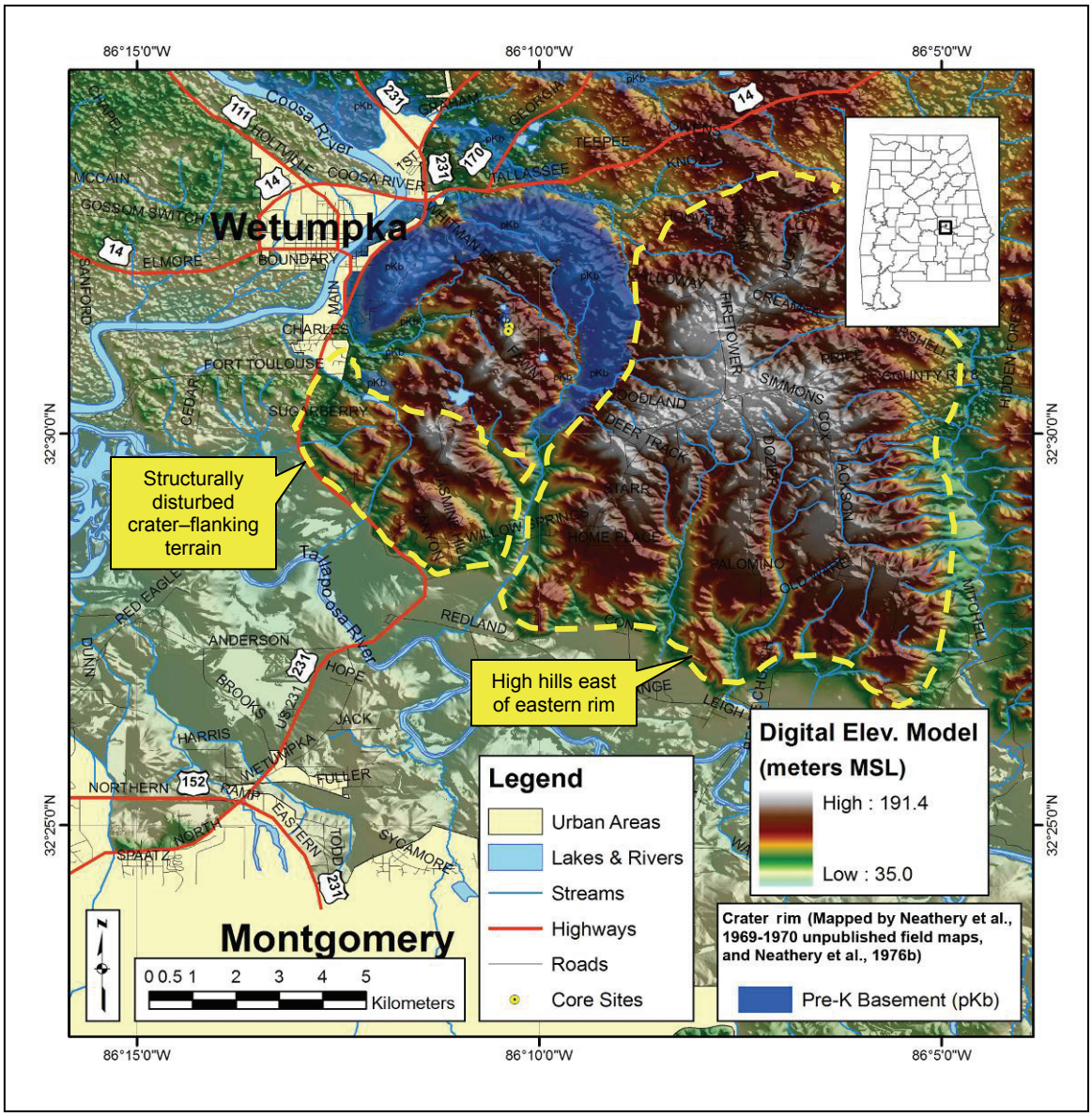

Figure 7. False-color shaded relief map of the Wetumpka region. The 7.6-km diameter Wetumpka impact structure is located in Elmore County, Alabama adjacent to the city of Wetumpka. The structure crops out as an eroded, crescent-shaped series of low hills composed of crystalline basement rock, mostly of the Emuckfaw Group (dark blue, labeled pKb). The crater bowl is filled with impact-related sediments. Note the structurally disturbed crater-flanking terrain and high hills east of the eastern crystalline rim. Two drill sites (yellow points near center of impact) indicate from where drill core for this study was extracted by King et al. (1999b). Map created by author using ESRI® ArcGIS® 9.1 and Extensions and data for Neathery et al.(1976b).

the crater bowl is filled with a mélange of impact-related sedimentary megaclasts in a sandy matrix (King, 1998; Nelson, 2000).

To the immediate south-southwest of the structure is what this report will term the *structurally disturbed crater-flanking terrain* (see Figure 7). This small region is a faulted series of generally parallel ridges and grabens of Cretaceous target strata, and is currently thought to have developed its structural characteristics during the modification stage of the impact event – probably during a *surgeback* event similar to that at the Chesapeake Bay impact structure (Poag et al., 2004; King et al., 2005).

Circumspectly, the label, "structurally disturbed crater-flanking terrain," is not to be confused with the label, "extra-crater terrain," used originally by Nelson (2000). The term "extra-crater terrain" was used ambiguously by Nelson to refer to *all* areas of the Wetumpka region anywhere outside of the elliptical region defined by the outer boundary of the structure's crystalline rim and crater fill. This is problematic because by that usage, *all of central Alabama* qualifies as "extra-crater terrain" (which is what she intended). Unfortunately, this ambiguity has caused some confusion. For example, King et al. (2002; 2004a; 2004b) used the similar label of "extra-structure terrain" when specifically referring only to a small fault and the disturbed area immediately south-southwest of the crater bowl – the small region this report is labeling the structurally disturbed crater-flanking terrain. Similarly, King et al. (2005) refer again to this same small region immediately south-southwest of the crater bowl, but they revert back to the label of "extra-crater terrain." In other words, these four papers misapplied Nelson's broad term in too limited a fashion. However, the phrase, structurally disturbed crater-flanking terrain, is not only narrower in scope than Nelson's broad term, it also focuses

attention on the distinct physiographic locale south-southwest of the crater bowl, it describes more precisely the nature and location of this unique area, and it corrects the misusage of Nelson's original label by other authors.

In similar fashion, there is another physiographic region adjacent to Wetumpka that also needs to be separated from Nelson's overly generalized "extra-crater terrain." East of the impact structure's eastern rim, a series of *high hills* rises ~155 m above the surrounding coastal plain and *exceeds* the highest point remaining anywhere on the crystalline rim (see Figure 7). In spite of their elevation, these high hills are part of the Cretaceous portion of the Alabama Coastal Plain (Szabo et al., 1988), and will be of use in creating a new reconstruction of the target paleostratigraphy and crater-forming sequence at time of impact. Note again that these high hills were originally included in the "extra-crater terrain" of Nelson (2000), but like the above structurally disturbed crater-flanking terrain, this report now separates them out as a distinct physiographic locale.

As a closing note, the impact structure itself will be discussed in detail in a coming section. This report now turns its attention to describing the present-day stratigraphy of the region surrounding the Wetumpka structure.

Description of Contemporary Stratigraphic Units in the Wetumpka Region

In ascending stratigraphic order, the units occupying the Wetumpka region today may be divided into three distinct packages: 1) pre-Cretaceous metamorphic crystalline basement; 2) Late Cretaceous sedimentary strata of the Tuscaloosa Group, Eutaw Formation, and Mooreville Chalk, all of which thicken southward and dip to the south at 9–15 m/km (~0.01°); and 3) Quaternary sediments of the *high terrace*, and *low terrace* deposits (Neathery et al., 1976b; Szabo et al., 1988). See Figure 8 for details. As will be explained later on, the importance of the Quaternary units has been overlooked until now.

The following three points are important to note. First, with exception to the crystalline basement, all overlying sedimentary material is highly friable, essentially uncompacted, poorly cemented, and not considered to be genuine rock by any reasonable definition (King, 1994). Second, the Mooreville Chalk is included in the above list, and in the descriptions to follow, only for purposes of thoroughness. In actuality, the Mooreville Chalk is only found in the Wetumpka region as anomalous outliers directly associated with the impact structure itself, and is not part of the *normal* stratigraphy in the Wetumpka region because it has been eroded away in this area. More details will be given in the section detailing the pre-impact paleoenvironmental setting. Third, although the two Quaternary units above are indeed labeled as "Quaternary" by Neathery et al. (1976b), Raymond et al. (1988), and Szabo et al. (1988), those authors also acknowledged the age of the units may actually range as follows: Quaternary high terrace may be Pliocene or Pleistocene to Holocene; and Quaternary alluvium and low terrace is probably Holocene. One may speculate the aforementioned authors lumped the ages in the interest of brevity, and the author of this report will follow suite.

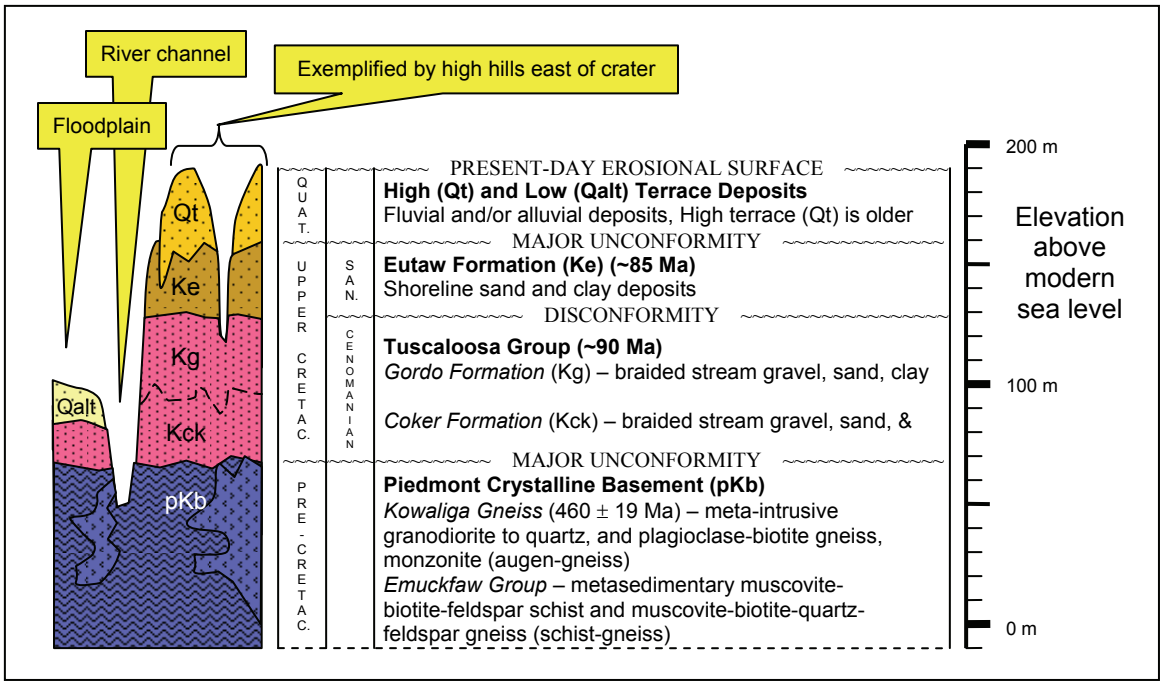

Figure 8. Idealized present-day stratigraphy of the Wetumpka region. For clarity, the impact structure and its associated stratigraphy are not depicted. Additionally, some relatively small outliers of Mooreville Chalk are found in association with the impact structure, but not the regional stratigraphy. For this reason and others outlined in the text, the Mooreville outliers are omitted here, but shown in other cross sections and maps in this report. Note the present-day 30-m thickness of the Eutaw strata owing to the regional major unconformity at the base of the Quaternary. Notice too the overlying Quaternary high and low terrace deposits. See text, maps, and cross sections for explanation. Adapted from Neathery et al. (1976b) and King (1997).

The following descriptions of the target units in their present-day form are derived largely from the work of Neathery et al. (1976b), Raymond et al. (1988), Szabo et al. (1988), and Nelson (2000) because it is not within this study's purpose to make a detailed investigation of the target strata itself. Moreover, because Raymond et al. (1988) and Szabo et al. (1988) generalized their descriptions for each unit's entire thickness and lateral extent, the descriptions herein are idealized toward what Neathery et al. (1976b) and Nelson (2000) reported specifically for the impact structure's *surrounding region*. In other words, although the Eutaw Formation is found in western and eastern Alabama, as well as at Wetumpka, that unit's description herein will excluded information pertinent to western and eastern Alabama, and focus only on the Eutaw's characteristics in the Wetumpka region. This section also excludes the impact-disturbed materials within and immediately around the impact structure itself, all of which are detailed in other sections of this report.

Crystalline Basement (metamorphic) [pKb]

The target region is underlain by low-relief crystalline basement rock of pre-Cretaceous metasedimentary and meta-igneous lithodemic units of the Emuckfaw Group (schist-gneiss) and Kowaliga Gneiss (augen-gneiss), the amalgamated surface of which currently dips ~10 to 20 m/km (~0.02°) to the south-southwest; this surface is thought to have had a similar dip at time of impact (Neathery et al., 1976b; Raymond et al., 1988; Szabo et al., 1988; King, 1997; King et al., 2005). The present author will usually homogenize these two units and generally refer to them as the pre-Cretaceous crystalline basement. Even so, separate descriptions follow.

Emuckfaw Group. The whole of the metasedimentary Emuckfaw Group includes the Josie Leg Member, Timbergut Member, and Glenloch Schist (Nelson, 2000) although not all of these are present in the Wetumpka region (Raymond et al., 1988). Overall, this Group is a varied sequence of medium-grained muscovite-biotite-feldspar schist, fine-grained muscovite-biotite-quartz-feldspar gneiss, graphite-garnet-muscovite schist, and quartzite; thin amphibolite and ultramafic pods are present, but few in number (Raymond et al., 1988). Thin, aluminous graphitic schists are also found in the region (Bentley and Neathery, 1970). The overall structure of this group is complex and shows evidence of several tectonic deformational episodes (Tull, 1978). In the Wetumpka region, Neathery et al. (1976b) and Nelson (2000) report that this group's prevailing foliation strikes northeast and dips southeast, and exposures commonly show tight crenulations (Neathery, 1975).

Kowaliga Gneiss. In the Wetumpka region, the Kowaliga Gneiss is a collection of several meta-igneous bodies intruding into the Emuckfaw Group (Nelson, 2000). Raymond et al. (1988) report these bodies are composed of gray, coarse-grained, granodiorite to quartz and plagioclase-biotite gneiss and monzonite, and that plagioclase or microcline augen therein have diameters up to 10 cm. These intrusions are usually sheared along their margins (Raymond et al., 1988), and foliation predominantly dips east to southeast at 20° to 25° (Nelson, 2000). Bieler and Deininger (1987) found the Kowaliga to contain abundant biotite and plagioclase, but only trace muscovite, and that these distinguishing characteristics render mineralogy a key factor when distinguishing

this unit from other granitoids in the region. The age of the gneiss is reported to be 460 ± 19 Ma (Raymond et al., 1988).

Tuscaloosa Group

A major unconformity separates the crystalline basement rock from the overlying Upper Cretaceous clays, sands, and gravels of the fluvial Tuscaloosa Group (Raymond et al., 1988; Szabo et al., 1988). Overall, Raymond et al. (1988) summarize this group as varicolored clay, sand, and gravel, which dip gently to the south and are probably part of the Cenomanian and/or Coniacian stage. Bedding typically fines upward in meter-scale packages consisting of sandy, pebbly conglomerates overlain by cross-stratified arkosic sands, which are topped off by massive to mottled, silty to sandy clays with pervasive bioturbation (Reinhardt et al., 1986).

In 1969, while Neathery et al. (1976b) were conducting their fieldwork for the Wetumpka region, they interpreted and mapped the Tuscaloosa Group as being differentiated into the Coker and Gordo Formations in this area based on sedimentologic differences between the two and the nature of their shared contact, which was later described as undulatory, sharp, and unconformable (Copeland, 1972; Taylor, 1973). Jones (1967) had previously specified that an ironstone at the base of the Gordo Formation is readily discernable, and Smith and King (1983) later pointed out that the Gordo is notably more gravel rich than the Coker. However, in this study, these two formations will commonly be referred to collectively as the Tuscaloosa Group and considered as an undifferentiated whole. Nonetheless, separate descriptions are provided here to enhance clarity.

Coker Formation [Kck]. The Coker Formation is summarized by Raymond et al. (1988) as consisting of light colored, very fine to medium micaceous sands, cross-bedded sands, varicolored micaceous clays, and a few thin gravel beds containing chert and quartz pebbles. The clay beds are typically "red-stained" (Nelson, 2000) and locally bioturbated (Taylor, 1973). Quartz and chert gravels at the formation's base are comprised of very fine pebbles to very large cobbles (Raymond et al., 1988). The above-cited authors also specify that in southwestern Elmore County (i.e., the region surrounding the Wetumpka structure), the formation includes marine sediments consisting of glauconitic, fossiliferous, fine- to medium-grained quartz sand, and medium-gray carbonaceous silty clay. Overall, the thickness ranges from 70 m to more than 152 m, and the Coker's stratigraphic age is reported as late Cenomanian to early Turonian (Raymond et al., 1988).

Gordo Formation [Kg]. Raymond et al. (1988) describe the Gordo Formation as having cross-bedded sand in massive beds that locally contain gravel, as well as having gray, "moderate-red," and "pale-red-purple" partly mottled clay in beds that generally are lenticular and locally carbonaceous. Nelson (2000) reports the clay beds are typically "purple-stained." The lower portion of the Gordo is predominately gravel-rich sand consisting of chert and quartz pebbles, and overall, this formation is rich in gravel (Smith and King, 1983). Thickness ranges from 35–91 m, and the stratigraphic age is thought to be Turonian to Coniacian (Raymond et al., 1988).

Eutaw Formation [Ke]

Lying disconformably atop the Tuscaloosa Group are the lithologically variable, transgressive marine-shoreline sands and clays of the Eutaw Formation (Frazier and Taylor, 1980; Raymond et al., 1988). In central Alabama, the Eutaw is composed of a basal layer of bioturbated gravelly sand overlain by alternating beds of well-sorted, cross-stratified, fine sands and muds, which are succeeded upwards by bioturbated muds containing fragments of shell and lignitized wood in addition to shark and fish teeth (Frazier and Taylor, 1980). Of note, the total thickness of the Eutaw Formation in west-central Alabama is reported as ranging from 107 to 122 m in outcrop (Raymond et al., 1988). Additionally, although the laterally extensive Tombigbee Sand Member is present in the upper Eutaw (Raymond et al., 1988), it is not found in the Wetumpka region – possibly owing to Quaternary weathering and erosion (see Figure 8). Finally, the formation's stratigraphic age range is Santonian to Campanian (Raymond et al., 1988).

A brief digression is necessary here. The reader may be tempted to point out that if the above explanation for the absence of the Tombigbee Sand were true, then the Mooreville Chalk would also not be present in the Wetumpka region, but it clearly is found in and around the impact structure. This author agrees completely, but makes the following two points: 1) Mooreville Chalk is present in the Wetumpka region *only* as anomalous outliers within the impact structure and in grabens immediately associated with the structure; 2) the Mooreville is *not* part of the typical Cretaceous strata in the Wetumpka region today because everything above the lower Eutaw has been eroded from this region. More details will be provided directly below and later in the section detailing the pre-impact paleoenvironmental setting.

Mooreville Chalk (Outliers) [Km]

Sixteen kilometers south-southwest of Wetumpka's geographic center, the Eutaw Formation is overlain by the hemipelagic, shallow-marine carbonate marl of the Campanian Mooreville Chalk (Raymond et al., 1988; Szabo et al., 1988). Note that *laterally continuous* Mooreville Chalk is not found any closer to Wetumpka than this 16 km distance (Neathery et al., 1976b; Szabo et al., 1988). Presently, the Mooreville chalk is found in the Wetumpka region only as relatively small outliers within, and immediately around, the impact structure (Neathery et al., 1976b; Szabo et al., 1988; Nelson, 2000). For this reason, the Mooreville has been omitted from the generalized stratigraphic column depicting the present-day Wetumpka region (Figure 8), but will appear in subsequent maps and cross sections within this work. By sequestering the Mooreville outliers, they will be better represented and better understood. That said, the Mooreville Chalk is described here.

King (1987) described the Mooreville in detail noting that its variable lithology ranges from clay and marl to limestone and sandstone. Raymond et al. (1988) summarize the Mooreville as a yellowish-gray to dark-bluish-gray, clayey, compact, fossiliferous chalk and chalky marl, and specify that near its base may be found a series of thin, glauconitic and clayey marls. Within the bottom meter is a compact calcareous sand containing scattered quartz pebbles, phosphatic pellets, and phosphatic internal molds of fossil shells (Raymond et al., 1988). In Montgomery County, ~16 to 20 km south of the Wetumpka region, the *lower portion* of the Mooreville is ~183 m thick, but remains unnamed (Raymond et al., 1988). This is unlike the upper 3 meters of the Mooreville, which are designated the **Arcola Limestone Member** – a unit composed of two to four

beds of light-gray, impure, dense, and brittle fossiliferous limestone with softer marl interbeds (Raymond et al., 1988). Significantly, no Arcola Limestone has been found in the outliers of Mooreville Chalk that are associated with the Wetumpka impact structure, and this observation has important bearing on the age constraint of the impact event (King, 1997).

The Mooreville weathers unlike any other unit in the Wetumpka region, and where exposed, forms a distinctive olive-brown to grayish-olive-brown, calcareous, clay-rich soil having white to light-gray, millimeter- to centimeter-scale caliche nodules that are irregular in shape (Nelson, 2000).

High Terrace Deposits [Qt]

Note: the unit described here is labeled as "Quaternary" by Neathery et al. (1976b), Raymond et al. (1988), and Szabo et al. (1988), but those authors also clearly acknowledged the age of the high terrace unit may range back into the Pliocene. In the interest of continuity and brevity, this report will follow the labeling of those authors.

In areas of high elevation within and surrounding the Wetumpka structure, a major unconformity, ranging in elevation from 90 to 180 m, divides the Upper Cretaceous units from remnants of an overlying "Quaternary" fluvial deposit partially covering the older geologic strata throughout much of the Alabama Coastal Plain (Neathery et al., 1976b). These high terrace deposits consist chiefly of lenses of varicolored, poorly sorted gravels, cross-bedded sands, silts, and clay that locally may be very hard, and may contain organic matter, peat, and unspecified shells and shell debris (Raymond et al., 1988). This fluvial unit should not be confused with the *younger*

alluvial and fluvial sediments (described next) found on the low floodplains and valleys currently occupied by the Coosa and Tallapoosa rivers and their major tributaries. To the contrary, the high terrace deposits are generally found in high areas *adjacent* to these major streams and their larger tributaries, and are thought to represent ancient floodplains that were abandoned when the streams became entrenched (Raymond et al., 1988). The overall thickness is reported to range from 0 to 46 m, and the deposits are believed to be late Pliocene or Pleistocene to Holocene (Neathery et al., 1976b; Raymond et al., 1988).

Alluvial, and Low Terrace Deposits [Qalt]

In the low lying areas of the Wetumpka region, a package of Quaternary alluvial and low terrace deposits shows a lithology that is much softer, but nearly identical to the *older*, though topographically higher, high terrace deposits (Neathery et al., 1976b; Raymond et al., 1988). These low-lying alluvial and fluvial sediments occupy the floodplains and valleys of the Coosa and Tallapoosa rivers and their major tributaries, and should not be confused with the older fluvial unit of higher elevation, described above. Like the high terrace deposits, these low terrace deposits also unconformably overlie units of older geologic age, but the low terrace deposits generally contain greater quantities of organic material, and are thought to be Holocene (Raymond et al., 1988). Topping everything is the present-day erosional surface cutting into and/or through all of the units described in this section.

The Impact Structure Itself as Currently Understood

As was mentioned, the impact structure itself is described here separately from the broad region surrounding it so that significant differences between the two may be clearly understood. Again, the reader is advised to read the present author's notes on impact-related nomenclature in Appendix 1.

Rim, Peak Ring, or Overturned Flap within what was a Larger Crater?

Although the Wetumpka structure is thought to be a marine-target complex impact structure, many authors have considered the horseshoe-shaped outcrop of crystalline basement rock to be the structure's outermost rim as depicted in Figure 9 below; published examples include Neathery et al. (1976b), Neathery et al. (1997), King et al. (2004b), and many others between these dates. Conversely, two published works have speculated this crystalline rim may be the "peak ring" of what was actually a larger crater (King, 1997; Nelson, 2000). However, the term "peak ring" was misapplied by those authors, and this idea has since been rejected. More recent work is exploring the possibility that Wetumpka's crystalline rim is actually an overturned flap of crystalline rock within a larger impact structure – a morphology similar to that found at the Lockne impact structure (Ormö et al., 2002). Lockne is a marine-target impact structure similar to Wetumpka in size and process of formation (Ormö and Lindström, 2000). In coming sections, this report uses Lockne – in addition to other marine-target impact structures – as an analogue to Wetumpka.

Unlike the outermost rims of most complex impact structures, Wetumpka's crystalline rim (overturned flap?) is comprised of structurally uplifted basement rock

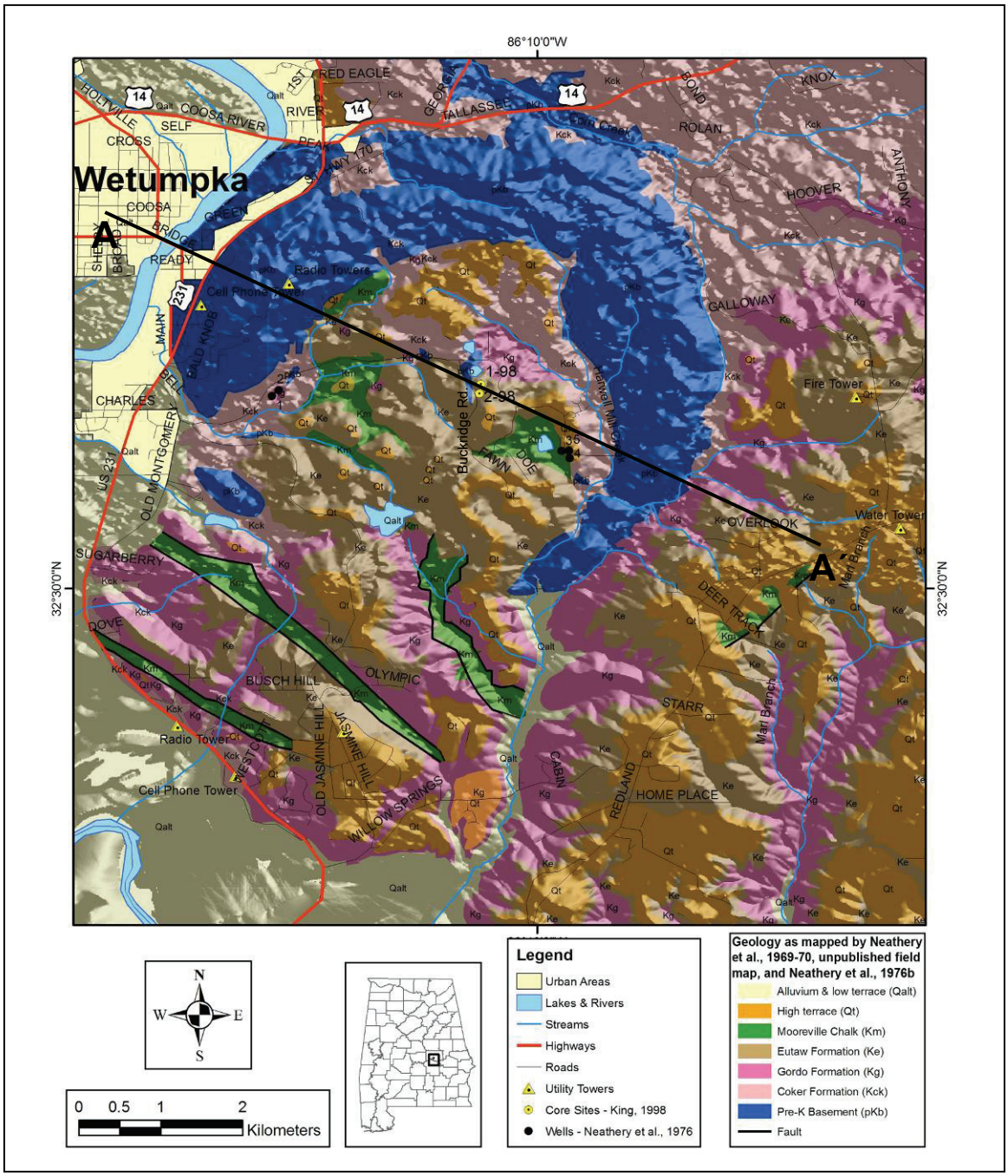

Figure 9. Geologic shaded relief map of Wetumpka impact structure. Dark blue (pKb) crystalline basement rock designates "rim." Note proximity of two drill core sites (1-98 and 2-98) near center of structure just east of Buckridge Road. Compare disturbed nature of crater fill and structurally disturbed crater-flanking terrain to high hills east of eastern rim. Outliers of Mooreville Chalk are associated with the impact structure and related faults. Schematic cross section along A–A´ shown in next figure. Utility towers are easily spotted while in the field and are indicated to assist framing the structure. Map compiled by author in ArcGIS® 9.1 from field maps used by Neathery et al. (1976b).

(Neathery et al., 1976b), and does not exhibit a series of concentrically arranged normal faults as would be expected if this were the structure's outermost rim (Nelson, 2000). Further, a comparative analysis by Nelson (2000) of Wetumpka with other terrestrial complex impact structures lends support to the idea that Wetumpka, as currently mapped, is probably just the crystalline rim within what was originally a larger impact structure.

Today, remnants of Wetumpka's crystalline rim (overturned flap?) crop out as a semicircle of low, deeply weathered hills of pre-Cretaceous crystalline basement rock mostly of the Emuckfaw Group (Neathery et al., 1976b; Nelson, 2000). Although this crystalline feature is ~6.5 km in diameter, the diameter of the overall structure is currently thought to be ~7.6 km as measured along the line of cross-section (Figure 9) from upturned basement rock in the Coosa River channel, to a small normal fault outside the eastern crystalline rim running northeast-southwest near Redland Road (Neathery et al., 1976b).

Nelson (2000) reported that within the rim (overturned flap?) itself, the following five characteristics may be observed in the crystalline rock: 1) atypical exposures of Upper Cretaceous target material do exist but are few in number; 2) a radial metamorphic foliation is virtually ubiquitous; 3) folds are concentrated in the northwestern sector; 4) a variety of lineations are widely present; and 5) impact-related joints and faults also may be found. Neathery (1976b) also mapped a relatively large enigmatic deposit of Coker formation on the flank of the northern crystalline rim (overturned flap?), and recorded data on the orientations of foliations, lineations, and folds in the exposed crystalline rock.

Presently, the highest remaining point on the crystalline rim (overturned flap?) is known as "Bald Knob" (Figure 10), which tops out at ~180 m elevation, and is roughly

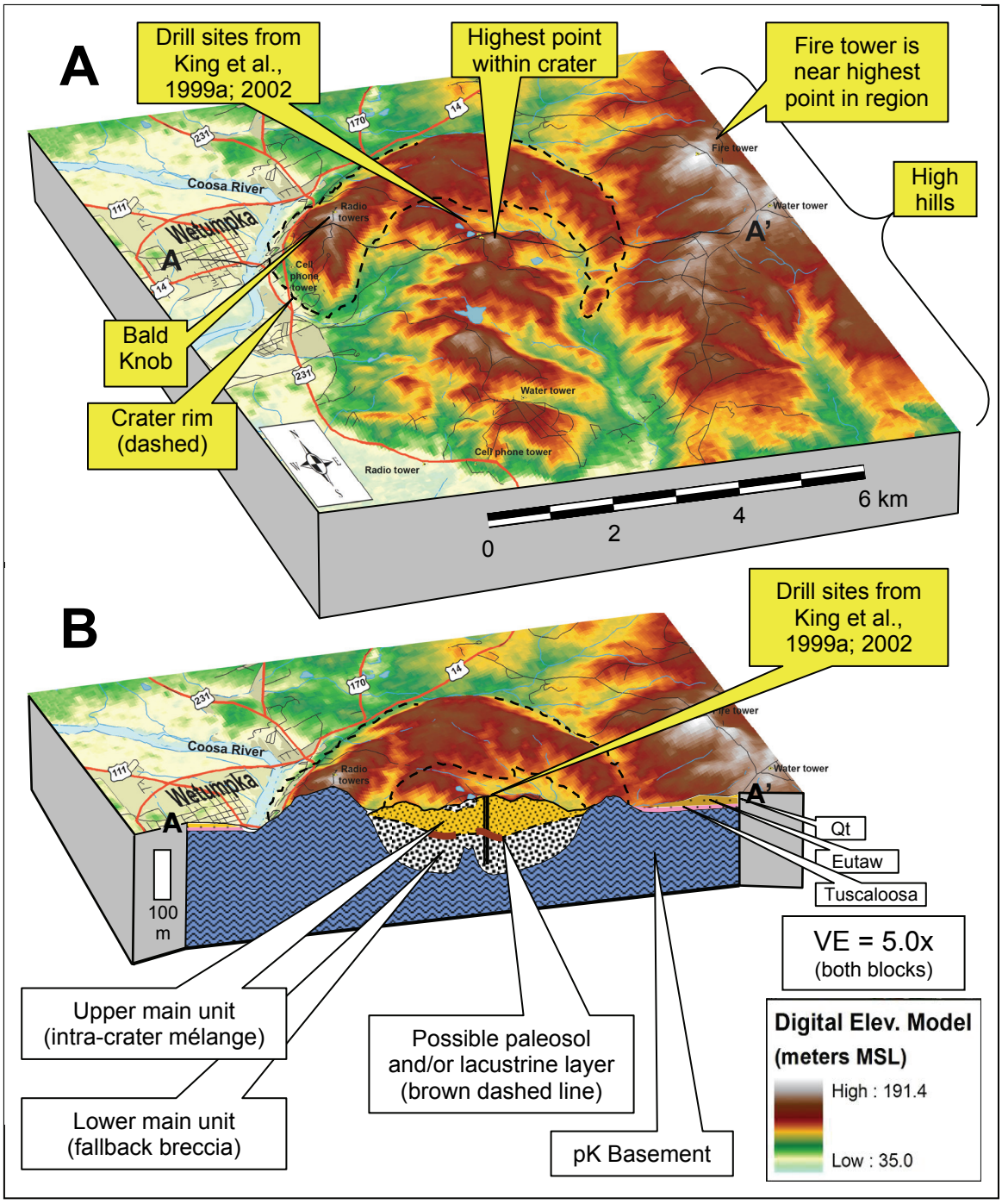

Figure 10. False-color block diagrams of A: Wetumpka impact structure, and B: generalized schematic cross section. Note two main crater-filling packages in part B. Lower unit (fallback breccia) may show two distinct facies – fallback material at bottom, and hydrodynamically reworked fallback material at top. A thin paleosol and/or lacustrine layer may partly overlie this unit. Upper unit (crater-filling mélange) contains reworked impact breccia and/or ejecta. Compiled by author using ArcGIS® 9.1 with data adapted from Neathery et al. (1976b), TOPO!® (2002), and King et al. (2004a).

150 m above the surrounding plains (Neathery et al., 1976b). However, Bald Knob is not the highest point in the region. Lastly, the southwest third of the rim (overturned flap?) is missing, and at least three ideas have been put forth to explain this phenomenon as will be outlined in the section on previous works.

Intra-crater Terrain and Crater-filling Stratigraphy

As mentioned, this report examines two drill cores extracted from near the geographic center of the Wetumpka impact structure. Thus, a detailed, top-down understanding of this central region is necessary to establish the geologic framework from which the drill core was taken. To that end, this section will first detail the region's surficial geology, then the crater-filling stratigraphy, and finally, issues regarding the central peak as it relates to the surficial topography.

Surficial Geology. Overall, the crater-filling material found at the surface of Wetumpka's interior region is a type of mélange (King, 1998) consisting of a highly disturbed, moderately shocked, chaotically oriented megabreccia (as classified using the modified Udden–Wentworth grain-size scale, which was proposed by Blair and McPherson, 1999). Nelson (2000) reported that within this interior region, numerous outcrops of mostly quartzose sand from (what appears to be) the Tuscaloosa Group are readily found. She also writes that outcrops of Eutaw sediments are smaller and fewer in number than Tuscaloosa material (contrary to what is mapped), and that exposures of Mooreville Chalk are rare but easy to discriminate.

King (1997) points out, and Nelson (2000) further confirms, that many of the exposed blocks of sedimentary target strata show at their edges evidence of deformation by faulting, shearing, folding, stretching, and flattening, but their interior regions show varying degrees of deformation and are commonly undeformed. Typifying the contacts between these sedimentary blocks are either iron-oxide-cemented sands, or small blocks and boulders of target strata in various orientations within sandy matrix (Nelson, 2000). King (1998) and Nelson (2000) also describe what may be clastic dikes of impact origin separating blocks of Tuscaloosa sediments, and other Upper Cretaceous block-to-block contacts appear to show fluidized sands (Nelson, 2000). In all, such traits are consistent with the notion that these blocks were rotated against each other and experienced compressional as well as tensional forces, possibly during a marine surgeback event (King et al., 2005).

Along some portions of the interior edge of the crystalline rim are large blocks of Upper Cretaceous target material. Orientations of relatively large normal faults within and bounding these large Upper Cretaceous blocks are roughly parallel to the crystalline rim's edge have been interpreted by Nelson (2000) as possibly being indicative of interior rim-wall slumping. However, the present author suspects such faults are perhaps equally consistent with megablock slumping into the inner basin within a larger impact structure, as exemplified by many marine-target impact structures (Poag et al., 2004). Reasons for this opinion will be explained in sections to follow.

In addition to the shattered Upper Cretaceous material filling the impact structure, Nelson (2000) also reported that there are limited exposures of impact breccia within the crater fill not far from the structure's geographic center, and that impact melt is

apparently absent in outcrop. Exposures of impact breccia within the interior region vary from matrix-supported to clast-supported, and contain numerous pebble- to block-size, angular to rounded clasts of biotite-muscovite-quartz schist and pebble- to boulder-size, angular to rounded clasts of sedimentary target strata all within a fine-grained matrix of pulverized target materials (Nelson, 2000). Shocked quartz is present within the matrix of this exposed breccia (J. Morrow, unpublished, 2005).

Problematically, Nelson (2000) describes "megaboulder-sized clasts" of crystalline rock within this impact breccia but she offers little indication of exactly how big this is, and the term is not well defined elsewhere. There are hints within Nelson's work that suggest "megaboulder" is meant to indicate dekameter-scale clasts up to ~30 m in diameter, and this accords with what has been observed by the present author and numerous others dating back to Neathery et al. (1976b). Curiously, King et al. (2005) indicate that large crystalline blocks within this impact breccia near the impact structure's geographic center have diameters of "hundreds of meters," but this seems speculative. Even though meter- to dekameter-scale boulders of crystalline rock do exist within the exposed impact breccia, no crystalline boulders "hundreds of meters" in size are known from anywhere at the surface of Wetumpka's interior region (Neathery et al., 1976b; Nelson, 2000).

Crater-filling Stratigraphy. Near the Wetumpka structure's geographic center are two drill sites on the Schroeder and Reeves properties for which drill holes 1-98, 2-98 (Figure 9), and their respective drill cores were named (King et al., 2002). Previously, King (1998) had examined outcrops within the impact structure and proposed that

material filling the crater bowl is comprised of three facies: 1) a monomict megablock breccia; 2) a clastic, dike-injected, deformed strata; and 3) a polymict megaconglomerate. But after extracting and examining the two drill cores from near the topographic high-point, King et al. (2002) simplified these three units into two main crater-filling units depicted schematically in Figure 11. Shocked quartz was found in the lower main unit by King et al. (1999b). Together, the two main crater-filling units are currently thought to indicate a two-stage crater-filling process, with the lower main unit having been formed by deposition of fallback breccia coeval with slumping typical of the early modification stage of complex crater formation (Melosh, 1989; King et al., 2004b). King et al. (2004b) speculate the top portion of this fallback breccia may have been reworked by a marine resurge into the fresh crater a short time after impact.

The upper main unit may result from the late modification stage also typical of complex impact structure formation in marine environments wherein portions of the rim and surrounding seafloor strata collapse into the new crater (Melosh, 1989; King et al., 2004b; Poag et al., 2004). Interestingly, this second marine resurge seems to have been associated with at least one major collapse event on the southwest crystalline rim (overturned flap?) (King et al., 2004b; King et al., 2005). Worth noting is that within the Chesapeake Bay impact structure, the crystalline rim (labeled a "peak ring") seems to be missing a portion as is the incomplete crystalline rim at Wetumpka (Poag et al., 2004).

Figure 12 illustrates that partly separating the two main units filling the crater bowl is what may be a paleosol and/or lacustrine mudstone ~1.65 m thick (King et al., 2006), located at 101 m drill depth in the Schroeder drill core (1-98). This package is not present in the Reeves drill core (2-98) since this hole was purposely not cored in the

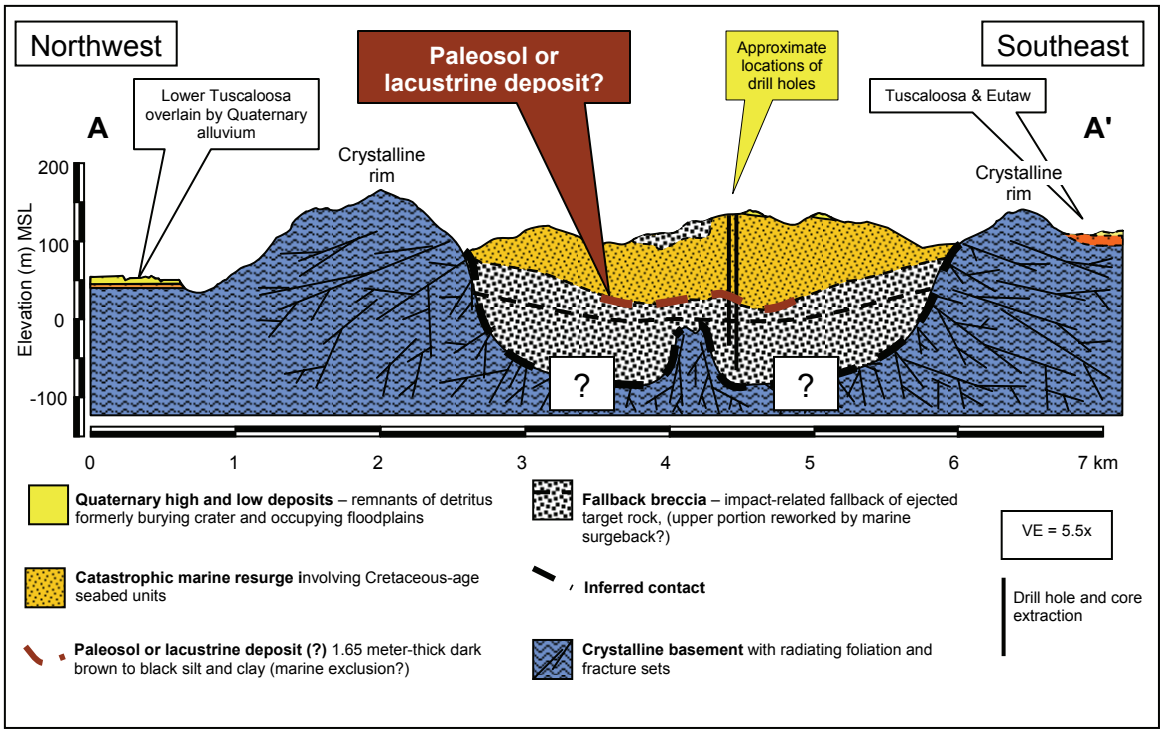

Figure 11. Schematic diagram of Wetumpka's crater-filling stratigraphy based primarily on King et al. (2004a) and data from 5 drill holes documented in Neathery et al. (1976b). Actual depth to the structural basement is not known. Crater-fill is mainly comprised of two thick breccia units: the lower unit is fallback breccia deposited during the impact event, and the upper unit is catastrophic rim-collapse and/or marine resurge breccia deposited in the crater some time later. Dividing these two units is an enigmatic mudstone that may be an intra-crater paleosol and/or lacustrine deposit (King et al., 2006) ~1.65 m thick with horizontal bedding (dashed brown line in diagram; see detail figure below). This thin unit may represent a unique intra-crater ecosystem that also might hold important clues about a possible time lapse between deposition of the underlying fallback breccia and the overlying surgeback material.

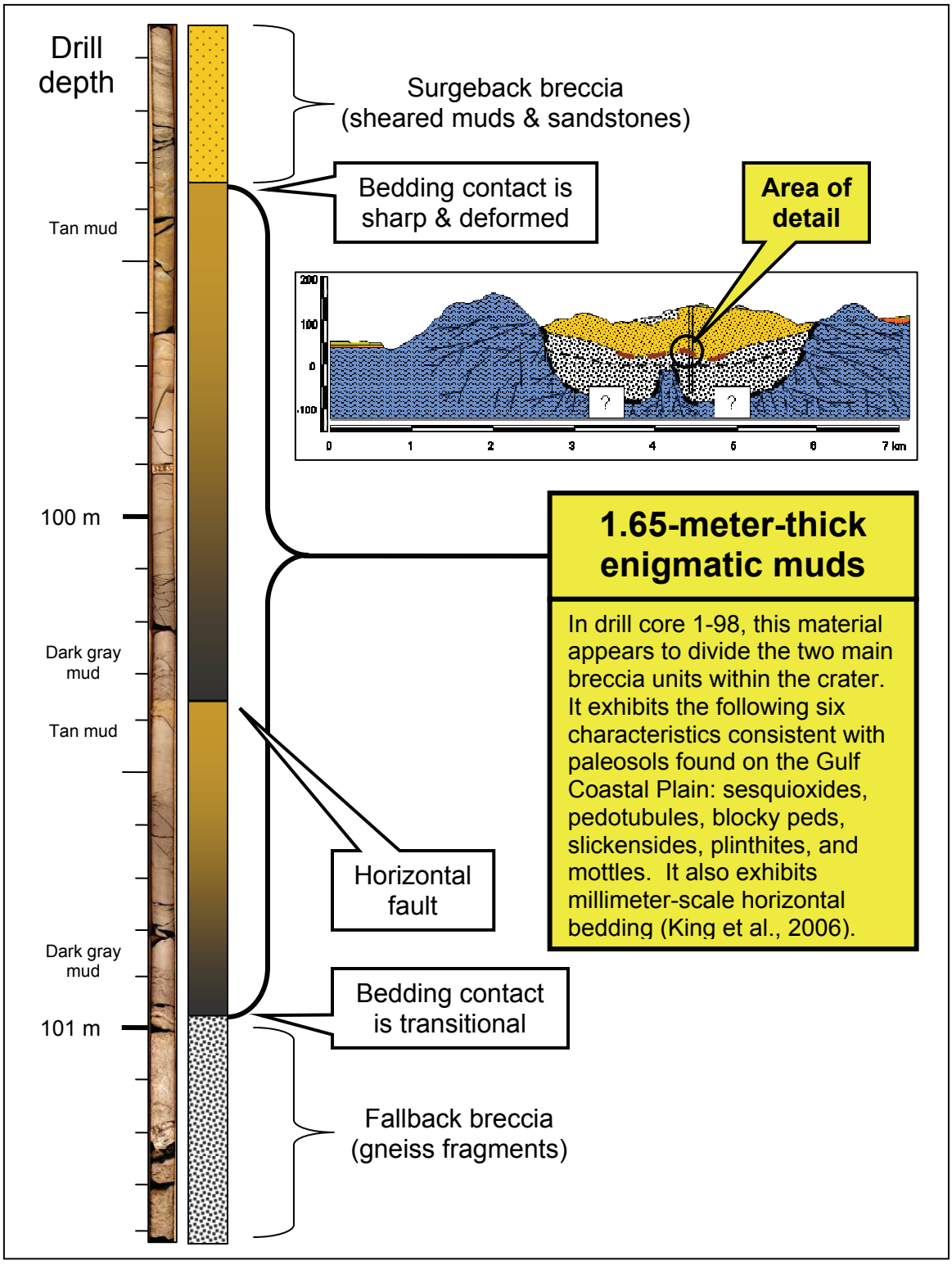

Figure 12. Detail of enigmatic mudstone unit that may be an intra-crater paleosol and/or a lacustrine deposit (King et al., 2006). As such, this material may hold clues about the timing of crater-filling events.

depth range corresponding to this unit because of drilling problems. This mudstone shares a transitional contact with the underlying main unit, and a sharp, highly distorted contact with the overlying main unit. Under a standard medical CT scan, horizontal, millimeter-scale laminations are evident, and it is thought this mudstone may constitute an unidentified intra-crater ecosystem indicating a significant hiatus between deposition of the upper and lower main units within the crater bowl (King et al., 2006). Conversely, it may simply be a horizontal block of Eutaw target strata. This report investigates these possibilities.

Central Peak versus Surficial Topography. The highest remaining topographic point within Wetumpka's central region is near the structure's geographic center, and is ~20–30 m below the current elevation of Bald Knob (Figure 10). Given the above data on the surficial geology near this location, Neathery et al. (1976b) and Nelson (2000) concluded that the breccia's characteristics indicate the high-point is an exposed central peak. Although impact-related breccia is found at the surface near this interior high-point, the lithology of the high-point itself is composed of strongly disturbed Upper Cretaceous target strata topped by undisturbed Quaternary sediments (Neathery et al., 1976b; Nelson, 2000). As such, the highest point within Wetumpka's interior region probably does not represent the weathered remnant of a central peak because its lithology is wrong (Melosh, 1989).

Consider the following. The poorly consolidated seafloor sedimentary material was likely far too friable to be uplifted with the crystalline basement to the elevation required by the present breccia exposure even though such is possible with more

indurated strata (Melosh, 1989). In other words, for this topographic high-point to be an exposed central peak, its lithology would have to be crystalline basement that shows signs of intense compressional, tensional, and shearing forces (Melosh, 1989). This requirement is vastly different from the characteristics of both the Upper Cretaceous-derived crater-filling material that the high-point is composed of, as well as the nearby impact breccia previously implicated. Furthermore, Melosh (1989) states that a central peak cannot be composed of these two materials. Finally, the crater bowl appears too deeply filled in for a true central peak to show at the present surface, as this report will illustrate.

The present author suspects the outcrops of breccia are perhaps better interpreted as exposures of impact breccia, which was originally deposited as ejecta and/or fallback material that became mobilized during the catastrophic marine surgeback into the new crater. As surgeback energy died off, the breccia was emplaced within the surgeback deposit and was later exhumed by subsequent weathering and erosion. Reasons for this opinion will be explained in sections to follow, but as a closing statement, the present author considers the topographic high-point near Wetumpka's geographic center to be just that – a topographic high that by chance alone happens to be near the structure's geographic center.

In spite of the above, evidence for a true, albeit buried, central peak does exist in a gravity survey from Wolf et al. (1997). This report will reexamine the gravity data and offer an updated interpretation in the context of marine-target impact structure morphology.

Structurally Disturbed Crater-flanking Terrain

As previously indicated, the structurally disturbed crater-flanking terrain is a faulted series of generally parallel ridges and grabens of Upper Cretaceous target strata, and is currently thought to have developed its morphology during the modification stage of the impact event – probably during a *surgeback* similar to that at the Chesapeake Bay structure (Poag et al., 2004; King et al., 2005). Neathery et al. (1976b) suggested linear outliers of exposed Mooreville Chalk confined to low elevations – and bordered by Tuscaloosa at high elevations – are impact-related extensional grabens, or are possibly related to a regional fault system. Nelson (2000) explained this region could be something like wall terraces formed by slumping of an undiscovered outer rim surrounding the structure, or that it could be a marine resurge deposit as was later documented at the Chesapeake Bay impact structure by Poag et al. (2004). King et al. (2005) also suggested catastrophic surgeback similar to that at the Chesapeake Bay structure. Whatever this region truly is, one must remember it is only an eroded remnant of what was there originally.

Chaotically oriented bedding within the structurally disturbed crater-flanking terrain indicates post-depositional deformation, and bedding dips range up to 90°, but strata are not overturned (Nelson, 2000). Further, some Upper Cretaceous material within the terrain does indeed show clear evidence of impact-related deformation, but much of the region does not (Nelson, 2000). This ambiguity is to be expected even if the terrain was formed during the impact event by marine surgeback (Poag et al., 2004). Such characteristics are not unlike those found in the highly disturbed blocks of Wetumpka's crater-filling mélange as previously summarized.

Within the structurally disturbed crater-flanking terrain, crystalline basement rock is not intermixed with the rest of the Upper Cretaceous sediments, even where those sediments are disturbed (Nelson, 2000). Additionally, unlike the crystalline basement rock comprising Wetumpka's rim (overturned flap?), exposed basement rock immediately surrounding the raised crystalline rim is relatively undisturbed and similar to the basement rock of the encompassing region (Neathery et al., 1976b; Nelson, 2000).

All of the above characteristics are consistent with slumping of partly deformed blocks of sedimentary target units within a developing crater's annular trough as the blocks rotate against each other on fault surfaces while collectively moving along a décollement at the surface of the crystalline basement (Poag et al., 2004).

Pre-impact Paleoenvironmental Setting

The Wetumpka impact event was an early Campanian catastrophic event resulting from a hyper-velocity celestial object impacting onto a shallow carbonate shelf ~30 to 100 m deep (King et al., 2002). As shown in Figure 13, impact occurred at ~82 m.y.a. in what was the larger paleo-Gulf of Mexico, roughly 30 km seaward of a barrier island chain (King, 1997; King and Neathery, 1998). At that time, dinosaurs roamed the nearby beaches and tropical forests of the Appalachian headland, while giant marine reptiles swam in the warm sea and flew through the coastal skies (Lacefield, 2000). Benthic life forms were also abundant within the carbonate ooze on the seafloor (King et al., 2006). The region's gently dipping homoclinal target stratigraphy was rather uncomplicated despite its proximity to the southernmost Appalachian massif.

Paleowater depth, as noted above, is based on ichnosedimentologic evidence and depth-sensitive eye morphology of ostracodes (King et al., 2002). Although this water layer shallowed to the north, it was deep enough to now be considered the uppermost unit of target stratigraphy given the effect surface water has on resultant crater forms and subaqueous strata during bolide impacts (Kieffer and Simonds, 1980; Melosh, 1982; Ormö and Lindström, 2000; Dypvik and Jansa, 2003).

The underlying paleo-seafloor is currently thought to have been unconsolidated, water-saturated, Upper Cretaceous marine, shoreline, and fluvial sediments previously interpreted to have been approximately 120 m thick (Neathery et al., 1976b; King, 1997) at time of impact. However, the author of this report suggests the overall thickness was probably well in excess of 170 m for reasons to be explained. In descending stratigraphic order, these units are the Mooreville Chalk, the Eutaw Formation, and the Tuscaloosa

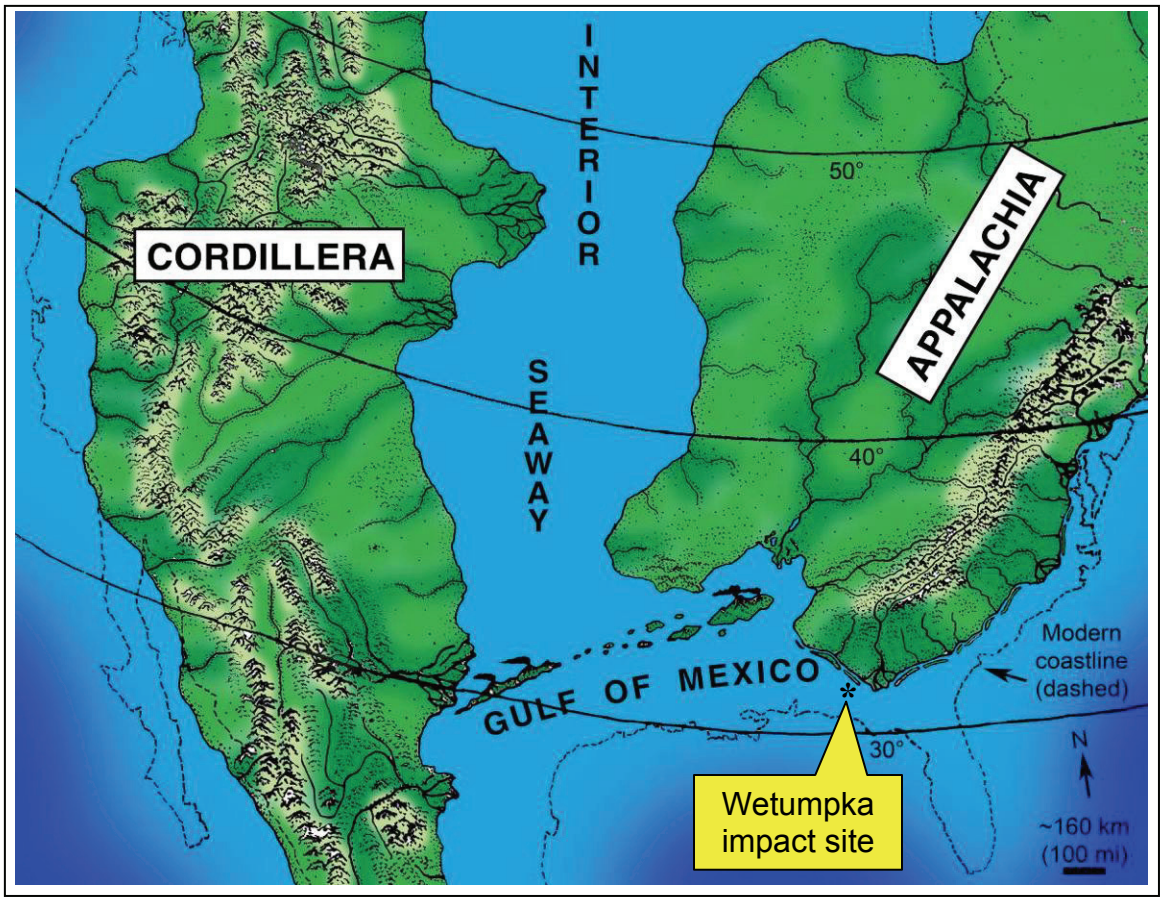

Figure 13. Wetumpka's early Campanian, shallow, nearshore, marine-target setting in the greater context of the then larger paleo-Gulf of Mexico and the Late Cretaceous Western Interior Seaway, both of which partially covered North America. Water depth at target is thought to have been ~30 to 100 m (King et al., 2002). Modified from Schwimmer (2002).

Group. At time of impact, they were resting unconformably atop the regional metasedimentary and meta-igneous pre-Cretaceous crystalline basement rock (Neathery et al., 1976b). A new interpretation of the marine-target paleostratigraphy is offered in the next section.

A New Interpretation of the Marine-target Paleostratigraphy

Since time of impact, most attributes of the target units have changed very little from their original condition. Nevertheless, an exception is found in the Eutaw strata. As previously indicated, the Eutaw Formation is *presently* only about 30 m thick in the vicinity of the impact structure, and many authors cited throughout this report have noted this thickness when examining the structure in its current form. However, several authors have also mistakenly cited this 30-m thickness when reconstructing the impact event itself as recently documented in King et al. (2005) and numerous other publications. That being said, the present author makes the following eight points about the Eutaw Formation in the target area:

1) In central Alabama, Eutaw thickness in outcrop can range up to ~107–122 m (Raymond et al., 1988). Therefore, there is at least the potential for the unit being thicker in the past than what is seen there today.
2) The Eutaw is conformable with the overlying Mooreville Chalk; there is no unconformity dividing these two layers in the target area (Raymond et al., 1988).
3) Eutaw strata (~30 m thick) has been mapped adjacent to the Wetumpka structure in the high hills just east of the eastern rim (Neathery et al., 1976b). See Figure 9 for details.
4) In the high hills, the Eutaw is capped by a Quaternary disconformity that was obviously not present in the region's paleostratigraphy (Neathery et al., 1976b; Szabo et al., 1988).

5) Neathery et al. (1976b) report that atop this disconformity is a Quaternary high terrace fluvial deposit having a base ranging between 90 and 180 m above modern sea level (see Figure 14).
6) In the target region, the Eutaw's thickness extends up to the maximum elevation given for the base of this terrace deposit, i.e., the Eutaw rises to the Quaternary disconformity at 180 m elevation.
7) It is exceedingly unlikely that the process forming this Quaternary disconformity eroded the overlying strata down to the exact level at which Eutaw deposition ceased and Mooreville deposition began. Neathery et al. (1976b) point this out where they discuss the nearly 100 m relief of this disconformity. Clearly then, weathering action eroded the strata down to some level *within* the thickness of the original Eutaw Formation such that the thinned remnant of this unit as seen presently no longer represents its original thickness in the target region at time of impact.
8) Because the Eutaw's current 30-m thickness is too thin, it is not necessary to invoke unusual depositional conditions or catastrophic alterations to interpret the Eutaw as having a significantly greater paleothickness.

Evidently, previous authors failed to recognize fully that, given the overlying Quaternary disconformity cutting into the Eutaw, 30 m is not necessarily the unit's *entire thickness at time of impact*. In essence, they appear to have forgotten they were not observing a perfectly preserved beach deposit that nature laid down, but instead, the thinned remnants of what weathering and erosion heretofore left behind.

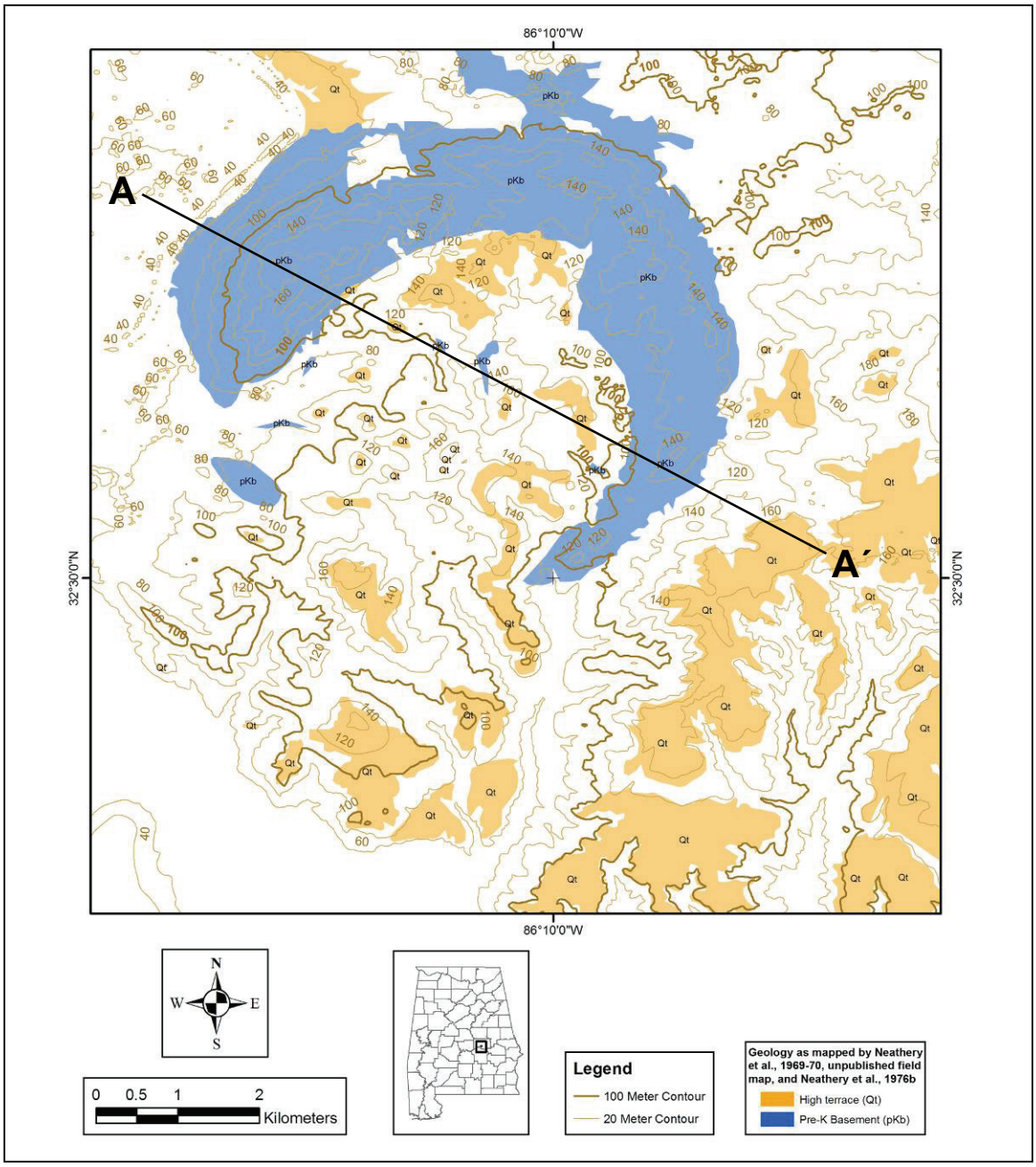

Figure 14. Topophysiographic map of Quaternary high terrace deposits capping the high hills east of the crystalline rim. The Eutaw Formation rises in thickness to the base of this Quaternary unit where a major regional unconformity exists. Neathery et al. (1976b) report this unconformity (the eroded top of the Eutaw) as ranging 90 – 180 m above modern sea level. It is unlikely this unconformity weathered to the exact paleo-top of the paleo-Eutaw. Therefore, paleo-Eutaw was thicker than what is left here today. See text above and cross section below for further explanation. Compiled by author in ArcGIS® 9.1 from field maps used by Neathery et al. (1976b), the published map from the same authors, and the Geologic Map of Alabama (Szabo et al., 1988).

Given the above eight points, this author suggests that, in the target area at time of impact, the Eutaw Formation was at least 30 m thicker than what is currently indicated by Neathery et al. (1976b), Nelson (2000), and several subsequent papers citing their work.

Figure 15 shows a reconstruction of the target based on the present-day stratigraphy of the high hills east of the eastern crystalline rim. Recall that the paleo-Eutaw must have *exceeded* the present elevation of the Quaternary disconformity. Therefore, the reconstructed Eutaw Formation must be depicted as having an original thickness that brings its paleo-top to some elevation *higher than* the 180-m basal elevation of the Quaternary disconformity. This author illustrates the top of the paleo-Eutaw as being a conservative 10 m above the Quaternary disconformity, which effectively makes the Eutaw's total thickness in the target region at time of impact greater than 60 m. This provisional 10 m (or more) was completely stripped away, and the 20 m beneath it were eroded down to the Eutaw's present-day 30-m thickness. Finally, Figure 16 offers a new interpretation of the Upper Cretaceous marine-target paleostratigraphy during the Wetumpka impact event. A thickness of 170 m is indicated for the Upper Cretaceous sediments overlying the crystalline basement, and 60 m of water is shown (schematically) above the sediments for a total thickness of approximately 230 m (give or take some tens-of-meters) for the marine-target stratigraphy of the Wetumpka impact event.

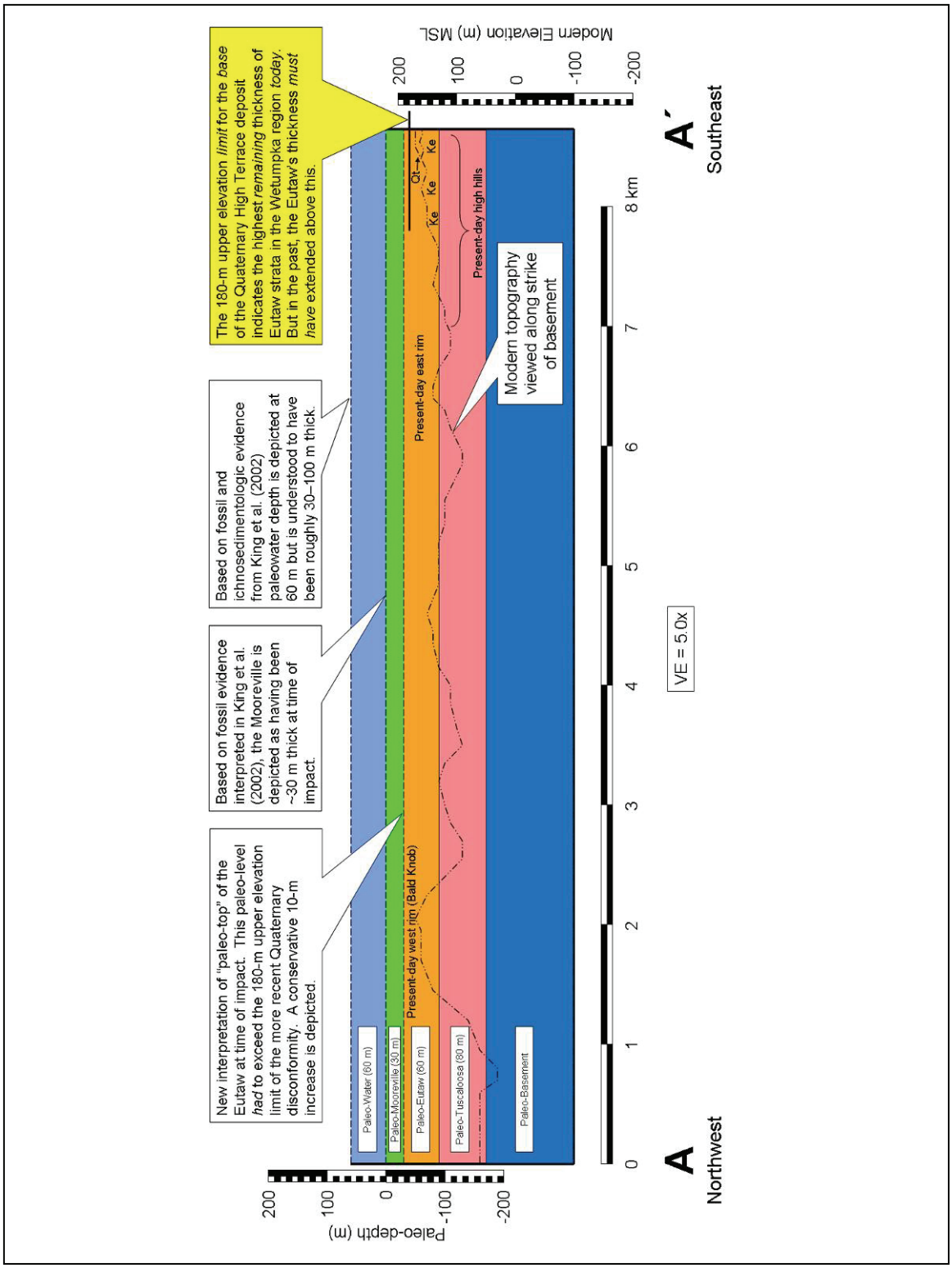

Figure 15. Schematic cross section of marine-target paleostratigraphy reconstructed from strata in high hills east of eastern rim. See text for explanation. The 80-m-thick depiction of the Tuscaloosa is merely a consequence of relief on the basement surface.

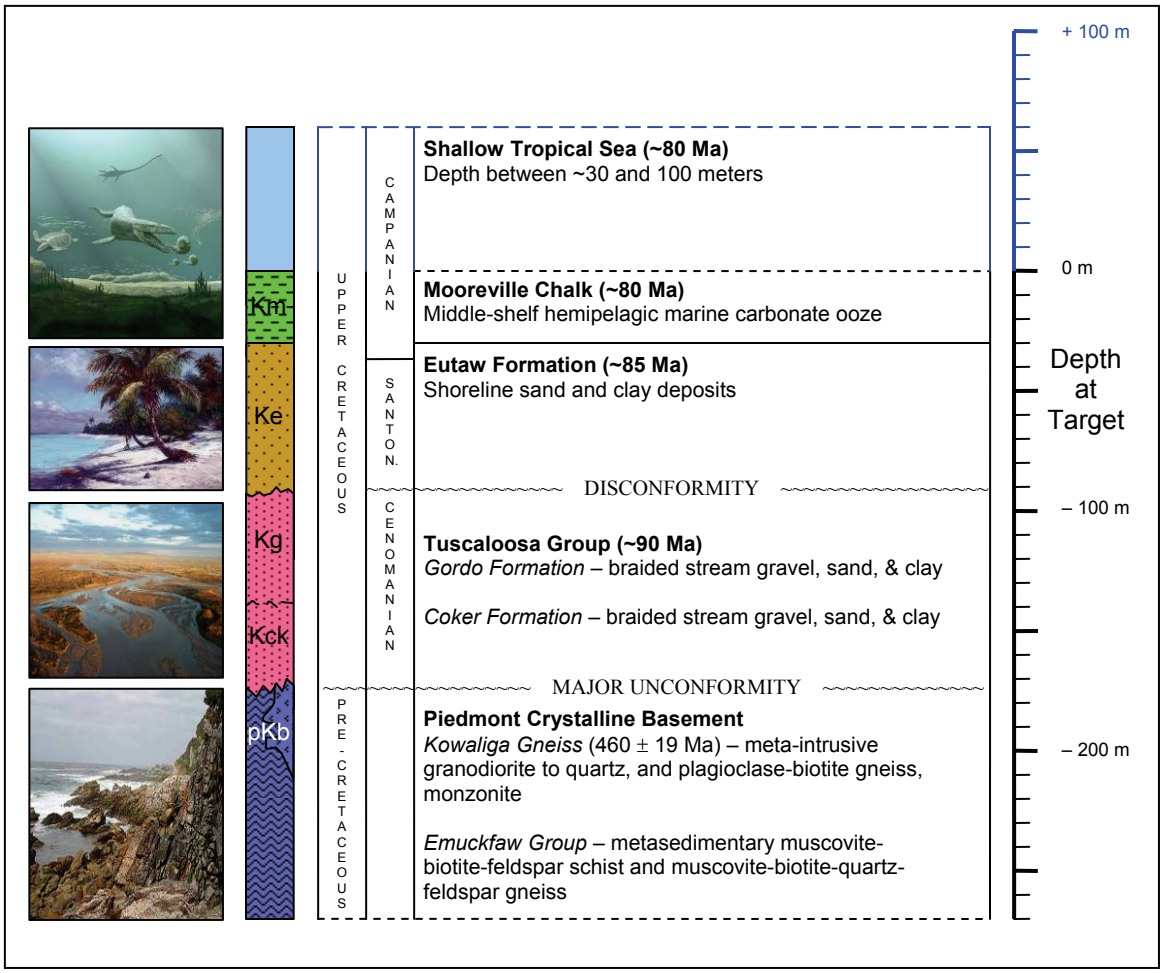

Figure 16. A new interpretation of the Upper Cretaceous marine-target paleostratigraphy during the Wetumpka impact event. Note seawater as uppermost target unit. Inclusion of the water layer is appropriate in characterizing marine-target bolide impact events because a water layer can strongly influence formation processes, structure, and morphology. Notice too that the target-age Eutaw Formation is depicted as significantly thicker. See text for full explanation. Adapted and modified from Neathery et al. (1976b), Raymond et al. (1988), King (1997), and Neathery et al. (1997). Usage of the photo thumbnails in this figure accords with U.S. Code, Title 17, Chapter 1, Section 107 (2006).

Post-impact Paleoenvironmental Setting as Presently Interpreted

Understanding the post-impact paleoenvironmental setting is of importance to understanding the crater-filling material comprising the two drill cores examined in this report. It has been speculated that, once formed, Wetumpka's crystalline rim may have stood exposed above the shallow tropical sea as an arcuate island sheltering a central lagoon, or that perhaps the rim totally excluded the sea to form a circular landmass surrounded by the water (Neathery et al., 1976b; King et al., 2004a). If the latter were true, then the entire rim would have to have been intact, and this would require a hiatus between deposition of fallback and surgeback material that ended with a catastrophic rim collapse and marine resurge. Further speculation casting Wetumpka as possibly hosting such a unique marine or terrestrial ecosystem during the time between fallback and rim collapse suggests the formation of the previously outlined intra-crater paleosol and/or lacustrine deposit as evidenced by sedimentary material at 100 m drill depth in the Schroeder drill core (1-98).

However, evidence (outlined earlier) suggests the Wetumpka structure is actually an overturned flap within a larger impact structure similar to the hypothetical crater produced in a numerical model of Lockne by Ormö et al. (2002). By chance, the parameters used in the Lockne model approximate the Wetumpka impact event (Figure 17). If the crystalline rim at Wetumpka is indeed an overturned flap similar to the flap at Lockne, the implications are far reaching. Such a scenario would allow the following five conclusions to be drawn: 1) an incomplete ring of crystalline rock would resemble the incomplete crystalline rim at both the Kärdla and Chesapeake Bay impact structures; 2) it would better-explain the structurally deformed crater-flanking terrain and faulting in

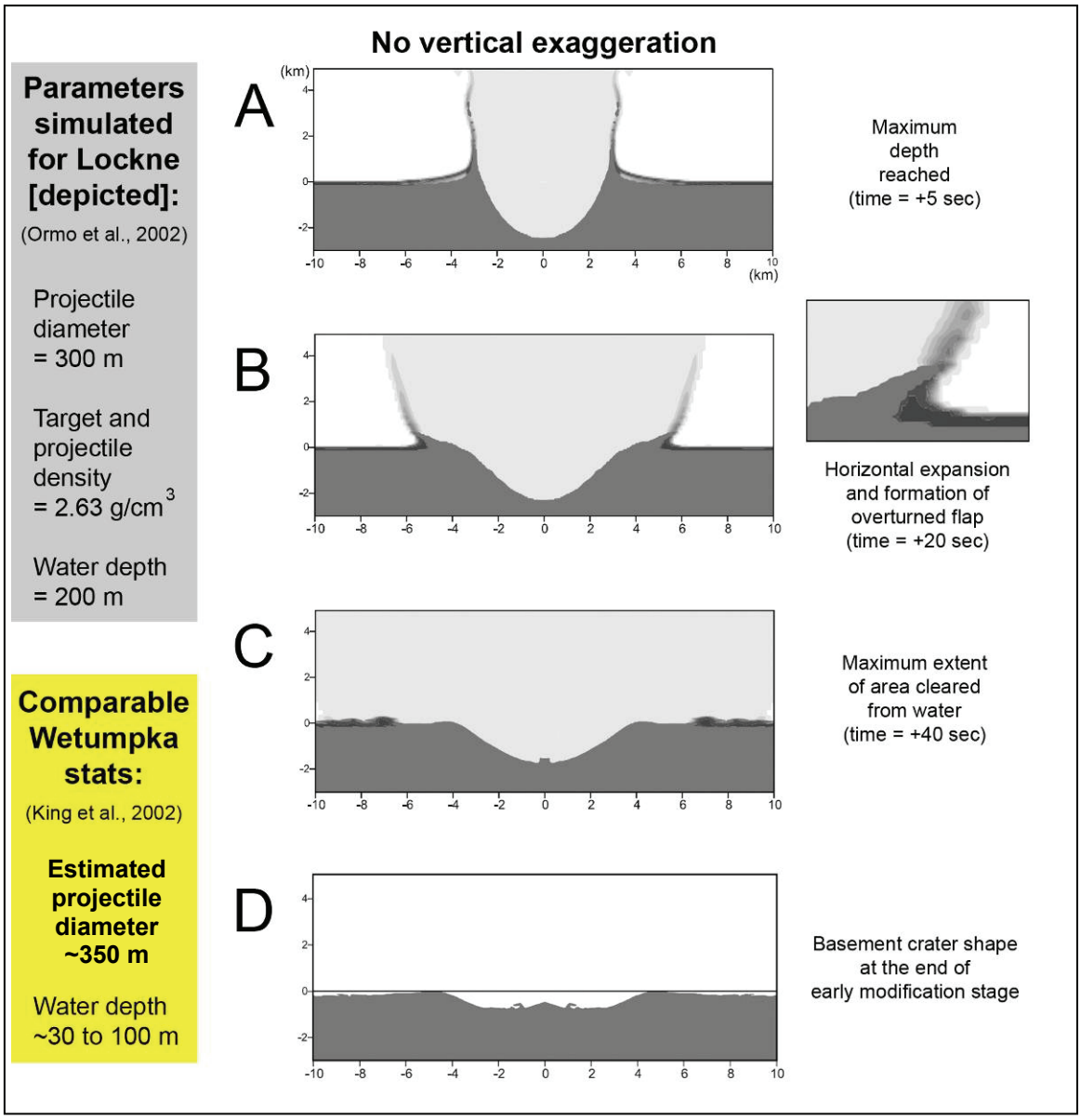

Figure 17. Hydrocode numerical simulation of shallow marine-target impact event. Model was developed for Lockne impact structure by Ormö et al. (2002) but its parameters and results are similar to those for Wetumpka. A: Transient crater opens to max depth in marine target of water (200 m thick) and soft sediments (thin, dark gray layer) overlying crystalline basement. B: Detail shows formation of overturned crystalline flap enveloping seafloor sedimentary layers in a process possibly similar to what may have taken place at Wetumpka. C: Water crater has opened to max extent, surgeback is about to begin. D: Final shape of impact structure after cratering process ends. Modified from Ormö et al. (2002).

the high hills as the consequence of surgeback; 3) it would account for the nature of the crater-filling materials as well as their stratigraphic positions and topographic elevations as fallback and surgeback deposits; 4) it would explain the enigmatic deposit of Coker Formation on the northern flank of the crystalline rim (overturned flap?) as a recently exposed remnant of Upper Cretaceous strata that was enveloped under the flap during impact; and 5) it would eliminate the possibility of any hiatus between crater-filling events because the fresh crater would have been filled during the impact event. Because these five conclusions fit observations, and because Wetumpka was probably formed in a shallow marine environment with a poorly lithified dichotomous stratigraphy, the present author gives preference to the numerical simulation (Figure 17) and its related conceptual model (Figure 18). Both figures depict the formation of an impact structure in a shallow marine environment resulting in the formation of an inner basin within a larger impact structure. Of importance is the resulting outermost rim that forms in the soft sediments as depicted in Figure 18D.

To produce a similar model for the Wetumpka impact structure, the hydrocode simulation's final crater form (Figure 17D) was adjusted slightly to match Wetumpka's scale, and given a vertical exaggeration of 5.0x as shown in Figure 19. This adjusted and exaggerated figure helped approximate the structure of the crystalline basement for the Wetumpka model. Additionally, a cross section of the Kärdla impact structure (Figure 20) from Puura and Suuroja (1992) was adjusted to the required scale and vertical exaggeration, and was used to help approximate both the structure-filling material as well as the structure of the crystalline basement for the Wetumpka model. Further, a depositional lithofacies model of the Chesapeake Bay impact structure (Figure 21) from

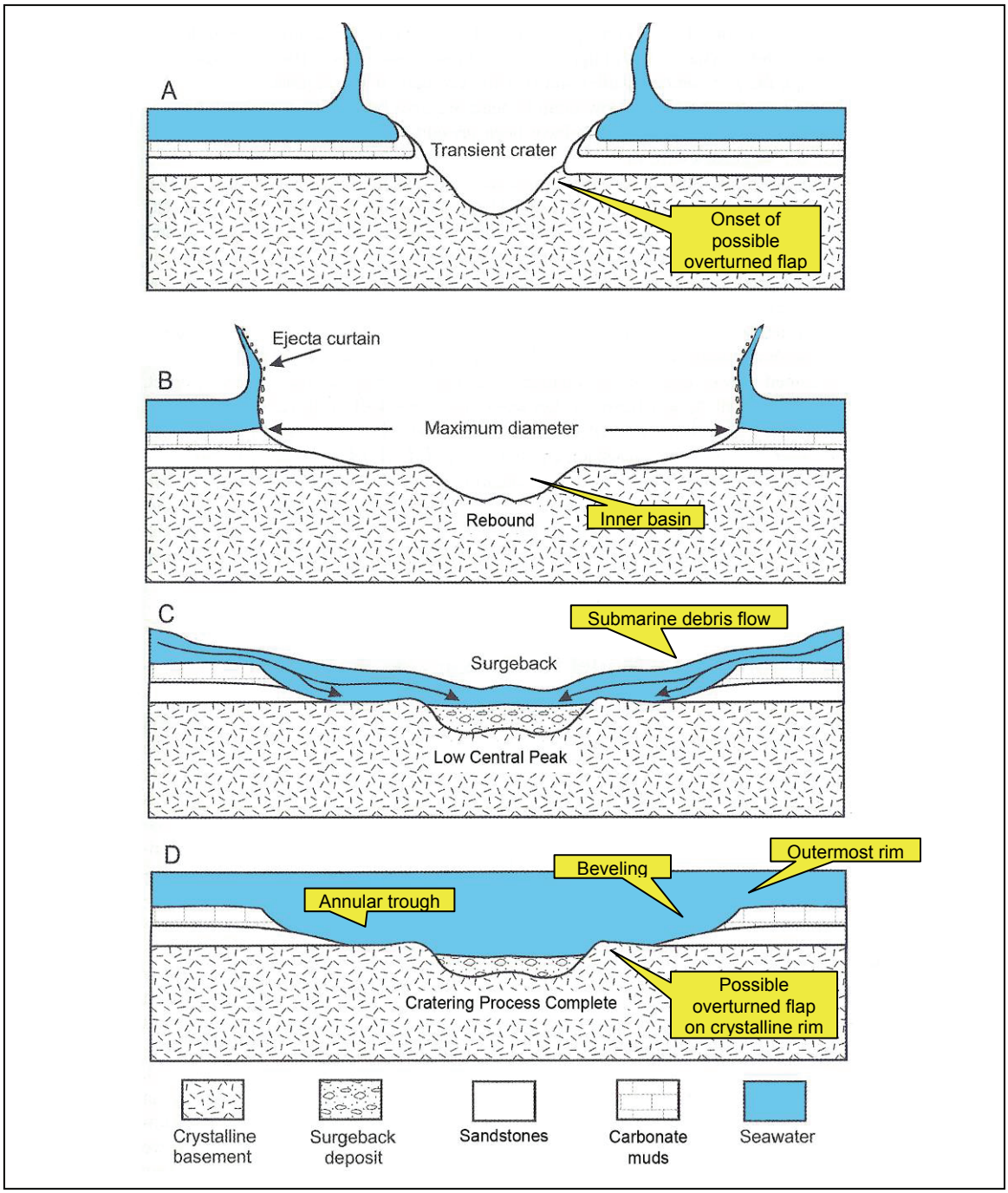

Figure 18. Conceptual model of impact-crater formation in a shallow-marine target of poorly lithified dichotomous stratigraphy. A: Transient crater opens. B: Inner basin has formed within larger crater. C: A catastrophic debris-flow of disturbed seafloor is driven in by surgeback. D: Notice the crater's final morphology, particularly the presence of an outermost rim in sediment and/or sedimentary rock. Notice too the overturned flap in crystalline basement, and the chaotically-filled inner basin. Modified from Poag et al. (2004) and their original derivation from Ormö and Lindström (2000).

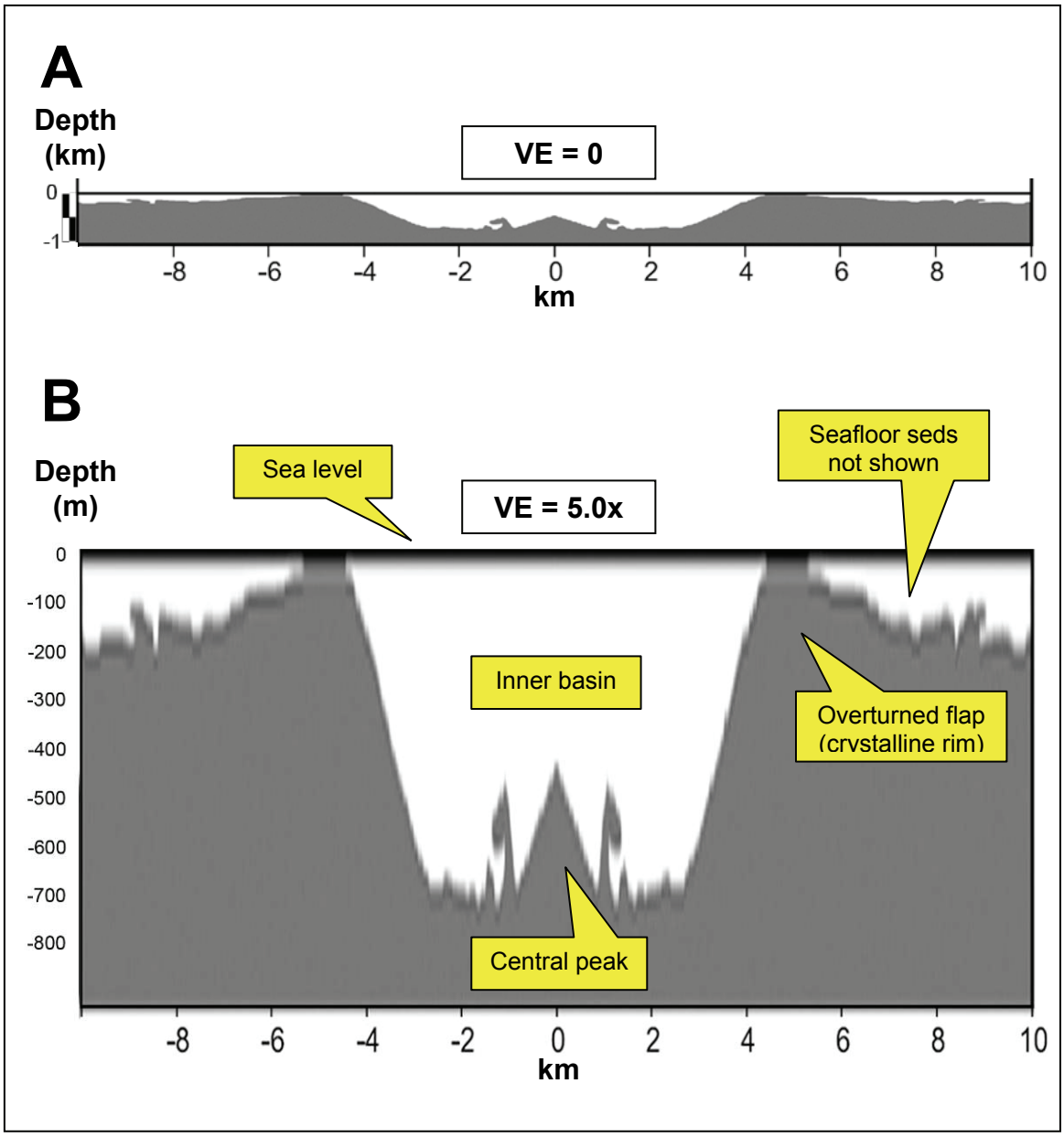

Figure 19. Detail of hydrocode simulation showing the final shape of the simulated impact structure. A: At a vertical exaggeration (VE) of zero, this undistorted view of the hypothetical impact structure shows a true-to-form profile of the simulated crystalline basement. The structure's features are nearly flat. B: At a VE of 5.0x, the structure's features falsely appear mountainous, and/or abyss-like. This exaggerated profile will be used in this report to help model the Wetumpka impact structure. Note the moderate central peak, and that the depth to basement is ~700 m. Modified from a simulation created for the Lockne impact structure by Ormö et al. (2002).

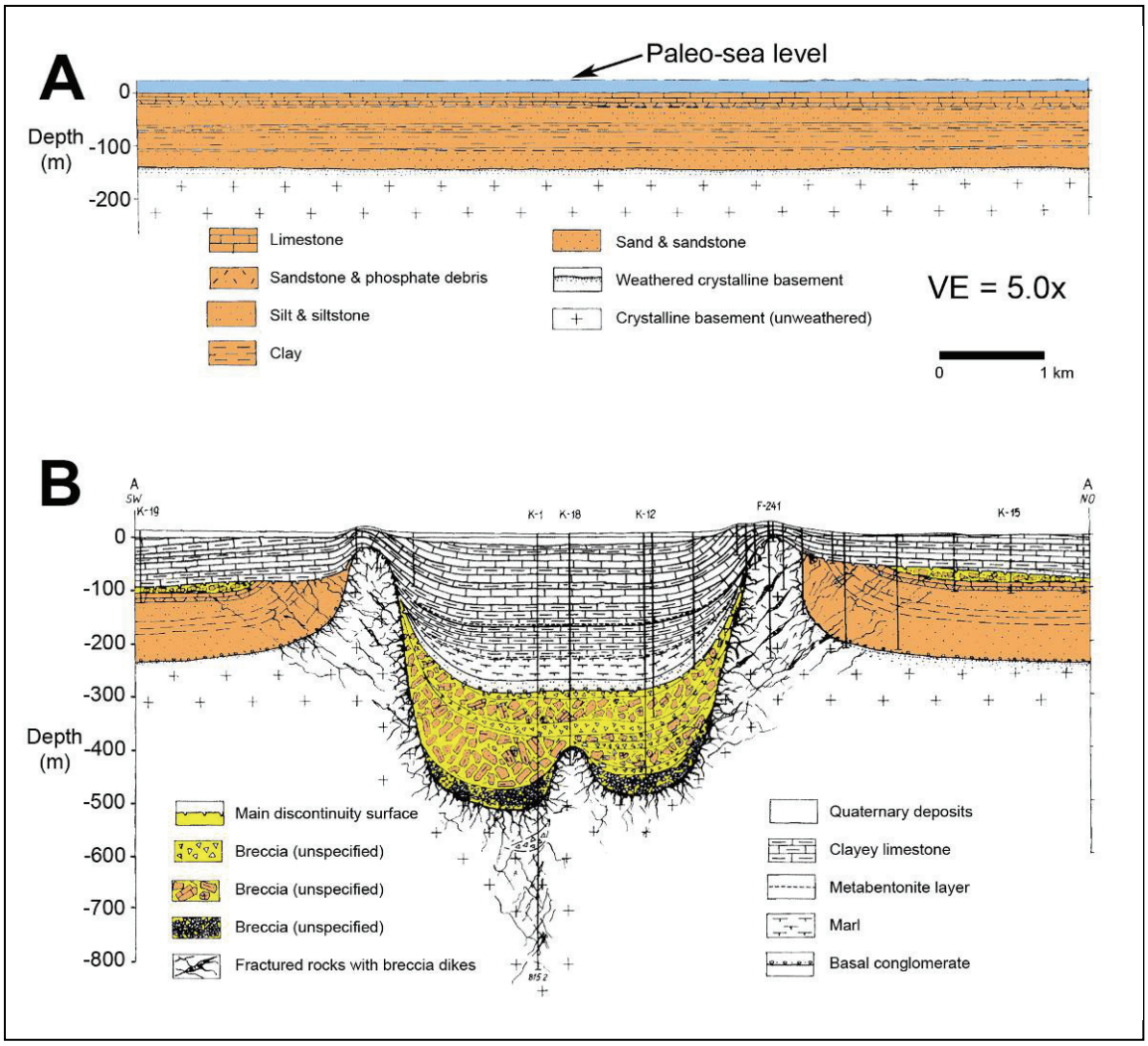

Figure 20. Cross section of the Kärdla impact structure showing structure-filling stratigraphy. Kärdla has been drilled in excess of 300 times (Puura and Suuroja, 1992). Some of the drill holes are depicted in the figure as vertical lines; a few are shown with labels. As with the previous figure, VE is set to 5.0x. A: Pre-impact marine-target stratigraphy. Note similarities to that of Wetumpka. B: At a VE of 5.0x, the structures features falsely appear mountainous, and/or abyss-like. Note the short central peak, and that the depth to basement is ~500 m. An overturned flap is not depicted in this reconstruction, probably because it has been largely eroded away. Even so, sedimentary target layers do fold upward at the edge of the crystalline rim. This may be a basal remnant of the overturned flap. The figure is brightly colored to aid recognition of various units. This exaggerated profile will be used in this report to help model the Wetumpka impact structure. Modified from Puura and Suuroja (1992).

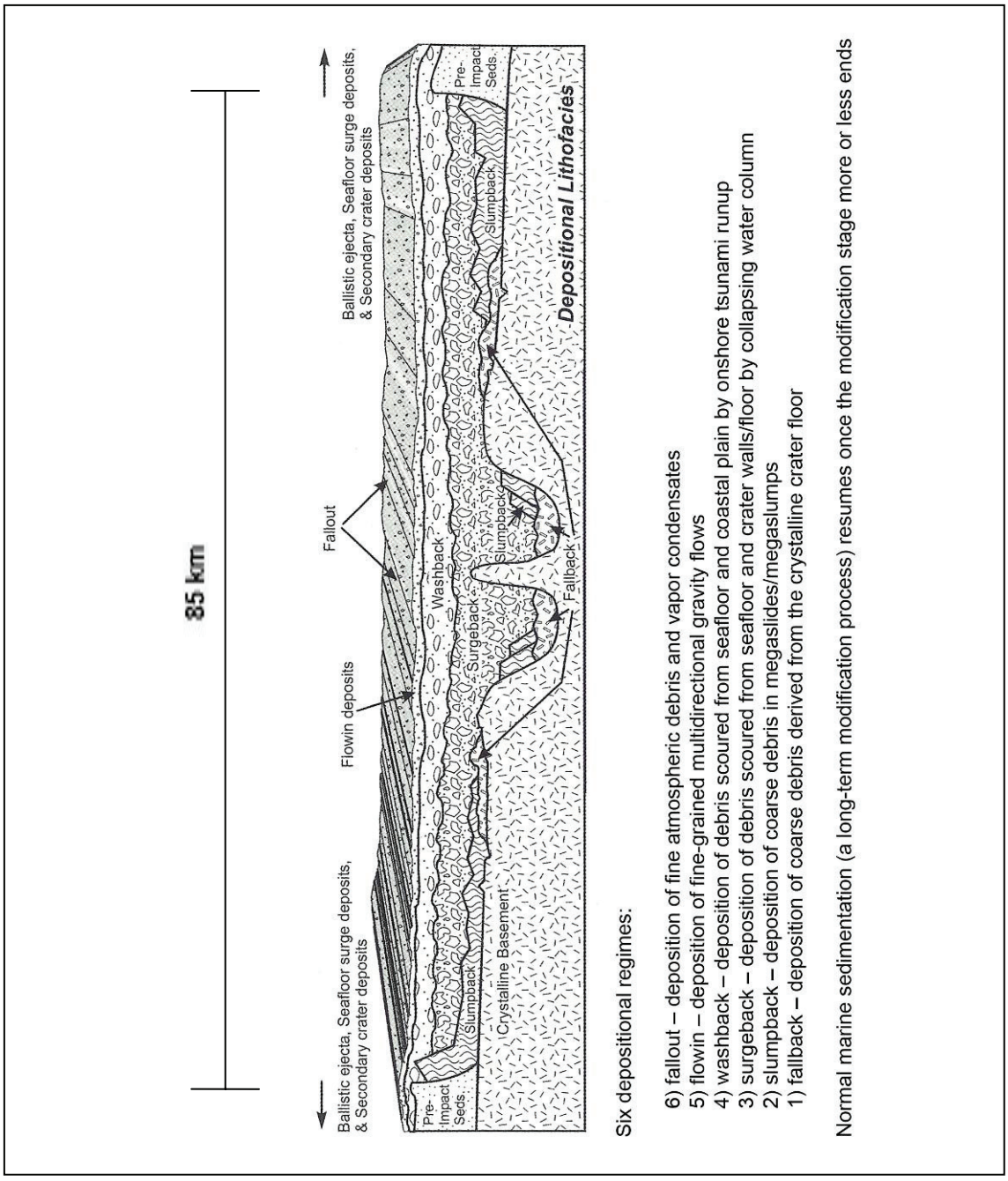

Figure 21. Depositional lithofacies model of the Chesapeake Bay impact structure. No indication of vertical exaggeration is offered in the schematic diagram, features must be judged relative to each other. The direction of the line of cross section is generic. Six depositional regimes are briefly outlined. Note the tall central peak rising above the crystalline rim of the inner basin. Poag et al. (2004) interpret the crystalline rim as a "peak ring," but the present author prefers the terms "crystalline rim," "inner ring," or "overturned flap." This lithofacies model was used in this report to help model the Wetumpka impact structure. Modified from Poag et al. (2004).

Poag et al. (2004) was also used to help approximate the structure-filling material and crystalline basement for the Wetumpka model. Finally, early drill core data from King et al. (2002) provided details of the structure-filling material as did King et al. (2005).

Figure 22 shows a map view of the Wetumpka model. Figure 23 illustrates the details of how some of the features used to help create the cross-sections had to be projected onto the cross sections from their nearby geographic positions. Figure 24 shows two conceptual cross sections of the same. Each figure uses the potential size range calculated by Nelson (2000) for the diameter of the outermost rim as 13.5 to 15.6 km. Although Neathery et al. (1976b) did not map Wetumpka's crystalline rim as an overturned flap, nor a peak ring within a larger impact structure, they did find several faults and grabens in the Upper Cretaceous sediments outside the crystalline rim (overturned flap?), including an arcuate fault in the high hills shown just southwest of transect B–B′ in Figure 22. Those authors also indicated on their structural cross section through the same region the possible existence of additional faults beyond the one already known. King (1997) pointed out that these potential faults could extend the impact structure's overall diameter to at least 10 km, but the original cross section ends at that point. Even so, the 10 km value does approach the smaller, 13.5-km-diameter from Nelson (2000).

In the model below, the structurally disturbed crater-flanking terrain is explained as a complex of slumped megablocks that moved towards and into the inner basin along a décollement at the surface of the crystalline basement similar to processes described in Poag et al. (2004) and King et al. (2005). This region shows clear evidence today of having undergone strong extensional forces probably attributable to mass movement into

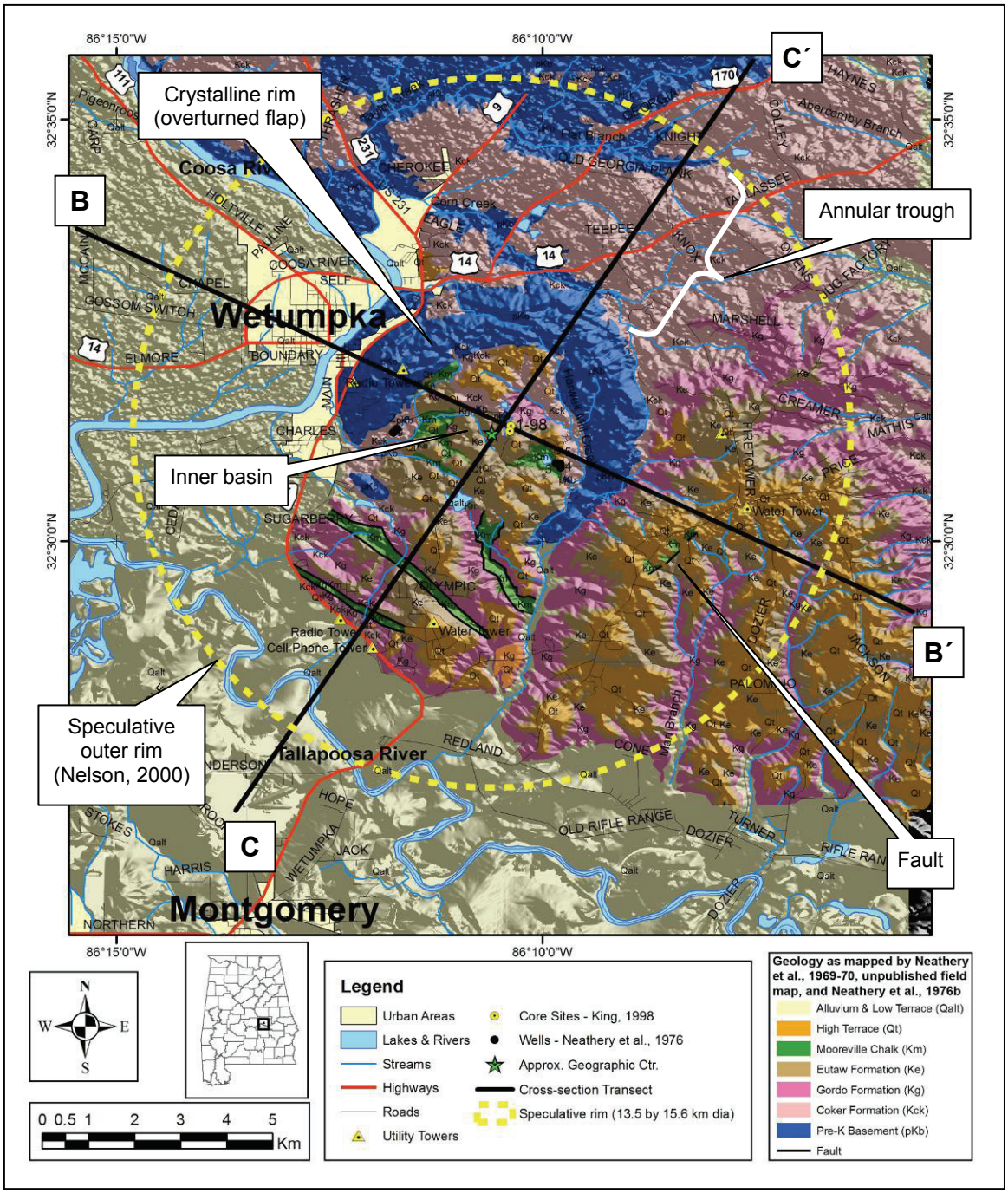

Figure 22. Index map for cross sections in the next figure depicting the Wetumpka structure as an inner ring within a 13.5- to 15.6-km-diameter crater. The dashed yellow circle represents the speculative outer rim diameter as calculated in Nelson (2000). Because of distortions associated with mapping (projecting) Earth's spherical surface onto a flat surface, the perfectly drawn circle is actually 13.5 km east-to-west, and 15.6 km north-to-south. That is, the map itself is slightly distorted, as are *all* maps of this projection. Map created using ArcGIS® 9.1 and data from Neathery et al.(1976b).

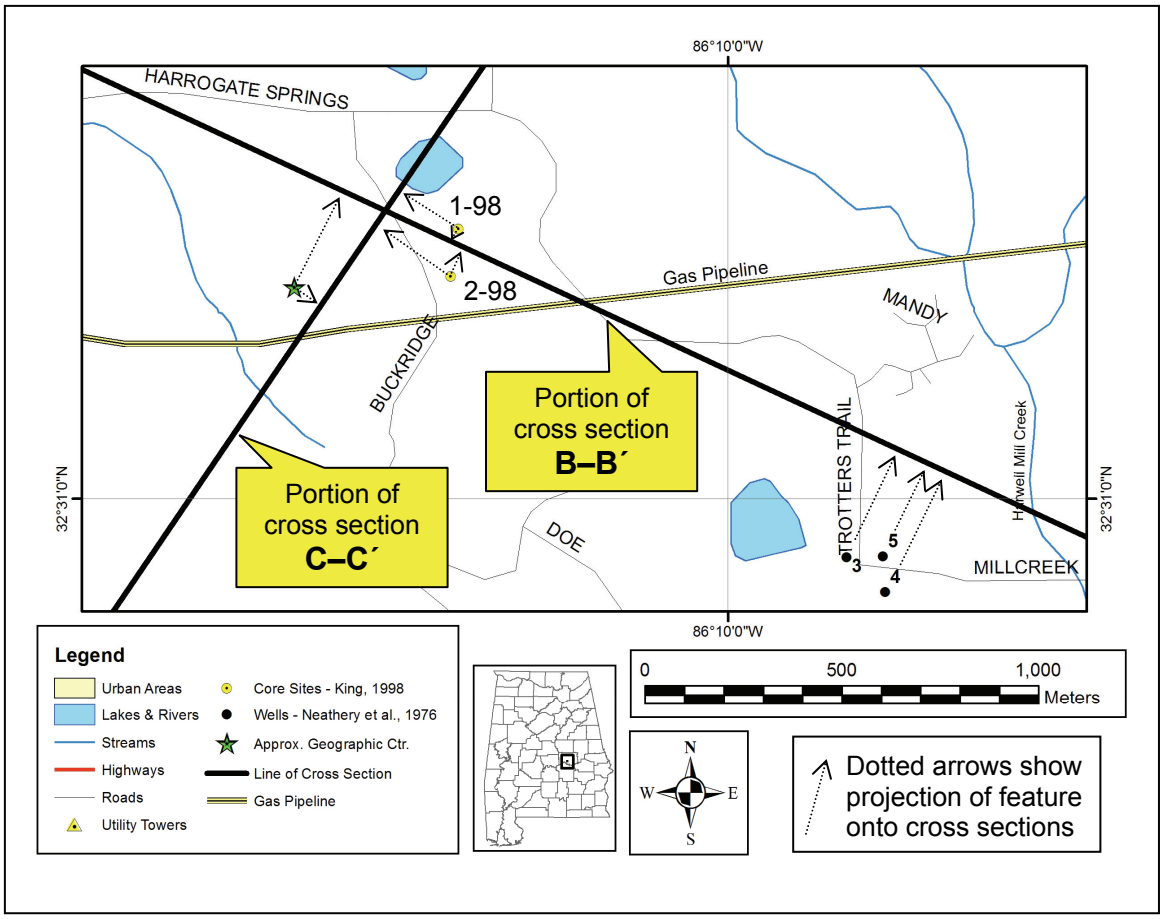

Figure 23. Detail map showing various subsurface features projected at right angles (dotted arrows) relative to cross sections B–B´ and C–C´ (next figure). This detail map is intended to pre-empt any potential for confusion. The reader should be aware that when viewing cross section B–B´ from the southwest, drill hole 1-98 will be projected on the left, and 2-98 will be on the right. Notice too that the drill holes will appear very close together. However, the opposite is true for viewing cross section C–C´ from the southeast, wherein 2-98 will be projected on the left, and 1-98 on the right. In this cross section, the drill holes appear at a greater separation than in the previous cross section. Adding to the potential for further confusion, the approximate geographic center (green star) will be to the left in each cross section. The overall effect is that the reader may be confused into mistakenly thinking the present author has misplaced the drill holes in the numerous cross sections of this report.

Figure 24. (Following page) Schematic cross section of the freshly-formed Wetumpka impact structure. A: Line of cross section B–B′ follows the strike of regional basement rock from Neathery et al. (1976b) and does not show any dip. Note the outlier of Mooreville Chalk in the normal fault mapped by Neathery et al. (1976b). Other grabens in this cross section are speculative and depicted with minimal dip values that appear exaggerated. As such, they could have been overlooked during mapping – especially if their sandy edges were fluidized or buried by Quaternary sediments. The high hills east of the crystalline rim may show what Ormö and Lindström (2000) refer to as "beveling," which is thought to be an indicator of marine-target impact. B: Line of cross section C–C′ cuts perpendicular to strike of regional basement rock from Neathery et al. (1976b) and shows a southward dip of roughly 10 to 20 m/km (~0.02°) for the basement, and 9 to 15 m/km (~0.01°) for the Cretaceous strata. Both dip values appear artificially steepened by the diagram's vertical exaggeration, but in reality, even over a distance of 20 km, the target is virtually flat. The southern rim (overturned flap?) is depicted as having been either poorly formed and/or collapsed to help form the grabens in the structurally disturbed crater-flanking terrain, and is based largely on King et al. (2005). Note the two grabens containing Mooreville Chalk that are still present today. As in the previous cross section, other grabens in this cross section are speculative and depicted with minimal dip values that also appear exaggerated. As such, they could have been overlooked during mapping – especially if their sandy edges were fluidized or buried by Quaternary sediments. Citations: Diameter of the overall impact structure is based on possible rim-to-rim size range calculated by Nelson (2000). Pre-impact target stratigraphy is based on this study's new interpretation thereof. Original height of the crystalline rim (overturned flap?) is based on calculations by King (1997) and matches well with hydrocode simulation. Faulting outside of the crystalline rim is based on Neathery et al. (1976b). The impact structure's post-impact stratigraphy and depth is based on the extensive drill record of the Kärdla structure summarized by Puura and Suuroja (1992), and on previous studies of Wetumpka by King et al. (2004b; 2005). The overall model is adapted from a depositional lithofacies model developed for Chesapeake Bay impact structure by Poag et al., (2004).

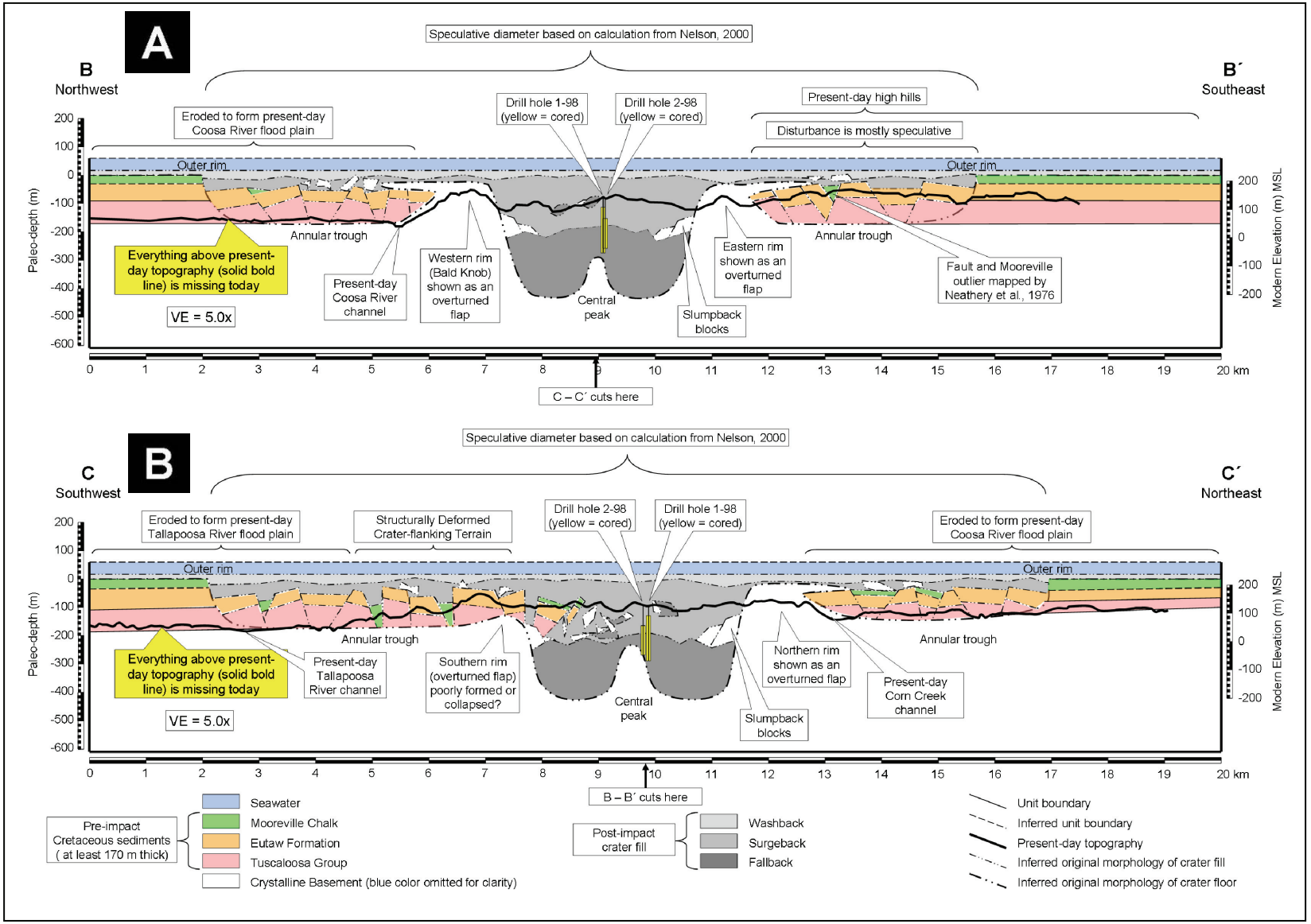
A
B
Northwest
B´
Southeast
Speculative diameter based on calculation from Nelson, 2000
Eroded to form present-day Coosa River flood plain
Drill hole 1-98 (yellow = cored)
Drill hole 2-98 (yellow = cored)
Present-day high hills
Disturbance is mostly speculative
Outer rim
Outer rim
Annular trough
Annular trough
Everything above present-day topography (solid bold line) is missing today
VE = 5.0x
Present-day Coosa River channel
Western rim (Bald Knob) shown as an overturned flap
Central peak
Slumpback blocks
Eastern rim shown as an overturned flap
Fault and Mooreville outlier mapped by Neathery et al., 1976
Paleo-depth (m)
Modern Elevation (m) MSL
C – C´ cuts here
B
C
Southwest
C´
Northeast
Speculative diameter based on calculation from Nelson, 2000
Eroded to form present-day Tallapoosa River flood plain
Structurally Deformed Crater-flanking Terrain
Drill hole 2-98 (yellow = cored)
Drill hole 1-98 (yellow = cored)
Eroded to form present-day Coosa River flood plain
Outer rim
Outer rim
Annular trough
Annular trough
Everything above present-day topography (solid bold line) is missing today
VE = 5.0x
Present-day Tallapoosa River channel
Southern rim (overturned flap) poorly formed or collapsed?
Central peak
Slumpback blocks
Northern rim shown as an overturned flap
Present-day Corn Creek channel
Paleo-depth (m)
Modern Elevation (m) MSL
B – B´ cuts here
Pre-impact Cretaceous sediments (at least 170 m thick)
Seawater
Mooreville Chalk
Eutaw Formation
Tuscaloosa Group
Crystalline Basement (blue color omitted for clarity)
Post-impact crater fill
Washback
Surgeback
Fallback
Unit boundary
Inferred unit boundary
Present-day topography
Inferred original morphology of crater fill
Inferred original morphology of crater floor

the inner basin owing to the absence of a well-developed crystalline rim (overturned flap?) at the southwest quadrant of the inner basin (King et al., 2005). That is, nothing prevented its catastrophic partial movement into the inner basin during surgeback.

Similarly, any deformation in the high hills east of the eastern rim (overturned flap?) may be explained as resulting from a corresponding mass movement, but to a lesser extent because that material was largely blocked from entering the inner basin by the presence of the well-developed crystalline rim (overturned flap?). It is perhaps because of the supportive nature of the crystalline rim that these high hills do not show strong evidence today of structural disturbance on par with the structurally disturbed crater-flanking terrain. As such, most of the blocks are depicted in Figure 24 as having shallow dips except where otherwise known to be steeply dipping. Such would have been the case for the rest of the Upper Cretaceous material moving within the annular trough. Of interest, the high hills may still show some evidence of "beveling" similar to that described at Lockne by Ormö and Lindström (2000). Further investigation of this issue is left to future studies.

Complicating the entire matter is the extensive weathering and erosion the Wetumpka impact structure has undergone since formation. Figure 24 nicely illustrates the point that we are not looking at what nature made, but the tattered remnants of what was left behind. This is even apparent in the map view of Figure 22 where one may notice the broad floodplains of the Tallapoosa and Coosa rivers. In essence, most evidence for the speculative existence of an outer rim in the Upper Cretaceous strata, and slumping of Upper Cretaceous megablocks in the annular trough has been washed away, or buried by Quaternary sediments, making it very difficult to identify with certainty.

The 30% that remains today (the structurally disturbed crater-flanking terrain and the high hills) needs extensive study to confirm or refute the model. This study's analysis of the two drill cores from Wetumpka will assist in that regard by comparing their stratigraphy to that of the recently drilled marine-target impact structure at Chesapeake Bay.

PREVIOUS WORK

> Impact cratering has been recognized as an important geologic process for only the last few decades. As recently as 1950 most astronomers believed that the lunar craters were giant volcanoes, and all but a few geologists derided the idea that the Earth's surface has been scarred by impact structures kilometers in diameter (Melosh, 1989).

The first person to document the disturbed geology just east of the Coosa River near the town of Wetumpka was Eugene Allen Smith, Professor of Geology at the University of Alabama, and Alabama State Geologist (Smith et al., 1894; Hall, 1996). When writing in his field notes of July 1, 1891 about an area now known to be within Wetumpka's interior region (Figure 25), Smith wrote that the geology is "… difficult to explain except upon the supposition of a depression of several hundred feet …" but he offered little more speculation than this (Smith et al., 1894).

Indeed, Wetumpka's unique geology is easy to recognize as unusual for its surroundings, but explaining the structure's features and origins outside the context of impact cratering is rather difficult as evidenced by the regional generalized mapping

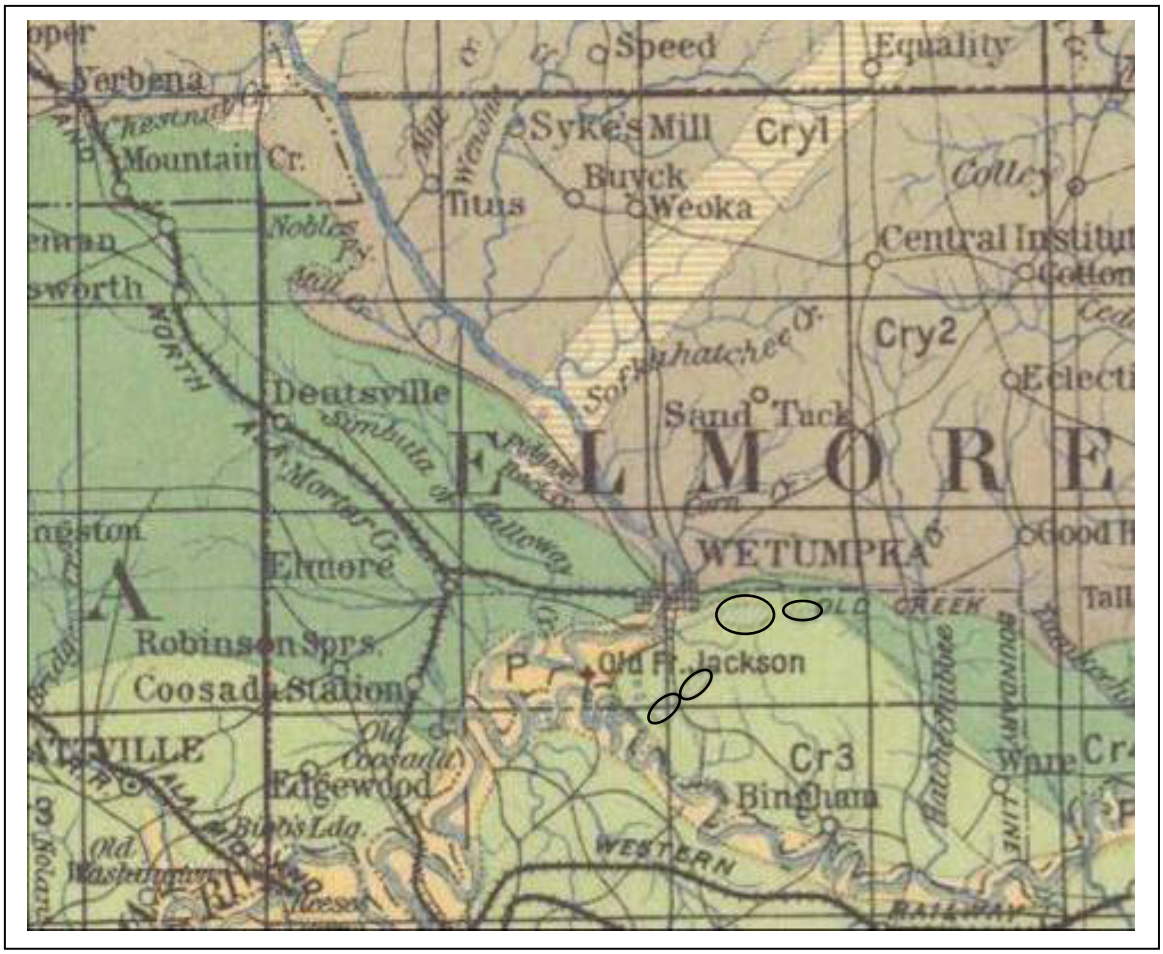

Figure 25. Portion of geologic map of Alabama from Smith et al. (1894) depicting oval-shaped outliers of Mooreville Chalk (green and white crosshatch pattern within the four small black ovals added by the present author) surrounded by Eutaw strata (pale green). A later map by Smith (1904) would omit these features.

efforts conducted by Smith et al. (1894), Stose (1926), and Monroe (1941), all of whom made note of the disrupted geology (Figure 26 and Figure 27). At the same time, and elsewhere in the world, unusual regions having disrupted geology similar to that at Wetumpka had been discovered and were being mapped. Beginning in 1905, some of these disturbed regions were labeled as "cryptovolcanic" despite their total absence of igneous rock (Melosh, 1989). As with those other poorly understood regions, Smith et al. (1894), Stose (1926), and Monroe (1941), were not specifically studying Wetumpka's odd features, they just happened to be mapping the area for other purposes. Nonetheless, it is noteworthy for this early work at Wetumpka that no geologist invoked volcanism of any sort to explain the broken features there as had been done at the other disturbed regions now known to be of impact origin (Melosh, 1989). Instead, they all interpreted the unusual geology as a depression or fault system, probably because they never observed any breccia.

Prior to the late 1960s, geologists took little notice of the anomalous horseshoe-shaped structure occupying the Coastal Plain–Piedmont boundary, but in 1969, the interest level would begin to change. Like those who came decades earlier to map the region for purposes unrelated to the unrecognized structure itself, a team composed of Thornton ("Tony") L. Neathery (team leader), Robert D. Bentley, and Gregory C. Lines was working on part of a new geologic map of Alabama for the Geological Survey of Alabama (Szabo et al., 1988). After mapping the Wetumpka region, these three geologists came forward with a rather bold idea for that time. An abstract by Bentley et al. (1970) submitted to the American Geophysical Union proposed the structure be named the "Wetumpka Astrobleme" based on five lines of evidence typically associated

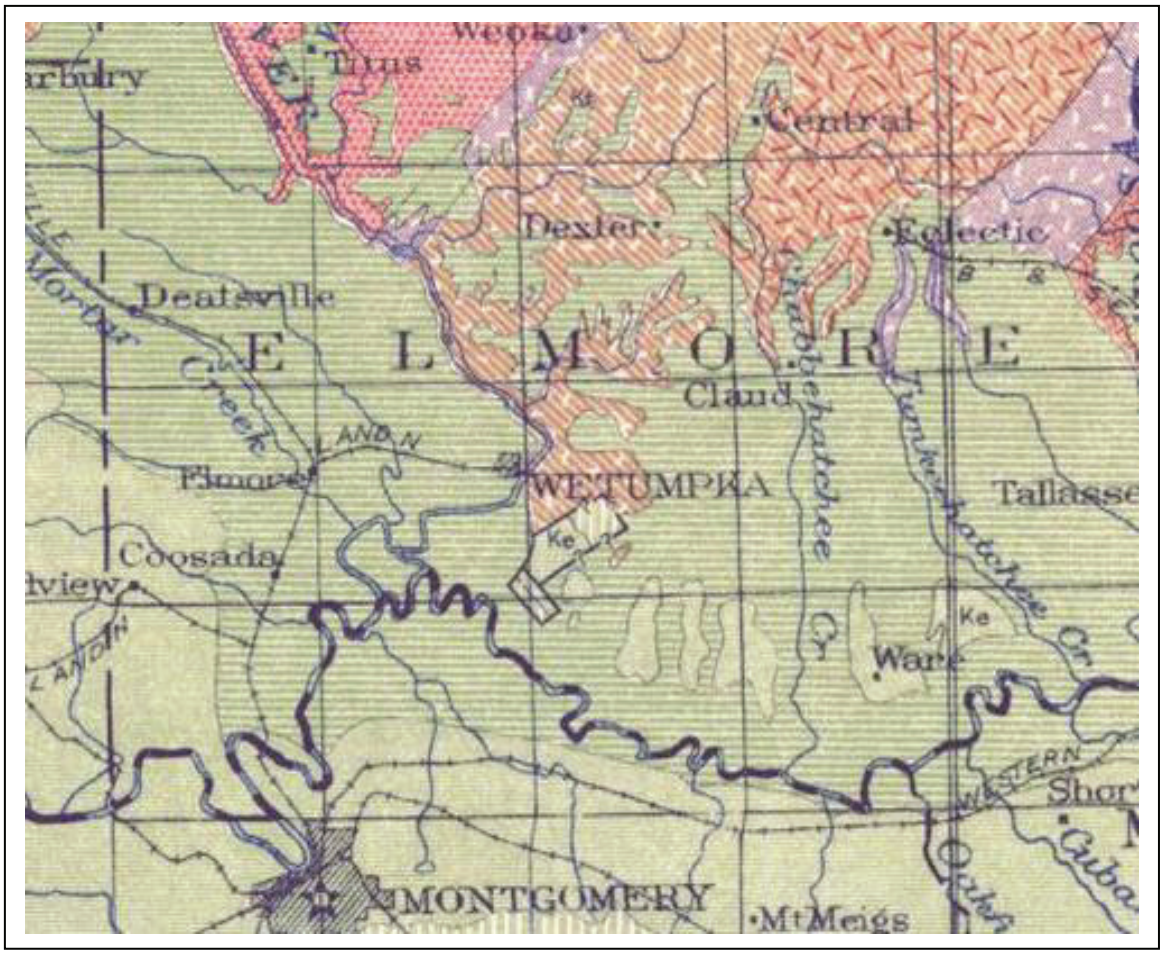

Figure 26. Portion of geologic map of Alabama from Stose (1926) wherein the Wetumpka structure was interpreted as a fault system with Eutaw (Ke) and Mooreville strata (vertical green and white stripes) exposed at the surface.

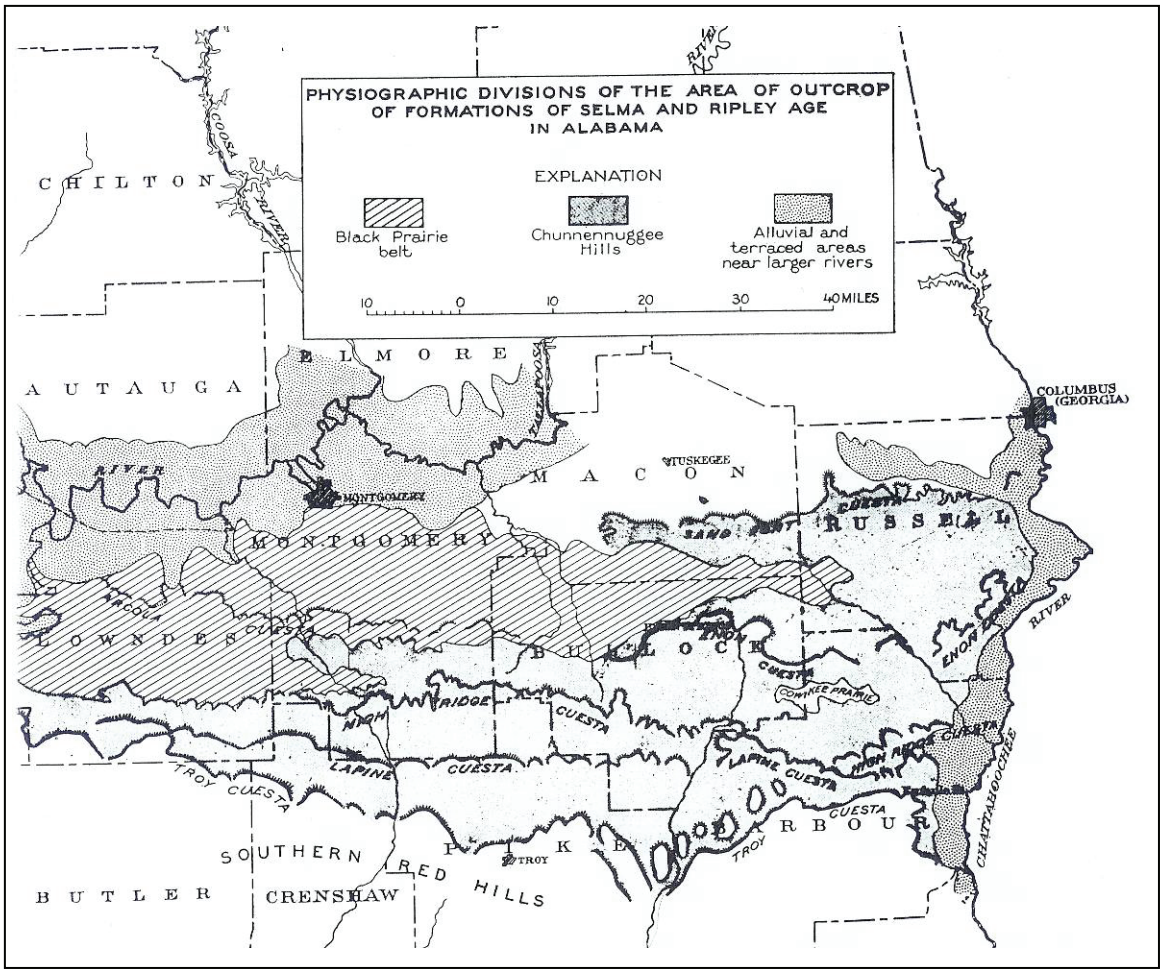

Figure 27. Portion of geologic map from Monroe (1941). Monroe reinterpreted the improbable fault system illustrated in Stose (1926) as a system of only two faults. Nonetheless, Monroe (1941) did not illustrate his new fault system with a figure anywhere in his text. Nor did he include the new faults on his final map (pictured), choosing instead to omit each interpretation from all figures in his work.

with known impact structures. However, their interpretation lacked conclusive evidence – namely, planar deformation features (PDFs) found within shock-metamorphosed quartz (Figure 28) taken from confirmed impact structures (French, 1998). In similar fashion, Bentley et al. (1971) tendered a comparable abstract to the *Journal of the Alabama Academy of Science*.

In March of 1973, these same three authors submitted a complete paper to the *Geological Society of America Bulletin* for peer review and publication. This work (Neathery et al., 1976b) more thoroughly described several features at Wetumpka for which the authors again proposed an impact event as the origin, and again proposed the name Wetumpka Astrobleme, but the work was not accepted for publication until April 1976 owing to controversy stemming from the persistent lack of conclusive evidence indicating such. As before, no shock-metamorphosed quartz had yet been found at Wetumpka. Moreover, the executive editor's pointed bias against the work also played a role in the three-year delay as indicated by his comment, "I don't believe a word of it, and I don't think it's worthy of publication" (McGowin, 1996). The paper was finally published with the compromise that its title would not indicate an extraterrestrial origin for Wetumpka, nor a volcanic origin, but would instead be *Cryptoexplosive structure near Wetumpka, Alabama* (T. Neathery, pers. comm., 2005). Clearly this was not the first choice of the paper's authors after thoroughly documenting the circumstantial evidence of impact (Neathery et al., 1976b). Nonetheless, impact science was still young and controversial (Melosh, 1989), and Wetumpka simply was not proven.

Two months later, the journal *Geology* published a new paper by Neathery et al. (1976a) wherein the authors gave an interpretation of aeromagnetic and aeroradioactivity

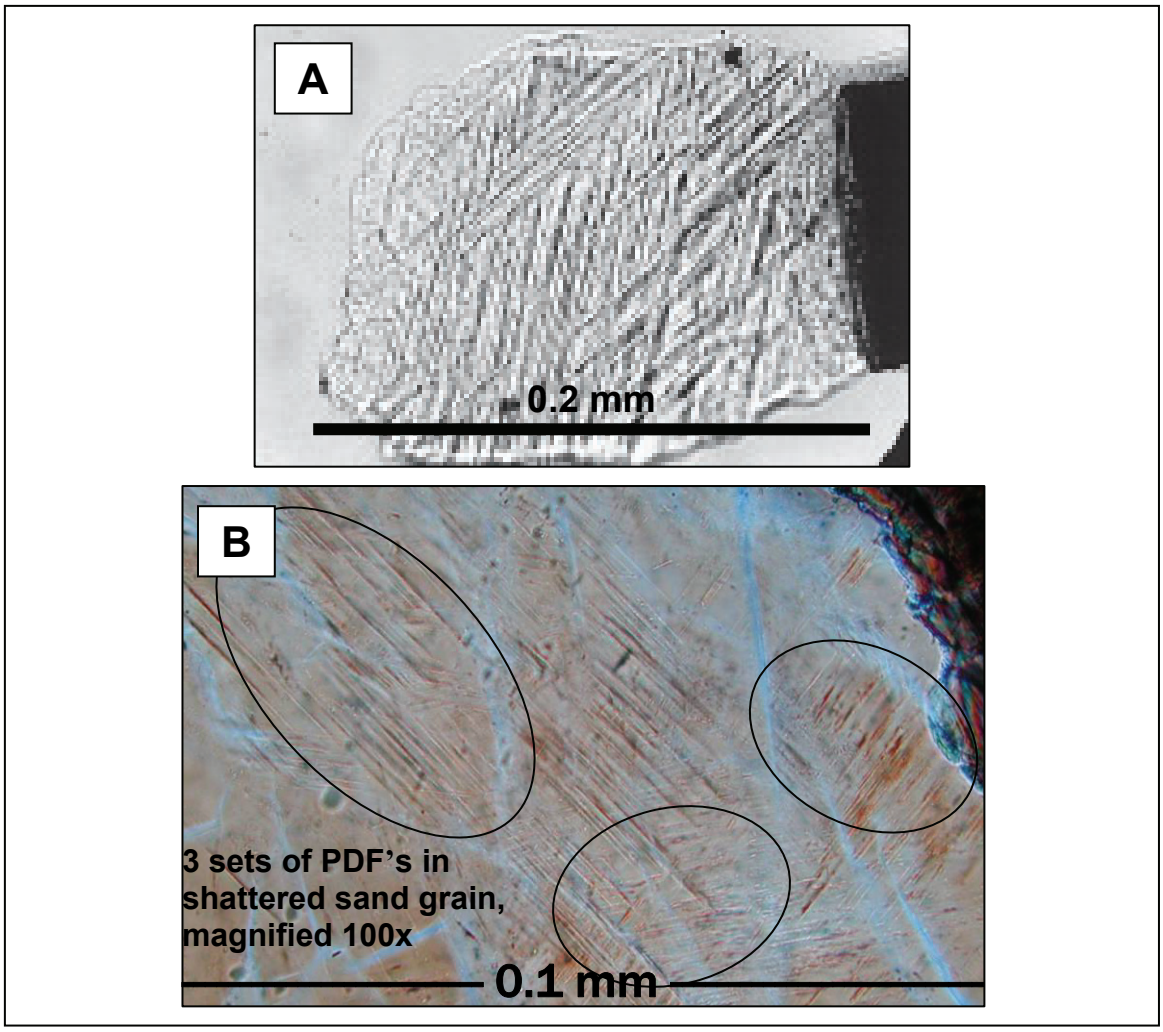

Figure 28. Multiple planar deformation features (PDFs) in a shock-metamorphosed quartz grains. A: Quartz grain from Chicxulub ejecta with amorphous lamellae indicative of shock pressures found only in cosmic impact events and atomic tests is shown in plane-polarized light. When found in association with a structure suspected of having an impact origin, such data are understood to be "proof" of impact provided the PDFs are oriented along a certain crystallographic axis (French, 1998). B: PDFs in shattered quartz grain from Wetumpka (photo courtesy of D. King, 2005).

maps of the Alabama Piedmont and described an aeromagnetic low coincident with what they labeled the "Wetumpka impact structure" (Figure 29). Nonetheless, few scientists of the day would have accepted this interpretation and characterization as having anything to do with each other (inferred from Melosh, 1989). Curiously, for nearly the next twenty years, little work was done on the still unproven Wetumpka structure.

During this lull, a new geologic map of Alabama was published (Szabo et al., 1988), which used the map and data from Neathery et al. (1976b) in depicting its representation of the surficial geology in the Wetumpka region. Even so, Szabo et al. (1988) offered no special representation of the widespread mélange documented by Neathery et al. (1976b) within the Wetumpka structure even though the mélange would have been easy to show and readily discernable at the map's scale. As with the map, authors of the map's associated stratigraphic descriptions made no mention of any mélange, and the mélange was not recognized as an official stratigraphic unit in spite of its size and distinct nature (Raymond et al., 1988).

By 1993, acceptance of impact events in Earth's past had grown significantly. At the time, Alvarez et al. (1993) were trying to explain an apparent "double" Cretaceous-Tertiary impact-related boundary in the sediments of the Western Interior Seaway. While looking for the source of this unusual boundary, Alvarez et al. (1993) considered Wetumpka's possible impact origin, its apparent Late Cretaceous age, the age of its basement rock, and the ostensible low trajectory of its projectile as hypothesized by Neathery et al. (1976b). With that in mind, these authors speculated the Wetumpka structure could explain the apparent double boundary if Wetumpka was a "ricochet" impact spawned from the Chicxulub impact event. However, the question of whether

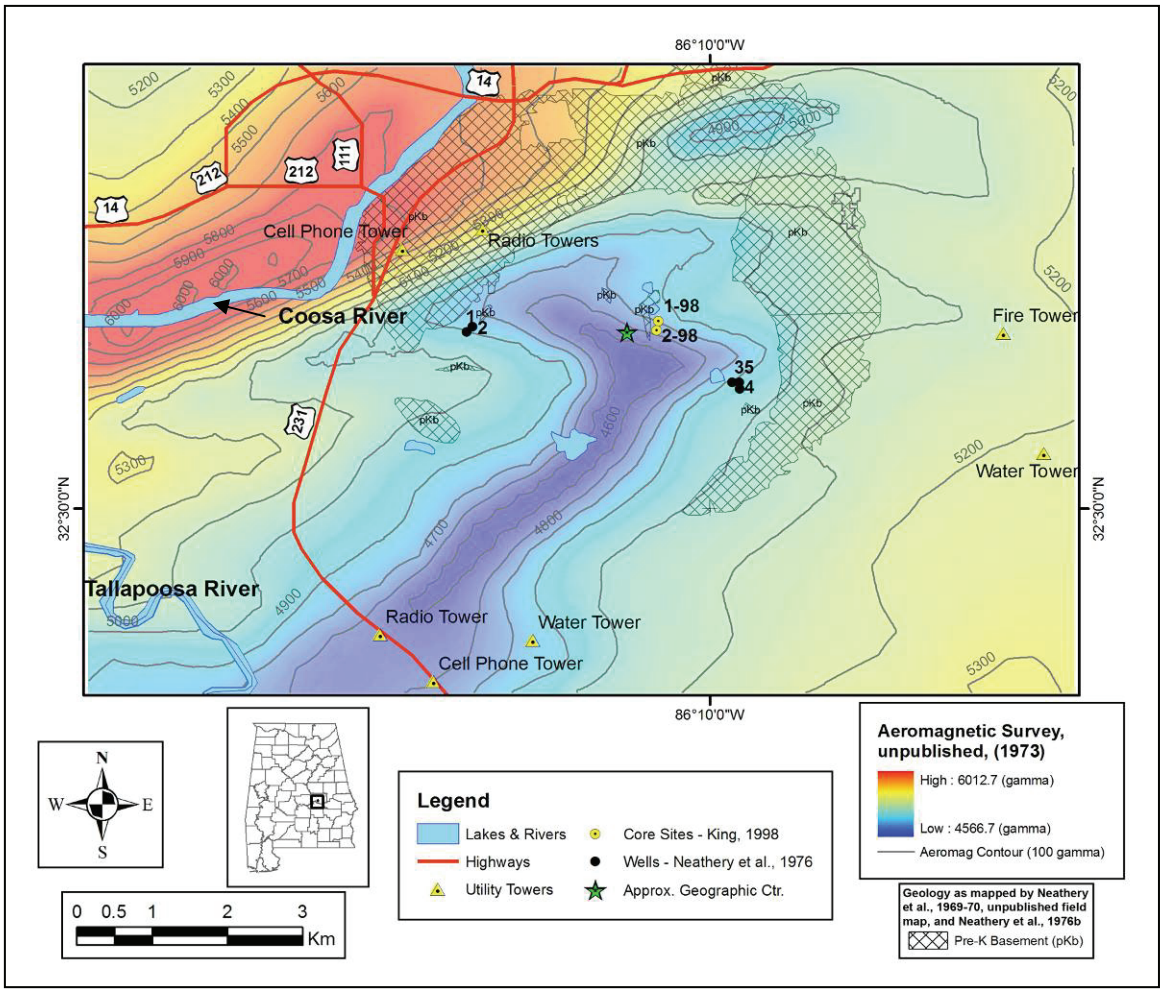

Figure 29. Digitized portion of a larger unpublished aeromagnetic survey map from 1973 that was later interpreted in Neathery et al. (1976a). The map as shown at this scale was derived from Neathery et al. (1997), and has been colorized and corrected for distortions in ArcMap by the author of this report. Additional details have been added as reference points to aid understanding. Note the remarkable correlation of the aeromagnetic low not only in its position relative to the crystalline rim (overturned flap?), but in its correlative shape too. Moreover, the deepest part of the aeromagnetic low is roughly coincident at its northeastern end with the structure's approximate geographic center, and its southwestern end is on-axis with what was probably the down-range trajectory of the projectile (King and Neathery, 1998).

Wetumpka was impact related remained unresolved because the earlier work done there was thus far inconclusive. To better understand Wetumpka, Walter Alvarez and Philippe Claeys visited the region in 1995 seeking evidence that it might be related to Chicxulub, but their work was largely inconclusive. Specifically, they failed to find shock-metamorphosed quartz and were unable to determine the structure's age with any more certainty than Neathery et al. (1976b). A short time later, the apparent double Cretaceous-Tertiary boundary was reinterpreted without invoking the suspicious structure at Wetumpka – or any confirmed impact structure – as a related feature (Alvarez et al., 1995).

Shortly thereafter, in a review of known and possible impact structures within the United States, Koeberl and Anderson (1996) listed Wetumpka as a "possible impact structure" considering its physical features, but they also noted there was still no positive evidence of shock metamorphism from the region (PDFs), and no chemical or physical meteorite signatures were yet identified there. The following year, Wolf et al. (1997) interpreted a 1994 gravity survey transecting the structure as showing features similar to those of known impact structures (Figure 30), but this too was not in itself conclusive evidence of an impact origin, nor was it conclusive when considered with all other evidence previously gathered. The paper by Wolf et al. (1997) was part of a larger field guide edited by Neathery et al. (1997) that detailed what was then understood about Wetumpka. The guidebook and associated fieldtrips showed a growing interest in the subject of impact structures.

With the arrival of 1998, over twenty years had passed since the work of Neathery et al. (1976b) had been published, and roughly ten years had gone by since Szabo et al.

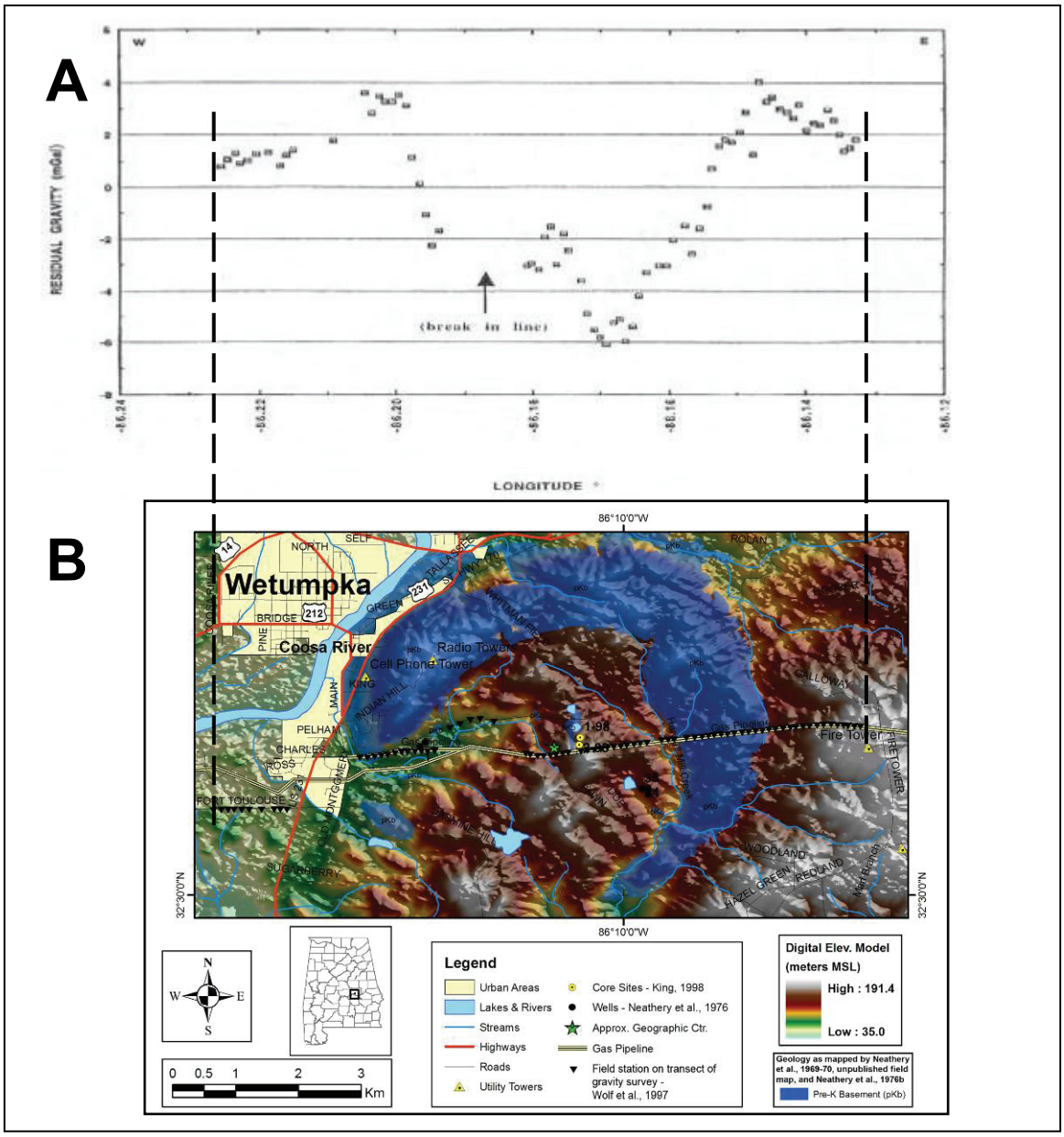

Figure 30. Residual gravity profile and index map. A: Original residual gravity profile as it appeared in Wolf et al. (1997) before an impact origin was confirmed. The break in line (arrow) is a portion where unusual data points were purposely omitted, probably to avoid confusing the readers. B: The old gravity profile is matched to the same horizontal scale used in the new index map created by this author in ArcMap. Field station locations were plotted using original GPS data from the 1994 survey.

(1988) produced their new geologic map of Alabama. Academic interest in the Wetumpka structure had been gaining momentum, and it was at this time that King (1998) proposed that the previously documented mélange be classified as an actual stratigraphic unit in Alabama. King and Neathery (1998) also presented the idea that if Wetumpka were an astrobleme, the projectile should have had a northeast-to-southwest trajectory, opposite of that originally speculated on in Neathery et al. (1976b). That same year, research at Wetumpka took a new direction.

Given the inconclusive geological and geophysical evidence of Wetumpka's origins, research efforts began to center on finding proof of shock metamorphism in quartz grains. In the summer of 1998, King et al. (1999b) took the first scientific drill cores from Wetumpka at two locations near the structure's geographic center. These drill cores were named after the property owners on whose land they were drilled, and are still referred to as the Schroeder drill core (1-98) and the Reeves drill core (2-98). Interestingly, it was on the 107th anniversary of Eugene A. Smith's discovery of "disturbed geology" at Wetumpka that this drilling operation produced the first impact breccia recovered from depth (D. King, pers. comm., 2004). Subsequent analysis of drill core 1-98 by King et al. (1999b) finally revealed PDFs in shocked-metamorphosed quartz, which was extracted from the matrix of the impact-breccia that partially fills the structure. Shortly thereafter, an elevated concentration of iridium (10x background, ~200 ppt) was identified by Dr. Christian Koeberl in samples from drill core 1-98 and interpreted as a further confirmation of Wetumpka's impact origin (King et al., 2000). Of significance to this report, King et al. (1999b; 2000) produced only general descriptions

of the two drill cores before they were stored, because a more detailed analysis was planed. This report will produce that planned detailed analysis of each drill core.

In the subsequent months and years, research at the now proven Wetumpka impact structure intensified. Nelson (2000) produced a new map of the structure, and importantly, described many small- and large-scale structural details inherent to the crystalline rim (overturned flap?), the surficial crater fill, and the region surrounding the structure. Additional data further confirming an impact origin were found in the form of multiple sets of intersecting PDFs within quartz grains, PDF angular measurements, and elevated concentrations of iridium, cobalt, nickel, and chromium (King et al., 2002). The concentrations of these and other elements identified in drill core samples indicated the Wetumpka projectile was probably a chondritic asteroid like those common to the distal regions of our solar system's Main Asteroid Belt (de Pater and Lissauer, 2001; King et al., 2002). The work by King et al. (2002) also confirmed a shallow marine target for the Wetumpka impact event based on ichnosedimentologic evidence and ostracode eye morphology from fossils in the Mooreville outliers at Wetumpka.

With an impact origin now considered all but irrefutable, work began to focus on further elucidating the nature of the crater-filling material within Wetumpka. Study of the two drill cores had already revealed at least five facies types (King et al., 1999a) comprising two distinct units indicative of a violent two-stage crater-filling process (King et al., 2002). An idea advanced by King et al. (2002), and again by King et al. (2005) proposed catastrophic rim collapse as a strong influence on the crater-filling stratigraphy and the structurally disturbed crater-flanking terrain. This report will draw from and build on these ideas.

Recently, investigations into the paleobiologic effects of terrestrial cratering have begun (Cockell and Lee, 2002), and Wetumpka is one impact structure among many being studied under this paradigm (King et al., 2006). Such work describes the patterns commonly found in post-impact biological changes resulting from crater formation as well as the chronological sequences of post-impact ecology, and it provides insight into paleoenvironments within and around impact structures that are spatially and temporally unique, and otherwise would not have existed. For example, within the Schroeder drill core (1-98), a mudstone layer ~1.65 m thick at 100 m drill depth appears to separate the two main crater-filling units. King et al. (2006) speculated that the apparent mudstone deposit might be an intra-crater paleosol or lacustrine unit. This report will explore that possibility.

Currently, two- and three-dimensional maps and animated flyovers of Wetumpka's topography, land use, soil type, geology, vegetative cover, etc. are being produced by this author. Many of these maps appear in print for the first time within this report and have already markedly improved our understanding of the Wetumpka impact event and the resultant structure. Further insight will come from coupling these maps to drill core examined in this report.

OBJECTIVES

The overarching objective of this report was to document the scientific investigation of two whole-round (not split) NX drill cores pulled in 1998 from near the geographic center of the Wetumpka impact structure as first reported by King et al. (1999a). This investigation had a three-tiered series of goals. The first tier of goals (*preparatory objectives*) was classified as non-interpretive preparatory work. The second tier (*main objective*) was both investigative and non-interpretive to the extent allowed by practicality. The third tier (*ancillary objectives*) was also investigative, but added the element of interpretation.

Preparatory Objectives

The *preparatory objectives* of this investigation focused exclusively on the two drill cores in their entirety. The objectives were to 1) clean the drill core thoroughly; 2) check the stratigraphic order of core pieces and reassemble as necessary; and 3) photograph each drill core in its entirety using a high-resolution digital format. Although these initial goals were purely non-interpretive and only preparatory in nature, they were exceedingly important because without clean, well-prepared samples, any observations (and hence, interpretations) stemming from the ensuing objectives may have been unnecessarily flawed.

Main Objective

The *main objective* of this study was to produce detailed geologic descriptions of each drill core using a digital log format. This effort was purely a data-collecting venture, and was to be non-interpretive so that the collected information may be most helpful to subsequent investigations and follow-on interpretations. In other words, the impartial descriptions born from achieving this *main objective* were at the hub of this investigation and report.

Ancillary Objectives

As indicated, the third tier of goals (*ancillary objectives*) was both investigative and interpretive. Here, the objectives centered on elucidating the nature and origin of the various crater-filling materials found within the drill core in terms of their possible modes of emplacement, their temporal relationships, and the post-impact paleoenvironments that particular sections of drill core may represent. Six goals were pursued in the third tier.

1. Clarify Structures and/or Patterns found in the Drill Cores

By its very nature, drill core is cylindrical. As such, its surface wraps around so that any structural features cut through during drilling are visible on what is an outside-curving face. That is, the two-dimensional surface of the drill core is effectively warped into the third dimension. Consequently, typical structural features that any geologist would immediately recognize in a flat face (folds, faults, kinks, etc.) are instead

commonly visible on the outside-curving surface of the drill core as peculiar loops, whorls, bull's-eyes, hyperbolae, chevrons, and more.

Certain portions of drill core show noteworthy patterns of different colored materials such as the concentric bull's-eye pattern wrapping around each core leg in Figure 31. Hypotheses to have been explored by this study included the ideas that these structures could be 1) large, roughly spherical accretionary lapilli or jacketed boulders not unlike those in Chicxulub ejecta at Albion Island, Belize (Pope et al., 1999); 2) simple folds in distorted target materials; 3) vertically oriented blocks of target strata; or 4) fluidized sands that have been swirled.

Intended Analysis. A schematic catalogue was to be created to show how different geologic structures such as faults, folds, layered spheres, and various bedding orientations would manifest in cylindrical drill core extracted from these structures. The catalogue's results were to assist in making interpretations of drill-core facies.

2. Determine the Position of the Drill Cores relative to the Central Peak

Meter-scale blocks of crystalline basement rock have been found near Wetumpka's geographic center (see Figure 24). Speculation about the origin of these blocks includes the possibilities that they are: 1) remnants of the southwest crystalline rim (overturned flap?) that collapsed into the fresh crater (King et al., 2005); 2) fragments of the central peak that broke off and dropped into the fresh crater during the peak's dynamic collapse (D. King, pers. comm., 2006); or 3) reworked fallback breccia, which became chaotically mixed with the surrounding surgeback material during its deposition atop the fallback breccia (Neathery et al., 1976b). Additionally, there is some question as

Figure 31. Two examples of bull's-eye patterns in drill core from the Wetumpka impact structure. The patterns wrap around much of each core leg. Both photos are of core legs taken from 1-98 (the Schroeder drill hole) at depths of 121.5 m (left) and 181.2 m (right).

to whether the two drill cores taken by King et al. (1999a) penetrated into the impact structure's crystalline central peak indicated on the Wolf et al. (1997) gravity profile (Figure 30), or whether they penetrated only brecciated material above and surrounding the central peak.

Intended Analysis. Map and drill-core data from this study (Figure 32), along with map data from earlier work, and residual gravity data from Wolf et al. (1997) was to be examined together in the context of marine-target impact structures.

3. Elucidate the Ostensible Intra-crater Paleosol

The temporal relationship between the two main crater-filling units (Figure 11) was of interest because the inferred paleosol and/or lacustrine deposit separating these two units (Figure 12) may have held important clues as to the magnitude of elapsed time between deposition of the underlying and overlying strata. King et al. (2006) have identified six criteria consistent with paleosol development in this portion of the drill core but further analysis was desirable because there was some doubt that a paleosol and/or lacustrine deposit could have had time to form before overlying material was deposited. The present study would explore the hypotheses that this unit is either 1) a genuine paleosol that formed atop the reworked fallback breccia over a significant period during the impact structure's post-impact modification stage; or 2) a horizontal block of an Upper Cretaceous target unit bearing a pre-impact paleosol.

Intended Analysis. This study outsourced samples of the apparent paleosol/lacustrine material to look for micropaleontological (especially palynological) evidence of soil development over time. Of particular interest was any material either

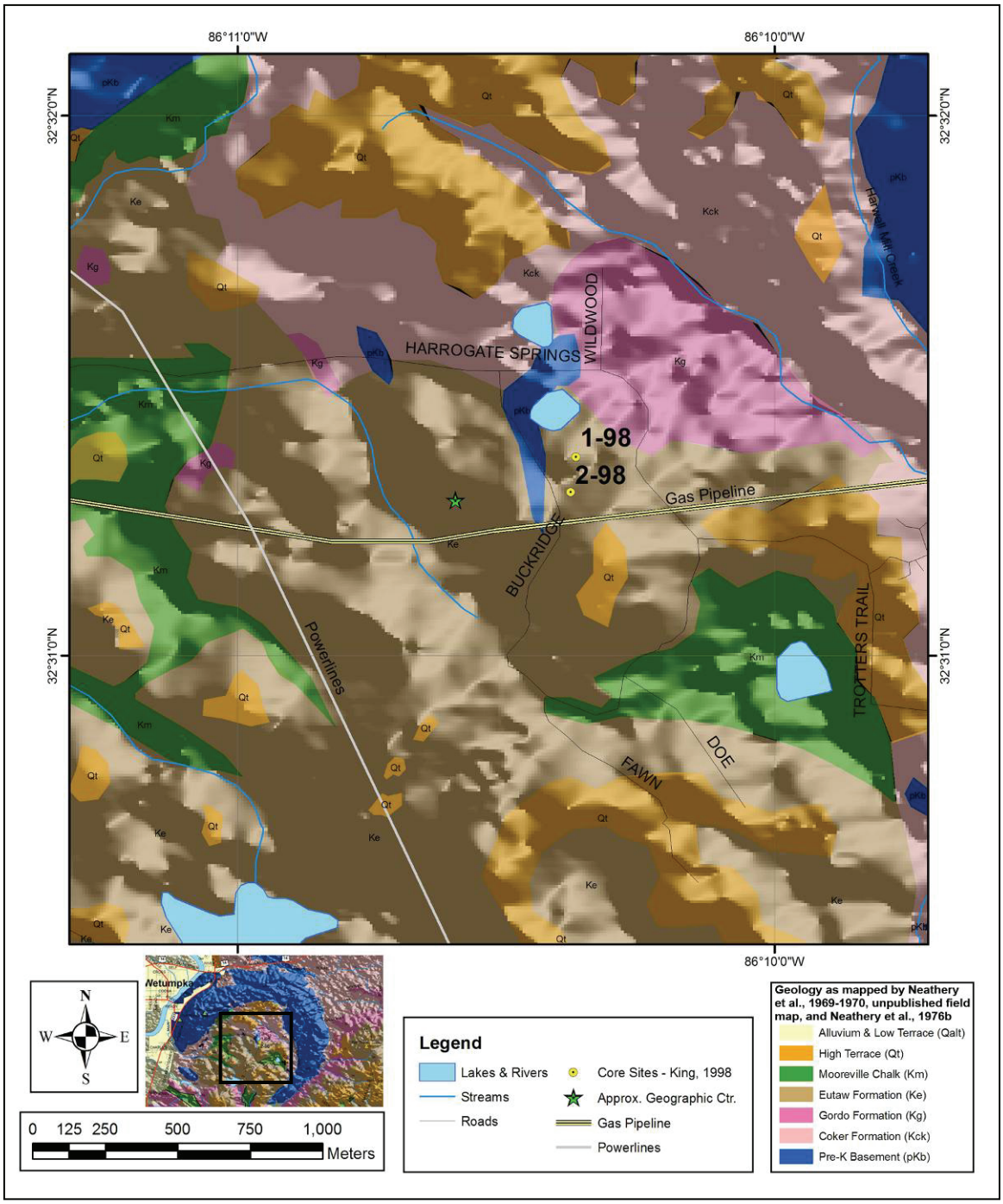

Figure 32. Detail map of drill hole locations. The small hill capped with Qt sediments immediately south-southeast of drill hole 2-98 is the highest point within Wetumpka's central region. The gas pipeline is the right-of-way along which the 1994 gravity survey was made. The impact structure's approximate geographic center (indicated by a small star) is in a diminutive valley on the flanks of an unnamed stream. Map created using ArcGIS® and data from Neathery et al. (unpublished field maps, 1969-1970; 1976b).

predating or post-dating the impact event. For example, the presence of large quantities of palynomorphs significantly post-dating the impact event would have indicated the mudstone layer is indeed a post-impact paleosol. To the contrary, a similar presence of palynomorphs pre-dating impact event would have indicated the mudstone is simply a block of Upper Cretaceous target material.

4. Determine the Age of Shock Metamorphism

The age of the Wetumpka impact structure is currently thought to be between 80 and 83.5 m.y. based on guide fossils and the absence of the Arcola Limestone Member of the Mooreville Chalk (King, 1997; King et al., 2006). However, a radiometric age is preferable to an age based on stratigraphic relations and/or guide fossils.

Intended Analysis. This study conducted $^{40}Ar/^{39}Ar$ dating of altered and unaltered muscovite crystals from the drill core to investigate the age indicated by evidence of shock metamorphism. Feldspars were not examined. Analysis was done using the Auburn Noble Isotope Mass Analysis Laboratory (ANIMAL).

5. Compare Drill Core 1-98 to Drill Core 2-98

Given the proximity of the two drill sites (Figure 32), the two drill cores presented a rare opportunity for comparison. Because the drill sites were so close together, the drill cores were collectively assessed for site-scale similarities and differences with the aim of identifying and possibly correlating distinct attributes of the crater-filling material typically not discernable between drill holes bored kilometers apart. Further, the characteristics of their intra-crater depositional processes were also assessed within the

context of formation and modification of marine-target impact structures. Identifiable characteristics were expected to include consequences of central peak-collapse dynamics, different modes of emplacement in the post-impact fallback breccia, imbricated megablocks within the marine surgeback unit, and further evidence in support of (or against) the postulated 1-m thick paleosol between these two units as interpreted by King et al. (2006).

Intended Analysis. After the bulk of all descriptions and ancillary objectives were complete, both full-length geological descriptions of the two drill cores were depth-matched and examined side-by-side for any similarities and differences.

6. Compare Wetumpka to Chesapeake Bay Impact Structure

To assist with the initial interpretation of geological data collected from the two Wetumpka drill cores, other marine-target impact structures such as Kärdla, Lockne, and Chesapeake Bay were used to provide a framework for the Wetumpka drill core data. Much of this framework has already been outlined in earlier sections of this report.

Intended Analysis. Poag et al. (2004) provide an excellent summary of the formational processes related to marine-target impact structures. They also provide a concise model of depositional regimes for the same. This summary and model were used to help gauge the nature of drill core facies from Wetumpka, formulate interpretations about the crater-filling material there, and draw appropriate conclusions about the overall sequence of events that played out during the Wetumpka impact event.

METHODOLOGY

The Methodology section describes the procedures developed and/or employed by the present author to achieve all the objectives of this study.

Methods of Achieving Preparatory Objectives

Before this study's *main objective* and six *ancillary objectives* could be addressed, the following three preparatory objectives had to be satisfied: 1) clean each drill core thoroughly; 2) reassemble each drill core in correct stratigraphic order; and 3) digitally photograph the entirety of each drill core in high resolution.

1. Cleaning the Drill Cores by Abrasive (Sand) Blasting

After extraction from the two drill holes, much of the drill core was not water-washed to remove the coat of drill mud covering it. A benefit of this was that the poorly consolidated drill core remained largely unaltered by the erosive effects of washing. However, because extensive portions of the drill core were boxed while still covered with ~2 mm of drilling mud that later dried to a hard crust (Figure 33), detailed study of the drill core in these intervals was rendered nearly impossible. Complicating the matter, the dried drill core was too weakly lithified to be cleaned using liquid solvents, and too clay-

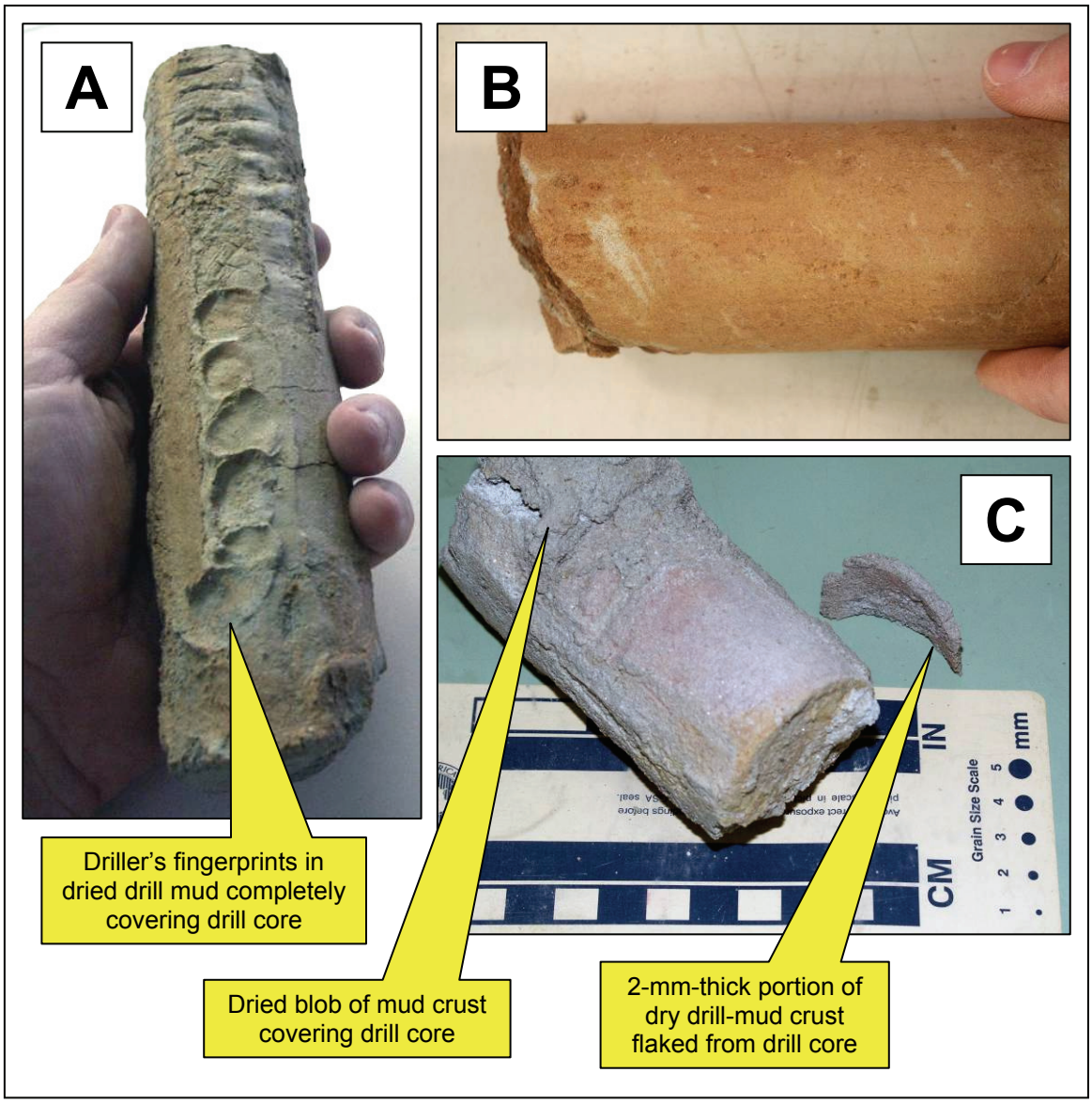

Figure 33. Examples of drill core pieces covered with dried drill mud that had to be cleaned off prior to photographing and describing each drill core. A: Drill mud on this core piece is so thick that it preserves the fingerprints of someone who handled it while still fresh from the drill hole. B: Smooth drill mud almost completely obscures the details of this core piece. C: Drill mud could be found covering core pieces in thick blobs as well as thin crusts.

rich for brushing or scraping, as this only polished the drill core and obliterated structural details.

A successful means of removing the undesired mud crust has been achieved through a process of abrasive (sand) blasting with commercially-produced 20/30 sieve-size silica sand blown through a common sand blaster (Figure 34). This method of drill-mud removal is a relatively quick, easy, inexpensive, one- or two-person job utilizing readily available equipment (Johnson et al., 2006). Nonetheless, this method posed one serious health hazard, and two minor health hazards, all of which had to be addressed in order to do this work. First, freshly broken, aerosolized silica dust is considered a carcinogen and represents a Class-3 (severe) health hazard (Mallincrodt Baker Inc., 2003). Because few people are aware of this danger, it was essential to post adequate warning signage on the blasting cabinet, vacuum apparatus, and sand storage containers (Figure 35). Also essential was that all blasting operations take place in a "fully enclosed" abrasive blasting cabinet under a partial vacuum. The term "fully enclosed" means enclosed with an exception – a factory-installed ambient-air intake port on the back of the cabinet, which allows for the proper flow of air between periods of actual blasting, is present. Additionally, operator respiratory protection is required. Typically, a full-face air-supplied respirator is necessary, especially where there is any question about whether the blasting cabinet is "fully enclosed" (U.S. Silica, 1997; Mallincrodt Baker Inc., 2003). In the instance of blasting work done for this report, a respirator equipped with two P-100 *High Efficiency Particulate Air filters* (HEPA filters) was sufficient and was worn by the equipment operator(s) during all active blasting work and while handling the bulk sand. Use of this filter type is acceptable *only* when blasting

Figure 34. Typical abrasive blasting apparatus modified by the present author to clean dried drill mud from friable drill core.

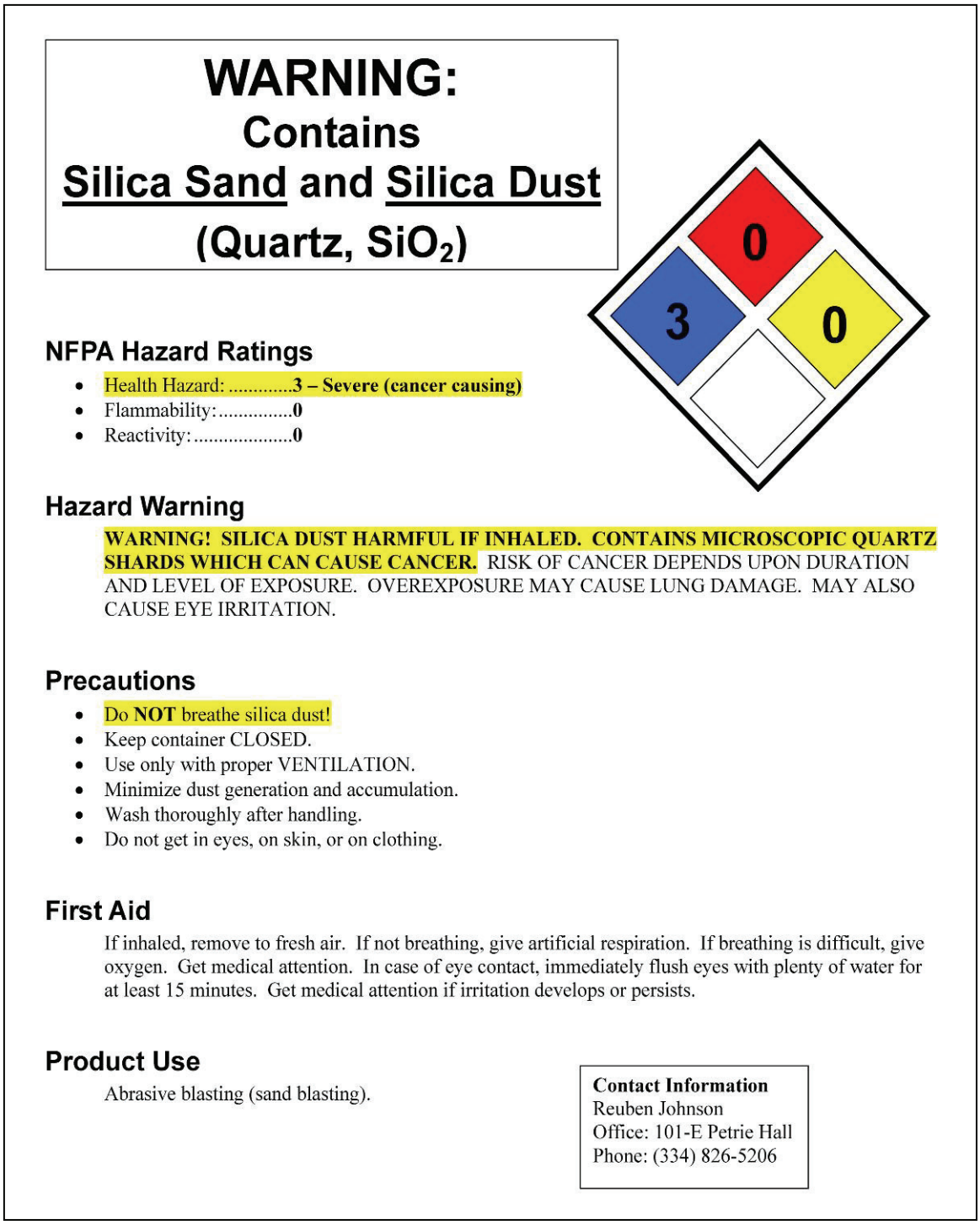

Figure 35. Warning sign posted on blasting cabinet, vacuum, and sand storage containers advising of health hazards stemming from exposure to crystalline silica. NFPA stands for the *National Fire Protection Association*. The blue, red, and yellow diamond symbol indicates the listed hazard ratings in a quickly recognizable, standard iconic format. Information derived from Mallincrodt Baker Inc. (2003) and U.S. Silica (1997).

takes place within a "fully enclosed" blasting cabinet under partial vacuum so the concentration of aerosolized silica dust outside the cabinet falls below 10x the mandated personal exposure limits according to Material Safety Data Sheets (MSDS) provided by U.S. Silica (1997) and Mallincrodt Baker Inc. (2003). As an alternative to using crystalline silica, other types of blasting media are safer and are readily available in various shapes, sizes, and hardnesses, including walnut-shell fragments; pellets of plastic, foam or gel; and beads of glass or metal. Second, because crystalline silica is a particulate, the equipment operator(s) must wear eye protection, especially while actively blasting. Finally, the necessary compressed-air source usually requires that the equipment operator(s) also wear proper ear protection.

Functions of the abrasive blasting apparatus itself are depicted in Figure 36 as a cut-away view. A diaphragm-type compressed-air source delivering 5.5 peak horsepower and capable of sustaining 5.1 standard cubic feet per minute (SCFM or 2.4 *l/s*) at a working pressure of 90 psi (620.5 kPa) supplies air to the blasting apparatus through a typical air hose equipped with standard ¼-inch (6.35-mm) NPT fittings. A pressure gauge and regulator mounted atop the blasting cabinet allow for convenient and frequent adjustment of the supplied air pressure, which is usually set between 40 to 90 psi (275.8 to 620.5 kPa).

Within the "fully enclosed" blasting cabinet are a work light and trigger-operated sand blasting gun with its air supply and sand feed hoses. These items rest on a heavy screen that functions as a work surface and separates the tools, drill core, and debris from the blasting media (20/30 sieve-size crystalline silica sand) stored in the hopper/reservoir below. The screen lets sand grains fall through back to the hopper/reservoir after they are

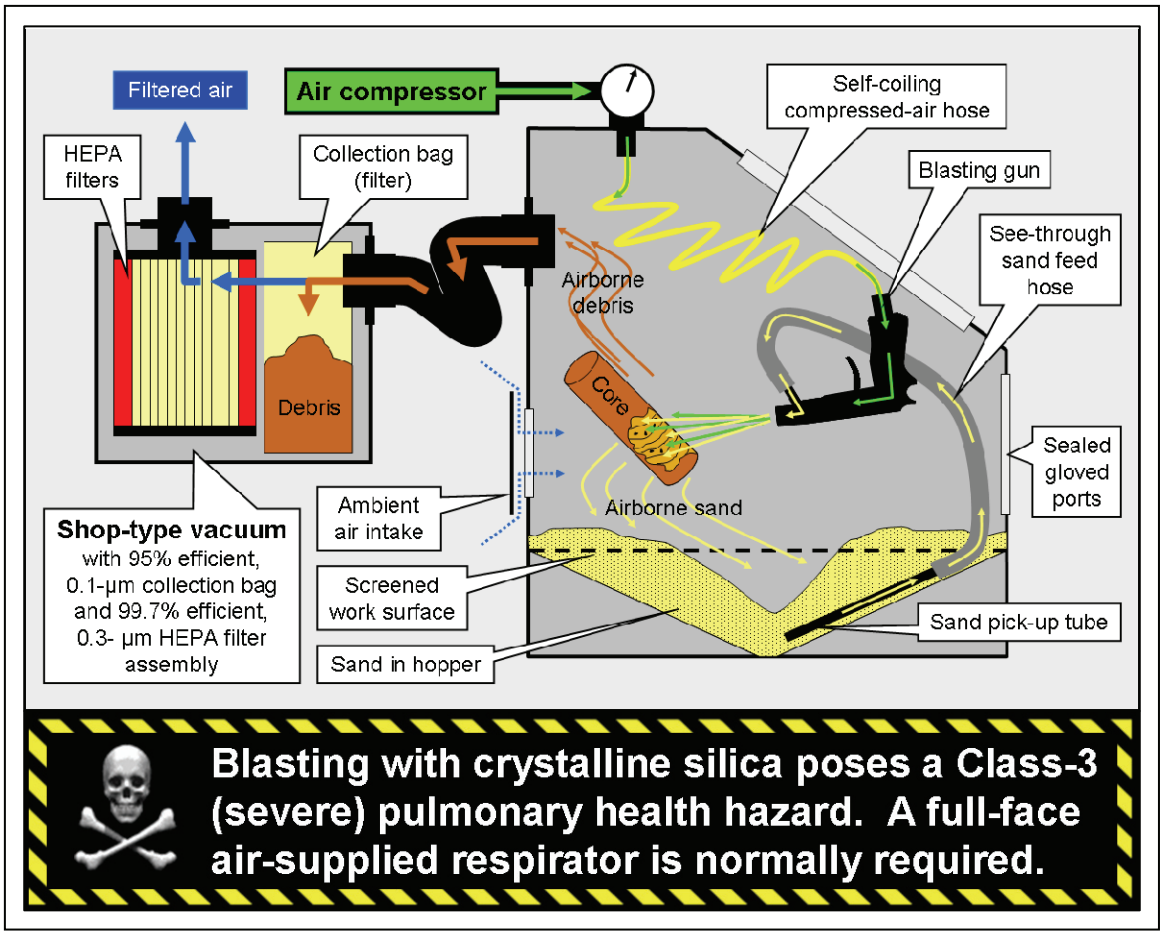

Figure 36. Cutaway schematic diagram of abrasive blasting apparatus.

sprayed from the gun, but prevents any core fragments >3 mm from entering the hopper/reservoir from where they may later enter and plug the blasting gun. It is convenient to have a piece of 50-grit sandpaper in the cabinet to aid with mud removal.

Outside of the cabinet, a 12-gallon (45.4-liter) shop-type vacuum connected to the cabinet's upper back exterior draws dust and aerosolized silica from the cabinet through the vacuum's 2.5-inch (6.35-cm) diameter suction hose into a 95% efficient 0.1-micron collection bag inside the vacuum. This bag collects virtually all the dust, stray sand grains, and any other material drawn from the cabinet during blasting, making for easy disposal of this waste. Air leaving the collection bag then passes through a 99.7% efficient, 0.3-micron HEPA filter also within the vacuum. These two special filters must be purchased separately from the vacuum as manufacturer-approved add-on accessories. The air then passes through a third filter (this one is non-HEPA) before being exhausted through a 2.5-inch (6.35-cm) diameter hose connected to a fume hood as an added precaution. The fume hood draws air at a rate in excess to that expelled by the vacuum.

Disposal of blasting waste and packaging is uncomplicated, but given the health concerns, it must not simply be dumped into an open indoor waste container. Rather, the materials should be carefully bagged and tightly sealed to minimize dust generation. Everything may be disposed of in a landfill unless doing so violates local, state, and/or federal law (U.S. Silica, 1997).

The blasting procedure itself is not unlike spray painting in an enclosed painting cabinet with a compressed-air-source spray gun (Figure 37). For soft lithologies, the blast pressure may be turned down to 40 psi (275 kPa) to gently remove drill mud and/or enhance numerous structural details otherwise obliterated or made difficult to discern by

Figure 37. Blasting procedure (*simulated* for purpose of photo) showing operator wearing protective gear as described in text. Blasting must be done only with the cabinet doors fully closed. Notice the sand hopper/reservoir is filled up to where sand completely overtops the screened work surface (not visible). This provides a soft bed for the core pieces, and helps keep the blasting gun well fed with sand.

more common cleaning methods. More durable segments of drill core can tolerate pressures of 90 psi (620 kPa) and higher, with similar positive results.

Given the harsh environment produced within the cabinet during blasting, the cabinet itself required certain protective measures to prevent it being damaged and rendered unusable, and to defend against the undue health hazard of fugitive aerosolized silica. For example, during blasting, the cabinet's window was susceptible to frosting caused by pitting from errant sand grains. This problem was solved by using strips of clear plastic packing tape to shield the window's interior surface. These strips could easily be applied in rows, and replaced as they became frosted. Additionally, the rubber gloves attached to the cabinet's glove ports would have eventually degraded in the abrasive environment. This would have caused a dangerous compromise to the cabinet's integrity. To alleviate this potential, typical leather work gloves were worn over the cabinet's attached rubber gloves to preserve the rubber from undue abrasion (Figure 37).

Pieces of drill core were cleaned individually, box-by-box, in order. When the piece at hand was sufficiently cleaned, it was returned to its storage box and checked against its neighboring pieces for proper continuity (which includes orientation). In effect, each drill core was carefully reassembled in its entirety after cleaning. The next section details the guiding principles used in this effort.

2. Reassembling Each Drill Core

Because of the way each drill core was cleaned, nearly every piece of core was removed from its box at some point. Care had to be taken to make sure the core pieces were not haphazardly replaced upside down or out of sequence. Additionally, before cleaning began, it was discovered that some pieces of drill core were boxed upside down, and/or out of sequence as originally packaged at the drill site. Although such errors were rare, they were obvious and needed correcting.

After each piece of drill core in the storage box at hand was cleaned, the individual piece was checked for lithic continuity and proper placement in the box. When matching each piece of drill core to another piece of drill core, careful attention was given to complimentary broken faces, lithology, color, and structure. These procedures were also applied to the assembly of pieces, within not only the particular box at hand, but also when comparing the start and end pieces in the given box to their corresponding start or end piece in the box preceding or following it. Where possible, effort also went into assembling the pieces in such a way as to give preference to the overall structure of the crater-filling material. For example, if all the core pieces in hypothetical boxes numbered n_1, n_2, and n_3 contained mud-rich layers which were dipping to the left, and the core pieces in box n_4 lithologically and structurally *matched* the core pieces in box n_3, then the core pieces in box n_4 were also positioned to have their mud-rich layers dipping to the left. Doing so gave this hypothetical drill-core segment (stored across four boxes) an appearance true to its original in situ format. Many lengthy portions of drill core were reassembled this way.

However, a complete reassembly that was true to the original in situ format of each drill core in its entirety was not possible because of missing core sections, abrupt breaks that coincided with sharp changes in lithology, and/or indefinite matching contacts. Continuing with the above example, the core pieces in those four hypothetical boxes above all had mud-rich layering, and the pieces were positioned in their boxes so their bedding was dipping to the left. Imagine now that there is ten feet of missing drill core between box n_4 and n_5. Suppose further that the hypothetical drill core pieces in box n_5 are composed of a bedded sandstone that is altogether different from the mud-rich sediments in box n_4. Although is easy to assemble the pieces of this different sandstone relative to its own bedding, there is no way to determine which way the bedding in this sandstone should dip relative to the lengthy reassembled section of drill core pieces extracted from ten feet higher in the hypothetical drill core. Given the chaotic nature of crater-filling materials, there is no way to deal with this other than to position each length of reassembled drill core relative to itself between missing sections. Interestingly, this minor problem provided the solution to another minor problem.

Some storage boxes contained segments of drill core that were too fragile and/or too broken to be repositioned or otherwise moved. The exposed faces of unmovable pieces could be cleaned while remaining in their storage box, but could not be rotated. The solution was simply to rotate the adjoining pieces above/below into the required correct positions relative to the unmovable pieces. Missing sections of drill core both above and below made this workaround quite feasible. Figure 38 illustrates some of the guiding principles of these procedures.

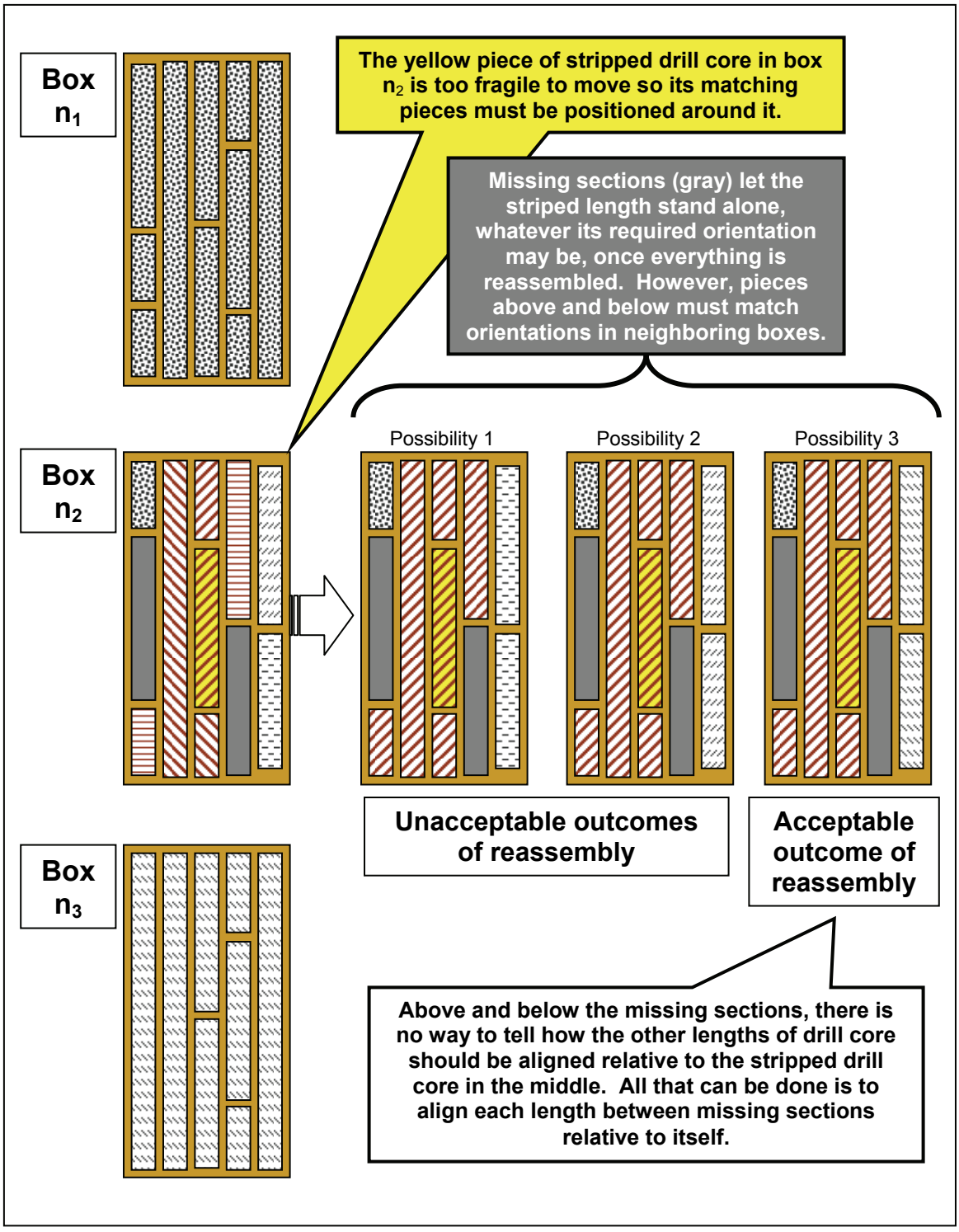

Figure 38. Illustration of reassembly protocol for cleaned drill core. When reassembling box n_2, several outcomes are possible, but only three are shown.

Once the content of each storage box was stratigraphically correct, the individual core pieces were shored up with custom-cut foam blocks, which then prevented movement of drill-core pieces within the box. With all of this complete, the two drill cores were ready to be photographed.

3. Photographing the Drill Cores

After the drill core was cleaned and reassembled, the entire length of each drill core was digitally photographed in high-resolution format. Tools for this included a 5.7 mega-pixel digital camera, and a professional-grade lighted copy stand (Figure 39). A jig (mechanical brace) was fashioned to serve the dual purpose of letting core boxes be positioned on the copy stand with consistency of position while displaying at the same time pertinent information at the photo's edge relative to the image's specific subject (Figure 40). This included the following information: 1) the drill core name, location, and dates drilled; 2) the depth interval of the drill core pieces shown; 3) a dimensional scale in feet and tenths, which are standard units of measure in U.S. drilling practice (metric units are provided in the subsequent geologic descriptions of drill core); 4) the orientation of the drill core in terms of which direction is stratigraphically up and the direction of deepening, both of which depend on how the core was boxed and/or placed in the jig; and 5) a Kodak color separation guide with gray scale (Kodak, 2000).

Once all photos were obtained, the originals (*master photos*) were checked for overall quality and batch-equalized using Adobe® Photoshop® CS2 to match each photo to all others in terms of contrast, and brightness. Without this step, the *drill-core photo mosaics* in each *digital geologic drill core description* (outlined in the next section) would have had an artificial, banded appearance. Next, the master photos were adjusted using Photoshop® to correct for natural fisheye lens distortion. Finally, all images were digitally sharpened using the same software, and archived as .jpg files. Note that the .jpg file extension is short for *Joint Photographic Experts Group*. The file extension was

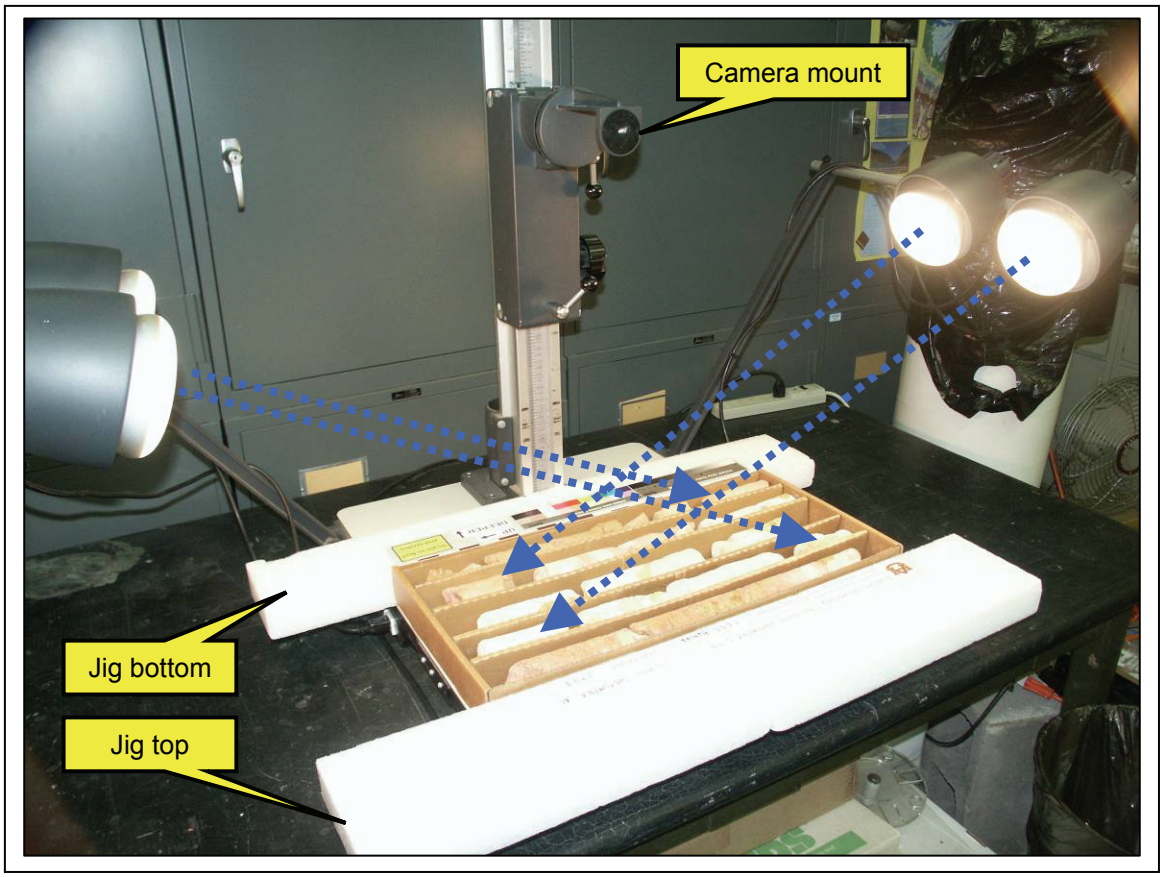

Figure 39. Lighted copy stand and jig (mechanical brace) used to photograph boxed drill core. The jig also displays information specific to each photo. The blue arrows depict how the four lights are aimed at the opposite end of the core box to help even out the lighting across the subject. Additionally, the two arms that the lights sit on are positioned at an angle of 45° away from center to give the light source greater distance from the subject. These two techniques produced a more consistent set of *master photos*.

Figure 40. Boxed drill core resting in the jig with relevant data specific to the box.

originally .jpeg but older web browsers and computers had problems interpreting four-letter file extensions (The Joint Photographic Experts Group, 2006).

Once archived, copies of the *master photos* were formatted into mosaics of stratigraphically correct stacked core lengths using Adobe® Photoshop®. These reformatted images are referred to as *stack photos*. To accomplish the reformatting, the five legs of drill core in each *master photo* (Figure 40) were digitally arranged according to drill depth as marked during drilling. Proper depth was tracked in the *stack photos* using a 10-foot dimensional scale crafted from the original 2-foot dimensional scale appearing in each *master photo*. The photographically reassembled lengths of drill core were then digitally labeled down-hole according to their drill depth as indicated by the *stack photo's* dimensional scale. These depth labels later served as a quality control once the *stack photos* were placed into the digital geologic drill core descriptions drafted in LogPlot 2005™. See Figure 41 for details of this procedure. Figure 42 depicts a completed *stack photo* ready for placement in the LogPlot™ software. This is accomplished by entering the start and end depths of the drill core depicted in the *stack photo*, along with the .jpg file name and file address for the *specific stack* photo.

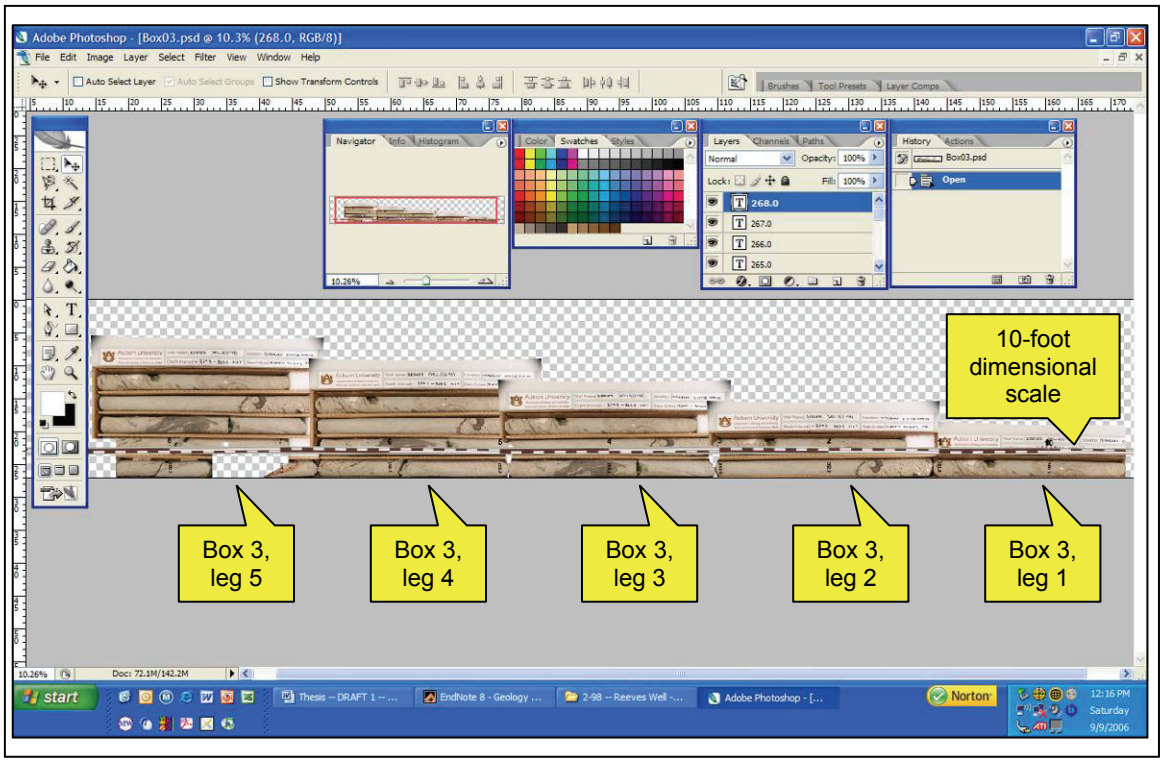

Figure 41. Screen capture illustrating *stack photo* creation process in Adobe® Photoshop® CS2. Because there are five legs of drill core in each box, five identical copies of the *master photo* for the box in processing are positioned stair-step fashion in correct stratigraphic order. Caution: correct stair-step orientation depends on how the drill core is boxed. Other drill cores boxed differently may have to be positioned with their stair-step pattern sloping in the opposite direction. Once the required five legs of drill core are positioned correctly along the bottom edge of the photo canvas (gray and white checkered area), the entire photo is cropped down to a thin rectangle containing only the assembled drill core legs along the bottom edge. The resulting image strip is rotated 90° counterclockwise and saved. Caution: direction of rotation also depends on how the drill core is boxed. The saved image is one of many *stack photos* that will be entered into the LogPlot 2005™ software.

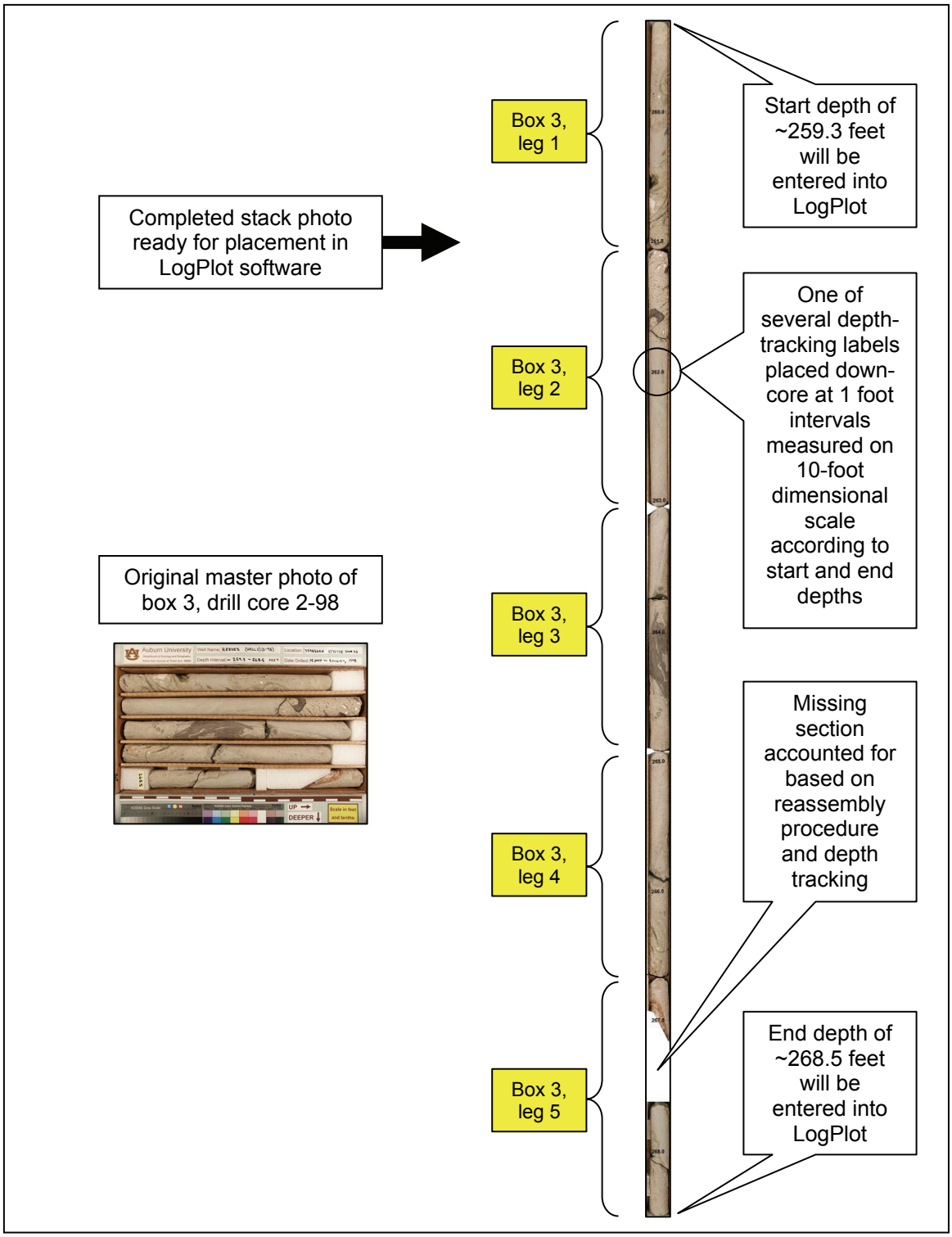

Figure 42. Completed *stack photo* after processing in Adobe® Photoshop® as compared to original *master photo*. Both photos are shown at the same scale.

Methods of Achieving the Main Objective

The *main objective* of this study was to provide non-interpretive, digitally formatted, geologic descriptions of both Wetumpka drill cores extracted from the structure in 1998. Commercially available, core-logging software was used in conjunction with the typical tools, charts, principles, and procedures commonly brought to bear during the geologic description of drill core.

1. Core-logging Software Used

Before this study began, it was decided that the non-interpretive geological descriptions of the drill core should be produced in a digital format that is widely used. It was also decided that photo-mosaics of the entire length of a particular drill core should accompany the description of that particular drill core's geology. To that end, a core-logging software application, namely LogPlot 2005™, was used to house and organize all data (including photos) collected during examinations of the two drill cores.

During data input, LogPlot™ functions like a typical spreadsheet file with rows, columns, and cells occupying a series of name-organized sheets into which raw textual and/or numerical data are entered according to drill depth. When data entry is complete, the data are automatically compiled by the software into a graphical representation of the drill core with accompanying text and figures positioned where appropriate in a series of columns based on drill depth. The software accomplishes this by dumping all the raw data into a digital template created in a previous step using the same LogPlot™ software.

The final digital output of all data can be in either a portable document format (.pdf), or a data (.dat) table format. Each of these formats is easily accessed by

commonly available software – the .pdf file by Adobe® Reader®, and the .dat file by Microsoft® Excel®. Further, these files are sized so that they may be printed on sheets of 8½ x 11 inch (U.S. letter-size) paper. The finished product's appearance and quality depends largely upon the skills of the software user who first created the various files, so it was necessary to work with the program for a time to gain experience. For the present study, all LogPlot™ data files, templates, and .pdf files were created by the current author.

An example of the blank template into which data for a given drill core was compiled is illustrated in Figure 43. The top of the first page in the template contains places to list the unique identifying characteristics of the drill core to be illustrated. Below this are the various legends and keys to assist the reader in understanding the graphical log. Below that are the data column headings indicating the information to be depicted in each data column under it.

Data columns include the following six *non-interpretive* columns from left to right. Column 1 – core box number and drill depth in meters and feet (subdivided into tenths). Column 2 – photos of drill core stacked as a mosaic of the drill core's entire length, shown in the correct stratigraphic positions. Column 3 – schematic lithology diagram to help illustrate the drill core's lithology. Column 4 – sketch of structures and various features manifest in the drill core. Column 5 – fining direction and notes on uncertain depth positions for given core pieces. Column 6 – lithologic descriptions and *detail graphics* with associated captions.

The next two data columns (7 and 8) are combined under *Interpretations*, and will be described in detail later. Together, they contain interpretive notes, sketches, and an

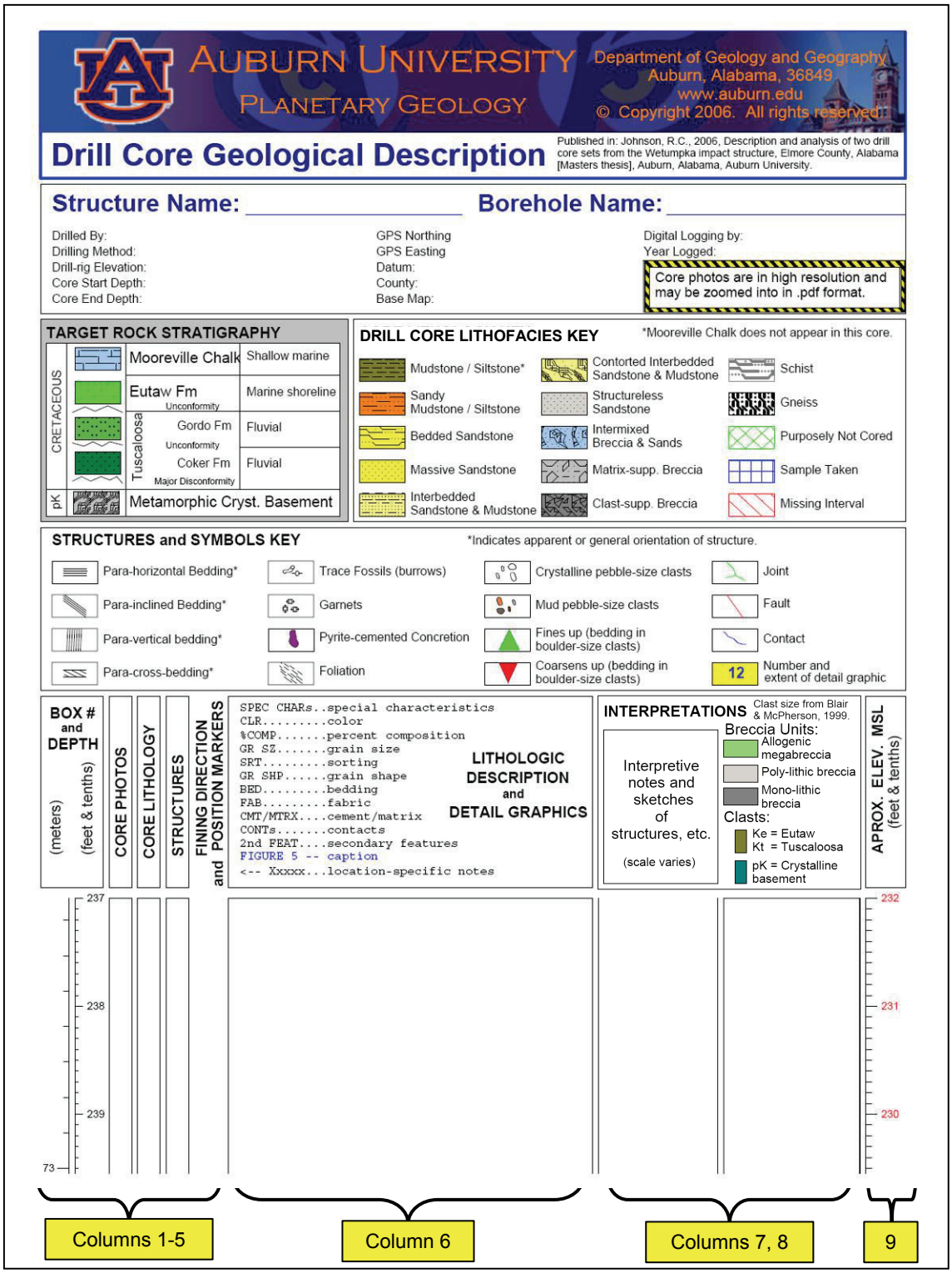

Figure 43. Example of the blank template into which data for a given drill core was compiled. The two columns under *Interpretations* will be described in a later section of this report. Template created by the present author in LogPlot 2005™.

interpretive representation of the entire drill core in an impact context based on the non-interpretive columns to the left. Finally, the data column at the far right (9) is a return to non-interpretive data with its depiction of the approximate elevation above/below mean sea level.

2. Describing the Drill Cores

Once all data files and templates in LogPlot™ are made ready for data entry, the software requires that data are entered in a manner not always intuitive in terms of the way that data will eventually appear in the final graphical log (.pdf file). For example, data about drill-core lithology and its associated lithologic description are entered on the same spreadsheet in the software, but they do not appear adjacent to each other in the final graphical log. For these reasons, the reader should not expect the following sequential explanations of data entry and core descriptions (i.e., the actual order of work) to correspond exactly with the order of columns appearing in the final graphical log. In addition, there will be *apparent* omissions of procedure in the following descriptions when compared to what is observed on the graphical log.

Drill core is typically described in a *down-hole* fashion because it is extracted that way. However, working *down-section* is contrary to the more common *up-section* method used, for example, in describing outcrop or interpreting stratigraphic order. Nonetheless, this study will follow what is typical of producing drill-core descriptions. Moreover, the core-logging software used in this study is set up to accept descriptions in a down-hole fashion. For examination and description of the drill core, boxed core was laid out on tables in a laboratory in its correct down-hole succession.

Columns 1 through 5

Drill depths for all lengths of drill core were entered into the LogPlot™ software according to values recorded at the time of drilling on each core box and/or on spacers between some core pieces. The depth values listed on/in the boxes were cross-checked

against the actual lengths of photographically reassembled drill core using the 10-foot dimensional scale in each photo mosaic of assembled drill core legs to accurately judge lengths. When no longer needed, the dimensional scale was omitted from the mosaic to declutter the image. Cross-checking of drill depth versus actual drill-core length revealed that most of the depth values listed on/in the boxes were indeed correct. Incorrect values, though rare, were readily apparent and commonly remedied for proper depiction of core-piece positions in the LogPlot™ software. However, the correct position of some core pieces could not be determined because of absent (*missing* or *purposely not cored*) portions in the drill core immediately above *and* below some pieces. Therefore, a note on correctness of position accompanies each of these rogue pieces in the *drill core geological description*.

Sketches of various structures manifest on the surface of the drill core were made using Adobe® Photoshop® CS2. The procedure involved drawing directly on the computer screen with a pressure-sensitive Graphire® stylus while working in a transparent Photoshop® layer placed over a given mosaic photo of drill core locked in the background. Sketches were then saved as .jpg files for eventual incorporation into LogPlot™.

Column 6

The next few paragraphs outline the methods of forming the actual descriptions of each drill core, but before continuing, a brief digression into the terminology used to refer to the various descriptions is necessary. The *Glossary of Geology* defines *lithofacies* as "… (c) A term that has been applied to "lithology", [*sic*] "lithologic type", [*sic*] and the

"manifestation" of lithologic characters" (Neuendorf et al., 2005). The present author used *lithofacies* in this sense when referring to the twelve categories of lithologic facies into which the drill cores were divided. These twelve categories are depicted in the *Drill Core Lithofacies Key* on the header of each *geologic drill core description* (Figure 43). Additionally, Neuendorf et al. (2005) define *lithozone* as "(a) An informal term to indicate a body of strata that is unified in a general way by lithologic features but for which there is insufficient need or information to justify its designation as a formal [separate] unit … ." The present author will use *lithozone* in this manner when referring to the various portions of drill core having a reasonably consistent lithofacies. Figure 44 illustrates the present author's usage of these two terms.

The intent of the *Lithologic Description and Detail Graphics* column (Figure 43) is to provide various details of the given drill core's geology while minimizing any process-associated descriptions and their implied interpretations. Each drill core's lithologic description was made using the standard tools, charts, principles, and procedures outlined in publications by Swanson (1981), Compton (1985), and Dietrich et al. (1989). Colors in the drill core were determined by comparison with the Geological Society of America Rock-Color Chart (1991). The data listed in this column follow a consistent pattern that varies as necessary depending on the lithology being described. Drill-core facies are generalized into twelve non-interpretive lithofacies based on grain size, texture, structure, and/or bedding (see *Drill Core Lithofacies Key*, Figure 43).

The descriptions for each lithozone list the various geologic attributes of the drill core's lithology for any given section of drill core having a consistent facies, regardless of its down-hole length. Within a particular description, the order of described

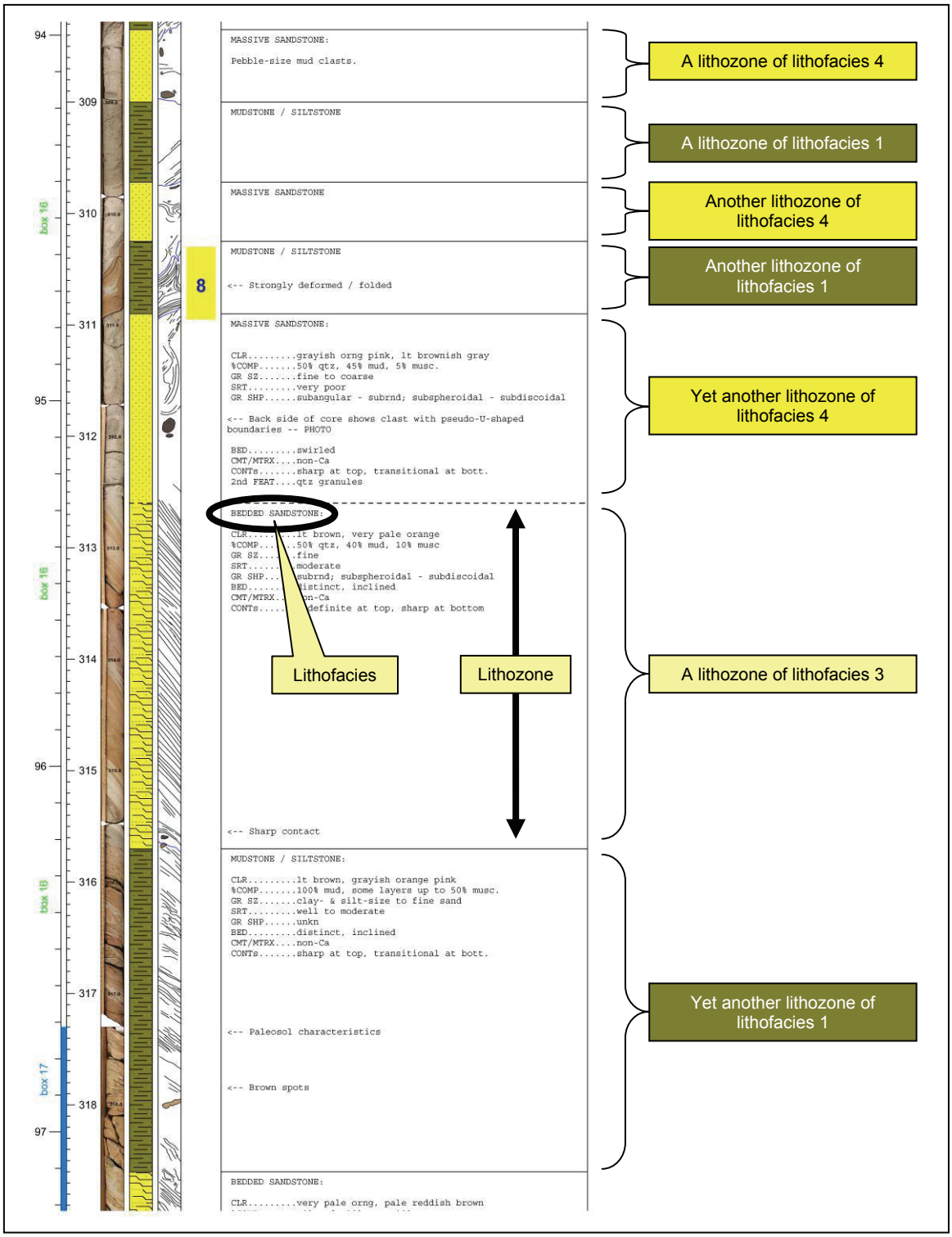

Figure 44. Example page from a *drill core geological description* illustrating the concept of several lithozones for a variety of lithofacies. Only columns 1 – 6 are shown. Columns 7 – 9 were omitted for clarity. A complete listing of lithofacies appears in the header of each *drill core geologic description*.

characteristics follows an order suggested by Compton (1985) because such an order simplified the process of describing the drill cores. These list-formatted descriptions accompany the lithofacies for a given lithozone and vary according to the subtleties and unique characteristics of the particular lithofacies within the boundaries graphically indicated for the lithozone.

Here it is important to remember that the crater-filling material at Wetumpka is composed of strongly disturbed and chaotically mixed target stratigraphy. As such, broken fragments originating from the same target unit(s) are found at various levels within both drill cores. Consequently, pieces of the same target units were being described repeatedly, as though they were individual units. Moreover, during the description process, no attempt was made to interpret the target unit of origin for the various lithozones in each drill core.

Finally, because of the drilling procedures used, gaps exist in the drill core, some of which were caused unintentionally, whereas others were caused intentionally. These gaps will be identified according to notes taken while drilling, lab notes from previous studies, and sample identification notes on papers inserted amongst the pieces of drill core. Gaps will be labeled in the *drill core geologic descriptions* as follows. Absent portions described as *Missing Interval* will indicate nonexistent portions of would-be drill core that were never recovered successfully from the drill hole despite normal drill-core recovery efforts. Absent portions described as *Purposely Not Cored* will indicate regions of the drill hole that were intentionally not cored because of problems encountered while drilling. Absent portions described as *Sample Taken* will indicate regions of previously existing drill core where samples have been cut from the drill core for destructive

analysis (1998 – 2006). No samples were taken from the drill holes (except for the two drill cores).

Methods of Achieving Ancillary Objectives

Work on the *ancillary objectives* was performed separately from most of the preceding non-interpretive effort. The methods used in these supplementary investigations are specific to the ancillary objectives and quite different from those previously described for the other objectives.

1. Clarifying Structures and/or Patterns Found in the Drill Cores

Because drill core has a cylindrically-curving surface that allows any structural features cored during drilling to be visible on its exterior, typical structural features that any geologist would immediately recognize in a flat face (folds, faults, kinks, etc.) are instead commonly manifest as peculiar loops, whorls, bull's-eyes, hyperbolae, chevrons, and other odd shapes (Figure 31).

To help clarify the true nature of these odd-looking features in the drill cores, it was necessary to create 3-D models of the actual structures that could have been drilled into and cored, thus resulting in the features observed within the drill cores (Figure 45). To that end, a software application designed for computer-aided drafting in three dimensions (TurboCAD® 11.1) was used to create several virtual blocks of strata, each having undistorted planar-parallel bedding. Next, the individual blocks were either faulted, folded, kinked, or otherwise distorted to create a variety of possible *starting structures*. Consideration was given to the *undeformed* block having undergone rotation before, during, and/or after the impact event. Additionally, for each structural deformation being modeled, careful attention was given to the deformation's magnitude and direction of both strike and dip relative to the block's original bedding, whatever

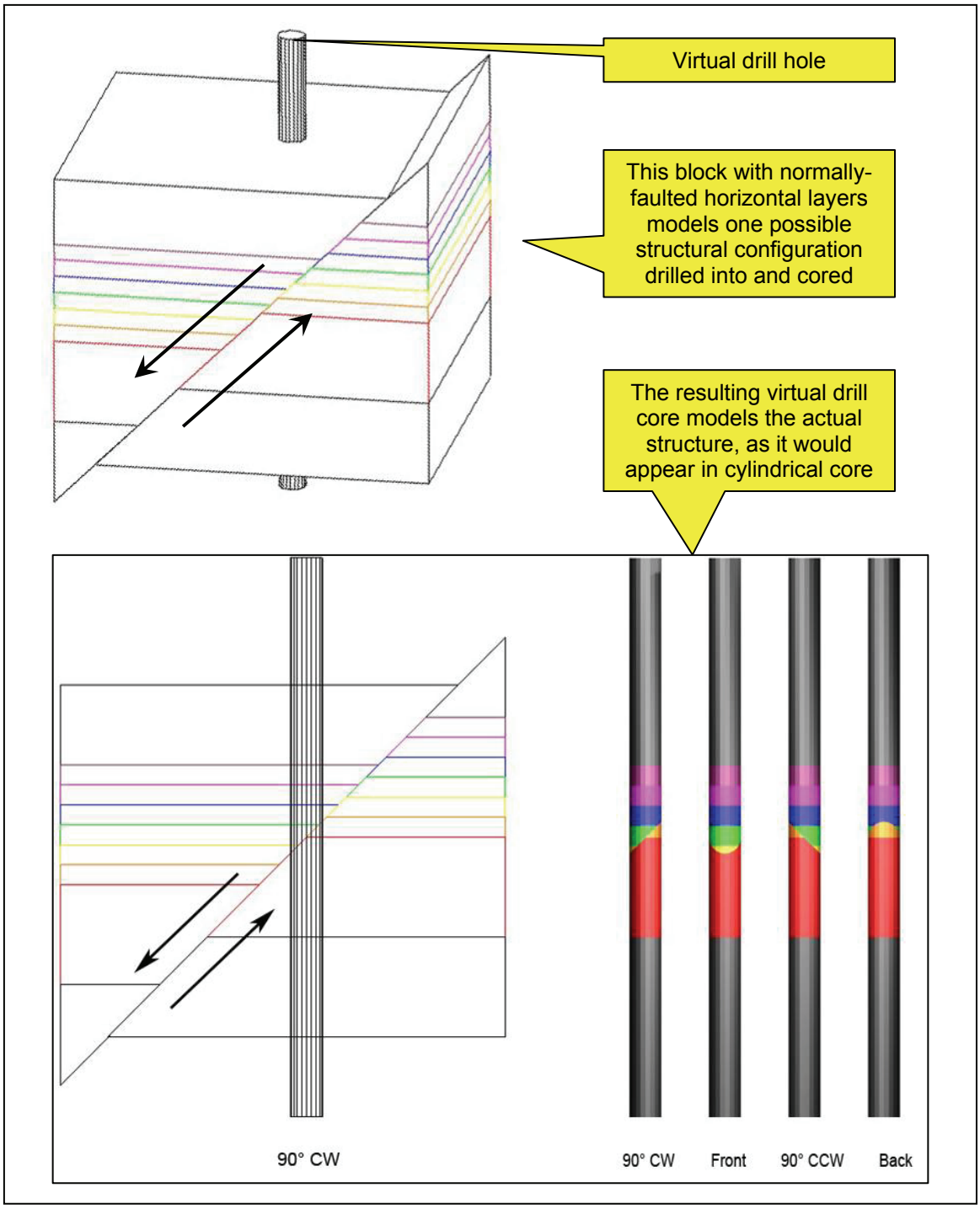

Figure 45. Example of a possible *starting structure* (normal fault in a target block having horizontally oriented bedding) cored within the crater-filling material at Wetumpka. The resultant virtual drill core (shown on four sides) models the given *starting structure* as it would appear in the actual drill cores. Features in each virtual drill core generated were compared against similar features in the actual drill cores to aid interpretation.

orientation that bedding may have originally had. Moreover, consideration was given to the *deformed* blocks' possible rotations before, during, and/or after the impact event. Finally, the observer's point of view was adjusted to best illustrate the structural disturbance within the block relative to bedding.

An additional special set of possible *starting structures* also had to be created. There is evidence to suggest that impact-related processes can form jacketed or layered boulders not unlike giant accretionary lapilli (Pope et al., 1999). Decimeter-scale bull's-eye features found within several drill-core intervals from Wetumpka were considered possible candidates for this (D. King, pers. comm., 2004). To investigate these features, layered spheres were also drafted as possible *starting structures*.

Once drafted and positioned appropriately, these structurally disturbed blocks and spheres served as unique models of the actual structures that could have been cored at Wetumpka. Using tools in the TurboCAD® software, each *starting structure* was "drilled" one-at-a-time by slicing a vertically-oriented cylinder from somewhere in the *starting structure* – usually down the center axis or off to one side. The resulting virtual drill core was then copied to show four *identical* intervals. Finally, three of the four intervals were rotated on their long axis as necessary so that a total of four different sides of the same length of virtual drill core were visible. Several possible outcomes of drill-core models were generated for each unique starting structure. These drill-core models could then be compared to features observed in the actual drill cores.

2. Determining the Positions of the Drill Cores versus the Central Peak

The 1994 gravity profile (Figure 30A) was used to help understand where the two drill cores are situated with respect to Wetumpka's central peak, as well as can be determined. The present author will apply the gravity data, and subsurface structure it implies, to further interpret the drill-core data within the context of the marine-impact depositional lithofacies model of Poag et al. (2004) as illustrated in Figure 21 of this report. Additional interpretations of the gravity data will also be made. To do this, the original numerical data used to produce the 1994 elevation and gravity profiles (Table 1) were both re-graphed in Microsoft® Excel® 2003 to show more clearly than before all the data points collected. Additionally, data points that were purposely excluded from some of the 1994 graphs were included in this report's new graphs. Lastly, map and drill-core data from the present study, along with map data from earlier work were examined in consideration with the gravity and elevation data to form interpretations about the position of Wetumpka's central peak.

	Field Station as numbered in 1994	West Longitude (decimal degrees)	North Latitude (decimal degrees)	Residual Gravity (mGal) [regional gravity removed]	Elevation (ft)	Elevation (m)
1	78	86.132843	32.524563	1.85	525.0	160.0
2	77	86.133736	32.524590	1.50	527.1	160.7
3	76	86.134644	32.524689	1.40	521.9	159.1
4	75	86.135284	32.524750	2.00	491.6	149.8
5	74	86.136116	32.524815	2.60	463.4	141.2
6	73	86.137070	32.524891	2.96	427.2	130.2
7	72	86.138153	32.524845	2.33	469.9	143.2
8	71	86.139084	32.524738	2.40	447.9	136.5
9	70	86.140152	32.524654	2.09	401.1	122.3
10	69	86.141052	32.524555	3.12	367.9	112.1
11	68	86.142105	32.524475	2.60	393.2	119.9
12	67	86.142899	32.524414	2.80	360.5	109.9
13	66	86.143974	32.524288	2.95	334.2	101.9
14	65	86.145065	32.524223	3.45	315.5	96.2
15	64	86.145981	32.524139	3.25	317.2	96.7
16	63	86.146912	32.524029	4.02	337.4	102.8
17	62	86.147903	32.523911	1.25	326.3	99.5
18	61	86.148888	32.523811	2.94	391.4	119.3
19	60	86.149818	32.523685	2.05	415.9	126.8
20	59	86.150925	32.523605	1.77	436.9	133.2
21	58	86.151909	32.523483	1.85	406.6	123.9
22	57	86.152809	32.523449	1.70	373.7	113.9
23	56	86.153801	32.523331	0.80	347.4	105.9
24	55	86.154640	32.523239	-0.90	346.7	105.7
25	54	86.155571	32.523106	-1.75	337.5	102.9
26	53	86.156593	32.523026	-2.55	342.0	104.2
27	52	86.157814	32.522907	-1.50	347.9	106.0
28	50	86.159531	32.522736	-2.01	333.0	101.5
29	49	86.160393	32.522655	-3.00	313.0	95.4
30	48	86.161369	32.522552	-3.00	313.5	95.6
31	46	86.163467	32.522255	-3.25	373.6	113.9
32	45	86.164413	32.522156	-4.10	407.8	124.3
33	44	86.165314	32.522007	-5.40	407.5	124.2
34	43	86.166321	32.521885	-5.99	385.7	117.6
35	42	86.167229	32.521755	-5.04	384.5	117.2
36	41	86.168221	32.521637	-5.10	387.1	118.0
37	40	86.169144	32.521515	-6.07	428.6	130.6
38	1	86.170090	32.521389	-5.90	456.0	139.0
39	2	86.170982	32.521252	-5.65	499.3	152.2
40	3	86.171967	32.521122	-4.95	506.2	154.3
41	4	86.172913	32.520988	-3.70	467.0	142.3
42	6	86.174759	32.520756	-2.40	493.5	150.4
43	7	86.175529	32.520672	-1.90	412.1	125.6
44	8	86.176506	32.520519	-3.00	356.5	108.7
45	9	86.177322	32.520420	-1.50	318.0	96.9
46	10	86.178284	32.520298	-1.95	353.6	107.8
47	11	86.179161	32.520294	-3.10	362.4	110.5
48	12	86.180206	32.520515	-3.05	333.7	101.7
49	13	86.180809	32.520676	-3.00	326.0	99.4
50	101	86.185379	32.525253	0.80	263.0	80.2
51	102	86.187347	32.525665	0.80	267.4	81.5
52	103	86.188766	32.525517	0.15	268.7	81.9
53	104	86.190247	32.524914	0.75	250.6	76.4
54	105	86.191719	32.524361	0.90	246.0	75.0
55	27	86.193901	32.521034	-1.85	228.8	69.7
56	26	86.194901	32.521023	-2.15	226.4	69.0
57	25	86.195763	32.521023	-1.09	227.9	69.5
58	24	86.196686	32.521015	0.09	232.8	71.0
59	23	86.197769	32.520927	1.10	244.5	74.5
60	22	86.198586	32.520908	3.07	249.6	76.1
61	21	86.199562	32.520710	3.60	267.3	81.5
62	20	86.200607	32.520493	3.25	265.1	80.8
63	19	86.201515	32.520355	3.25	239.0	72.9
64	18	86.202507	32.520222	3.60	224.7	68.5
65	17	86.203514	32.520088	2.90	215.1	65.6
66	16	86.204597	32.520023	3.70	186.9	57.0
67	91	86.215057	32.512566	1.55	190.5	58.1
68	90	86.216011	32.512600	1.30	187.9	57.3
69	89	86.216866	32.512596	0.90	185.7	56.6
70	87	86.218697	32.512562	1.50	180.5	55.0
71	85	86.220467	32.512531	1.45	178.0	54.3
72	84	86.221558	32.512543	1.09	178.2	54.3
73	83	86.222649	32.512535	1.00	178.3	54.4
74	82	86.223480	32.512527	1.40	178.8	54.5
75	81	86.224487	32.512497	1.10	179.0	54.6
76	80	86.225601	32.512463	0.90	180.0	54.9

Table 1. Original numerical data collected during a gravity survey transecting the Wetumpka impact structure in 1994 (courtesy of J. Plescia, pers. comm., 2005).

3. Elucidating the Ostensible Intra-crater Paleosol

Figure 11 and Figure 12 of this report illustrate that within Wetumpka's crater-filling material is an enigmatic mudstone of undetermined lateral extent that might be a thin paleosol and/or lacustrine deposit dividing the two larger, much thicker, main units filling the impact structure's central region (King et al., 2006). This paleosol and/or lacustrine mudstone is found only in drill core 1-98. Drill hole 2-98 was purposely not drilled at this depth because of drilling problems.

The enigmatic mudstone is either 1) a genuine post-impact, intra-crater paleosol, or 2) simply a block of pre-impact Upper Cretaceous target strata containing a pre-impact paleosol. Analysis of palynomorphs within the mudstone should reveal the mudstone's approximate age to within a range sufficient for elimination of one of the above possibilities.

To find the approximate age of palynomorphs in the mudstone, samples were prepared by the present author as follows. The outer surface of the drill core's entire length had already been cleaned by the abrasive (sand) blasting procedure outlined earlier. However, additional cleaning measures were necessary for the 1.65-meter-thick section of mudstone from which the micropaleontological samples would be taken. This was a precautionary measure to help ensure sample integrity and avoid cross-contamination by errant palynomorphs from elsewhere in the drill core. These additional cleaning procedures included dry brushing the drill core with a clean horsehair brush, then blowing the drill core clean with compressed air. It was not necessary to prevent contamination by modern palynomorphs because they cannot be mistaken for fossil forms.

Once cleaned, two samples were taken from the enigmatic mudstone unit. This was done because a small fault divides the mudstone and the throw of this fault is not precisely known. Sample A was taken above the fault, and sample B from below (Figure 46). Using a clean, *dry* rock saw, each sample was cut top-down from the drill core in the form of a single 3-cm-wide strip along the entire length of drill core indicated by the bracket corresponding to each sample letter in Figure 46. Each strip of mudstone was then broken into centimeter-scale chips and sealed in its own small airtight plastic container, which was itself sealed in a plastic bag. Sample A weighed ~75 grams and was essentially a collection of homogenized material from above the fault. Sample B weighed ~65 grams and was a similar collection of homogenized material from below the fault. The two samples were then sent to Global Geolab Ltd. in Medicine Hat, Alberta, Canada for chemical dissolution and separation of organics. All analysis of residual organics was done by palynologists at the IRF Group Inc. in Anchorage, Alaska.

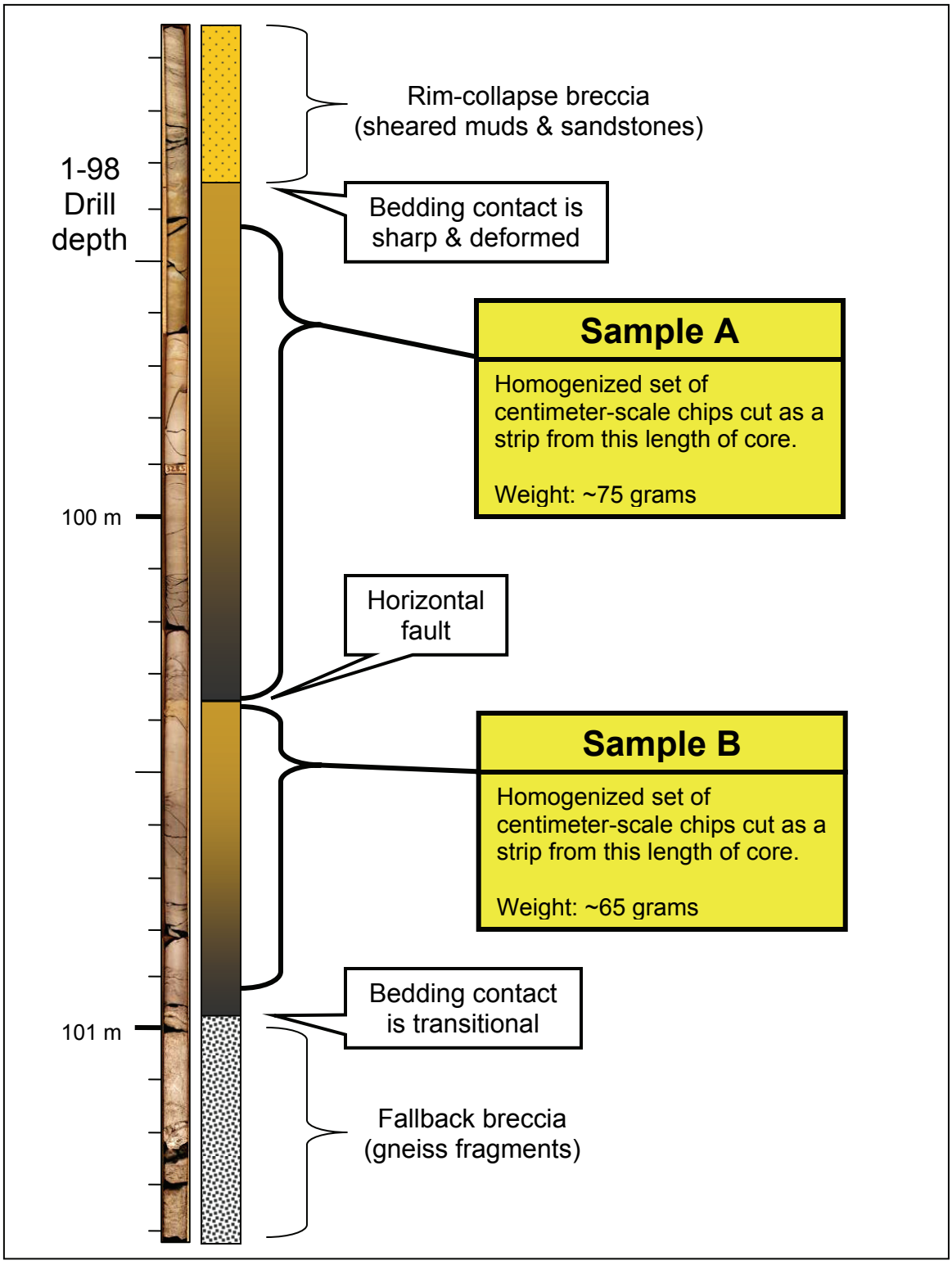

Figure 46. Detail of drill core 1-98 showing the enigmatic mudstone interval between the two main crater-filling units.

4. Determining the Age of Shock Metamorphism

Wetumpka's age estimate of early Campanian is a stratigraphic age assignment based on guide fossils and interpretations about target stratigraphy (King, 1997). A radiometric age determination is preferable and may be acquired by $^{40}Ar/^{39}Ar$ dating of potassium-bearing sheet silicates sampled from materials involved in an impact structure's formation (Bottomley et al., 1990).

The presence of shock-metamorphosed potassium-bearing sheet silicates was first identified at Wetumpka by Neathery et al. (1976b). Shock features are also evident within grains of garnet, feldspar, kyanite, and quartz (Neathery et al., 1976b; King et al., 1999b). Specifically, potassium-bearing sheet silicates from the matrix of Wetumpka's fallback breccia present an opportunity to investigate a possible thermal and/or mechanical loss of radiogenic ^{40}Ar, and a resetting of the $^{40}Ar/^{39}Ar$ ratio within individual crystal grains. This possible resetting can potentially yield an age estimate for the impact event because Wetumpka has not experienced any significant thermal or tectonic alteration subsequent to its formation (Neathery et al., 1976b; Nelson, 2000). Therefore, resetting can be inferred to result from loss of radiogenic ^{40}Ar from individual mineral grains that were strongly heated by the thermal pulse characteristic of impact events (Faure, 1986; Melosh, 1989; King, 1997; King et al., 2006).

Samples for this analysis were taken from drill core 1-98 at drill depths of 127.45 m (impact breccia matrix), and 182.5 m (contorted interbedded sandstone and mudstone). Bulk samples were disaggregated separately using a sonicator and water bath. After disaggregation, unwanted fines were washed away with water. The remaining grains were then placed in a bath of ethyl alcohol (ETOH) from which individual crystals of

potassium-bearing sheet silicates (particularly muscovite) ~1 mm in diameter were selected. Grains were initially divided into four groups based on their physical appearance (Figure 47).

The four sample sets were then packaged as required for outsourcing to the McMaster Nuclear Reactor at McMaster University in Hamilton, Ontario, Canada. This reactor facility performed the irradiation process necessary to generate ^{39}Ar from ^{39}K through activation by epithermal neutrons ("fast neutrons") as elucidated by Merrihue and Turner (1966). Depending on the sample's position in the reactor core, other reactions similar to the one above are also generated, which may produce radiogenic by-products. However, low quantities of calcium and/or chlorine in the muscovite studied will preclude these other unwanted reactions (Faure, 1986).

After the sample's return from the irradiation process, dating analysis was performed by laser fusion and vaporization of individual grains using the Auburn Noble Isotope Mass Analysis Laboratory (ANIMAL). Fish Canyon sanidine was used as the monitor mineral because of its widely preferred status as a monitor. Baksi et al. (1996) reported an age of 27.90 to 28.09 Ma for the Fish Canyon tuff, and a more recent paper by Dazé et al. (2003) assigned an age of 28.13 ± 0.47 Ma (2σ). For the present study, a value of 28.09 Ma was used for the age of the monitor mineral. Table 2 lists the values of other variables used to process the raw numerical results of the laser fusion analysis.

All processing and graphing was done in Microsoft® Excel® 2003 using the principles and equations summarized in chapter 7 of Faure (1986). Figure 48 depicts an example of this processing for a single muscovite crystal (i.e. the *sample*). Figure 49 exemplifies its companion processing for a *blank* run. Each crystal sample and blank was

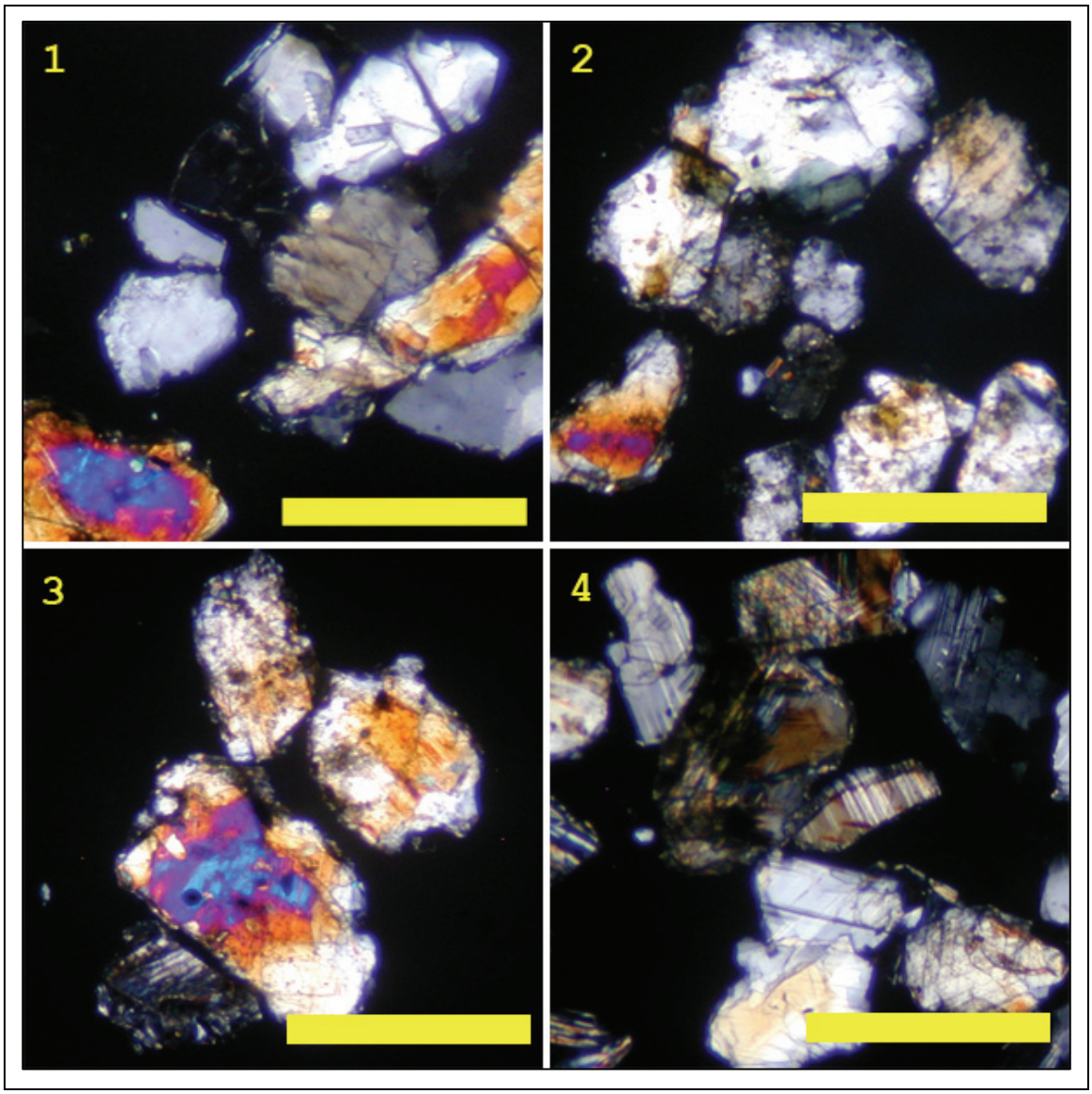

Figure 47. Photos of muscovite grains that were assayed for their $^{40}Ar/^{39}Ar$ ratio in an attempt to determine a radiometric age for the Wetumpka impact event. Views are divided based on their physical appearance as follows: 1) unshocked grains, 2) "flash-fried" (?), foamy-looking grains, 3) shocked "flash-fried" (?) grains, and 4) shocked grains with polysynthetic, mechanical twins dominating in this image. Yellow bars are ~1 mm. All photos were taken in cross-polarized illumination.

Sensitivity (Moles/volt):	1.89E-14 ± 1.89E-16
J-Value (production factor of ^{39}K to ^{39}Ar):	0.00928 ± 3.71E-05
Measured $^{40}Ar/^{36}Ar$ ratio of Air:	295.5 ± 2
Mass Discrimination (% per amu):	0.03% ± 0.14%
$^{36}Ca/^{37}Ca$ ratio:	0.000254 ± 0.00009
$^{39}Ca/^{37}Ca$ ratio:	0.000651 ± 3.1E-06
$^{40}K/^{39}K$ ratio:	0.00268 ± 0.0002
$^{38}Cl/^{39}K$ ratio:	3.21 ± 0.321

Table 2. Values of variables used in processing the numerical data resulting from laser fusion analysis in ANIMAL.

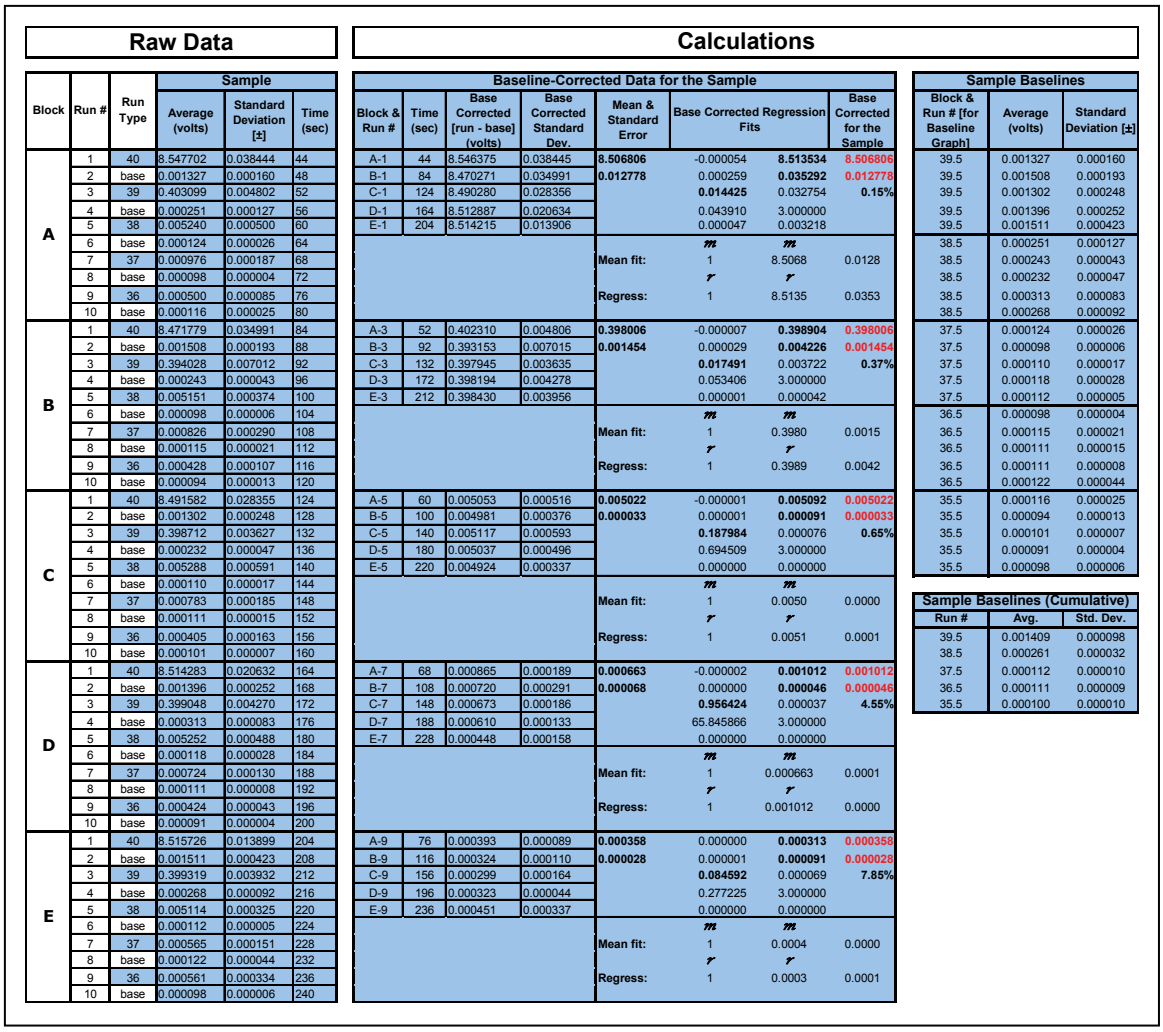

Raw Data

Block	Run #	Run Type	Sample: Average (volts)	Sample: Standard Deviation [±]	Sample: Time (sec)
A	1	40	8.547702	0.038444	44
	2	base	0.001327	0.000160	48
	3	39	0.403099	0.004802	52
	4	base	0.000251	0.000127	56
	5	38	0.005240	0.000500	60
	6	base	0.000124	0.000026	64
	7	37	0.000976	0.000187	68
	8	base	0.000098	0.000004	72
	9	36	0.000500	0.000085	76
	10	base	0.000116	0.000025	80
B	1	40	8.471779	0.034991	84
	2	base	0.001508	0.000193	88
	3	39	0.394028	0.007012	92
	4	base	0.000243	0.000043	96
	5	38	0.005151	0.000374	100
	6	base	0.000098	0.000006	104
	7	37	0.000826	0.000290	108
	8	base	0.000115	0.000021	112
	9	36	0.000428	0.000107	116
	10	base	0.000094	0.000013	120
C	1	40	8.491582	0.028355	124
	2	base	0.001302	0.000248	128
	3	39	0.398712	0.003627	132
	4	base	0.000232	0.000047	136
	5	38	0.005288	0.000591	140
	6	base	0.000110	0.000017	144
	7	37	0.000783	0.000185	148
	8	base	0.000111	0.000015	152
	9	36	0.000405	0.000163	156
	10	base	0.000101	0.000007	160
D	1	40	8.514283	0.020632	164
	2	base	0.001396	0.000252	168
	3	39	0.399048	0.004270	172
	4	base	0.000313	0.000083	176
	5	38	0.005252	0.000488	180
	6	base	0.000118	0.000028	184
	7	37	0.000724	0.000130	188
	8	base	0.000111	0.000008	192
	9	36	0.000424	0.000043	196
	10	base	0.000091	0.000004	200
E	1	40	8.515726	0.013899	204
	2	base	0.001511	0.000423	208
	3	39	0.399319	0.003932	212
	4	base	0.000268	0.000092	216
	5	38	0.005114	0.000325	220
	6	base	0.000112	0.000005	224
	7	37	0.000565	0.000151	228
	8	base	0.000122	0.000044	232
	9	36	0.000561	0.000334	236
	10	base	0.000098	0.000006	240

Calculations

Baseline-Corrected Data for the Sample

Block & Run #	Time (sec)	Base Corrected [run - base] (volts)	Base Corrected Standard Dev.	Mean & Standard Error	Base Corrected Regression Fits		Base Corrected for the Sample
A-1	44	8.546375	0.038445	**8.506806**	-0.000054	**8.513534**	**8.506806**
B-1	84	8.470271	0.034991	**0.012778**	0.000259	**0.035292**	**0.012778**
C-1	124	8.490280	0.028356		**0.014425**	0.032754	**0.15%**
D-1	164	8.512887	0.020634		0.043910	3.000000	
E-1	204	8.514215	0.013906		0.000047	0.003218	
					m	***m***	
				Mean fit:	1	8.5068	0.0128
					r	***r***	
				Regress:	1	8.5135	0.0353
A-3	52	0.402310	0.004806	**0.398006**	-0.000007	**0.398904**	**0.398006**
B-3	92	0.393153	0.007015	**0.001454**	0.000029	**0.004226**	**0.001454**
C-3	132	0.397945	0.003635		**0.017491**	0.003722	**0.37%**
D-3	172	0.398194	0.004278		0.053406	3.000000	
E-3	212	0.398430	0.003956		0.000001	0.000042	
					m	***m***	
				Mean fit:	1	0.3980	0.0015
					r	***r***	
				Regress:	1	0.3989	0.0042
A-5	60	0.005053	0.000516	**0.005022**	-0.000001	**0.005092**	**0.005022**
B-5	100	0.004981	0.000376	**0.000033**	0.000001	**0.000091**	**0.000033**
C-5	140	0.005117	0.000593		**0.187984**	0.000076	**0.65%**
D-5	180	0.005037	0.000496		0.694509	3.000000	
E-5	220	0.004924	0.000337		0.000000	0.000000	
					m	***m***	
				Mean fit:	1	0.0050	0.0000
					r	***r***	
				Regress:	1	0.0051	0.0001
A-7	68	0.000865	0.000189	**0.000663**	-0.000002	**0.001012**	**0.001012**
B-7	108	0.000720	0.000291	**0.000068**	0.000000	**0.000046**	**0.000046**
C-7	148	0.000673	0.000186		**0.956424**	0.000037	**4.55%**
D-7	188	0.000610	0.000133		65.845866	3.000000	
E-7	228	0.000448	0.000158		0.000000	0.000000	
					m	***m***	
				Mean fit:	1	0.000663	0.0001
					r	***r***	
				Regress:	1	0.001012	0.0000
A-9	76	0.000393	0.000089	**0.000358**	0.000000	**0.000313**	**0.000358**
B-9	116	0.000324	0.000110	**0.000028**	0.000001	**0.000091**	**0.000028**
C-9	156	0.000299	0.000164		**0.084592**	0.000069	**7.85%**
D-9	196	0.000323	0.000044		0.277225	3.000000	
E-9	236	0.000451	0.000337		0.000000	0.000000	
					m	***m***	
				Mean fit:	1	0.0004	0.0000
					r	***r***	
				Regress:	1	0.0003	0.0001

Sample Baselines

Block & Run # [for Baseline Graph]	Average (volts)	Standard Deviation [±]
39.5	0.001327	0.000160
39.5	0.001508	0.000193
39.5	0.001302	0.000248
39.5	0.001396	0.000252
39.5	0.001511	0.000423
38.5	0.000251	0.000127
38.5	0.000243	0.000043
38.5	0.000232	0.000047
38.5	0.000313	0.000083
38.5	0.000268	0.000092
37.5	0.000124	0.000026
37.5	0.000098	0.000006
37.5	0.000110	0.000017
37.5	0.000118	0.000028
37.5	0.000112	0.000005
36.5	0.000098	0.000004
36.5	0.000115	0.000021
36.5	0.000111	0.000015
36.5	0.000111	0.000008
36.5	0.000122	0.000044
35.5	0.000116	0.000025
35.5	0.000094	0.000013
35.5	0.000101	0.000007
35.5	0.000091	0.000004
35.5	0.000098	0.000006

Sample Baselines (Cumulative)

Run #	Avg.	Std. Dev.
39.5	0.001409	0.000098
38.5	0.000261	0.000032
37.5	0.000112	0.000010
36.5	0.000111	0.000009
35.5	0.000100	0.000010

Figure 48. Example of spreadsheet portion in Microsoft® Excel® 2003 used to process raw data from laser fusion of individual muscovite crystal *samples* in ANIMAL.

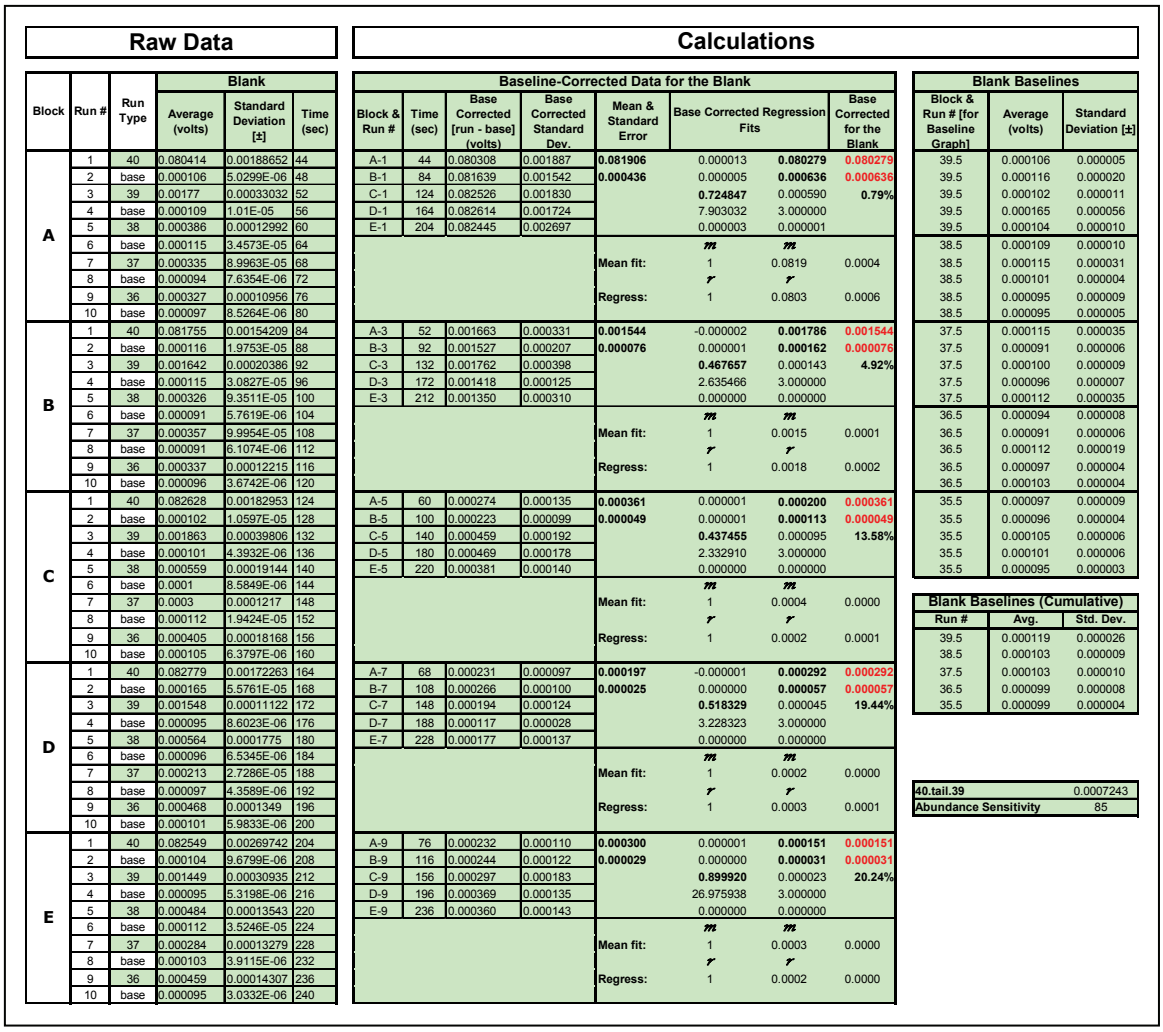

Raw Data

Block	Run #	Run Type	Blank: Average (volts)	Blank: Standard Deviation [±]	Blank: Time (sec)
A	1	40	0.080414	0.00188652	44
	2	base	0.000106	5.0299E-06	48
	3	39	0.00177	0.00033032	52
	4	base	0.000109	1.01E-05	56
	5	38	0.000386	0.00012992	60
	6	base	0.000115	3.4573E-05	64
	7	37	0.000335	8.9963E-05	68
	8	base	0.000094	7.6354E-06	72
	9	36	0.000327	0.00010956	76
	10	base	0.000097	8.5264E-06	80
B	1	40	0.081755	0.00154209	84
	2	base	0.000116	1.9753E-05	88
	3	39	0.001642	0.00020386	92
	4	base	0.000115	3.0827E-05	96
	5	38	0.000326	9.3511E-05	100
	6	base	0.000091	5.7619E-06	104
	7	37	0.000357	9.9954E-05	108
	8	base	0.000091	6.1074E-06	112
	9	36	0.000337	0.00012215	116
	10	base	0.000096	3.6742E-06	120
C	1	40	0.082628	0.00182953	124
	2	base	0.000102	1.0597E-05	128
	3	39	0.001863	0.00039806	132
	4	base	0.000101	4.3932E-06	136
	5	38	0.000559	0.00019144	140
	6	base	0.0001	8.5849E-06	144
	7	37	0.0003	0.0001217	148
	8	base	0.000112	1.9424E-05	152
	9	36	0.000405	0.00018168	156
	10	base	0.000105	6.3797E-06	160
D	1	40	0.082779	0.00172263	164
	2	base	0.000165	5.5761E-05	168
	3	39	0.001548	0.00011122	172
	4	base	0.000095	8.6023E-06	176
	5	38	0.000564	0.0001775	180
	6	base	0.000096	6.5345E-06	184
	7	37	0.000213	2.7286E-05	188
	8	base	0.000097	4.3589E-06	192
	9	36	0.000468	0.0001349	196
	10	base	0.000101	5.9833E-06	200
E	1	40	0.082549	0.00269742	204
	2	base	0.000104	9.6799E-06	208
	3	39	0.001449	0.00030935	212
	4	base	0.000095	5.3198E-06	216
	5	38	0.000484	0.00013543	220
	6	base	0.000112	3.5246E-05	224
	7	37	0.000284	0.00013279	228
	8	base	0.000103	3.9115E-06	232
	9	36	0.000459	0.00014307	236
	10	base	0.000095	3.0332E-06	240

Calculations

Baseline-Corrected Data for the Blank

Block & Run #	Time (sec)	Base Corrected [run - base] (volts)	Base Corrected Standard Dev.	Mean & Standard Error	Base Corrected Regression Fits		Base Corrected for the Blank
A-1	44	0.080308	0.001887	**0.081906**	0.000013	**0.080279**	0.080279
B-1	84	0.081639	0.001542	**0.000436**	0.000005	**0.000636**	0.000636
C-1	124	0.082526	0.001830		**0.724847**	0.000590	**0.79%**
D-1	164	0.082614	0.001724		7.903032	3.000000	
E-1	204	0.082445	0.002697		0.000003	0.000001	
					m	*m*	
				Mean fit:	1	0.0819	0.0004
					r	*r*	
				Regress:	1	0.0803	0.0006
A-3	52	0.001663	0.000331	**0.001544**	-0.000002	**0.001786**	0.001544
B-3	92	0.001527	0.000207	**0.000076**	0.000001	**0.000162**	0.000076
C-3	132	0.001762	0.000398		**0.467657**	0.000143	**4.92%**
D-3	172	0.001418	0.000125		2.635466	3.000000	
E-3	212	0.001350	0.000310		0.000000	0.000000	
					m	*m*	
				Mean fit:	1	0.0015	0.0001
					r	*r*	
				Regress:	1	0.0018	0.0002
A-5	60	0.000274	0.000135	**0.000361**	0.000001	**0.000200**	0.000361
B-5	100	0.000223	0.000099	**0.000049**	0.000001	**0.000113**	0.000049
C-5	140	0.000459	0.000192		**0.437455**	0.000095	**13.58%**
D-5	180	0.000469	0.000178		2.332910	3.000000	
E-5	220	0.000381	0.000140		0.000000	0.000000	
					m	*m*	
				Mean fit:	1	0.0004	0.0000
					r	*r*	
				Regress:	1	0.0002	0.0001
A-7	68	0.000231	0.000097	**0.000197**	-0.000001	**0.000292**	0.000292
B-7	108	0.000266	0.000100	**0.000025**	0.000000	**0.000057**	0.000057
C-7	148	0.000194	0.000124		**0.518329**	0.000045	**19.44%**
D-7	188	0.000117	0.000028		3.228323	3.000000	
E-7	228	0.000177	0.000137		0.000000	0.000000	
					m	*m*	
				Mean fit:	1	0.0002	0.0000
					r	*r*	
				Regress:	1	0.0003	0.0001
A-9	76	0.000232	0.000110	**0.000300**	0.000001	**0.000151**	0.000151
B-9	116	0.000244	0.000122	**0.000029**	0.000000	**0.000031**	0.000031
C-9	156	0.000297	0.000183		**0.899920**	0.000023	**20.24%**
D-9	196	0.000369	0.000135		26.975938	3.000000	
E-9	236	0.000360	0.000143		0.000000	0.000000	
					m	*m*	
				Mean fit:	1	0.0003	0.0000
					r	*r*	
				Regress:	1	0.0002	0.0000

Blank Baselines

Block & Run # [for Baseline Graph]	Average (volts)	Standard Deviation [±]
39.5	0.000106	0.000005
39.5	0.000116	0.000020
39.5	0.000102	0.000011
39.5	0.000165	0.000056
39.5	0.000104	0.000010
38.5	0.000109	0.000010
38.5	0.000115	0.000031
38.5	0.000101	0.000004
38.5	0.000095	0.000009
38.5	0.000095	0.000005
37.5	0.000115	0.000035
37.5	0.000091	0.000006
37.5	0.000100	0.000009
37.5	0.000096	0.000007
37.5	0.000112	0.000035
36.5	0.000094	0.000008
36.5	0.000091	0.000006
36.5	0.000112	0.000019
36.5	0.000097	0.000004
36.5	0.000103	0.000004
35.5	0.000097	0.000009
35.5	0.000096	0.000004
35.5	0.000105	0.000006
35.5	0.000101	0.000006
35.5	0.000095	0.000003

Blank Baselines (Cumulative)

Run #	Avg.	Std. Dev.
39.5	0.000119	0.000026
38.5	0.000103	0.000009
37.5	0.000103	0.000010
36.5	0.000099	0.000008
35.5	0.000099	0.000004

40.tail.39	0.0007243
Abundance Sensitivity	85

Figure 49. Example of spreadsheet portion in Microsoft® Excel® 2003 used to process raw data from *blank* runs in ANIMAL.

cycled five times. These data are further processed as exemplified in Figure 50, and the reduced data finally produces a result as illustrated in the example shown in Figure 51. Raw numerical data from every crystal analyzed (and its associated *blank*) had to be run individually through the spreadsheet portions depicted in these four examples.

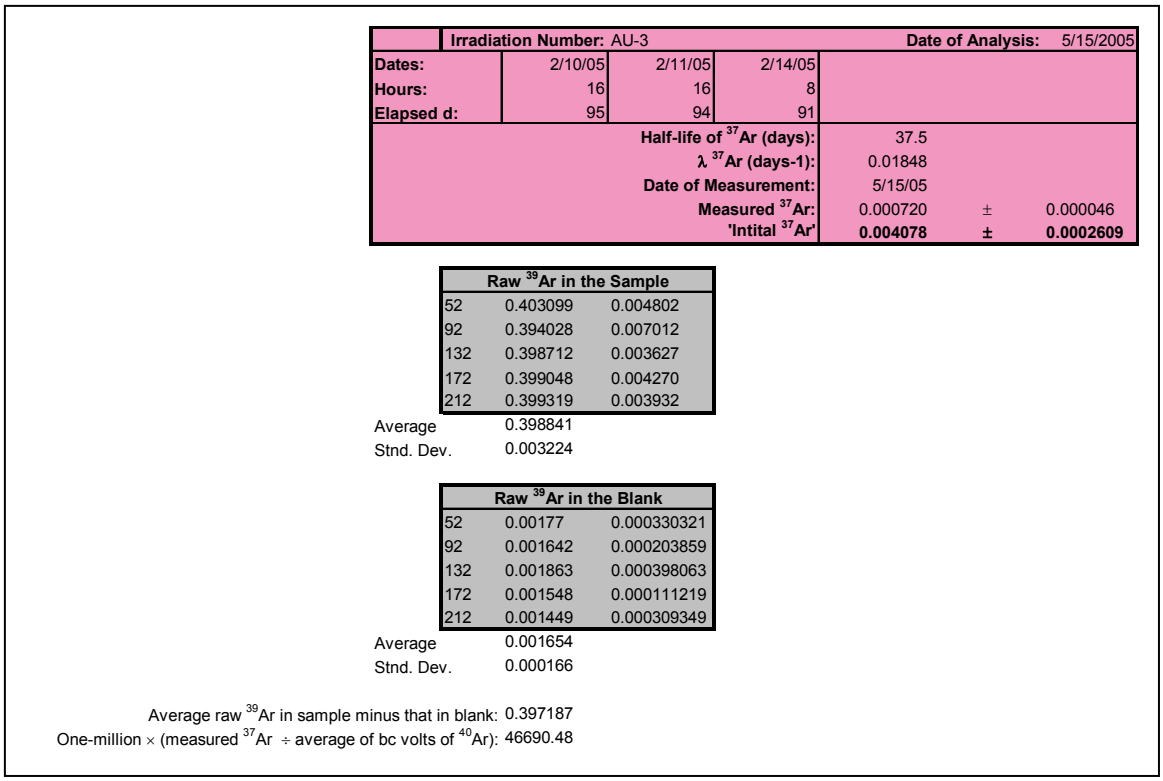

	Irradiation Number: AU-3			Date of Analysis:	5/15/2005
Dates:	2/10/05	2/11/05	2/14/05		
Hours:	16	16	8		
Elapsed d:	95	94	91		
			Half-life of ^{37}Ar (days):	37.5	
			λ ^{37}Ar (days-1):	0.01848	
			Date of Measurement:	5/15/05	
			Measured ^{37}Ar:	0.000720 ±	0.000046
			'Intital ^{37}Ar'	**0.004078 ±**	**0.0002609**

Raw ^{39}Ar in the Sample		
52	0.403099	0.004802
92	0.394028	0.007012
132	0.398712	0.003627
172	0.399048	0.004270
212	0.399319	0.003932
Average	0.398841	
Stnd. Dev.	0.003224	

Raw ^{39}Ar in the Blank		
52	0.00177	0.000330321
92	0.001642	0.000203859
132	0.001863	0.000398063
172	0.001548	0.000111219
212	0.001449	0.000309349
Average	0.001654	
Stnd. Dev.	0.000166	

Average raw ^{39}Ar in sample minus that in blank:	0.397187
One-million × (measured ^{37}Ar ÷ average of bc volts of ^{40}Ar):	46690.48

Figure 50. Example of spreadsheet portion in Microsoft® Excel® 2003 used to assess data from the previous two portions depicted above for the *sample* and *blank*.

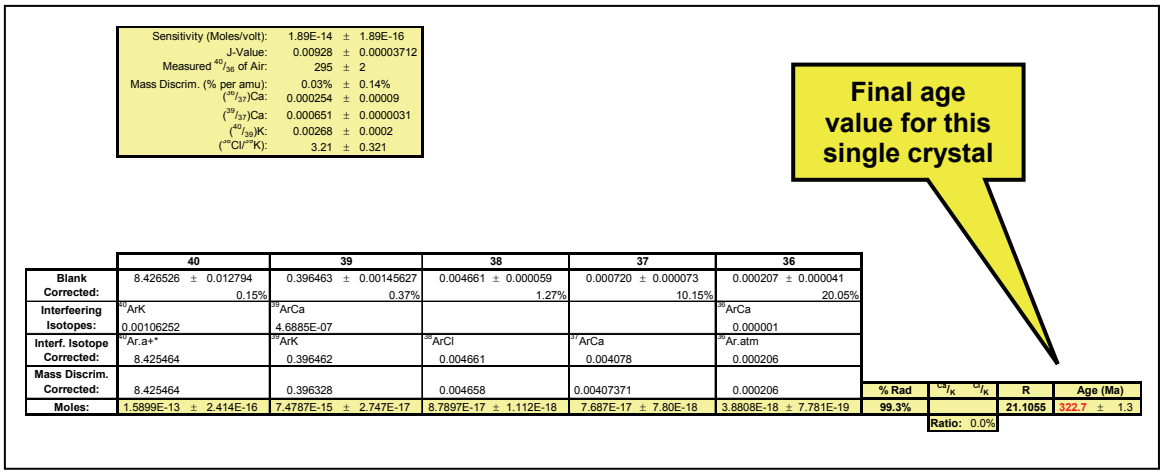

Figure 51. Example of spreadsheet portion in Microsoft® Excel® 2003 depicting final processing of reduced data from previous three portions illustrated above. The result is an age value in millions of years for the analyzed muscovite crystal.

5. Comparing Drill Core 1-98 to Drill Core 2-98

Given the proximity of the two drill sites, they may be collectively assessed for drill-site-scale similarities and differences with the aim of identifying and possibly correlating distinct attributes of the crater-filling material typically not discernable between drill holes bored kilometers apart. After the main objective and the preceding five ancillary objectives were complete, full-length printed versions of the two *drill core geological descriptions* for both drill cores were laid out side-by-side and corrected at first according to each drill site's elevation above modern sea level. These two core-log descriptions were then examined for any similarities and differences. The results were then used to guide further interpretations of the two drill cores, and ultimately, the Wetumpka structure itself.

6. Comparing Wetumpka to Chesapeake Bay Impact Structure

Once described and analyzed as previously mentioned, the Wetumpka drill cores were compared to other marine-target impact structures via comparative analysis of literature on marine impact processes and resultant structures. Of particular interest were the marine-target impact structures at Chesapeake Bay, U.S.A., Kärdla Island, Estonia, and Lockne, Sweden. Comparative analysis was then used to guide further interpretation of the Wetumpka drill cores. The three impact structures listed above provided important examples and analogues to the possible marine-target impact process and their results as manifest in impact-related drill core. Some of these examples have already been documented in this report to help establish the geological setting from which the drill core at Wetumpka was taken.

RESULTS

Results of Preparatory Objectives

1. Results of Cleaning by Abrasive (Sand) Blasting

The method of abrasive (sand) blasting developed for removing dried-on drill mud, which covered the two drill cores, thoroughly removed virtually all drill mud without damaging the drill core, regardless of its lithology (Figure 52 and Figure 53). Mud crust virtually melted away leaving the drill core's true lithology intact. Consequently, countless millimeter-scale structures, patterns, lithologies, and other features were revealed that otherwise would have gone unnoticed (Figure 54). A negligible amount of fine component was removed from the drill core itself, especially when using low blast pressures. In essence, the drill core itself remained, for the most part, unaffected by any surficial erosion caused by the blasting process. The overall result was somewhat like natural weathering of an outcrop. Because all unwanted debris was both blasted and vacuumed away, contamination by dust and debris from previously blasted drill core was minimal and substantially less than the contamination that would have been left on the core by other cleaning methods. For example, the abrasive medium (i.e., sand) did not penetrate into the drill core (except along minor fractures) as a solvent would have.

Figure 52. Example of sedimentary drill-core facies in especially poor condition before and after cleaning by abrasive (sand) blasting. Cleaning not only exposed immediately recognizable small-scale sedimentary structures and millimeter-scale garnets, but also revealed that what originally appeared to be a core piece of homogeneous lithology is actually composed of two distinct lithofacies. Modified from Johnson et al. (2006).

Figure 53. Example of crystalline drill-core facies before and after cleaning by abrasive (sand) blasting. Cleaning exposed the pre-impact metamorphic fabric within this core piece. Although the crystal faces of the mineral grains were mildly etched by the blasting process, etching was no more destructive than that caused by the drilling process itself.

Figure 54. Close-up of millimeter-scale details brought out and left undamaged by abrasive (sand) blasting of a drill core piece containing fluidized and plastically deformed sands and muds. Such details would have been obliterated or at least strongly altered by other cleaning methods.

2. Results of Reassembling Each Drill Core

Reassembly of each drill core resulted in having a collection of drill core that was more accurate in terms of depth and orientation (Figure 55). As an example, an analogy with a jigsaw puzzle will be made. Before assembly, one may indeed be able to discern the general nature of the puzzle's image by looking at its scattered or partially assembled fragments, but it is usually easier to appreciate the puzzle's image more fully once most of the pieces are assembled correctly. In essence, reassembly of the two drill cores lent itself to an improved ability to describe and interpret the drill core. Additionally, reassembly enhanced recognition of the drill core's structural features. With exception to absent portions, each reassembled drill core took on a "complete" appearance not unlike what one might see in a continuous exposure of rock on the face of a tall road cut. Finally, the quality of the photo mosaics of drill core in each graphical geologic description (.pdf file) was greatly improved upon by reassembly of the drill core.

Figure 55. Example of boxed drill core before and after reassembly. The same box is depicted in each photo.

3. Results of Photographing

Photographing the entire length of each drill core has produced a detailed and complete visual record of the crater-filling material pulled from near the geographic center of the Wetumpka impact structure. As a result, these high-resolution digital photographs (*master photos*) of each drill core perform at least four functions: 1) allow researchers to preview the fragile collection without unnecessary handling; 2) provide a means for reconstructing the order of drill-core fragments if they should become degraded or disarranged; 3) offer some tangible product in the event of permanent damage or loss of the drill core; and 4) provide a means for accessing particular attributes of the regional geology not otherwise available.

There are 49 *master photos* for drill core 1-98, and 22 *master photos* for drill core 2-98, giving a combined total of 71 *master photos* (Table 3). The full size of each image is approximately 35 inches wide, by 26 inches tall (~ 90 x 70 cm). Rather than print all of these photos in the text, the complete set of *master photos* has been archived to a CD-ROM, which is part of the present report. Additionally, scaled-down versions appear in Appendix 2 of this report.

The processing of *master photos* into *stack photos* produced a graphical set of drill-core data in a manner similar to that outlined above. These *stack photos* were successfully incorporated into the digital geological descriptions of the two drill cores with excellent accuracy as to their drill depth. For results, see the photo mosaics of drill core in each *drill core geological description* (.pdf file). There are 77 *stack photos* for drill core 1-98, and 46 for drill core 2-98, giving a combined total of 123 *stack photos*. The full size of most of these images is roughly 3.5 inches wide, by 10 feet tall (~ 9 cm x

1-98				
Box Number	Start Depth (ft)	End Depth (ft)	Length of Drill Hole Represented (ft) [includes absent portions]	File Name
1	104.80	127.00	22.20	Box01.jpg
2	127.00	139.80	12.80	Box02.jpg
3	139.80	149.80	10.00	Box03.jpg
4	149.80	159.60	9.80	Box04.jpg
5	159.60	170.00	10.40	Box05.jpg
6	170.00	222.50	52.50	Box06.jpg
7	222.50	232.20	9.70	Box07.jpg
8	232.20	243.50	11.30	Box08.jpg
9	243.50	253.00	9.50	Box09.jpg
10	253.00	262.50	9.50	Box10.jpg
11	262.50	271.40	8.90	Box11.jpg
12	271.40	280.20	8.80	Box12.jpg
13	280.20	289.90	9.70	Box13.jpg
14	289.90	298.50	8.60	Box14.jpg
15	298.50	308.20	9.70	Box15.jpg
16	308.20	317.30	9.10	Box16.jpg
17	317.30	327.00	9.70	Box17.jpg
18	327.00	337.50	10.50	Box18.jpg
19	337.50	350.30	12.80	Box19.jpg
20	350.30	361.50	11.20	Box20.jpg
21	361.50	371.10	9.60	Box21.jpg
22	371.10	381.30	10.20	Box22.jpg
23	381.30	388.90	7.60	Box23.jpg
24	388.90	399.50	10.60	Box24.jpg
25	399.50	403.50	4.00	Box25.jpg
26	403.50	413.90	10.40	Box26.jpg
27	413.90	424.20	10.30	Box27.jpg
28	424.20	432.10	7.90	Box28.jpg
29	432.10	440.50	8.40	Box29.jpg
30	440.50	457.10	16.60	Box30.jpg
31	457.10	466.30	9.20	Box31.jpg
32	466.30	475.40	9.10	Box32.jpg
33	475.40	483.20	7.80	Box33.jpg
34	483.20	492.30	9.10	Box34.jpg
35	492.30	501.70	9.40	Box35.jpg
36	501.70	514.80	13.10	Box36.jpg
37	514.80	525.50	10.70	Box37.jpg
38	525.50	538.50	13.00	Box38.jpg
39	538.50	548.00	9.50	Box39.jpg
40	548.00	557.00	9.00	Box40.jpg
41	557.00	566.00	9.00	Box41.jpg
42	566.00	575.60	9.60	Box42.jpg
43	575.60	583.70	8.10	Box43.jpg
44	583.70	592.50	8.80	Box44.jpg
45	592.50	598.50	6.00	Box45.jpg
46	598.50	607.00	8.50	Box46.jpg
47	607.00	615.90	8.90	Box47.jpg
48	615.90	625.50	9.60	Box48.jpg
49	625.50	638.50	13.00	Box49.jpg

2-98				
Box Number	Start Depth (ft)	End Depth (ft)	Length of Drill Hole Represented (ft) [includes absent portions]	File Name
1	239.60	251.50	11.90	Box01.jpg
2	251.50	259.30	7.80	Box02.jpg
3	259.30	268.50	9.20	Box03.jpg
4	268.50	277.00	8.50	Box04.jpg
5	277.00	286.60	9.60	Box05.jpg
6	286.60	298.50	11.90	Box06.jpg
7	298.50	349.30	50.80	Box07.jpg
8	349.30	359.40	10.10	Box08.jpg
9	359.40	377.10	17.70	Box09.jpg
10	377.10	384.90	7.80	Box10.jpg
11	384.90	395.10	10.20	Box11.jpg
12	395.10	409.30	14.20	Box12.jpg
13	409.30	441.60	32.30	Box13.jpg
14	441.60	454.30	12.70	Box14.jpg
15	454.30	463.50	9.20	Box15.jpg
16	463.50	479.70	16.20	Box16.jpg
17	479.70	489.30	9.60	Box17.jpg
18	489.30	510.60	21.30	Box18.jpg
19	510.60	527.45	16.85	Box19.jpg
20	527.45	545.60	18.15	Box20.jpg
21	545.60	559.30	13.70	Box21.jpg
22	559.30	589.00	29.70	Box22.jpg

Table 3. File names and depths of all *master photos* for both drill cores. Depth and length data are from each drill core's .dat file, and do not always agree with the generalized values written on the actual core box because of rounding of depth values at time of drilling.

3 m). The *stack photos* were also archived to a CD-ROM, which is part of this report, but are not printed in the appendix.

Results of Main Objective

The main objective of the study was to describe in a digital format the geological features of two drill cores without intruding into interpretation. Although description was a singular objective, four separate results were produced: 1) geological descriptions as raw alphanumerical .dat files in a spreadsheet format; 2) geological descriptions as refined, graphical .pdf files; 3) geological descriptions of lithofacies within the drill cores; and 4) a quantitative breakdown of lithologic data from both drill cores. Together, these results give an overview of the drill cores, which will perform at least six functions: 1) allow researchers to preview the fragile collection without unnecessary handling; 2) give direct access to a broad array of raw data from the collection in two practical file formats (.dat and .pdf); 3) provide a means for reconstructing the order of core fragments if they should become degraded or disarranged; 4) offer some tangible product in the event of permanent damage or loss; 5) provide a means for accessing particular attributes of the regional geology not otherwise accessible because those lithologies are completely buried; and 6) let researchers view the entirety of each drill core in detail without having to open a core box.

1. Geological Descriptions as Raw Alphanumerical (.dat) Files

All .dat files are in a spreadsheet format archived to CD-ROM. This data may be sorted, manipulated, statistically analyzed, etc. just as with any other spreadsheet. Consequently, future researchers may examine the datasets in ways that the present author did not.

2. Geological Descriptions as Graphical (.pdf) Files

The completed *drill core geological descriptions* are in a graphical .pdf format (Figure 56). The drill core in each file is drawn at a scale of ~1 foot per inch (~0.3 m per 2.54 cm). When printed on 8½ x 11 inch paper (U.S. letter-size), approximately 10 feet (~3.0 m) of drill core are depicted on a single page. Consequently, the .pdf files for drill cores 1-98 and 2-98 are 51 and 34 pages long, respectively. Each file may be viewed on-screen or printed as individual pages that may be subsequently taped together to form a continuous strip log of each description. Doing so allows a researcher to examine each strip either by itself, or side-by-side for comparison. Given their extensive length and size, the files were archived to CD-ROM, which is part of the present report. Columns under the heading *Interpretations* (in the *drill core geological descriptions*) are described in a later section. Because each data set is too large to view in this printed format, the schematic portion of each drill core's lithology column is depicted in its entirety in Figure 57 along with information on drill depth and box number.

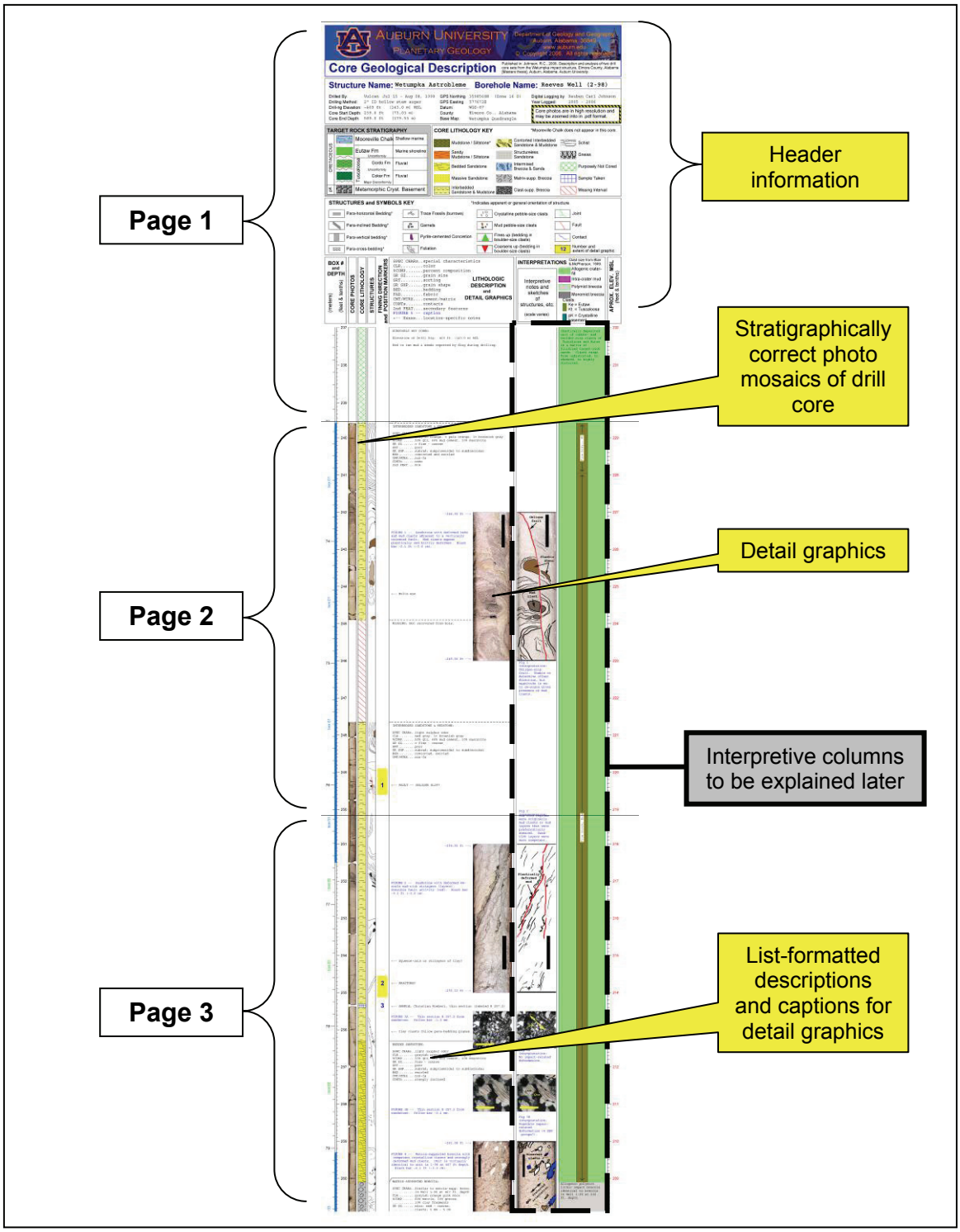

Figure 56. Scaled-down depiction of the first three pages of a completed graphical *drill core geological description* (.pdf file). The normal page size is 8½ x 11 inches (U.S. letter-size).

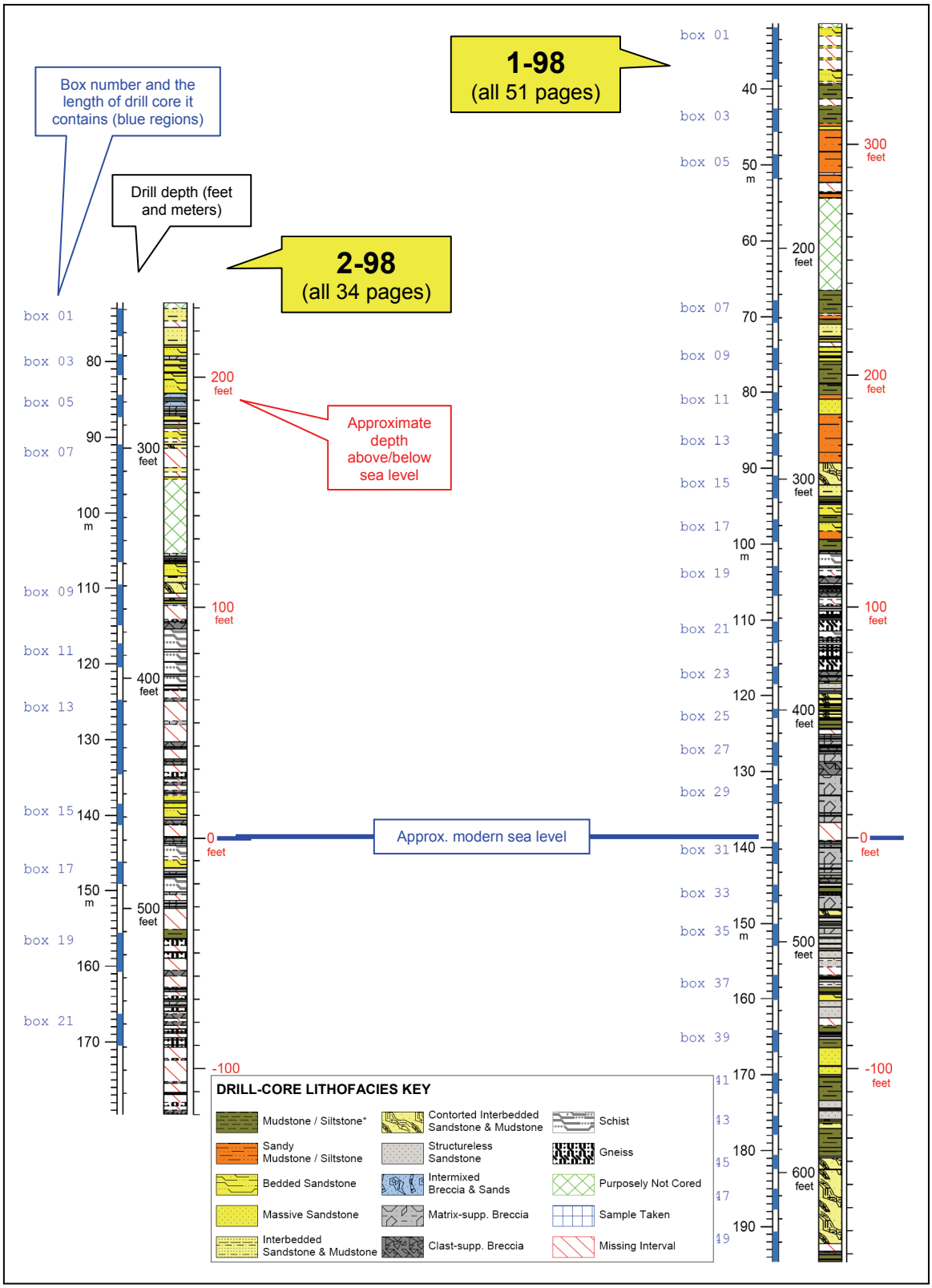

Figure 57. Schematic of drill core lithologic data greatly reduced in size.

3. Refined Geological Descriptions of Lithofacies within the Drill Cores

To lend a better understanding of the geologic characteristics observed in the various lithofacies within both drill cores, all list-formatted verbal descriptions of similar lithozones have been collectively merged into their respective twelve categories of lithofacies as indicated in the *drill-core lithofacies key* on the first page of each *drill core geological description*. Once all list-formatted descriptions for the given categories were collated and merged, the resulting merged descriptions (still in list format) were further refined into paragraph-formatted generalized, narrative descriptions of each lithofacies.

The narrative descriptions detailed below are ordered according to texture and lithology. This order generally follows the top-down (reverse) stratigraphic order of the drilled crater-filling material in the Wetumpka impact structure. Quantitative data collected at the time the descriptions were gathered, such as percent composition and grain size, are included in these descriptions. However, other quantitative data such as the collective thickness of the various lithozones for each lithofacies, etc. are summarized in the next section. Finally, several example photos of each lithofacies are included, but it is important to keep in mind that these photos are merely exemplary representations of the lithofacies described. That is, the photos are not actual results, just visual aids to understanding the resultant descriptions.

Mudstone / Siltstone Lithofacies

This lithofacies (pictured in Figure 58) is an orange-to-grayish-black siltstone to mudstone with commonly indistinct bedding and well-defined bioturbation. Paleosol-like characteristics such as slickensides, splotchy or mottled coloration, a wax-like texture, peds, and oxidized zones with reduction splotches, plinthites, and centimeter-scale clay clasts are common. Some regions have numerous *Taenidium* burrows (C. Savrda, pers. comm., 2005). Quartz granules are present in some places. At least one portion of this lithofacies type exhibits 1-mm flakes of gray clay. Overall coloration is splotchy to solid, and varies widely. The most common colors are grayish-orange-pink and pale reddish-brown. Also common are various browns and several shades of orange, red, and gray. Lithozones having this lithofacies are essentially 100% muds and silts largely composed of microscopic mica grains. Grain-size distribution is composed entirely of clay- and silt-size particles with the exception of some (rare) portions of this lithofacies having a fine sand component. Individual lithozones of this lithofacies are very well sorted. Under a microscope, grain shape (roundness and sphericity) for the silt component is very angular and platy. Bedding is mostly nonexistent to indistinct, but some portions show fine, distinct bedding ranging from near horizontal to steeply inclined. All lithozones of this lithofacies are entirely non-calcareous. Contacts (where present) are equally either sharp or transitional, and are commonly distorted or irregular in shape. One of the lithozones exhibiting this lithofacies is the possible paleosol and/or lacustrine mudstone interval in drill core 1-98 reported by King et al. (2006). This lithofacies will easily dissociate in water. Importantly, no facies resembling the Mooreville Chalk, nor any of its constituent assemblages (fossil or otherwise), was observed anywhere in either of the two drill cores.

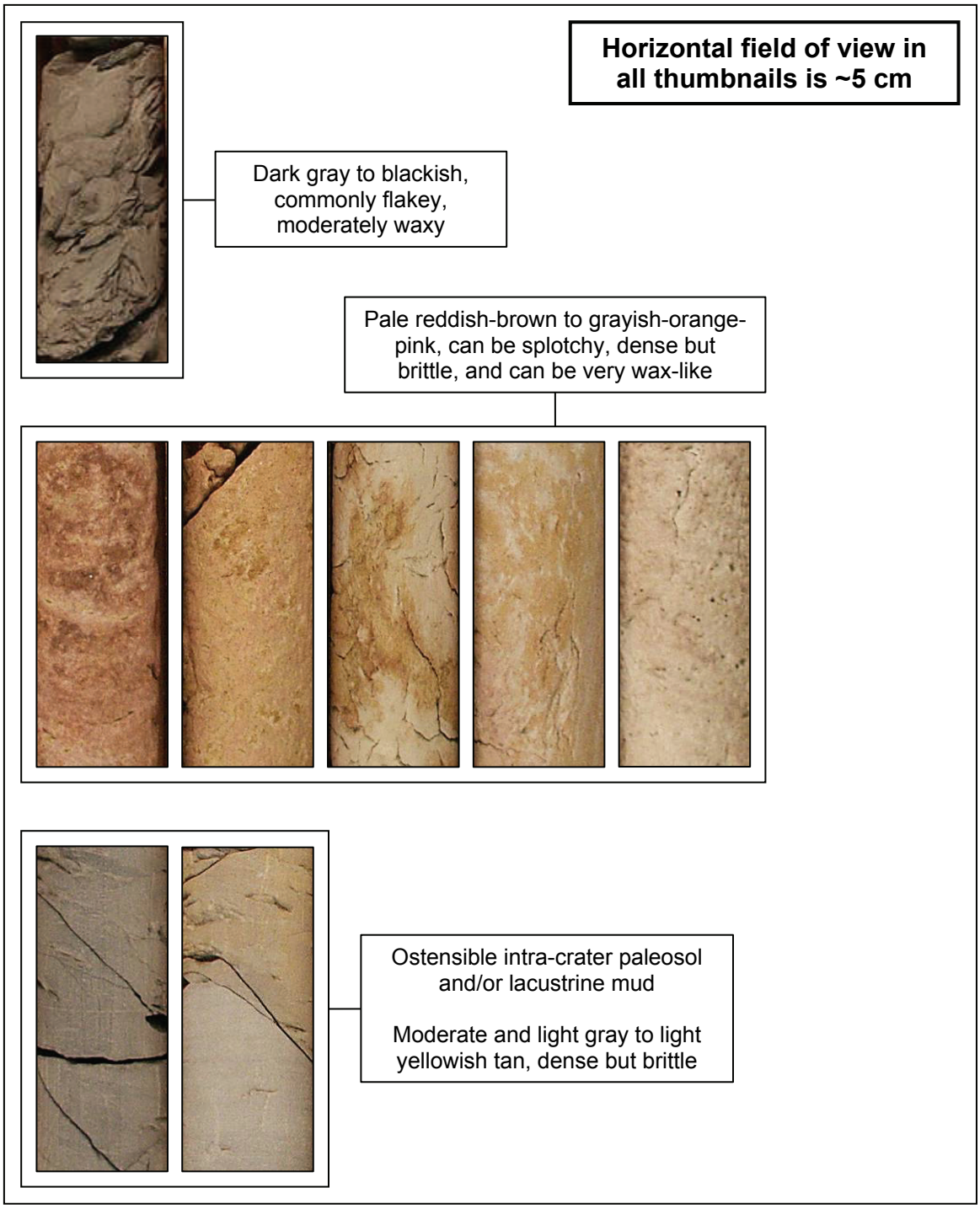

Figure 58. Representative examples of various *Mudstone/Siltstone* lithofacies. (Author's note: the histogram-like appearance of the photographs as grouped is of no particular meaning. Rather, certain lithologies categorized under this lithofacies presented a need to show their wider variety of appearances. Hence, five photographs of reddish-brown to pinkish-gray mud, and one photograph of the dark gray to blackish mud. Some of the other (following) figures of lithofacies examples share this trait.)

Sandy Mudstone / Sandy Siltstone Lithofacies

This lithofacies (Figure 59) is a grayish-orange-pink-to-brown, sand-bearing mudstone to siltstone with distinct bedding and bleaching along some fracture sets. Overall, this lithofacies is similar to the mudstone/siltstone lithofacies, except for a significant sand component herein. Colors in this lithofacies vary from grayish-orange-pink to several shades of orange, brown, and gray. Typical percent-composition shows broad variation in this lithofacies; ranges are 10-90% for muscovite, 5-100% for mud, and 5-50% for quartz sand. Minor biotite is present in some lithozones of this lithofacies. Grain-size distribution ranges from clay- and silt-size to coarse sand, and sorting varies from very poor to well. Grain shape (roundness and sphericity) ranges from subangular to subround, and subspheroidal to subdiscoidal. Bedding is primarily distinct but is also obscure in some places. Some regions appear plastically deformed. This lithofacies is entirely non-calcareous. Contacts (where present) range from distinct and sharp to transitional. Other features include *Taenidium* burrows (C. Savrda, pers. comm., 2005), fracture sets with reduction bleaching, splotchy coloration, pyrite concretions, lignite, and granules of quartz and mud. This lithofacies will easily dissociate in water, and a light sulfurous odor is common.

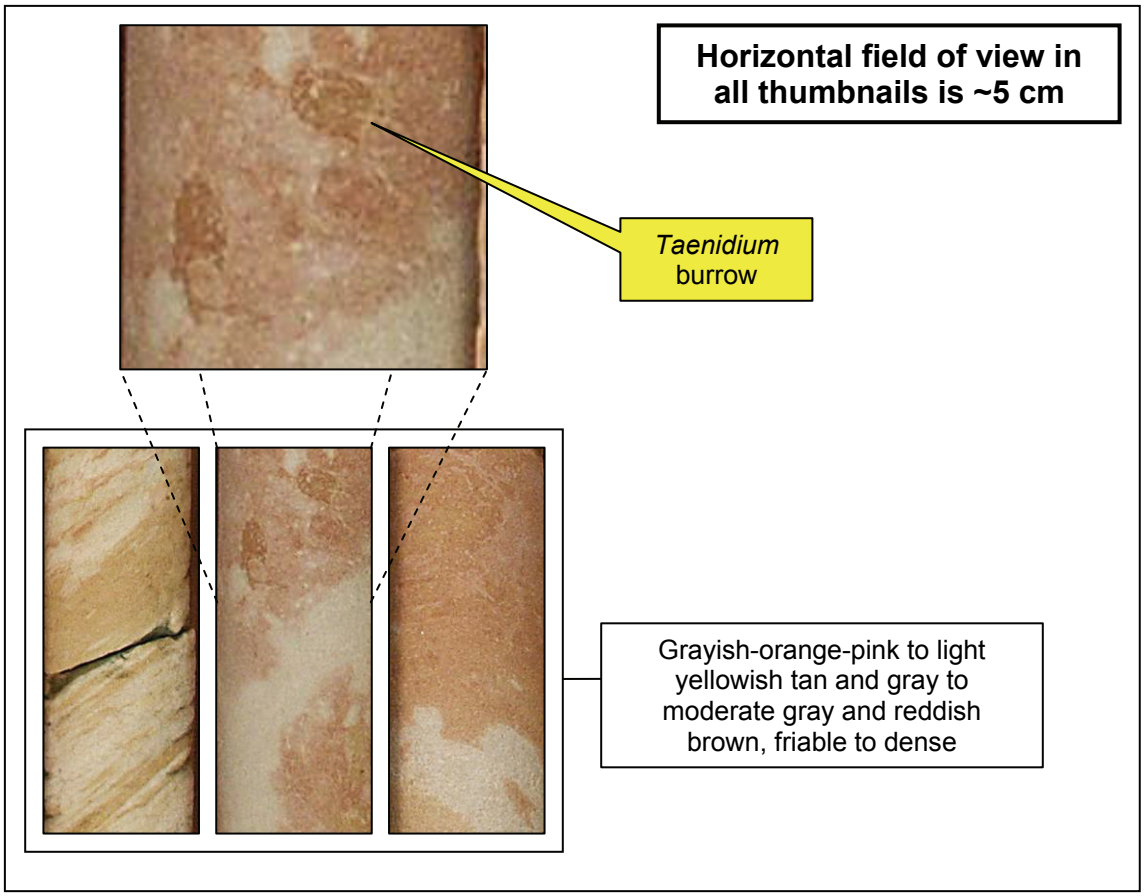

Figure 59. Representative examples of various *Sandy Mudstone/Sandy Siltstone* lithofacies.

Bedded Sandstone Lithofacies

This lithofacies is a grayish-orange-pink-to-brownish-gray, friable, bedded sandstone with non-calcareous cement and a light sulfurous odor (Figure 60). Granule- and pebble-size clasts of quartz and mud are common, with distorted mud clasts in some portions. Fragments of lignite and pyrite-cemented concretions are also present. Common color range is grayish-orange-pink, very pale orange, and light brownish-gray, with various other shades of browns, oranges, and grays. Typical percent-composition is approximately 50% quartz, 40% matrix, and 10% muscovite. Trace amounts of biotite may be found in some portions. One portion of this lithofacies exhibits approximately 80% muscovite, 10% quartz, and 10% biotite. Clasts of mud and quartz typically do not exceed ~5%. Grain-size distribution for most portions ranges from fine to very coarse with some sections exhibiting very fine sand. Sorting in most portions is uniform and ranges from very poor to poor. Some lithozones of this lithofacies exhibit moderate sorting throughout, while other lithozones show an alternating pattern of sorting within their overall thickness ranging from very poor to moderate. Grain shape (roundness and sphericity) in this lithofacies is typically subround to subangular, and subprismoidal to subdiscoidal. Bedding is mostly distinct and centimeter-scale. Many portions of this lithofacies type are inclined, and some appear to be nearly vertical or overturned. Distorted patterns that may or may not be bedding appear in some regions. This lithofacies type is non-calcareous throughout, and its contacts (where present) range from distinct to indefinite, sharp to transitional, planar to distorted, and horizontal to steeply inclined. Unusual features such as Liesegang banding, and 1 mm garnets are rare though present in some portions. This lithofacies will easily dissociate in water.

Figure 60. Representative examples of various *Bedded Sandstone* lithofacies.

Massive Sandstone Lithofacies

This lithofacies is a grayish-orange-pink-to-pale-reddish-brown, friable, massive sandstone with non-calcareous cement throughout, although calcite-cemented concretions and bioturbation are found in some regions (Figure 61). Some massive sands in the two drill cores are enigmatic and unusually clean while others hold distorted mud clasts. Color is primarily grayish-orange-pink, but light brownish-gray, pinkish-gray, dark yellowish-orange, and pale reddish-brown are also present. Typical percent-composition is approximately 50% quartz, 40% matrix, and 10% muscovite. Grain-size distribution for most portions of this lithofacies typically ranges from fine to coarse. Pebble-size quartz granules and mud clasts are present in some portions, but others hold distorted mud clasts >20 cm thick as measured down-hole. Sorting varies from one lithozone to the next, and within individual lithozones, although not in a manner consistent with graded bedding of any type or scale. Additionally, sorting may be either very poor, poor, poor to moderate, or moderate to well. Grain shape (roundness and sphericity) in this lithofacies is typically subangular to subround, and subspheroidal to subdiscoidal. Bedding is usually absent, although rare bedding-like structures may be observed. This lithofacies is non-calcareous except for a few centimeter-scale calcite-cemented concretions in some portions. Contacts (where present) are usually transitional and/or irregular. Distorted *Taenidium* burrows are found in some portions (C. Savrda, pers. comm., 2005). This lithofacies will easily dissociate in water.

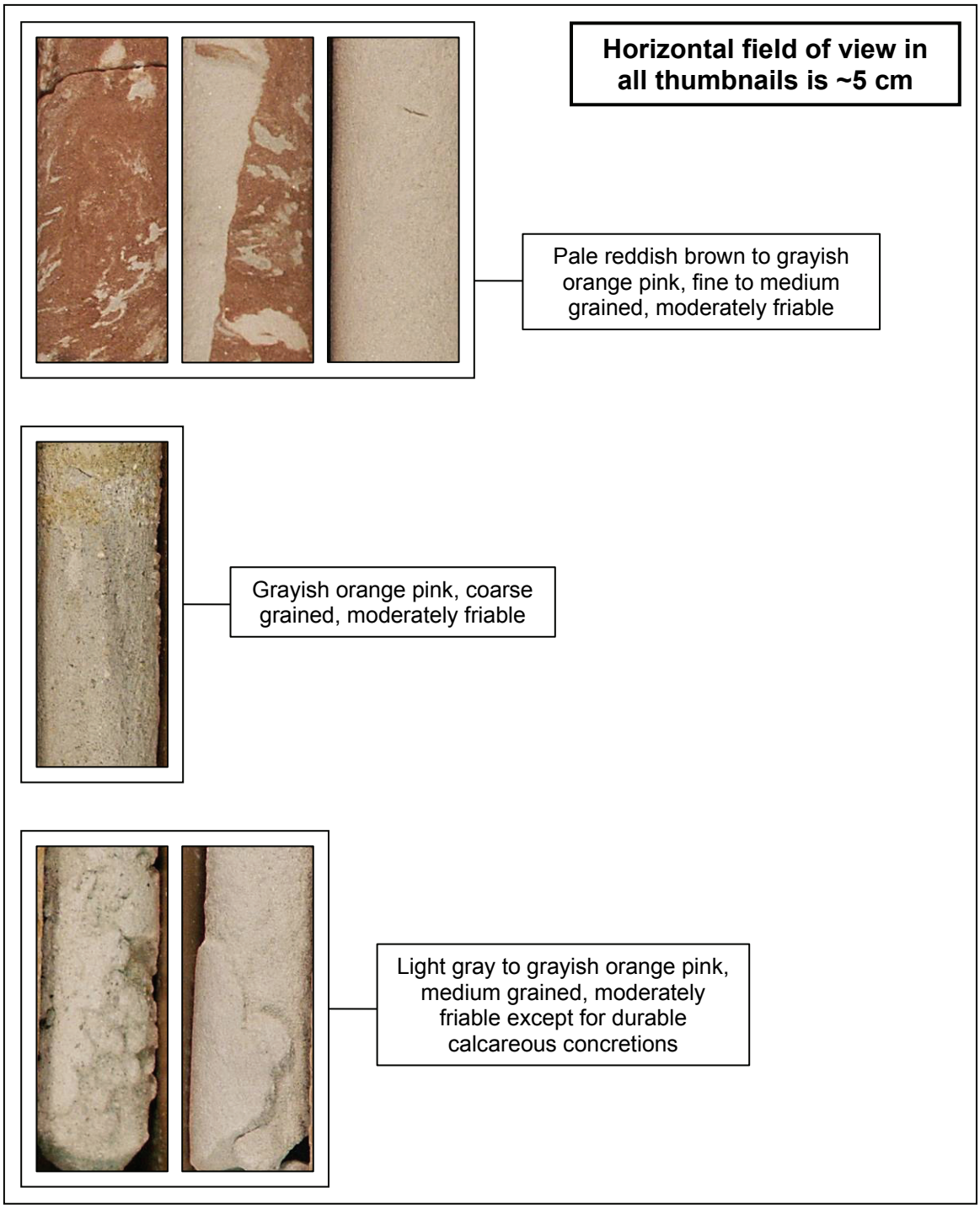

Figure 61. Representative examples of various *Massive Sandstone* lithofacies.

Interbedded Sandstone and Mudstone Lithofacies

This lithofacies is a grayish-orange-pink-to-pale-reddish-brown, friable, interbedded sandstone and mudstone with non-calcareous cement and distinct pyrite-cemented concretions (Figure 62). A moderate sulfurous odor is common in this lithofacies, and sub-millimeter lignite fragments are also present. Coloring is splotchy in regions and ranges from light brownish-gray to grayish-orange-pink to pale reddish-brown. Other colors present include medium dark gray, yellowish-gray, moderate reddish-orange, very pale orange, grayish-orange, and medium gray. Typical percent-composition is approximately 50% quartz, 40% mud matrix, and 10% muscovite. Some interbeds are 100% sand, others are variously mixed sand and mud, and still others are 100% mud. Grain-size distribution for most portions of this lithofacies ranges from clay- and silt-size in mud-rich zones, to very fine through coarse sand in sand-rich zones. Sorting is typically poor in sand-rich zones, though some regions range from moderate to very well. Grain shape (roundness and sphericity) in this lithofacies is typically subround, and subprismoidal to subdiscoidal. Bedding is centimeter-scale and alternates between mud-rich and sand-rich. As such, bedding is always distinct, although it is commonly very strongly distorted. Some bedding is very near vertical making it difficult to perceive as being other than massive. This lithofacies is non-calcareous throughout and its contacts (where present) are sharp to transitional, and are sometimes distorted. Centimeter-scale pyrite-cemented concretions are rare though easily spotted. Granule- to pebble-size quartz and mud clasts are present. This lithofacies will easily dissociate in water.

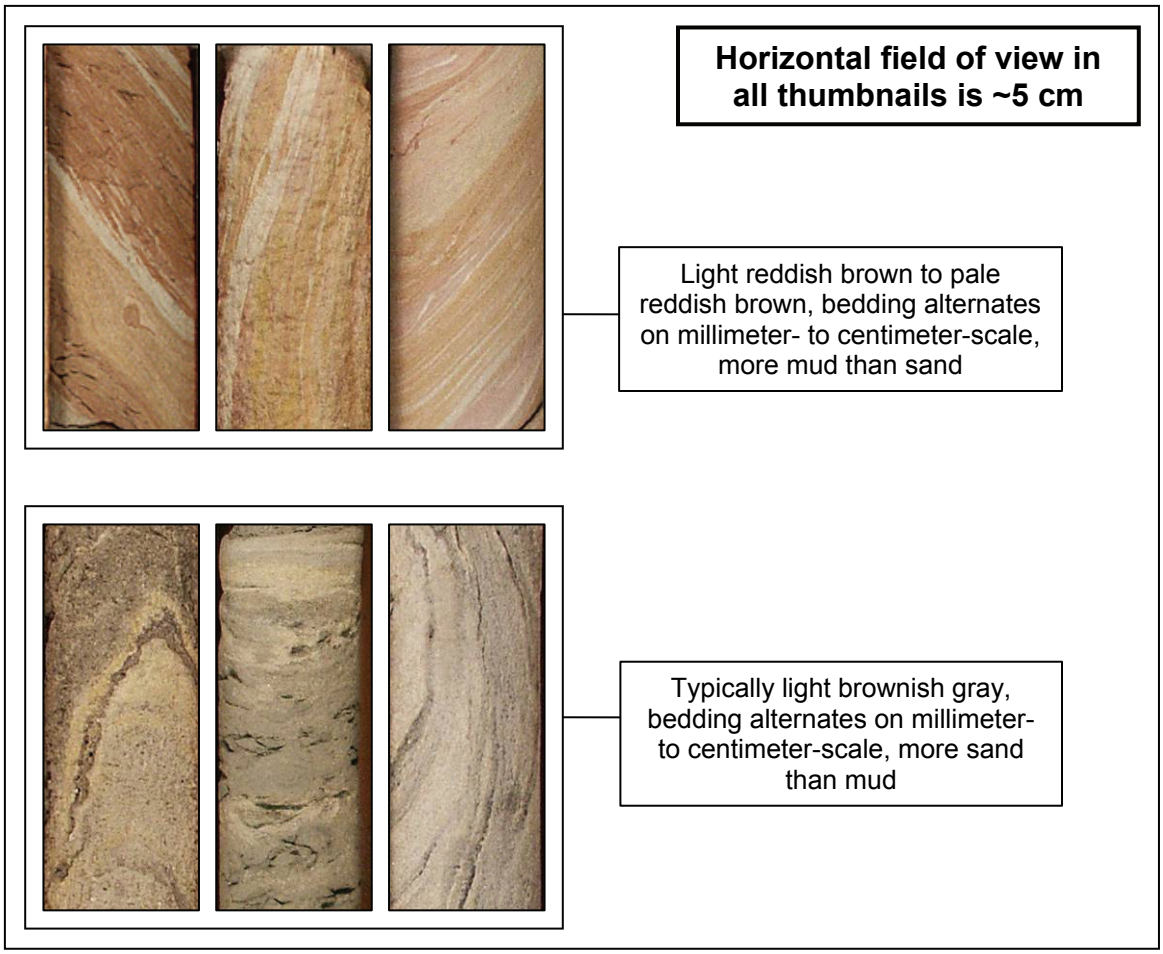

Figure 62. Representative examples of various *Interbedded Sandstone and Mudstone* lithofacies.

Contorted Interbedded Sandstone and Mudstone Lithofacies

This lithofacies is a grayish-orange-pink-to-light-brown, friable, interbedded sandstone and mudstone having a strongly disturbed appearance with non-calcareous cement and distinct pyrite-cemented concretions (Figure 63). Common features of this lithofacies are a light to moderate sulfurous odor, garnets in some portions, and "bull's-eye" patterns. Colors are typically grayish-orange-pink and light brownish-gray but yellowish-gray and light brown are also present. Typical percent-composition is approximately 50% quartz, 40% matrix material, and 10% muscovite. Grain-size distribution for most portions ranges from fine to medium, but some regions exhibit very fine to very coarse sand. Sorting typically ranges from very poor to moderate, but some portions are well sorted. Grain shape (roundness and sphericity) is typically subround, and subspheroidal to subdiscoidal. Bedding is centimeter-scale and strongly distorted, folded, and/or swirled, and varies from near horizontal to near vertical. This lithofacies is entirely non-calcareous except for a few centimeter-scale calcite-cemented concretions in no particular pattern or association. Contacts with other lithofacies types (where present) are commonly transitional, though discernable to distinct. Centimeter-scale pyrite-cemented concretions are rare but easily spotted, and granule- to pebble-size quartz and mud clasts are also found. This lithofacies will easily dissociate in water.

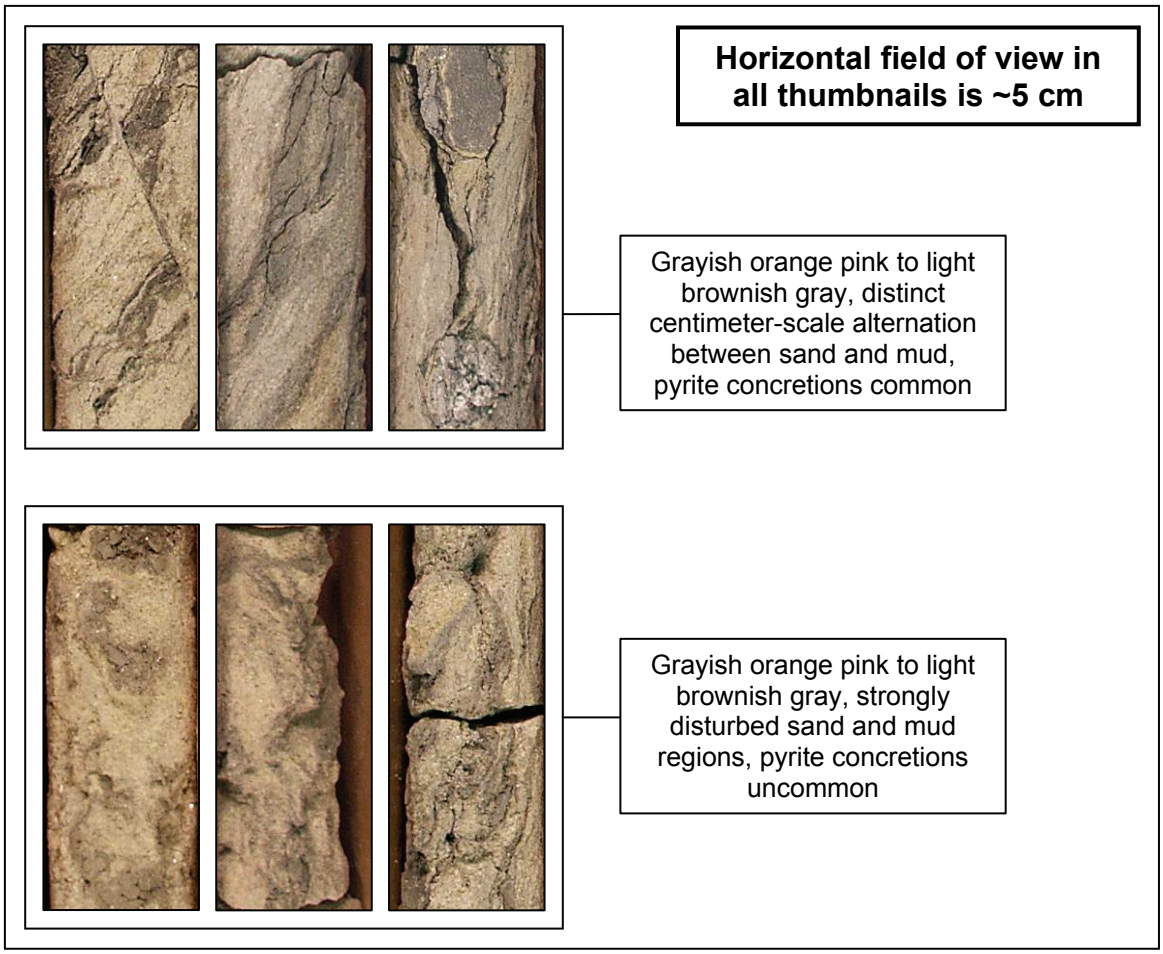

Figure 63. Representative examples of various *Contorted Interbedded Sandstone and Mudstone* lithofacies.

Structureless Sandstone Lithofacies

This lithofacies is a grayish-orange-pink, primarily massive sandstone with non-calcareous cement (Figure 64). Many portions of this lithofacies contain fragments of crystalline basement in addition to the mud clasts and quartz pebbles commonly found in the other lithofacies. This is an important distinction because fragments of crystalline basement are virtually absent from all other sandstone lithofacies in the two drill cores. This lithofacies is typically grayish-orange-pink, though browns and oranges are also present. Typical percent-composition is approximately 50% quartz, 40% matrix, and 10% muscovite. Grain-size distribution commonly ranges form fine to very coarse. Sorting in this lithofacies varies from lithozone to lithozone. Some lithozones show very poor or poor sorting throughout, while others display a range such as poor to moderate, or very poor to very well. Grain shape (roundness and sphericity) is typically subround, and subspheroidal to subdiscoidal, but some lithozones have grain shapes that are angular to subround, and subspheroidal to subdiscoidal. Importantly, bedding is usually absent; hence the adjective *structureless*. However, very rare bedding-like structures (where present) may be observed as faint to obscure, and distorted to swirled. This lithofacies is entirely non-calcareous. Contacts (where present) are commonly distinct or sharp, though some are transitional and/or distorted. This lithofacies will easily dissociate in water.

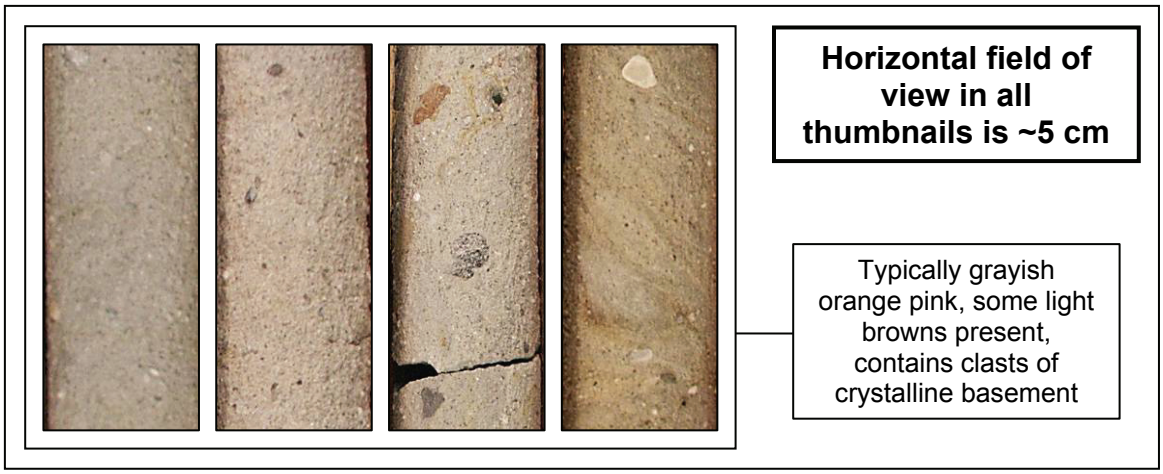

Figure 64. Representative examples of various *Structureless Sandstone* lithofacies.

Intermixed Breccia and Sands Lithofacies

This lithofacies is unique in that it is comprised of grayish-orange-pink, friable sands that are distinctly although incompletely intermixed with brownish-gray breccias containing centimeter-scale crystalline clasts (Figure 65). Colors are found in irregular patterns of grayish-orange-pink, dark yellowish-orange, and light brownish-gray. Typical percent-composition for the breccia component is approximately 80% matrix of muscovite/biotite, and 20% fragments of gneiss. The sands range from 90% matrix and 10% quartz to 50% quartz, 40% matrix, and 10% mica. Grain-size distribution for the matrix ranges from fine to very coarse and typical clast sizes are 3 mm to 4 cm. Sorting is very poor throughout. Grain shape (roundness and sphericity) is very angular to subround, and prismoidal to subdiscoidal. Bedding is irregular to swirled with possible flow lines. This lithofacies is entirely non-calcareous. The contact between the two lithologies is commonly chaotic but distinct and sharp, and appears to be near vertical in most regions of this lithofacies. Within the breccia are 1-2 mm garnets. This lithofacies will easily dissociate in water.

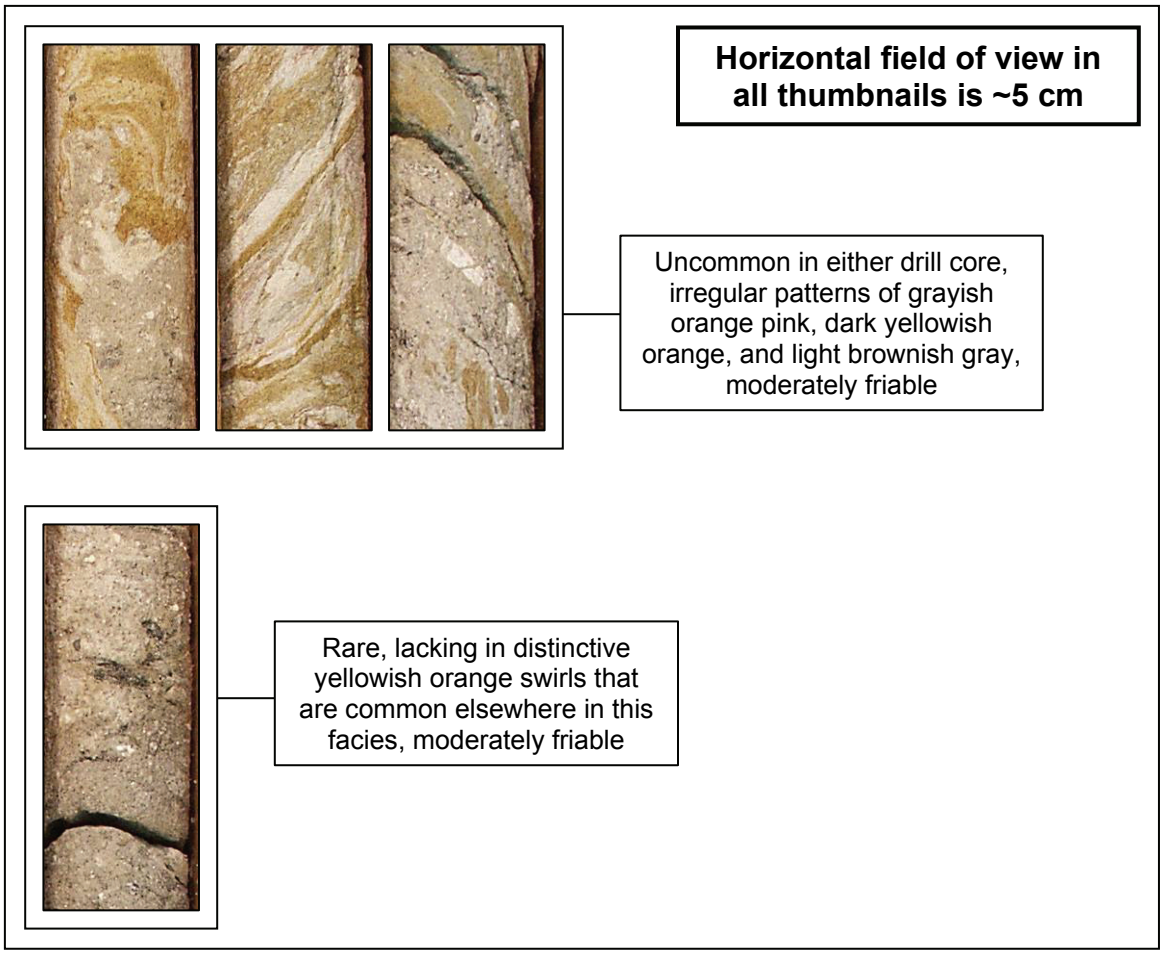

Figure 65. Representative examples of various *Intermixed Breccia and Sands* lithofacies.

Matrix-supported Breccia Lithofacies

This lithofacies is a grayish-orange-pink-to-light-brownish-gray matrix-supported breccia containing sedimentary and/or crystalline clasts within a sandy to powdery matrix (Figure 66). Some portions of this lithofacies are strikingly similar within both drill cores. Some regions show only crystalline clasts while others are a mix of crystalline and mud clasts. However, clasts are primarily gneiss and are typically undistorted. Where present, mud clasts are either distorted or undistorted. Some portions of this lithofacies alternate between fabrics that are distinctly wavy and not wavy. Overall color is consistently grayish-orange-pink to light brownish-gray. Clasts range from medium light gray to white. Matrix is generally light brownish-gray. Clast size is typically 1-4 cm but can range from 5 mm up to 15 cm. Matrix material is usually silt-size, although sand-size matrix is also present. Sorting is generally regarded as very poor, but certain grain-size assemblages are common, such as 1-4 cm clasts in silt-size matrix, or 1-9 cm clasts in silt-size matrix. Grain shape (roundness and sphericity) in this lithofacies is typically very angular to subround, and prismoidal to subdiscoidal. Bedding within lithozones of this lithofacies is primarily regarded as nonexistent because distinct changes in the overall facies of a given breccia were divided into separate, sometimes interbedded, breccia lithozones. However, some lithozones of this lithofacies do show distinctly wavy or chaotically intermixed regions. This lithofacies is entirely non-calcareous. Contacts (where present) are mainly distinct, and/or transitional, but few are actually sharp or well defined. There are no sandstone clasts in this lithofacies. This lithofacies will easily dissociate in water. Two lithozones (one in each drill core) show a distinct preferred orientation of both competent and sheared clasts (Figure 66, top).

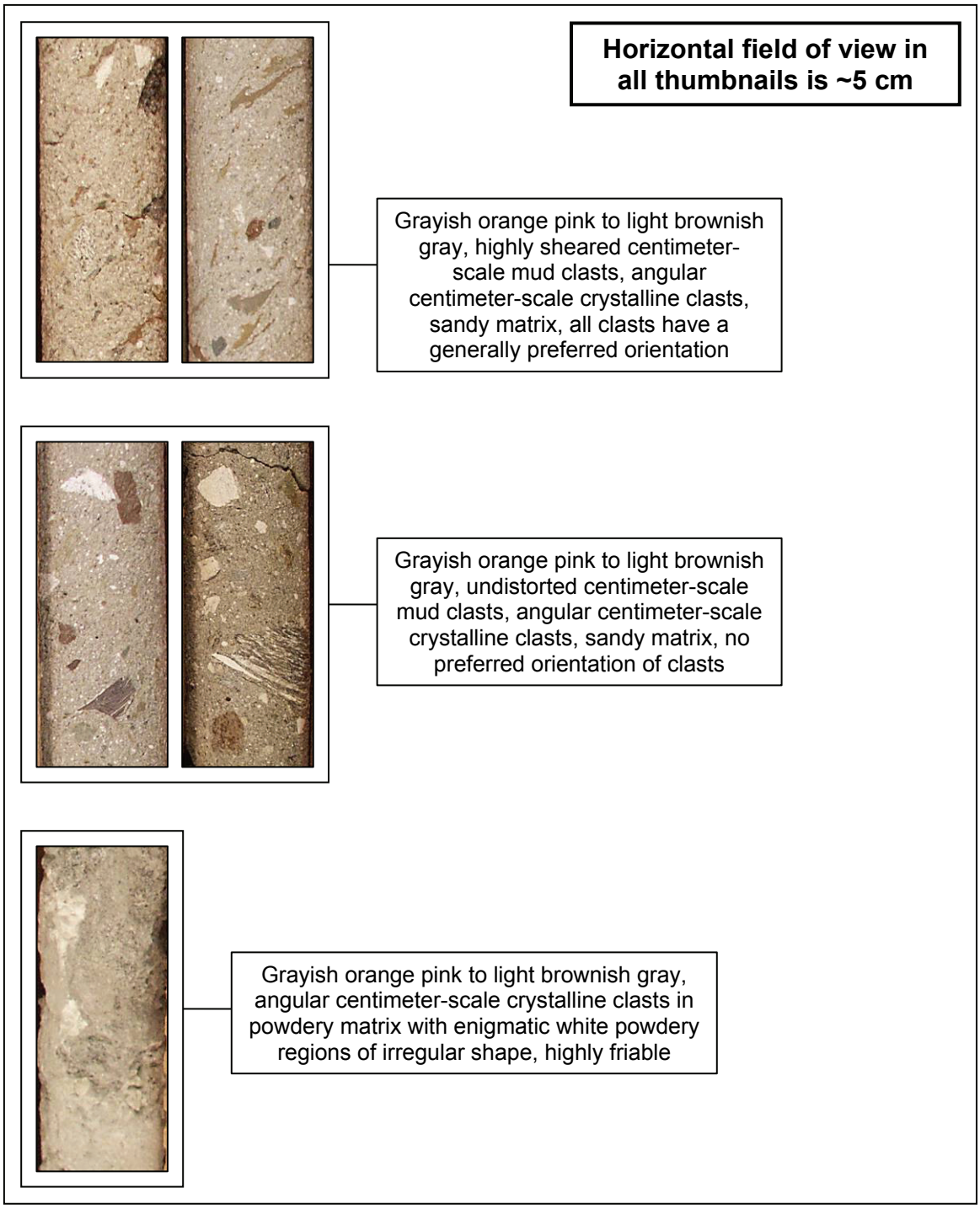

Figure 66. Representative examples of various *Matrix-supported Breccia* lithofacies.

Clast-supported Breccia Lithofacies

This lithofacies is a light-brownish-gray clast-supported breccia virtually devoid of sedimentary clasts, but containing numerous crystalline clasts within a sandy to powdery matrix (Figure 67). Lithozones of this category typically exhibit clasts of highly fractured gneiss, and to a lesser extent, highly fractured schist. Gneiss clasts are usually more competent than schist clasts. Although these crystalline clasts are solid and difficult to break while dry, they will easily dissociate when exposed to water. Overall color is light brownish-gray and very consistent. Grain color is usually medium light gray, but some gneiss fragments have been bleached white. The matrix material is typically light brownish-gray, although it is grayish-orange-pink in some lithozones. Clast size is generally 1 to 4 cm, but can range from 5 mm up to 20 cm. Matrix material is usually silt-size, but sand-size matrix is also present in some portions. Sorting is regarded as very poor, although certain grain-size assemblages are common, such as 1- to 4-cm clasts in silt-size matrix, or 1- to 9-cm clasts in silt-size matrix. Grain shape (roundness and sphericity) in this lithofacies is typically very angular to subround, and prismoidal to subdiscoidal. Bedding is regarded as nonexistent because distinct changes in this lithofacies were divided into separate, sometimes interbedded, lithozones of breccias. All breccia lithofacies are non-calcareous throughout. Contacts (where present) range from indeterminate to transitional to distinct, and may be irregular to contorted, as well as horizontal to steeply inclined. Some lithozones of this lithofacies show few 1-mm garnets in their clasts and matrix material. There are no sandstone clasts in this lithofacies. This lithofacies will easily dissociate in water.

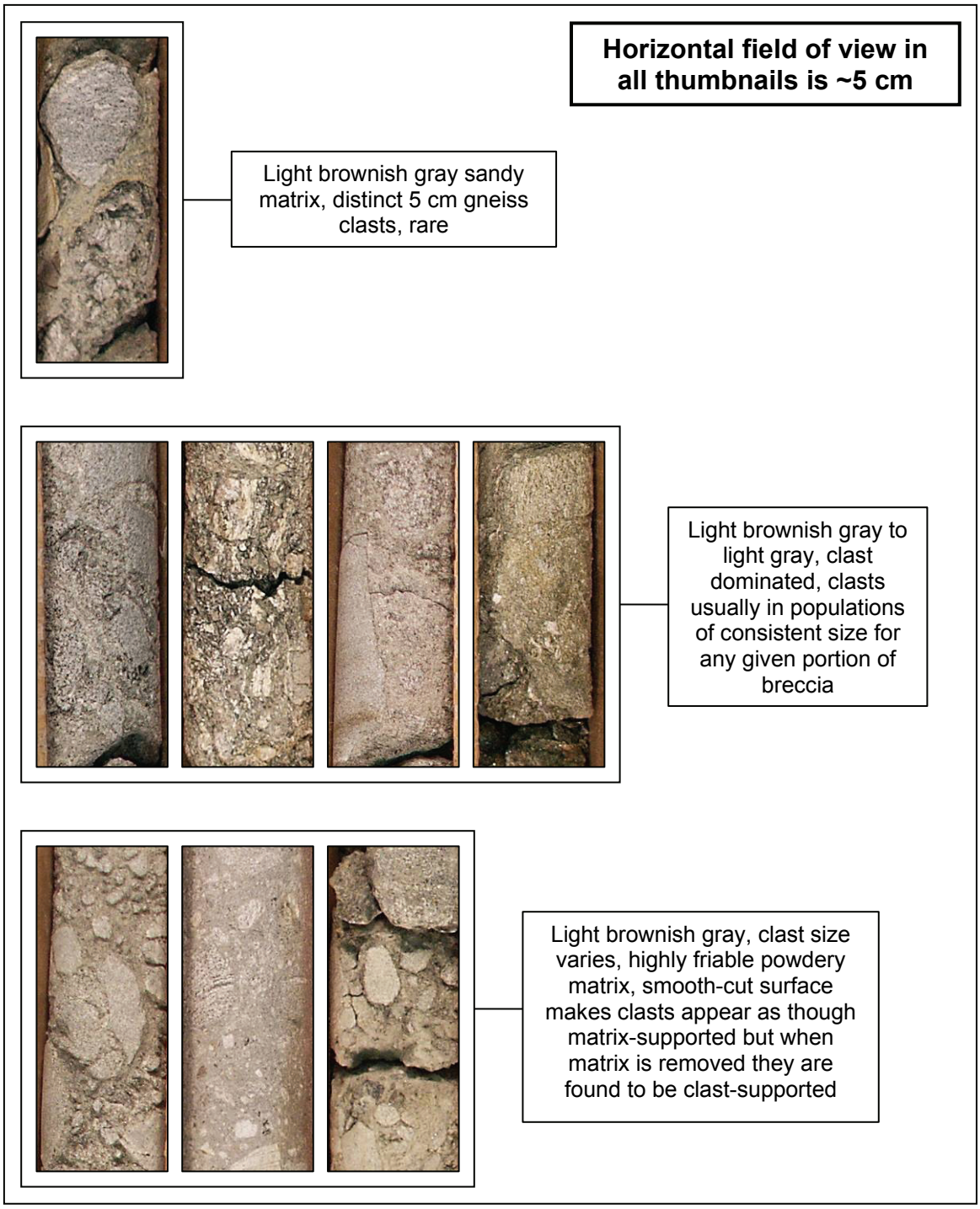

Figure 67. Representative examples of various *Clast-supported Breccia* lithofacies.

Schist Lithofacies

This lithofacies is a light-gray-to-goldish, strongly foliated, muscovite-biotite-quartz-garnet schist with the garnets not found throughout (Figure 68). In the drill cores, this lithofacies is commonly fractured along foliation planes and some portions appear highly altered and oxidized. Gneiss is present in some regions as are numerous 1- to 3-mm oxidized garnets. Light gray is the most common color, although one unusually extensive portion of this lithofacies displays a goldish hue. Others colors present are moderate to dark yellowish-brown, and grayish-orange-pink. Typical percent-composition shows varying quantities of muscovite (30-95%), biotite (5-60%), and quartz (5-20%). Texture is typically schistose with some granitic regions. Crystal size ranges from 1-3 mm. Grain shape is equant. Foliation is usually present and strong, but ranges from distinct to incoherent. Contacts (where present) are primarily transitional and fragmental, but some are distinct. Many regions are devoid of garnets while others contain numerous 1- to 2-mm oxidized garnets. Centimeter-scale quartz-rich zones are present but rare. This lithofacies will easily dissociate in water, even though hard and seemingly competent while dry.

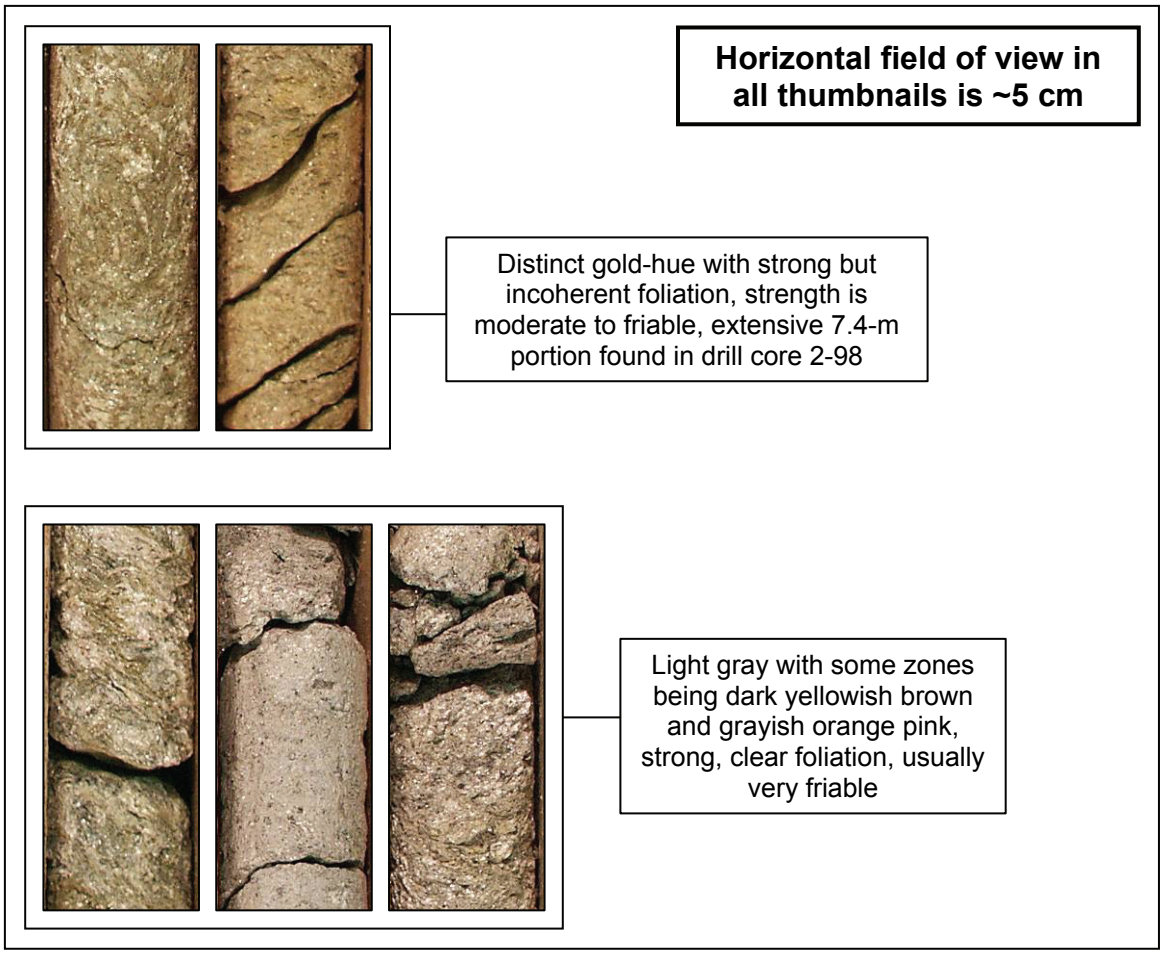

Figure 68. Representative examples of various *Schist* lithofacies.

Gneiss Lithofacies

This lithofacies is a light-gray, strongly foliated, plagioclase-biotite-quartz gneiss (Figure 69). Centimeter-scale fragments are a common trait of this lithofacies and may be competent or highly fractured (appearing as though an autobreccia). Regions of these clasts are often bordered by genuine breccias, although the clasts of this *Gneiss lithofacies* are clearly not part of those breccias. Overall color is generally light gray, but light yellowish-tan and light pinkish gray regions also exist. Typically, smaller clasts of this lithofacies are medium light gray to white. Grayish-orange-pink and grayish-orange zones are also present. Typical percent-composition is approximately 45% plagioclase, 35% biotite, and 20% quartz. Texture is granitic to schistose. Crystal size is ~1 mm. Crystal shape is typically equant, and the overall fabric is distinctly foliated. Certain extensive portions of this lithofacies at the bottom of drill core 2-98 exhibit a vertically oriented foliation. Contacts (where present) are mostly angular owing to the competent nature of the fragmented gneiss, but some contacts are transitional and/or rubbly. Millimeter-scale garnets are present in the more schistose zones, although they are few in number. Quartz-rich zones are also few. Durable portions of seemingly competent, solid gneiss will easily dissociate in water.

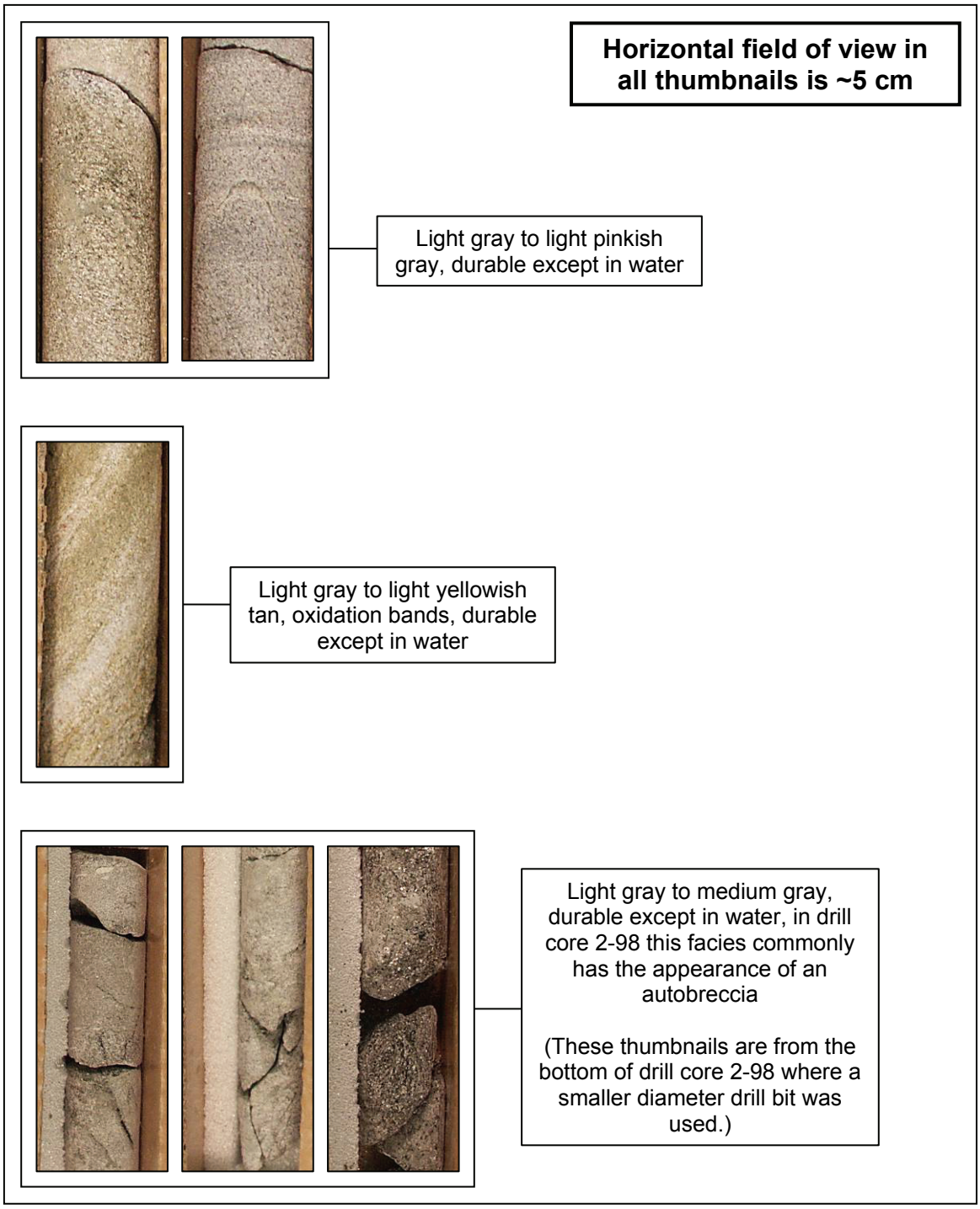

Figure 69. Representative examples of various *Gneiss* lithofacies.

4. Quantitative Breakdown of Lithozone Data

In this section, data for the lithozones from both drill cores are pooled into one dataset. The graphs that follow provide a quantitative breakdown of raw data from both drill cores combined to give an overall picture of the crater-filling materials at the two 1998 drill sites. The reader must remember that these data represent lithozones, as defined earlier, not lithologies or individual large clasts in the crater-fill.

Before one may fully understand the two drill cores, one must also understand the drill *holes* from which they were pulled. Taken together, the two drill *holes* represent a combined drill-length of approximately 374.14 m. The total thickness of all recovered drill core from this combined length is roughly 196.65 m, or approximately 53% of the total drilled length. This apparent half-recovery stems from two different origins, each taking place during drilling. The first origin of non-recovery is due to ~127 m of drill *hole* that were *purposely not cored*. The rationale was that the top several tens-of-meters in each drill hole were thought to be unnecessary at the time of drilling. Additionally, problems encountered while coring further down hole forced the drillers to purposely abandon core recovery attempts at one depth interval in each drill hole. The second origin of non-recovery relates to the additional ~51 m of drill *hole* wherein recovery of drill core was attempted, but was unsuccessful.

The total combined thicknesses of the various lithozones for each lithofacies within both drill cores are plotted as a histogram in Figure 70. Missing sections, and regions purposely not cored, are also depicted. This breakdown shows that ~86% of drill core was recovered successfully where attempts were made. These data also show that total combined thicknesses of the lithozones for each of the twelve lithofacies are

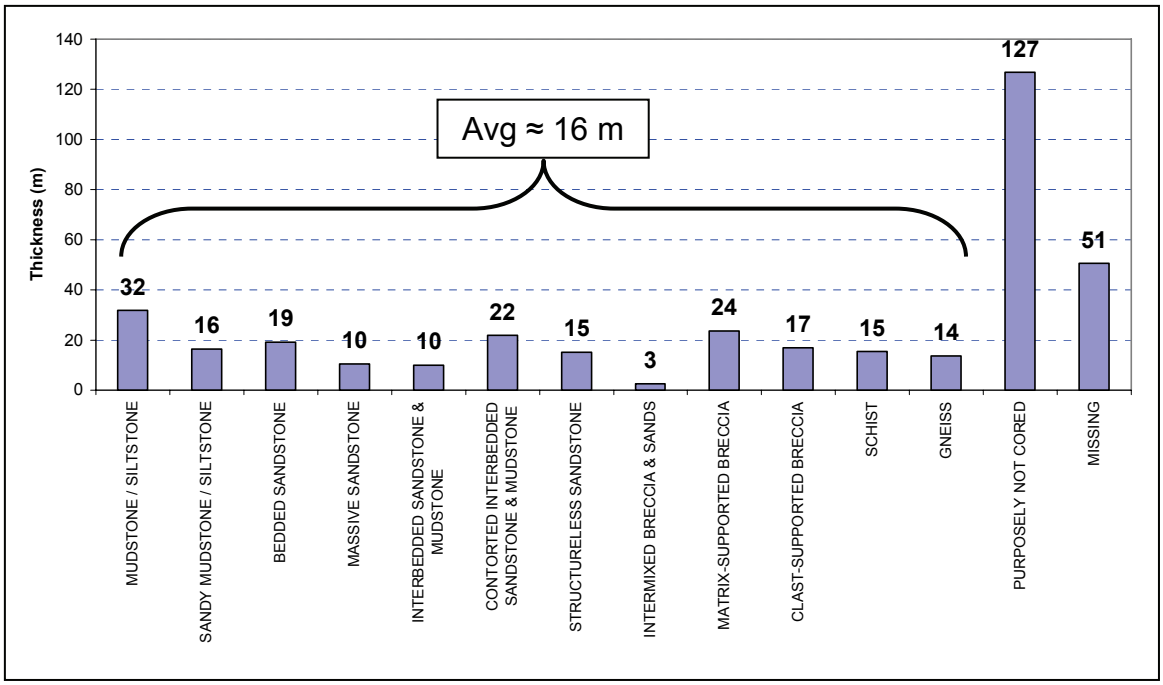

Figure 70. Total combined thicknesses of lithozones for each lithofacies within both drill cores. Absent sections were also graphed for comparison. Data graphed using Microsoft® Excel® 2003.

generally consistent from one drill core to the other, with little variation by lithology. The average total combined thickness is ~16 m.

Percentages of the combined thicknesses of each lithozone were plotted by lithofacies against the total combined length of the two drill holes (Figure 71). These data show that, overall, each category of lithofacies accounts for only a small percentage of the entire length of both drill holes. Quantitatively, each lithofacies represents ~4% of the combined length of the two drill holes. There was little variation by lithology. The graph also shows that ~34% of the combined length of both drill holes was purposely not cored, and an additional ~14% of the overall length did not yield any drill core despite efforts to retrieve it.

Percentages of the combined thicknesses of each lithozone were also plotted against the total length of recovered drill core (Figure 72). In other words, missing portions, and sections purposely not cored were excluded from this quantitative analysis. These data show that, overall, each of the twelve lithofacies accounts for ~8% of the combined length of the two drill cores. As with the previous graphs, there was little variation by lithology.

Figure 73 illustrates the thicknesses of individual lithozones (grouped by lithofacies) as entered in the LogPlot™ software. These data show that MISSING portions are by far the most commonly logged "zone" but that they are also consistently less than 1 meter thick. The four most frequently logged lithofacies are the two breccia lithofacies, along with the STRUCTURELESS SANDSTONE, and the MUDSTONE / SILTSTONE lithofacies. Each of these four lithofacies were logged approximately thirty times, and except for the MUDSTONE / SILTSTONE lithofacies, the majority of

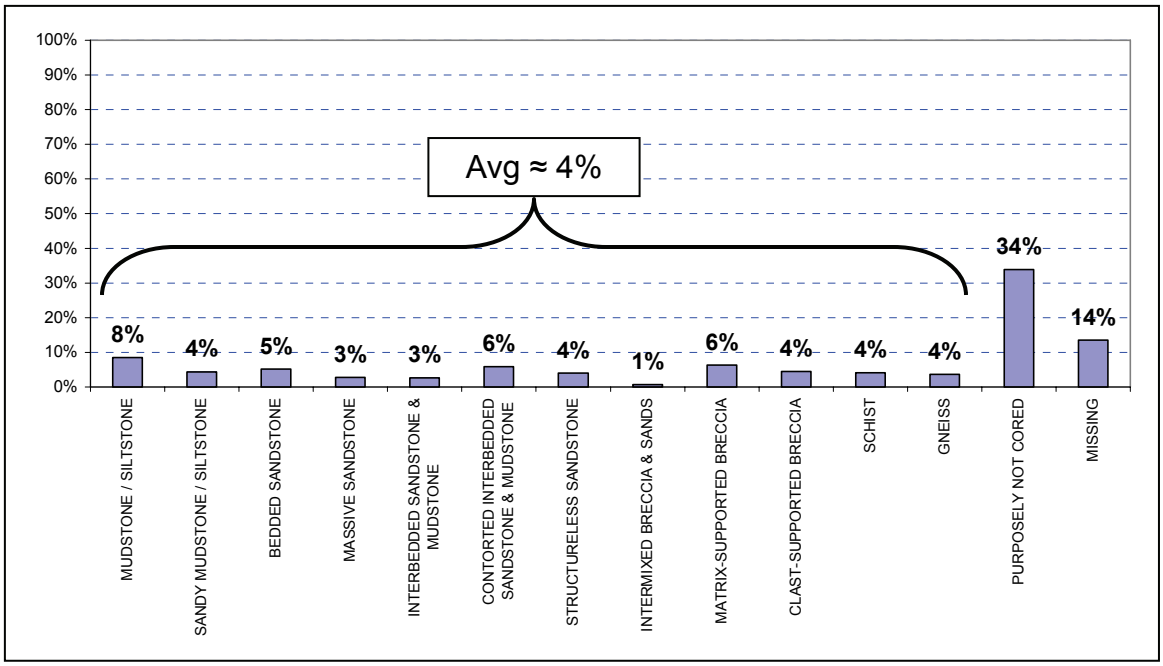

Figure 71. Percentages of lithofacies versus total depth of drill holes. Absent sections were also graphed for comparison. Data graphed using Microsoft® Excel® 2003.

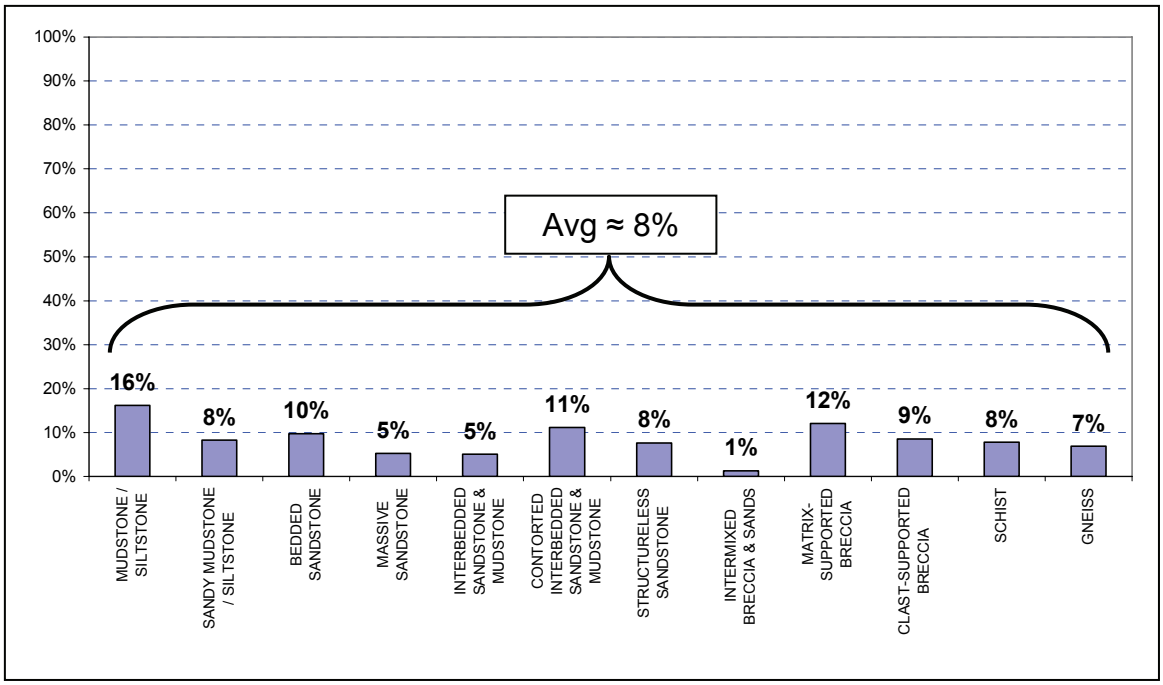

Figure 72. Percentages of lithofacies versus total recovered drill core. Data graphed using Microsoft® Excel® 2003.

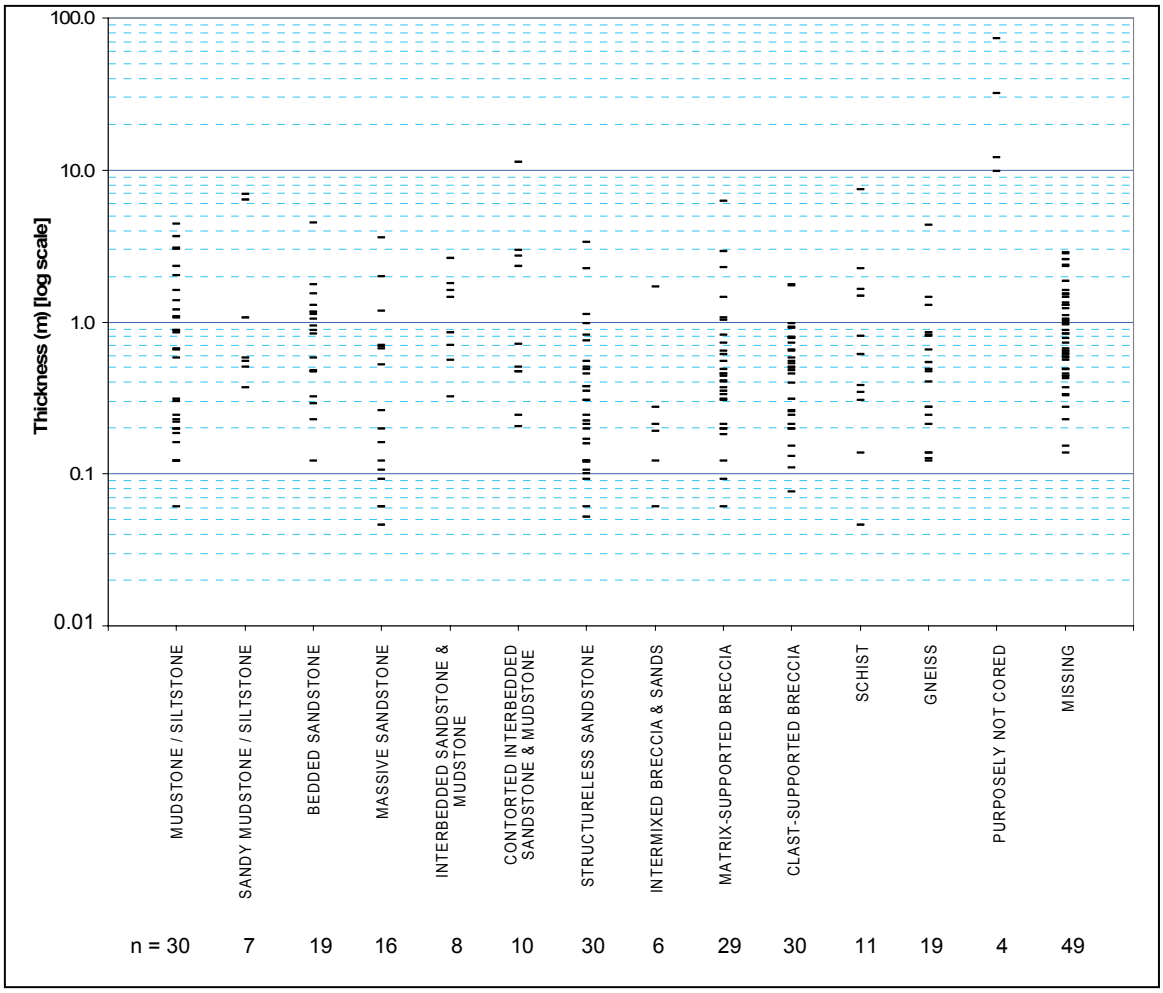

Figure 73. Scatter plot showing thicknesses of individual lithozones for each lithofacies as logged in the LogPlot 2005™ software. Note that "scatter" is on the Y-axis only, as data are grouped on the X-axis into their respective lithofacies categories. Absent sections were also graphed for comparison. Data graphed using Microsoft® Excel® 2003.

their thicknesses are typically less than 1 meter. These four lithofacies show the most evenly spread thickness distribution of all lithofacies. GNEISS was logged 19 times, and SCHIST was logged 11 times, but the latter shows a larger distribution of thicknesses. Together, the thickness distributions for these lithofacies range from ~4 cm up to nearly 8 m. Lithozones of BEDDED SANDSTONE and MASSIVE SANDSTONE were logged 19 and 16 times respectively, and show thickness distributions on par with that of the GNEISS. The remaining lithofacies were each logged 10 times or less. Even so, they share similar thickness distributions amongst themselves, except for the rarely present INTERMIXED BRECCIA & SANDS lithofacies, which is skewed toward being less than 0.5 m thick. Portions logged as PURPOSELY NOT CORED show up as being the thickest "zones" logged. These four sections range between ~10 m and ~75 m thick.

Results of Ancillary Objectives

The six ancillary objectives were both investigative and interpretive. These goals, centered on elucidating the nature and origin of the various crater-filling materials found within the drill core in terms of their possible modes of emplacement, their temporal relationships, and the post-impact paleoenvironments that particular sections of drill core may represent.

1. Results of Clarifying Structures and/or Patterns found in the Drill Core

The process of using the TurboCAD® software to simulate drill core taken from virtual models of various 3-D geological structures gave useful insight into the patterns and structures that could manifest in such drill core. The eleven figures that follow (Figure 74 through Figure 84) contain a graphical depiction of the results from the virtual coring process.

The set of modeled structures begins with simple parallel, planar bedding in different orientations, and moves into progressively more complex models. No attempt was made to simulate all possible structures because many structures are combinations of those depicted in the figures.

The resulting simulated drill core is depicted to the right of each structure by showing all four sides of the same leg. The viewpoint of each leg of simulated drill core is labeled as either Front, Back, 90° CW (rotated 90° clockwise from the Front view), or 90° CCW (rotated 90° counterclockwise from the Front view). The Back view was rotated 180° from the Front view.

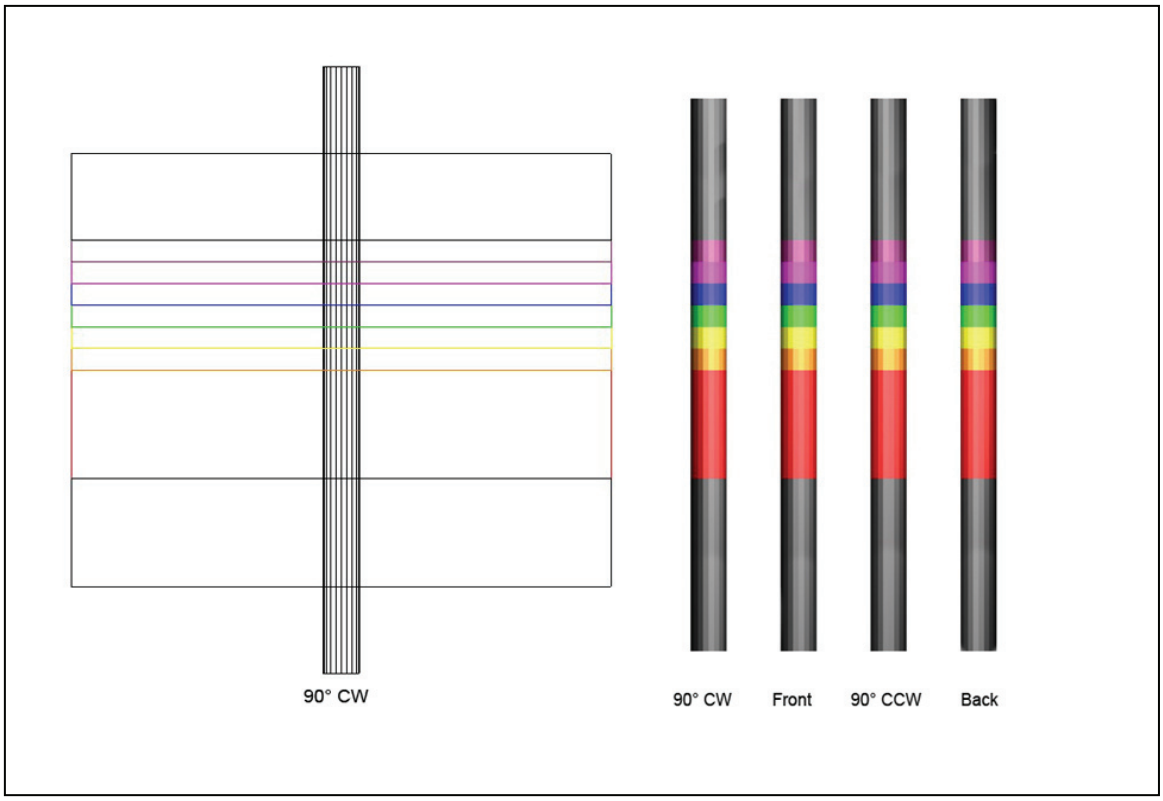

Figure 74. TurboCAD® simulation of *Bedding/Lithozone Contact – Horizontal*. Coring through a block with its layers in a horizontal orientation is uncomplicated. There is no repetition of the bedding pattern as is a common result of coring other, more complicated structures.

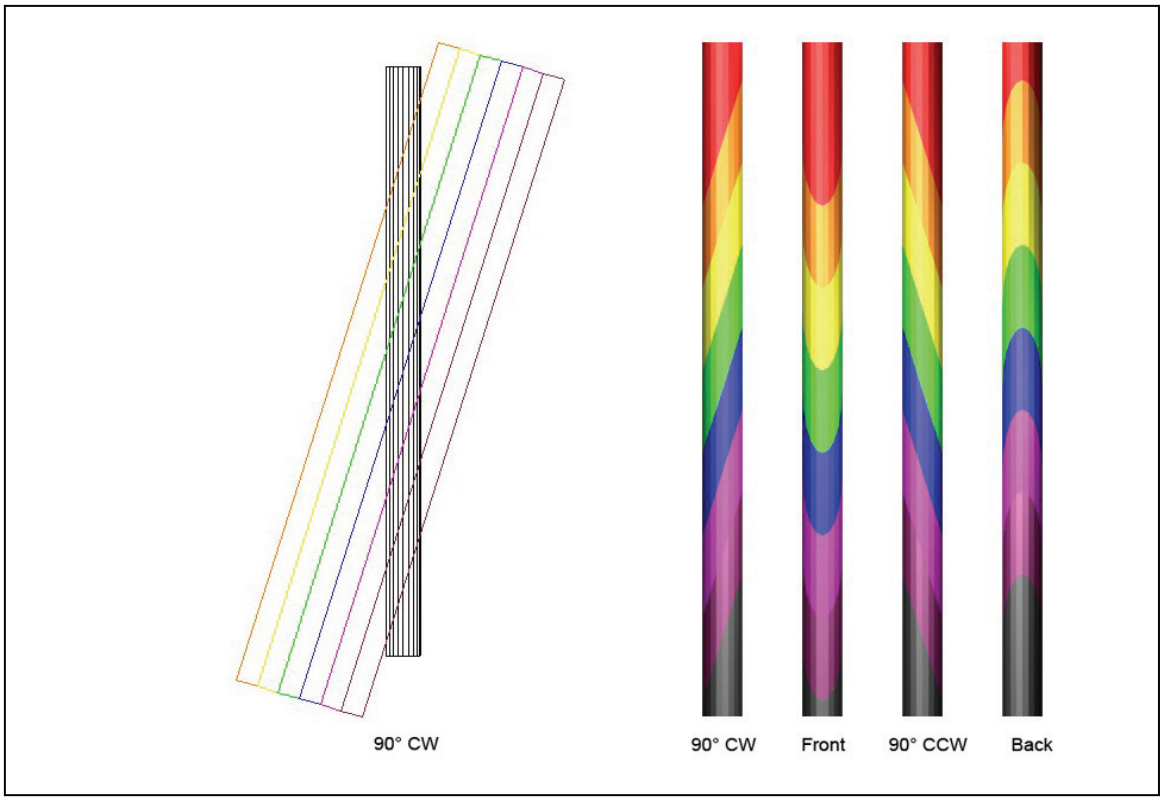

Figure 75. TurboCAD® simulation of *Bedding/Lithozone Contact – Inclined*. Coring through a block with previously horizontal layers now oriented in an inclined fashion produces units that, for example, may be mistakenly interpreted in drill core as cross-bedding in a thick horizontal bed. Note the upright and inverted U-shapes on the front and back views.

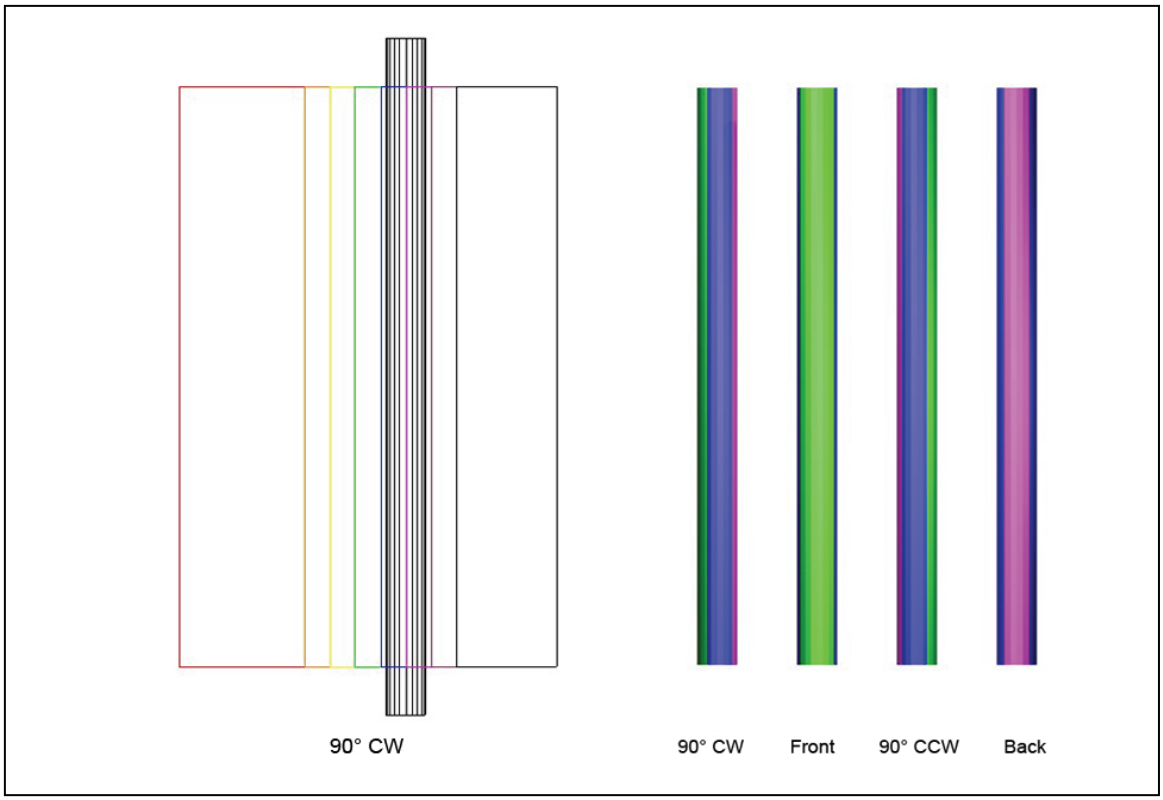

Figure 76. TurboCAD® simulation of *Bedding/Lithozone Contact – Vertical*. Coring through a block with its previously horizontal layers now oriented in a vertical fashion produces long, narrow strips of bedding parallel to the core's long axis. Such narrow strips may be difficult to recognize if they are at all distorted, or discontinuous.

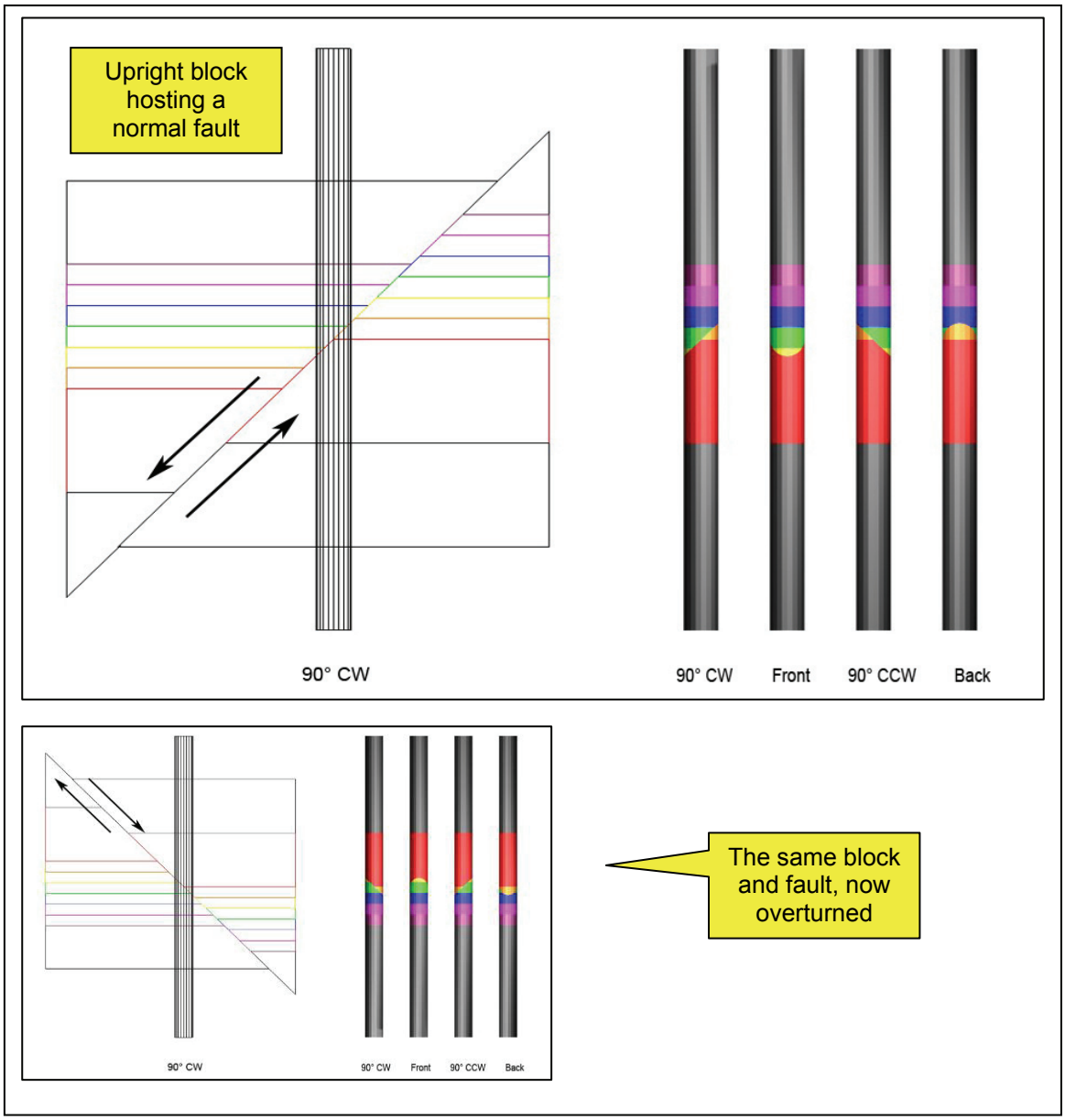

Figure 77. TurboCAD® simulation of *Fault – Normal*. Normal faults will manifest as normal faults regardless of whether their host blocks are right side up or upside down. They will not manifest as a reverse fault. An effect is that beds actually present in the block can be artificially thinned when manifest in the drill core, or altogether missed by the drill core. Patterns in the drill core will be the same for oblique slip on normal faults.

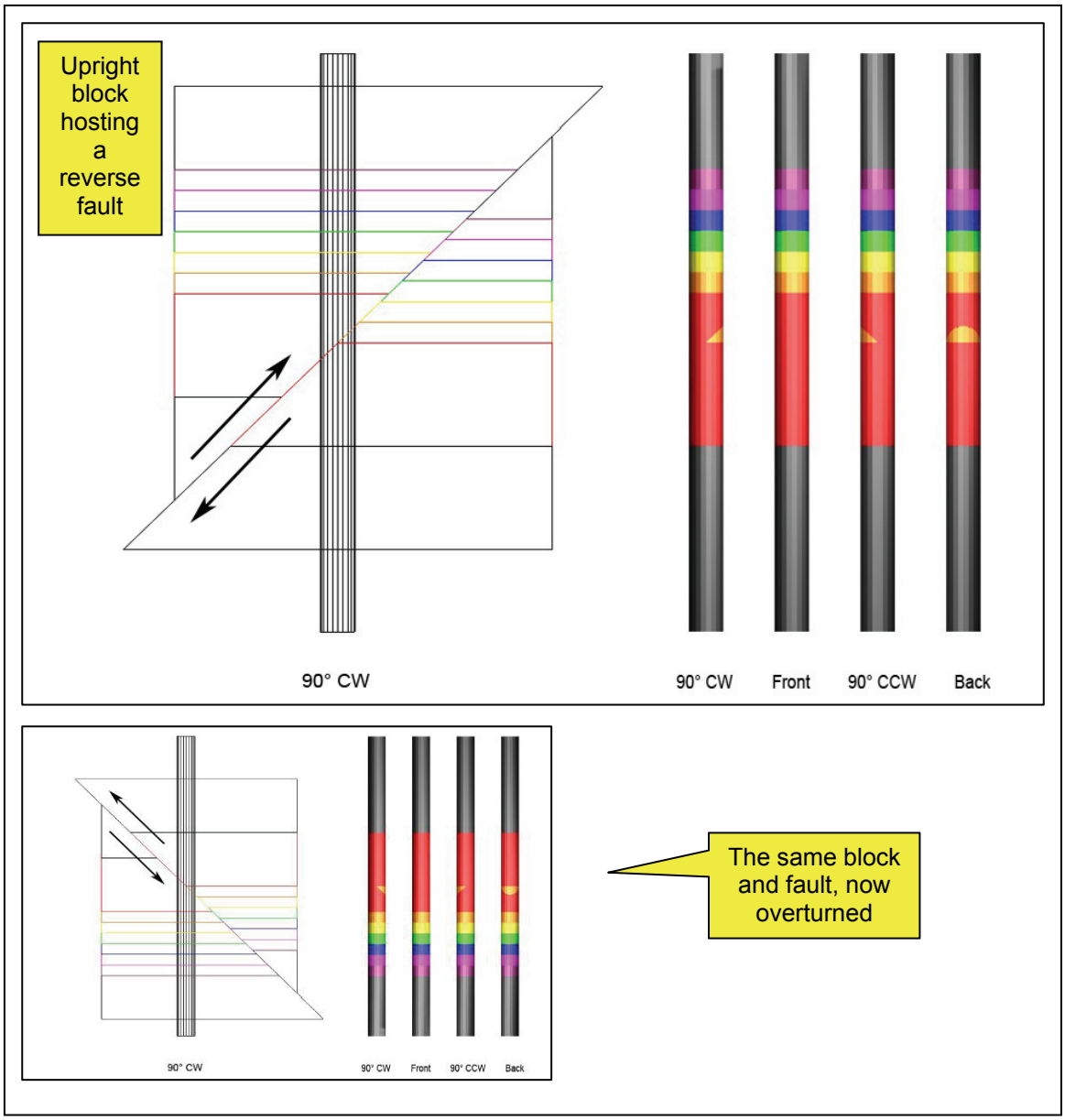

Figure 78. TurboCAD® simulation of *Fault -- Reverse*. Reverse faults will manifest as reverse faults regardless of whether their host blocks are right side up, or upside down. They will not manifest as a normal fault. An effect is that beds present in the block can be artificially thickened when manifest in the drill core, but not missed by the drill core (unlike cored normal faults). Patterns in the drill core will be the same for oblique slip on reverse faults.

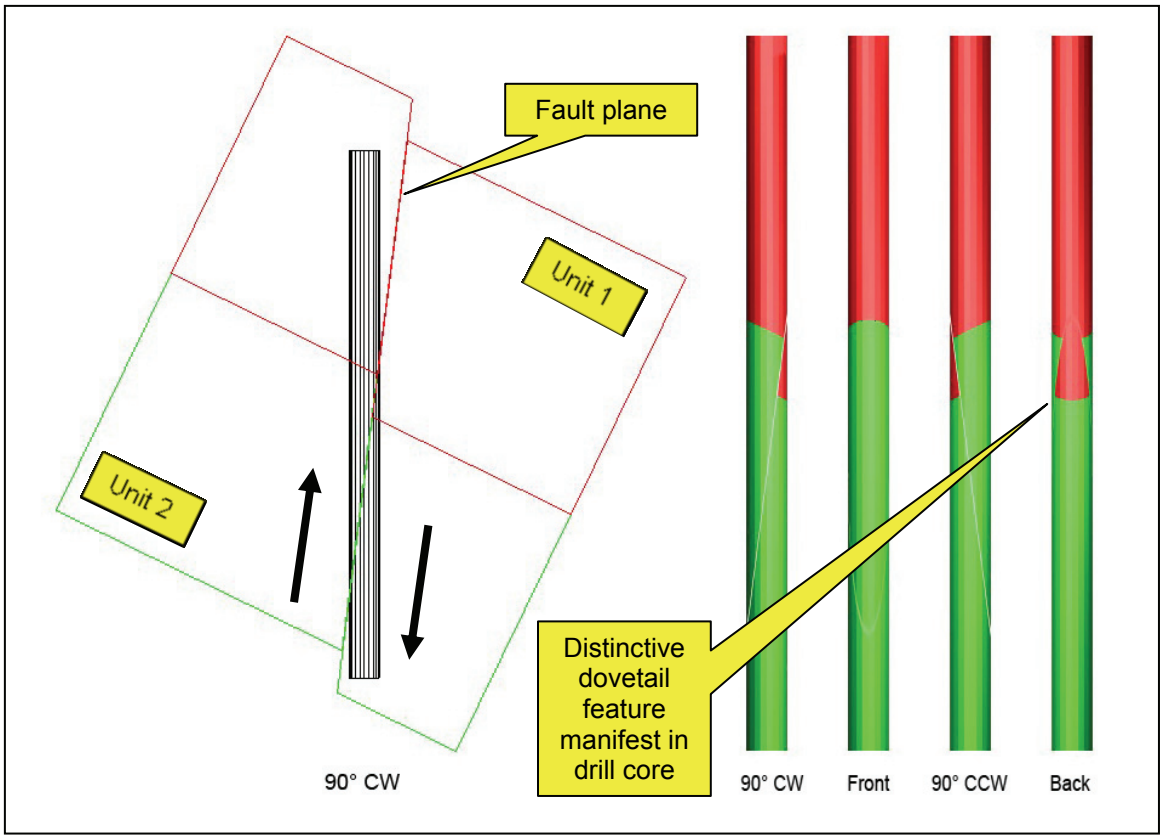

Figure 79. TurboCAD® simulation of *Fault – Near vertical with resulting dovetail feature in drill core*. This is a special case of faulting as manifest in drill core. In the model, two beds are steeply inclined, and a fault cutting through them is even more steeply inclined. The outcome is essentially the same, regardless of whether the fault is normal or reverse, but the dovetail feature will be inverted.

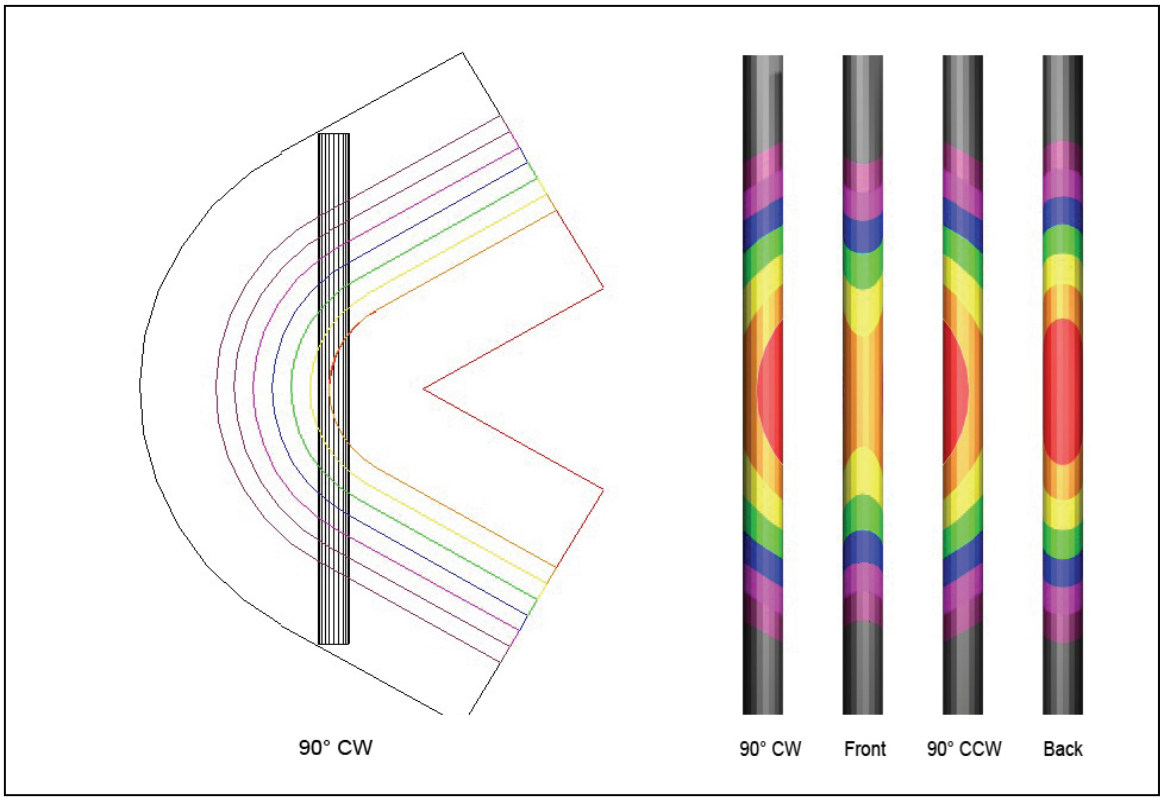

Figure 80. TurboCAD® simulation of *Fold – C-shaped*. When cored, this structure produces a distinctive bull's-eye pattern. When coring S-shaped folds, stacked bull's-eyes facing opposite directions will be produced.

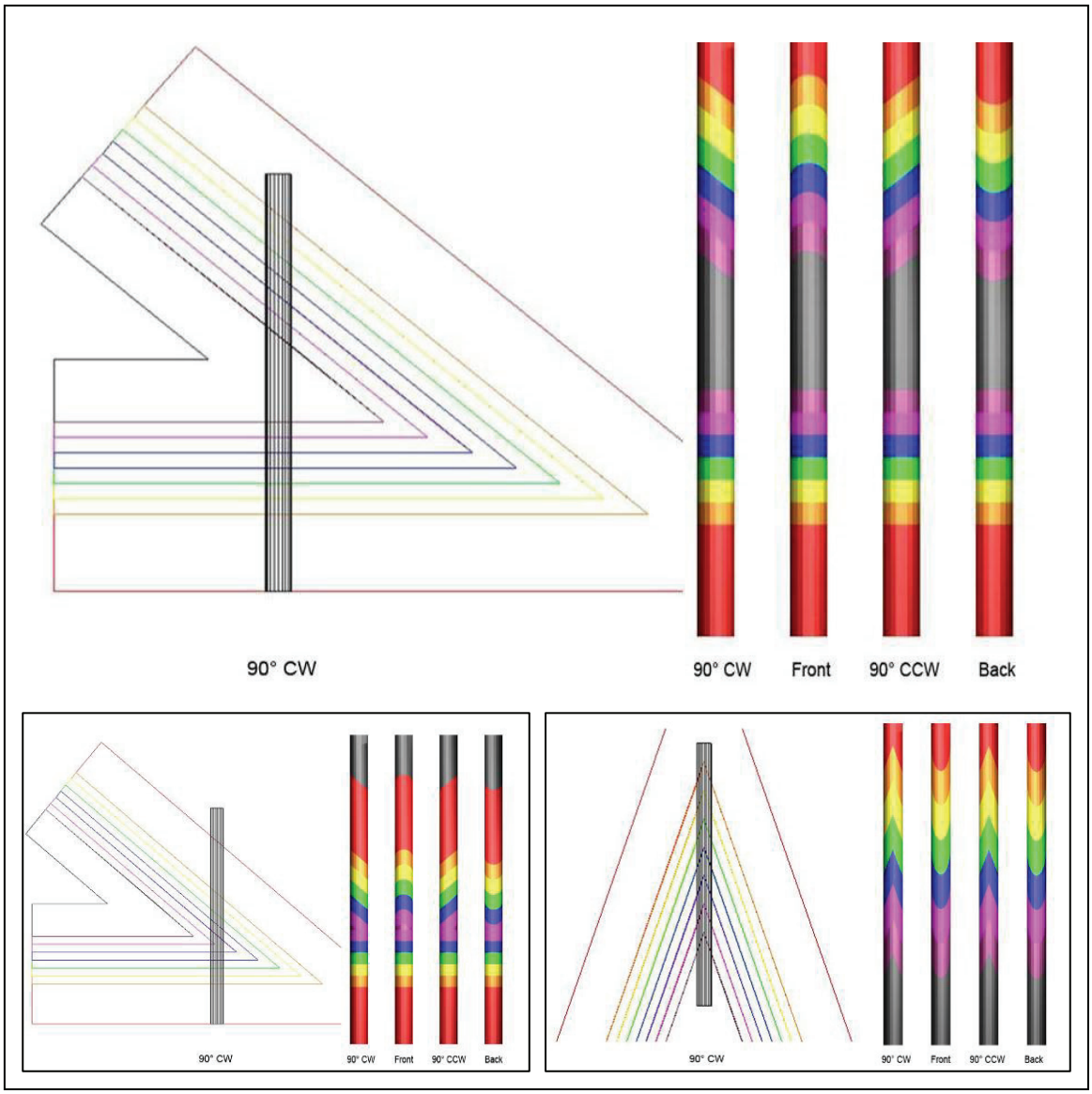

Figure 81. TurboCAD® simulation of *Fold – V-shaped*. Notice the mirrored bedding pattern except in the vertically oriented fold, which instead forms chevrons in drill core on the two faces rotated 90° from the Front view.

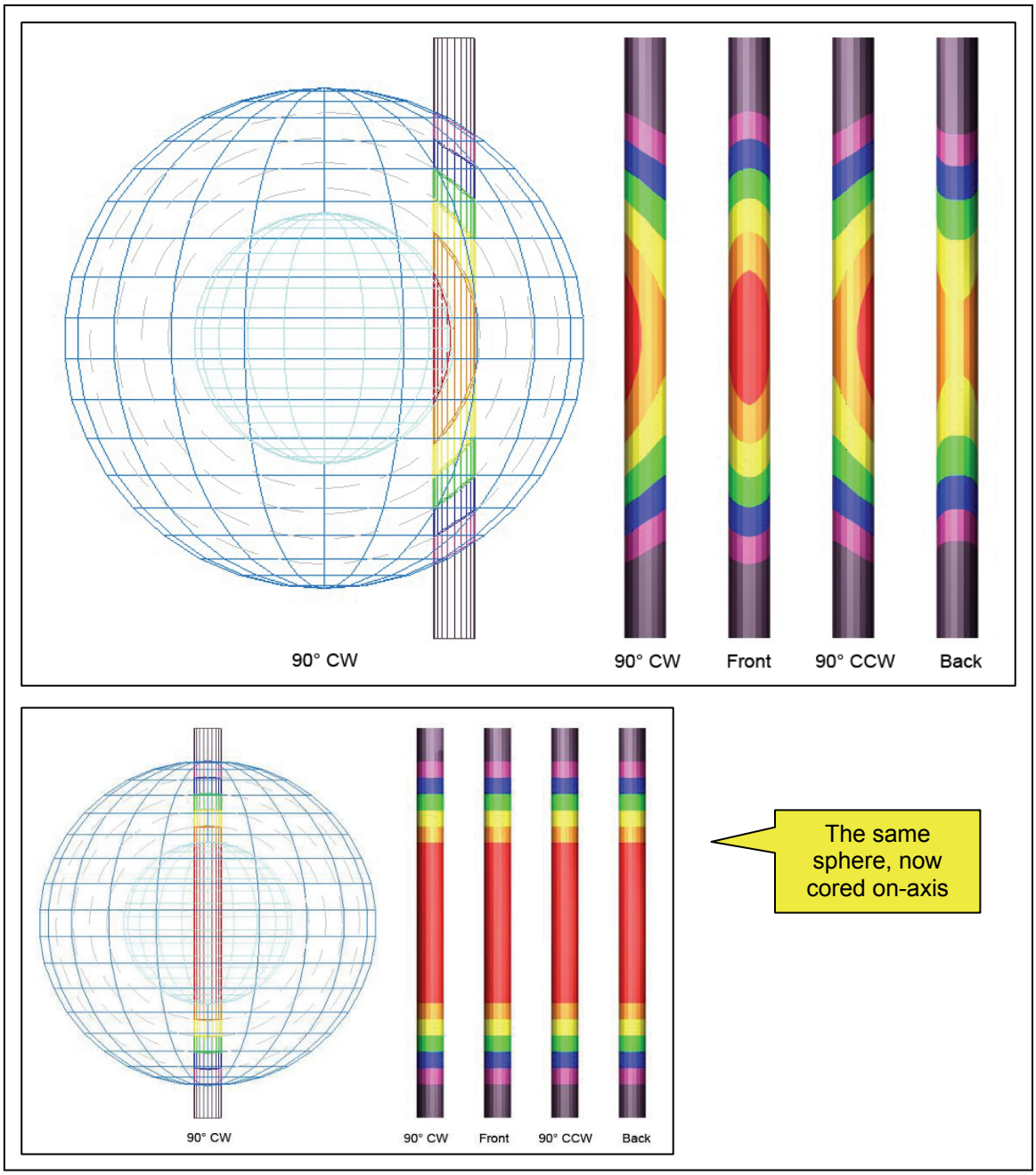

Figure 82. TurboCAD® simulation of *Sphere – Layered*. When cored off center, a bull's eye pattern is manifest in the drill core, but when cored on center, a mirrored pattern of horizontal beds is formed.

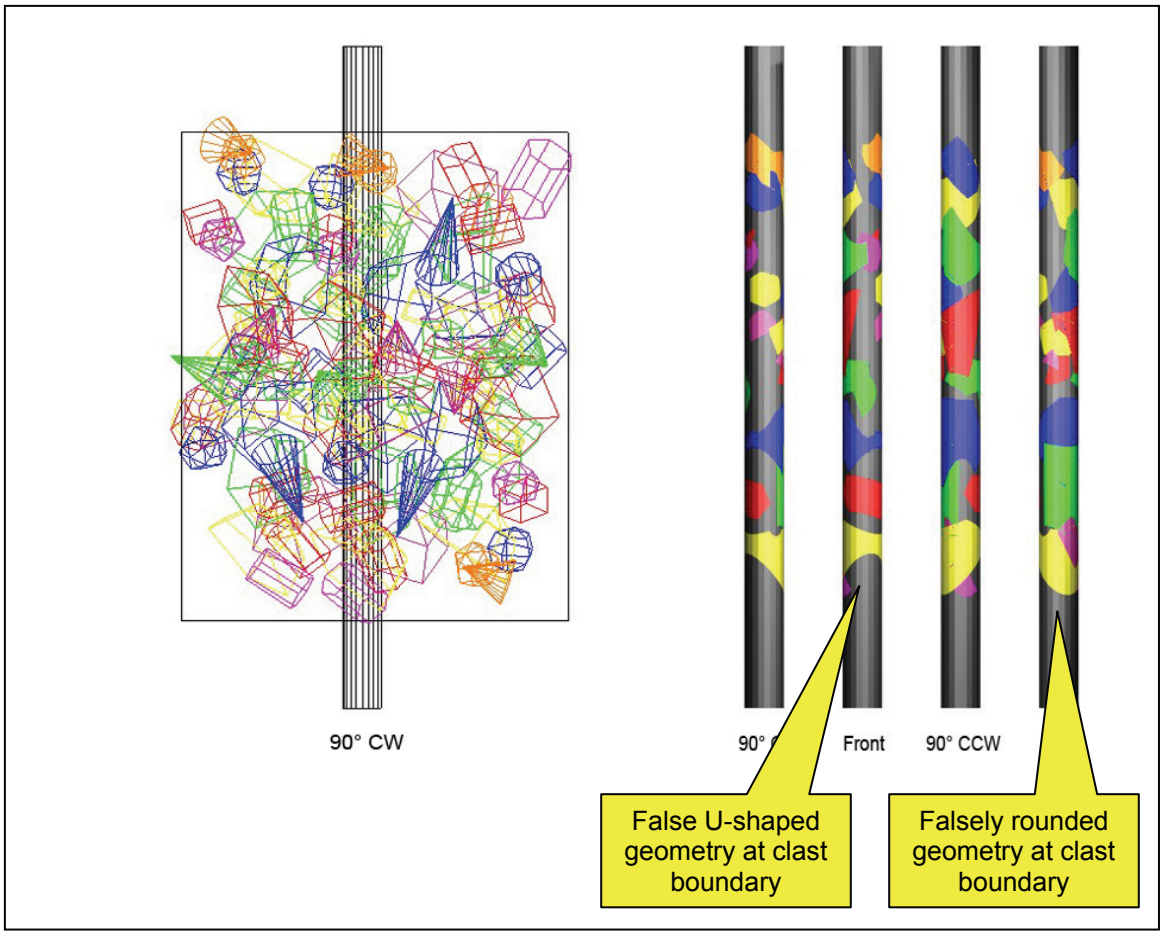

Figure 83. TurboCAD® simulation of *Breccia – Clast-supported*. Coring clast-supported breccia of angular to rounded clasts can give a false rounded geometry to clasts that actually have flat faces. False U-shaped clast geometries are also rendered in clasts having what are actually flat faces. Note most clasts appear to touch on the surface of the drill core, but some appear suspended in matrix. These clasts appearing as though suspended probably touch in places not visible on the drill core's surface.

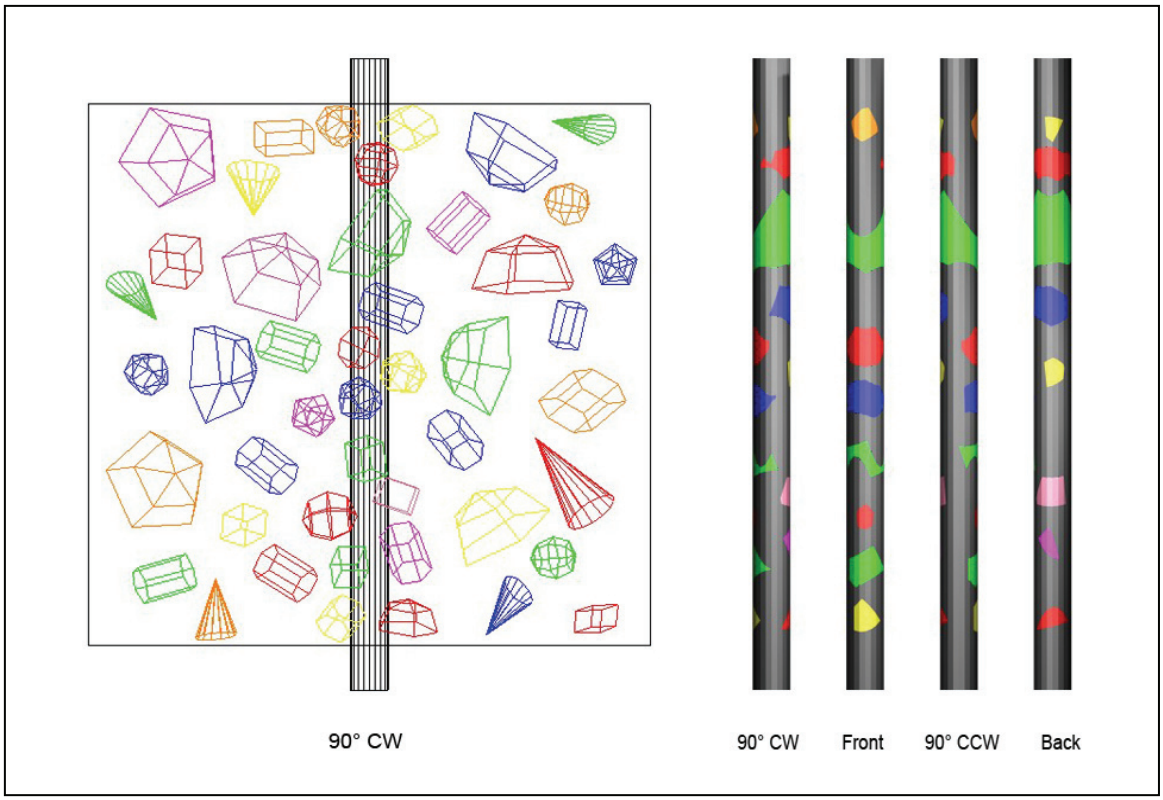

Figure 84. TurboCAD® simulation of *Breccia – Matrix-supported*. Coring matrix-supported breccia of angular to rounded clasts can produce upright and upside-down U-shaped geometries on clast boundaries. These U-shapes are oriented with the core's long axis and indicate flat surfaces on the clasts. As expected, few (if any) of the clasts touch other clasts.

2. Results of Determining the Position of Drill Core versus the Central Peak

Data for the 1994 gravity transect documented in Wolf et al. (1997) were collected along a gas pipeline right-of-way managed by the Alabama Gas Company. Some data had to be collected away from the right-of-way because of access issues. In all, 76 field stations were spaced across the impact structure at intervals of roughly 100 m (Wolf et al., 1997). The elevation of each station was surveyed to an accuracy of 0.3 m, and geographic positions were ascertained with a GPS receiver of unspecified make (Wolf et al., 1997). Gravitational data were collected with a Lacoste-Romberg gravimeter.

Using the actual numerical data collected in 1994, the present author remapped and colorized the field stations according to their gravitational strength in mGal (Figure 85A). Similarly, the actual elevation data from the 1994 survey has been newly graphed, and is depicted in Figure 85B. The vertical scale used in the elevation profile matches that used in other cross sections in this report. Finally, the actual numerical residual gravity data were also re-graphed, and these data are depicted in profile format in Figure 85C. The left edge of this graph is color-coded to match the colors of the field stations on the new map. All horizontal scales in the three portions of the figure match.

Several things have become apparent on these new maps and graphs. First, drill cores 1-98 and 2-98 were taken from just east of the central peak's two highest points as manifest in the gravity profile. Depth for the gravity profile has not been determined. Therefore, the two drill cores may or may not penetrate into the upper eastern flank of this central peak.

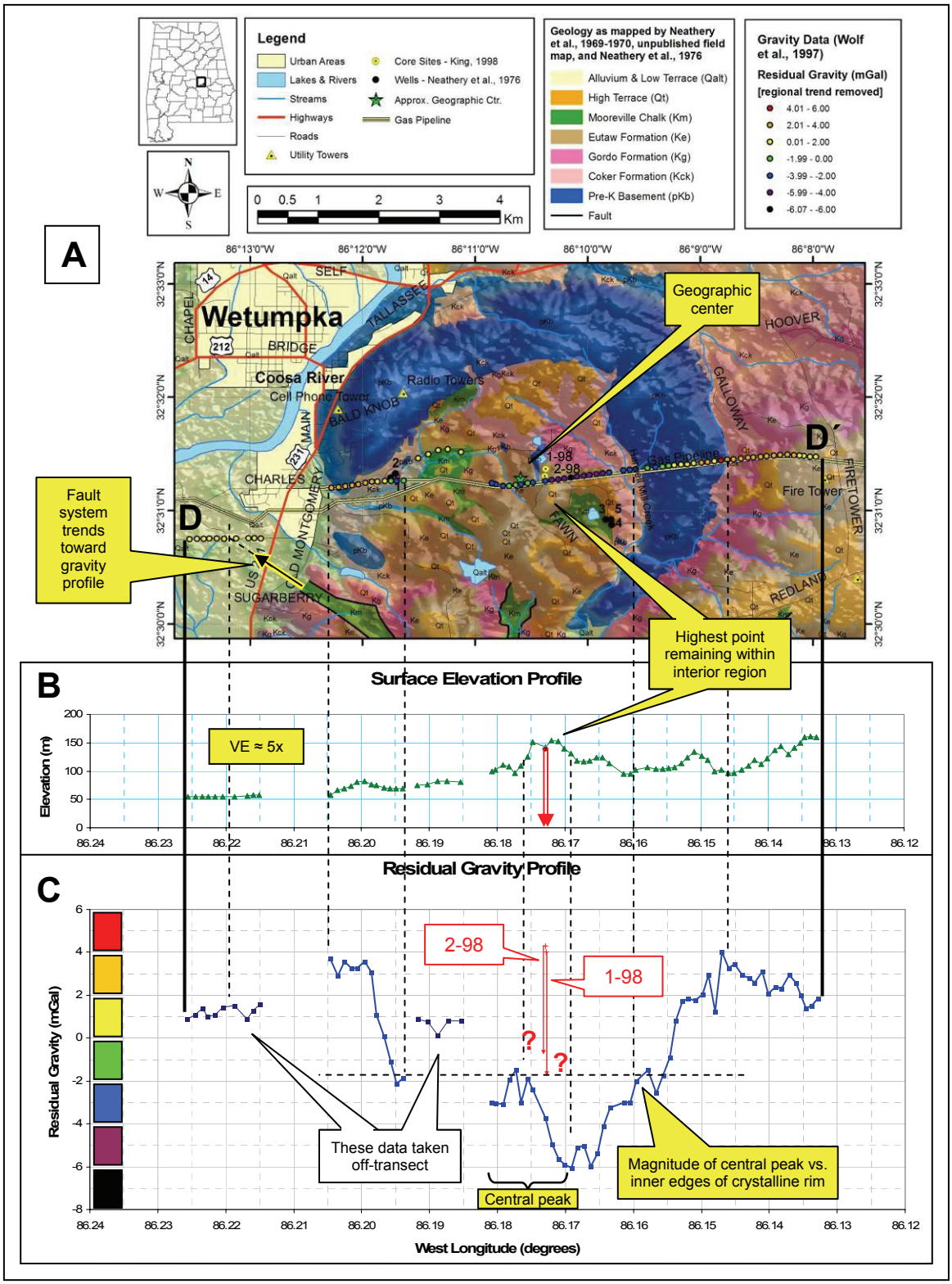

Figure 85. Results of remapping and re-graphing all data from the 1994 gravity survey of Wolf et al. (1997).

Second, the magnitude of the central peak versus that of the inner edges of the crystalline rim is indicated by dashed index lines. The magnitude of the central peak is approximately equal to the magnitude of the crystalline rim's inner edges. Conversely, each outer edge of the crystalline rim is significantly higher in magnitude than the inner edge, but even these locales are approximately equal in magnitude to each other.

Third, the fault system near Sugarberry road (southwest corner of the map, Figure 85A) is trending toward the westernmost data points on the gravity transect. There is little evidence that the graben between the two faults is manifest on the gravity profile.

Forth, the topographically highest point of elevation within Wetumpka's interior region is clearly discernable on both the map and elevation profile. This topographic high point is not coincident with the lateral position of the central peak on the gravity profile, but it is very close. Additionally, the topographically highest point of elevation within Wetumpka's interior region is significantly higher than the remaining eastern crystalline rim.

Fifth, small regions of enigmatic crystalline-clast breccia material crop out to the northwest of the two 1998 drill sites (Figure 32). This material is positioned just northeast of where the top of the central peak may reside. Additionally, this material is on axis with the presumed flow of surgeback material (King et al., 2005), and is immediately down-flow from the top of the central peak.

Finally, for reference while in the field at the highest point of elevation within Wetumpka's interior region, the eastern rim may be viewed from the pipeline right-of-way as the second low ridgeline towards the east as seen from the high point (Figure

85B). The third and largest ridgeline (the eastern horizon) is part of the high hills east of the eastern crystalline rim.

All of the aforementioned data will be collectively interpreted in the context of marine-target impact cratering processes and their results, and detailed in the *Discussion* section of this report.

3. Results of Investigating the Ostensible Intra-crater Paleosol

Two samples were collected from the mudstone in drill core 1-98 thought to be a possible intra-crater paleosol and/or lacustrine deposit (King et al., 2006). Both samples were outsourced for processing and analysis. All results documented here are as they were reported in the final lab write-up.

Both samples contained abundant, diverse and well-preserved assemblages of terrestrial origin, consisting of pollen (angiospermous and gymnospermous), spores, and rare fresh-water algae (Table 4, R. Ravn and D. Goodman, pers. comm., 2006). Photomicrographs were taken (at the lab) of representative palynomorphs collected from both of the two samples. Table 5 provides a numbered index identifying the palynomorphs in the individual photomicrographs appearing in Figure 86.

Before continuing, a cautionary note is necessary to preclude any potential confusion. Because the palynology work was done as a part of the present study (unlike the published gravity data, for example), the reader may be tempted to red flag the following results as interpretations. The present author would agree if this were a paleontological study of palynomorphs. However, in this study of the Wetumpka impact structure, the following pieces of information were data that were used later in this study to form interpretations about the depositional history of crater-filling material in the Wetumpka impact structure. In other words, the *age* of the palynomorphs as interpreted by paleontologists at the IRF Group Inc. was *data* in this report. Essentially, it is the *age* information (*data*) that the present author used to form interpretations documented later in this report.

Sample A	Sample B
Ovoidites parvus	*Rugubivesiculites rugosus* - common
Deltoidospora minor	*Sabalpollenites scabrus*
Costatoperforosporites foveolatus	*Deltoidospora hallii*
indet. bisaccate gymnosperm pollen – common	*Cicatricosisporites* spp. - indet.
Rousea sp. - indet., prolate	*Foveosporites* spp. - indet.
Cicatricosisporites venustus	*Triporoletes reticulatus*
Pristinuspollenites sp. - indet.	*Cicatricosisporites venustus*
Granulatisporites sp. - indet., fine ornament	*Plicatella* sp. - indet.
Densoisporites microrugulatus	*Costatoperforosporites foveolatus*
Ischyosporites pseudoreticulatus	*Exesipollenites tumulus*
Laevigatosporites haardtii	*Ischyosporites pseudoreticulatus*
Tigrisporites sp. - indet.	*Gleicheniidites senonicus*
Cicatricosisporites spp. - indet. - common	indet. bisaccate gymnosperm pollen – common
cf. *Thomsonisporites rasilis*	*Distaltriangulisporites perplexus*
Equisetosporites sp. - indet.	*Osmundacidites wellmanii*
Dictyophyllidites cf. *impensus*	*Thomsonisporites rasilis*
Plicatella spp. - indet.	*Laevigatosporites haardtii*
Triporoletes cenomanianus	*Balmeiopsis limbatus*
Plicatella cristata	*Lycopodiacidites* sp. - indet., small
Distaltriangulisporites perplexus	*Rousea* sp. - indet., subspherical
Deltoidospora hallii	*Leptolepidites* sp. - indet.
Rugubivesiculites rugosus	*Echinatisporis varispinosus*
Rugubivesiculites woodbinensis	*Foveosporites subtriangularis*
Lycopodiacidites sp. - indet., arcuate ridge, fine hamulate ornament	
Osmundacidites wellmanii	
Ischyosporites estheriae	
Sabalpollenites scabrus	
Foveosporites sp. - indet., triangular, fine	
Microreticulatisporites sp. - indet.	
Cicatricosisporites crassiterminatus	
Atlantopollis sp. - indet.	
Foveomonocolpites sp. - indet.	
Retimonocolpites sp. - indet.	
Rugubivesiculites reductus	
Exesipollenites tumulus	
cf. *Nicholsipollis*? sp. - indet.	

Table 4. Listing of all palynomorphs reportedly found within samples A and B from the sedimentary material in drill core 1-98 thought to be a possible intra-crater paleosol and/or lacustrine mudstone deposit. Items are listed exactly as they were reported (presumably in the order found) by paleontologists at the IRF Group Inc. where the samples were outsourced (R. Ravn and D. Goodman, pers. comm., 2006).

Photo Number and Name		Found within Sample A	Found within Sample B
1	*Laevigatosporites haardtii* (Potonié & Venitz) Thomson & Pflug 1953	yes	yes
2	*Triporoletes cenomanianus* Agasie 1969	yes	no
3	*Foveosporites senomanicus* (Chlonova) Dettmann 1963	indeterminate	indeterminate
4	*Foveosporites subtriangularis* Brenner 1963	indeterminate	indeterminate
5	*Ischyosporites pseudoreticulatus* (Couper) Döring 1965	yes	yes
6	*Ischyosporites estheriae* Deák 1964	yes	no
7	*Scopusporis spackmanii* (Brenner) Wingate 1980	no	no
8	*Plicatella* sp.	yes	yes
9	*Costatoperforosporites foveolatus* Deák 1962 (proximal and distal surfaces)	yes	yes
10	*Densoisporites microrugulatus* Brenner 1963	yes	no
11	*Retimonocolpites* sp.	yes	no
12	*Atlantopollis* sp.	yes	no
13	*Rousea* sp.	yes	yes
14	*Sabalpollenites scabrus* (Brenner) Wingate 1980	yes	yes
15	*Rugubivesiculites rugosus* Pierce 1961	yes	yes
16	*Equisetosporites* sp.	yes	no

Table 5. Numbered index listing the palynomorphs appearing in the next figure, and indicating whether each specific grain was found in sample A or B taken from the enigmatic paleosol mudstone deposit in drill core 1-98 (R. Ravn and D. Goodman, pers. comm., 2006).

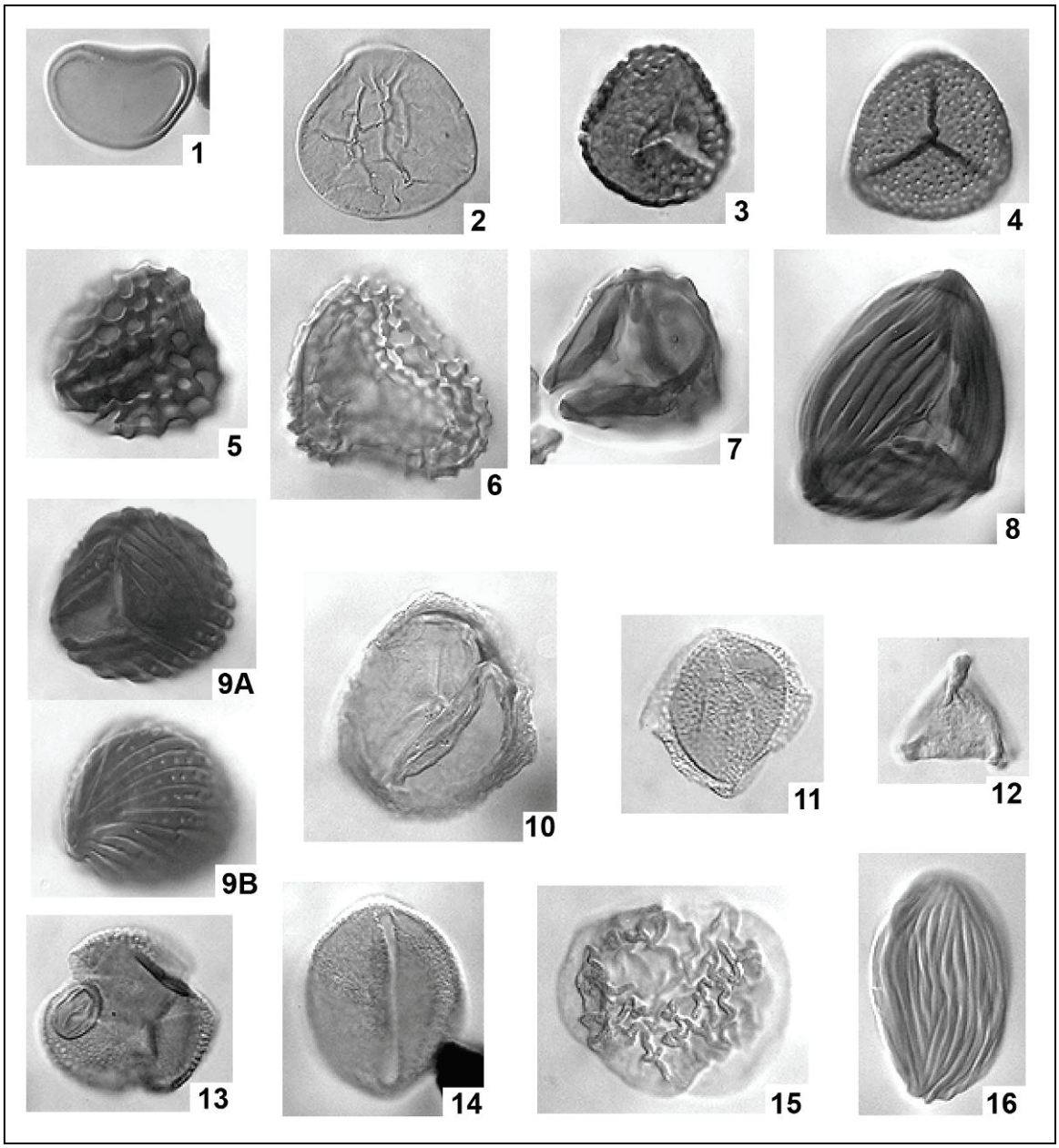

Figure 86. Photomicrographs of palynomorphs found in both sample A and B from the ostensible paleosol in drill core 1-98. See table above for number index. Scale in each photo is unknown, as are relative sizes. However, scale is not what was important. All that mattered was the identification of the populations and finding their approximate age. (Photomicrographs by the IRF Group Inc., R. Ravn and D. Goodman, pers. comm., 2006).

Each sample contained relatively similar populations, but the presence of certain forms in each lead to the following conclusions by the paleontologists. For sample A, the presence of a variety of angiospermous pollen (notably *Rousea* sp., *Atlantopollis* sp., and *Retimonocolpites* sp.), in conjunction with the spore assemblage present, suggests a Cenomanian age, possibly early Cenomanian (R. Ravn and D. Goodman, pers. comm., 2006). Sample B contains only very rare angiospermous pollen, along with some spore taxa, notably *Echinatisporis varispinosus* and *Foveosporites subtriangularis*, which are usually considered characteristic of late Albian material (R. Ravn and D. Goodman, pers. comm., 2006). To summarize, the age of the mudstone deposit predates the Wetumpka impact event by approximately 20 million years (Figure 87).

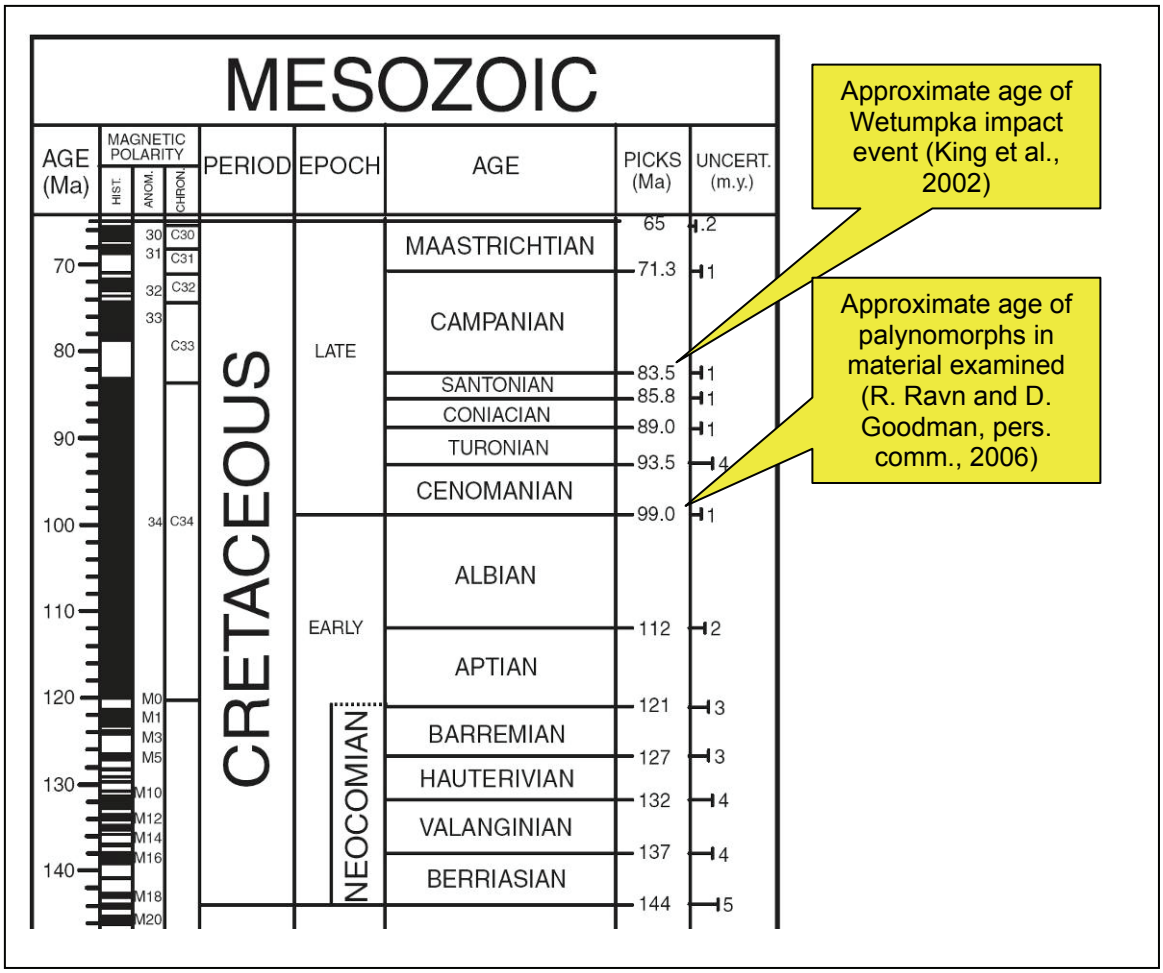

Figure 87. Geologic time scale showing Cretaceous global chronostratigraphy and markers depicting the age of palynomorphs in samples A and B (R. Ravn and D. Goodman, pers. comm., 2006) versus the age of the Wetumpka impact event reported by King et al. (2002). Time scale derived from (Palmer and Geissman, 1999).

4. Results of Investigating the Age of Shock Metamorphism

Initial laser fusion analyses of individual, shock-deformed muscovite crystals (exhibiting polysynthetic, mechanical twins) yielded ages approximately coeval with the regional Appalachian (crystalline) basement deformation of roughly 300 Ma, not the Wetumpka impact event (Johnson et al., 2006). Shocked muscovite crystals from a drill depth of 127.45 m (impact breccia matrix), and 182.5 m (contorted interbedded sandstone and mudstone) in drill core 1-98 generally show little variation in age or effects of extraneous argon, with a mean age of 325.9 ± 3 Ma (standard deviation), and a weighted mean age of 325.9 ± 2 Ma (standard error of the mean). The reduced data are shown in Table 6. The graph in Figure 88 shows there was essentially no contamination by excess argon from air in the samples.

Reduced Data

Sample Set:	AU3.1A.mus
Date Run:	May 8, 2001
Irradiation Package:	AU-3
J-Value	0.00928 ± 3.3408E-05
Air $^{40}Ar/^{36}Ar$:	295.5

	Sample Name	^{40}Ar (*+atm)	^{39}Ar (K)	^{39}Ar (Cl+atm)	^{37}Ar (Ca)	^{36}Ar (atm)	% Rad	$^{40}Ar^*/^{39}Ar$ (K)	Age (Ma)
1	AU3.1A.mus.3	3.535E-14 ± 3.21E-17	1.649E-15 ± 3.60E-18	1.958E-17 ± 9.04E-19	7.044E-18 ± 2.68E-18	-1.038E-18 ± -8.39E-19	100.9%	21.629	330.0 ± 0.8
2	AU3.1A.mus.4	1.496E-13 ± 2.04E-16	7.027E-15 ± 1.26E-17	8.183E-17 ± 3.09E-18	-5.181E-18 ± -3.44E-18	1.053E-18 ± 9.96E-19	99.8%	21.242	324.6 ± 0.7
3	AU3.1A.mus.5	1.182E-13 ± 1.59E-16	5.518E-15 ± 1.61E-17	6.010E-17 ± 1.86E-18	-1.222E-17 ± -9.70E-18	9.205E-19 ± 9.08E-19	99.8%	21.377	326.5 ± 1.1
4	AU3.1A.mus.6	1.135E-13 ± 2.67E-16	5.370E-15 ± 1.32E-17	6.668E-17 ± 3.91E-18	1.017E-17 ± 3.43E-18	6.664E-19 ± 6.02E-19	99.8%	21.096	322.5 ± 1.1
5	AU3.1B.mus.1	1.228E-13 ± 7.06E-16	5.669E-15 ± 1.27E-17	6.826E-17 ± 3.07E-18	1.121E-17 ± 6.09E-18	-6.907E-19 ± -8.26E-19	100.2%	21.690	330.9 ± 2.0
6	AU3.1B.mus.2	4.067E-14 ± 1.81E-16	1.903E-15 ± 9.43E-18	2.218E-17 ± 1.62E-18	2.466E-17 ± 7.96E-18	1.916E-19 ± 9.49E-19	99.9%	21.343	326.0 ± 2.2
7	AU3.1B.mus.3	4.650E-14 ± 5.44E-17	2.187E-15 ± 2.14E-17	2.357E-17 ± 1.05E-18	2.305E-17 ± 8.07E-18	4.954E-19 ± 7.78E-19	99.7%	21.193	323.9 ± 3.2
8	AU3.1B.mus.4	1.590E-13 ± 2.41E-16	7.479E-15 ± 2.75E-17	8.790E-17 ± 1.11E-18	7.687E-17 ± 7.80E-18	3.881E-18 ± 7.78E-19	99.3%	21.105	322.7 ± 1.3

Mean Age, Standard Deviation:	325.9 ± 3
Weighted Mean Age, Standard Error:	325.9 ± 2

Table 6. Results of $^{40}Ar/^{39}Ar$ dating of eight shock-metamorphosed muscovite crystals from drill core 1-98.

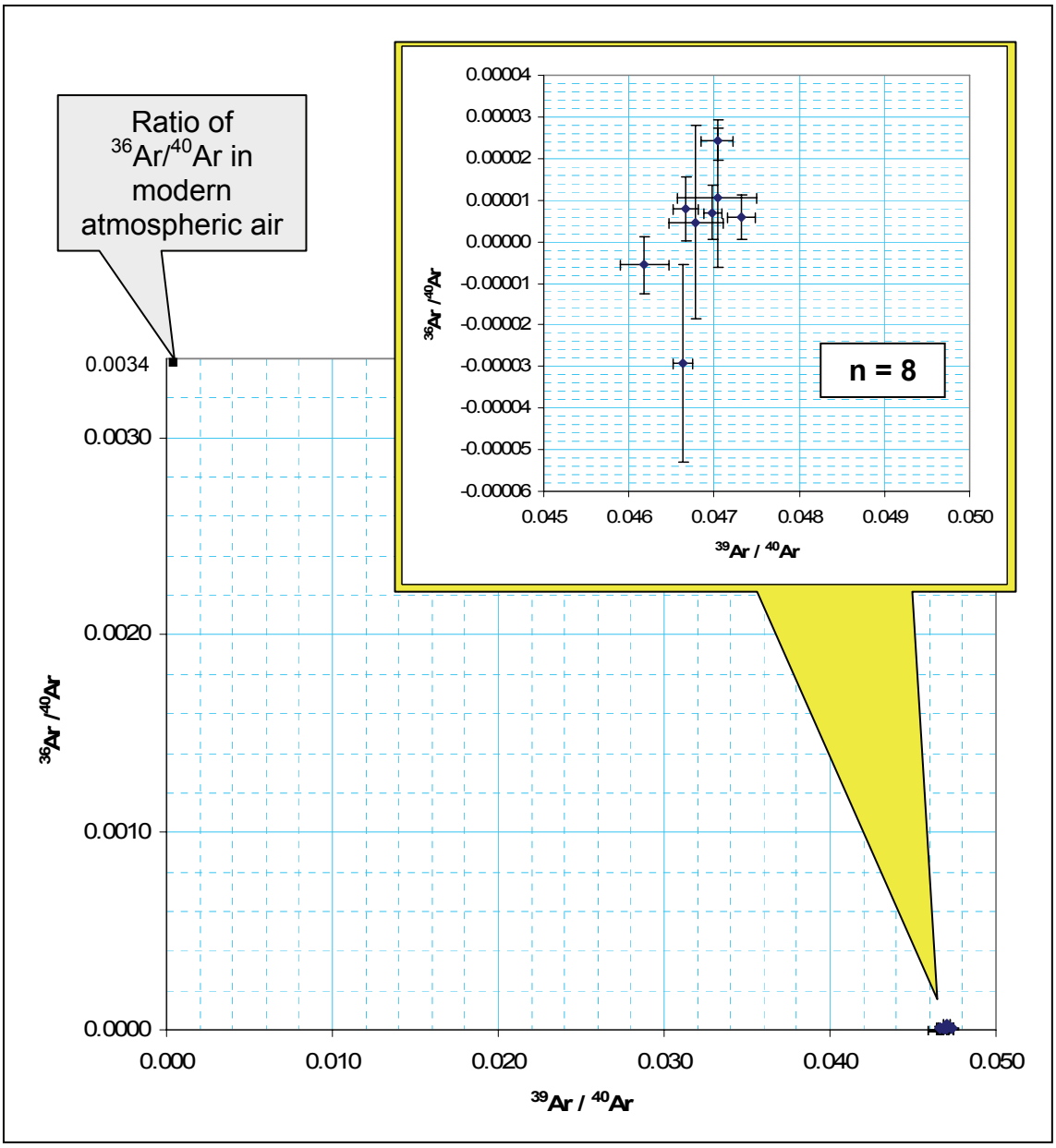

Figure 88. Graph of argon isotope ratios indicating magnitude of contamination by atmospheric argon. The tight cluster of eight data points together indicate there was essentially no air in the samples to provide excess argon. Callout box (yellow) depicts enhanced scale for detail.

5. Results of Comparing Drill Core 1-98 to Drill Core 2-98

When compared side-by-side, the two drill cores show significant differences as well as similarities. Figure 89 depicts a schematic version of each drill core's lithology. Most importantly, note the variations and similarities in the overall dominance of particular lithofacies in the different sections of each drill core. In the figure, each drill core is aligned using modern sea level as a common datum. Sea level in each drill core was determined from the elevation of the drill hole's top (i.e., ground surface at each drill site).

Each drill core is divided into three sections. The first two sections of both drill cores are remarkably similar. Except for two breccia lithozones in 2-98, each upper section is dominated by lithozones of sands, silts, and muds. The middle sections of each drill core are dominated by breccia and crystalline lithozones. Contrary to the similar stratigraphy thus far, the third and bottommost sections of each drill core are different from each other. The bottom of 2-98 exhibits breccia and crystalline lithozones only, whereas the bottom of 1-98 exhibits lithozones of strongly disturbed sands, silts, and muds. It is noteworthy that the boundaries of these three sections in each drill core are closely aligned (when using sea level as the datum). Figure 90 and Figure 91 break out the percentages for each lithofacies in the three sections just mentioned for each drill core; the percentages include absent portions in the drill core. Figure 92 illustrates the lithofacies data normalized to the quantity of drill core recovered for each section; absent portions are omitted from these graphs. Dashed lines in the figures help separate the general divisions. All data were processed and graphed using Microsoft® Excel® 2003.

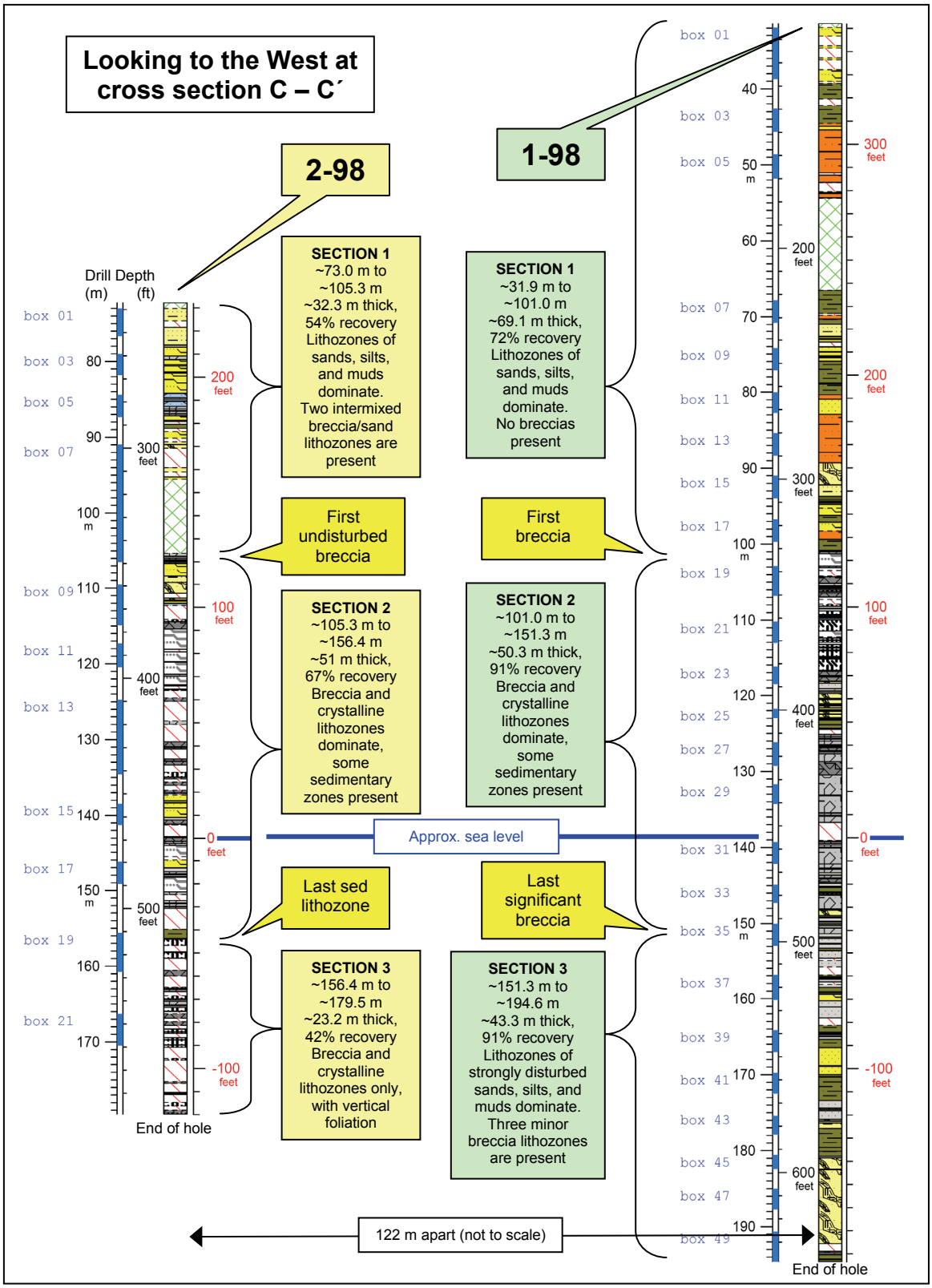

Figure 89. Comparison of sections in drill core 1-98 with sections in drill core 2-98.

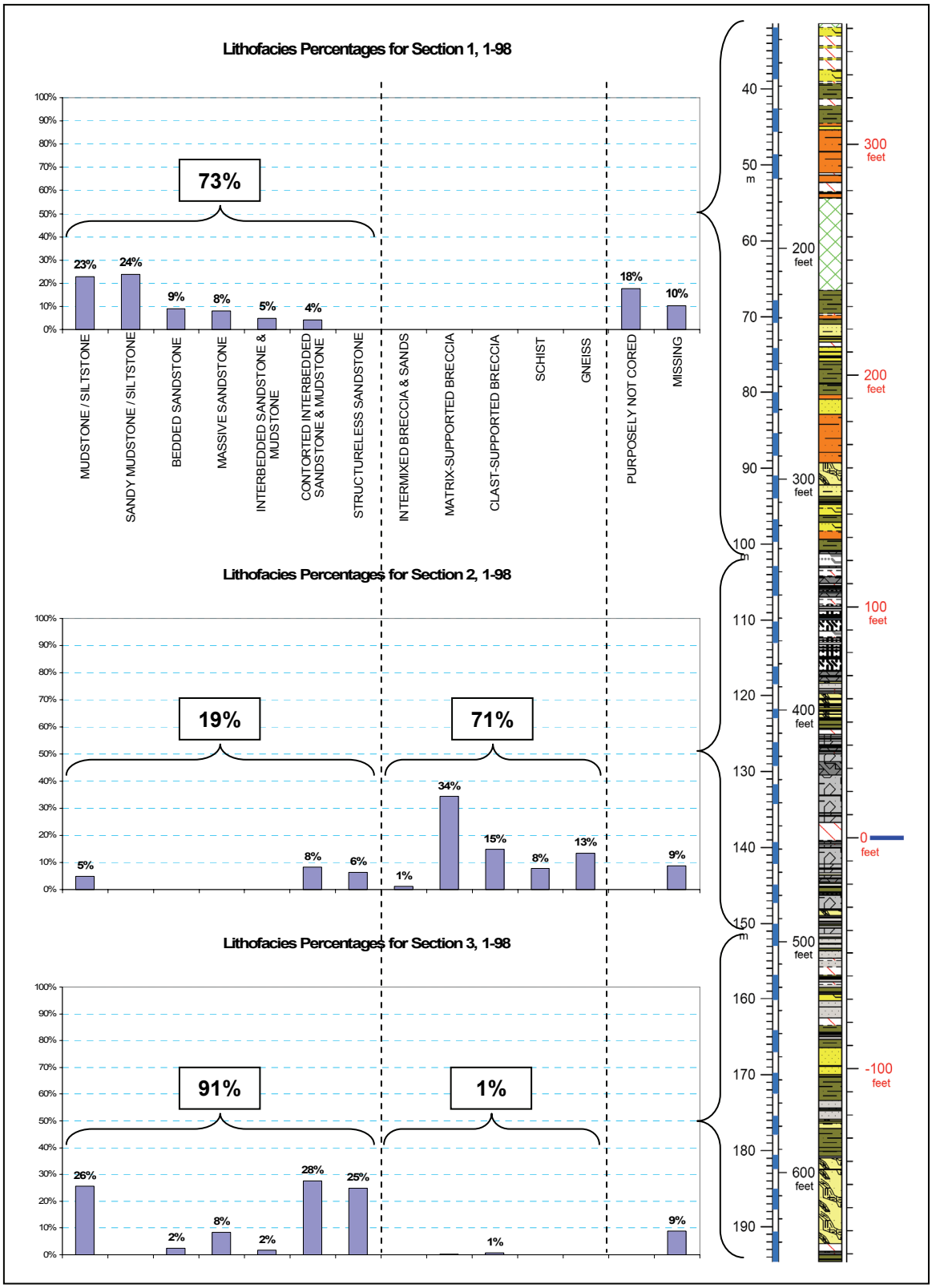

Figure 90. Lithofacies percentages by section for drill core 1-98. Values are rounded.

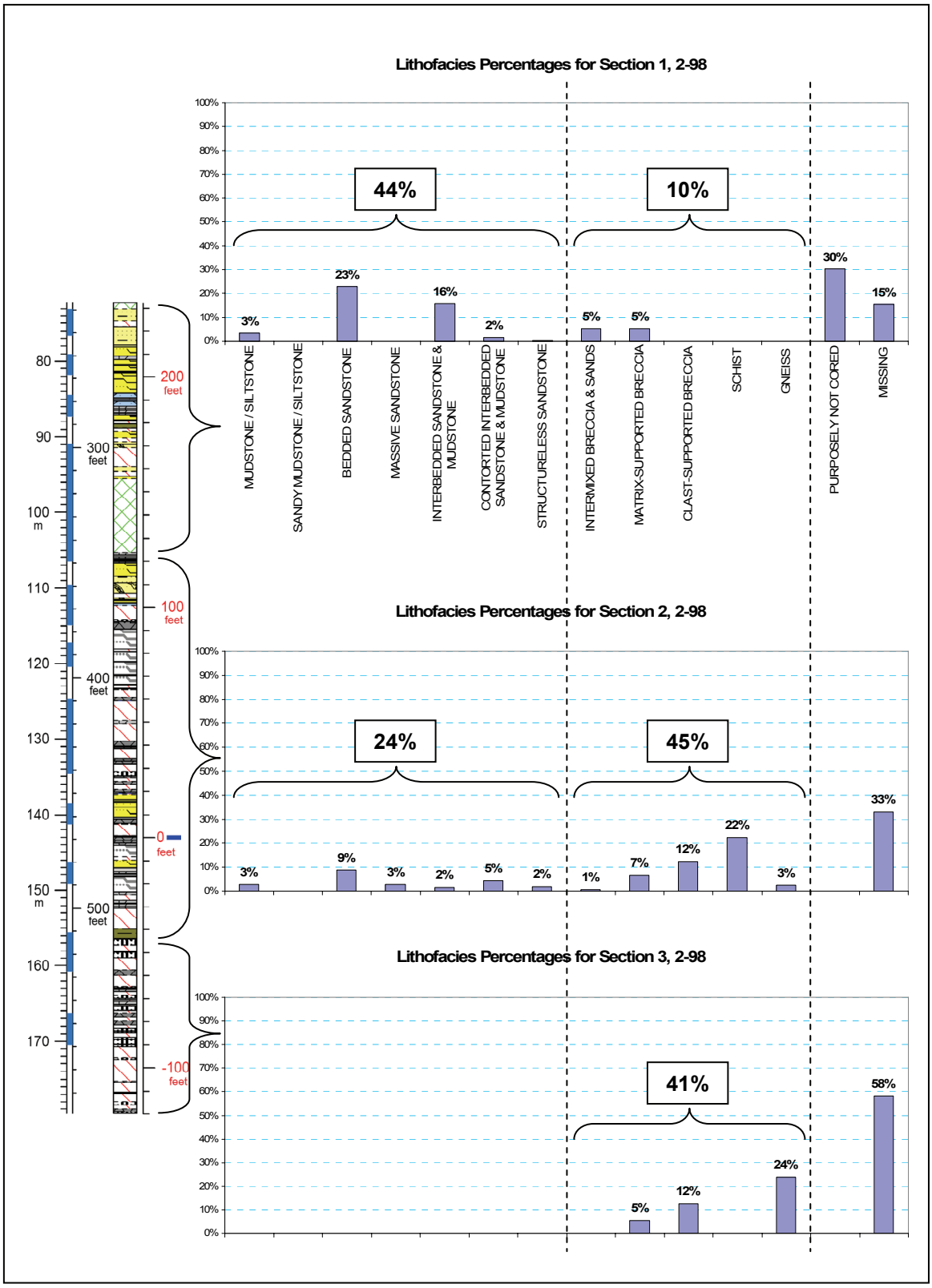

Figure 91. Lithofacies percentages by section for drill core 2-98. Values are rounded.

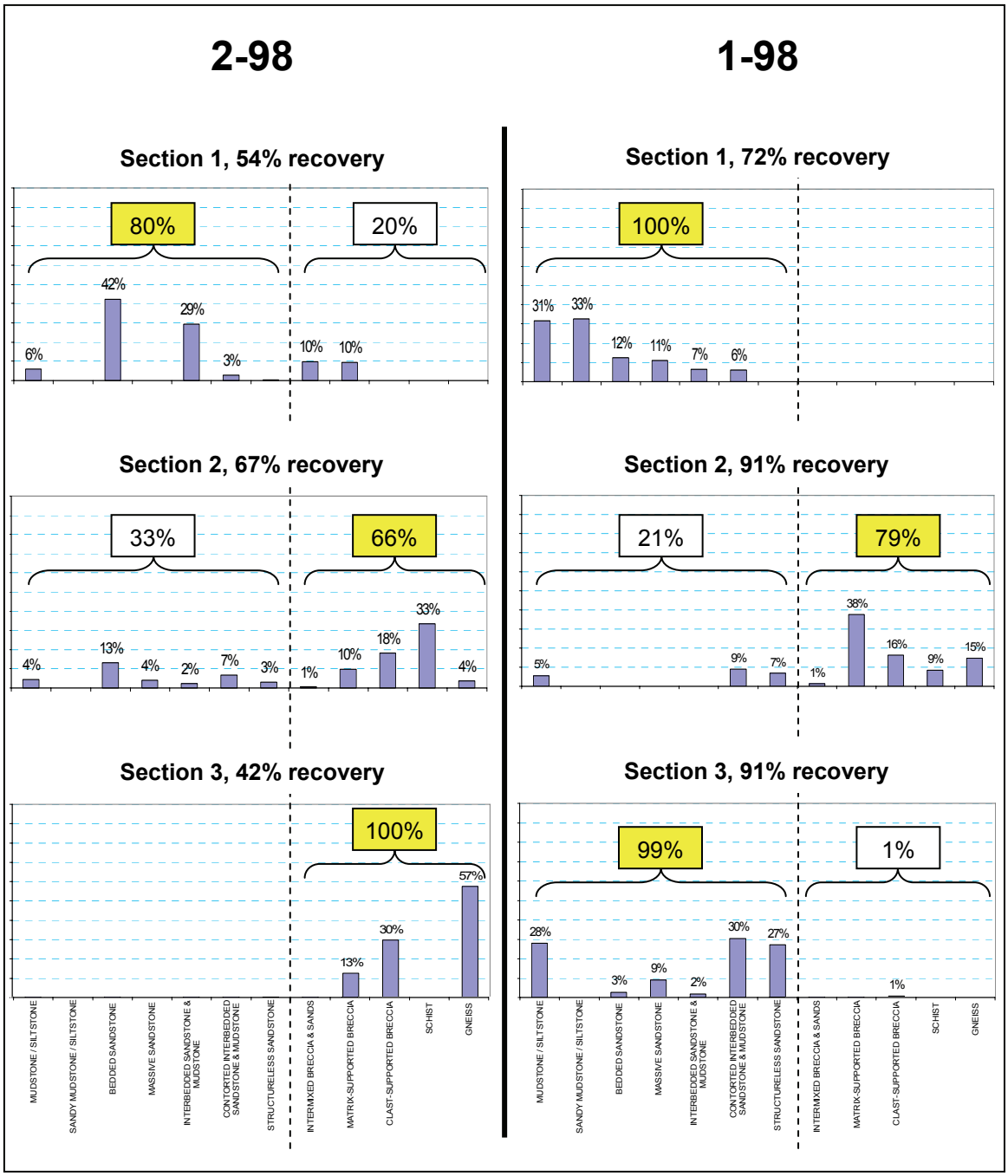

Figure 92. Lithofacies percentages normalized to the quantity of drill core recovered from each section. Dominant lithofacies are highlighted yellow. In both drill cores, section 1 is dominated by Upper Cretaceous material, whereas section 2 is dominated by breccias and material from the crystalline basement. Conversely, the composition of section 3 in both drill cores is diametrically opposed.

6. Results of Comparing Wetumpka to Chesapeake Bay Impact Structure

As outlined in the *Background and Geologic Setting*, the present author prefers to model Wetumpka as a filled inner basin within what was originally a larger marine impact crater. To test this model, geological features from the Wetumpka structure, and the descriptive data from the two drill cores, were compared to general models of the Chesapeake Bay impact structure presented in Poag et al. (2004).

Although the Chesapeake Bay impact structure is much larger than the Wetumpka structure, both have many similar characteristics. Examples include the following: 1) both impact events took place in a near-shore marine environment; 2) each projectile struck poorly consolidated water-saturated sediments and sedimentary rock overlying crystalline basement rock; 3) the uppermost layer of target strata at both impact sites was largely removed from the target area of each impact structure; 4) the crystalline basement rock at both locales is metasedimentary and meta-igneous; and 5) both impact regions have remained largely undisturbed since the impact event (Poag et al., 2004; King et al., 2006). Differences between the two structures can be generalized by saying that most aspects and features at Chesapeake Bay were/are larger than its corresponding aspect or feature at Wetumpka. Specifically, thicknesses of the target water and sedimentary strata were greater, the projectile was larger, the explosion greater, the crater deeper and wider, the surgeback stronger, etc. (Poag et al., 2004; King et al., 2006). In essence, if scale is taken into account, comparison of the two is justifiable and can be quite useful.

Comparative geologic cross sections of the Wetumpka and Chesapeake Bay structures (Figure 93) illustrate that the two compare nicely when the latter is proportionately reduced to Wetumpka's size. Note the tall central peak depicted at

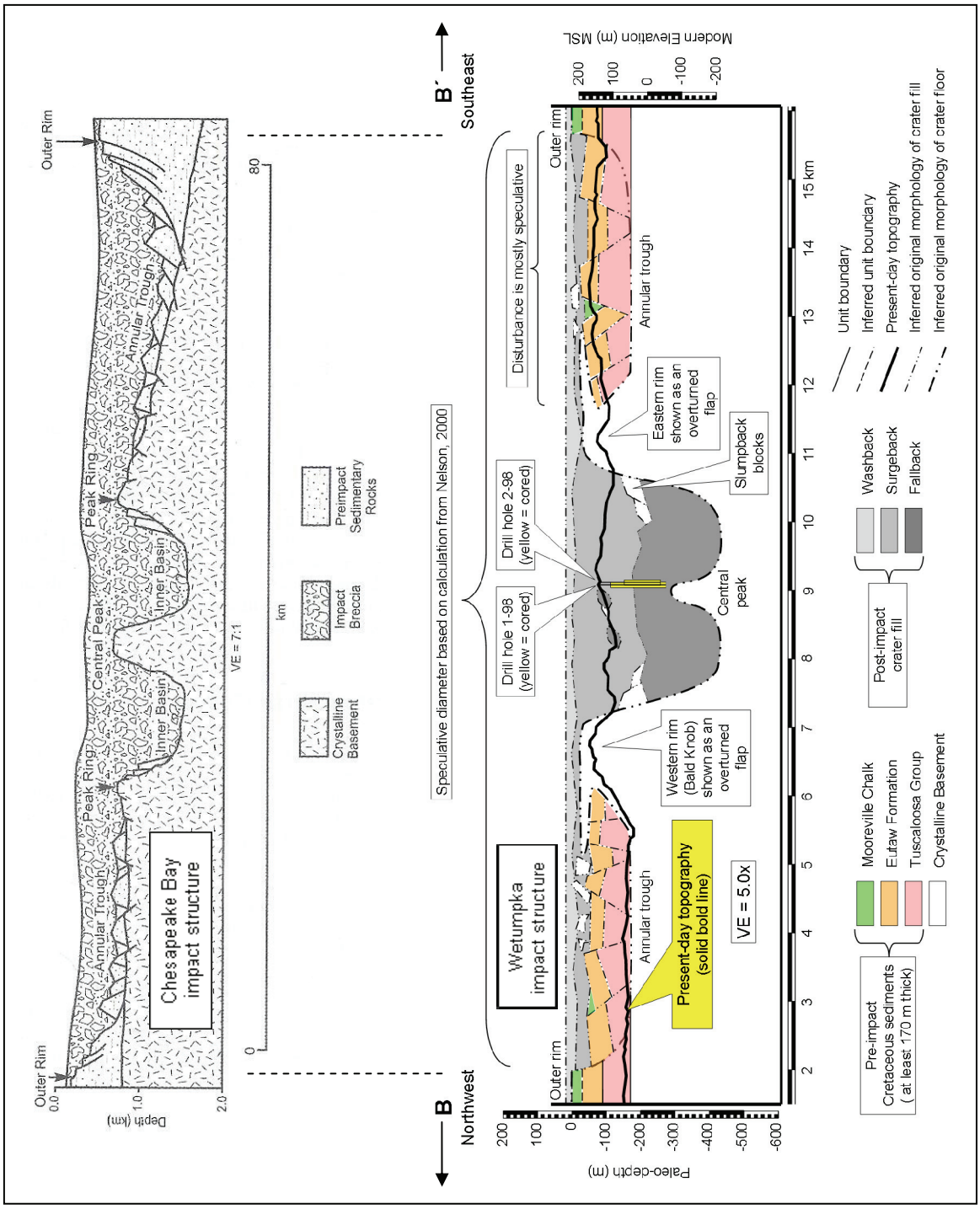

Figure 93. Comparative geologic cross sections of the impact structures at Chesapeake Bay and Wetumpka. Note the cross section for Wetumpka is only a portion of cross section B – B´. Cross section of Chesapeake Bay impact structure derived from Poag et al. (2004).

Chesapeake Bay. The height of Wetumpka's central peak is not known, but may extend higher than what is illustrated.

Figure 94 and Figure 95 both depict maps of Wetumpka's crystalline rim and its speculative outer rim (Nelson, 2000) as compared to the same known features at the Chesapeake Bay structure. The Wetumpka structure is illustrated at the same scale in both figures. However, in Figure 94, the Chesapeake Bay structure is scaled down to Wetumpka's speculative outer rim, and in Figure 95, it is scaled further down to match Wetumpka's crystalline rim. Note in this latter figure the correlation between the distal faults mapped at Wetumpka by Neathery et al. (1976), and the outer rim of the Chesapeake Bay structure.

Figure 96 depicts a schematic illustration from Poag et al. (2004) illustrating crater-filling breccia stratigraphies, general compositions, and depositional origins of the crater-filling materials found in six impact structures. A text-box schematic of data from this report's descriptions of Wetumpka drill core accompanies the adjacent schematic and illustrates a general correlation in crater-filling material for all seven impact structures.

Finally, Figure 97 provides a geologic cross section of the Chesapeake Bay impact structure from Poag et al. (2004), which outlines the relationships between the lithic texture, origin, and depositional regime for each crater-filling unit at Chesapeake Bay. Figure 98 applies this model to Wetumpka. However, full application of this model to drill core material from Wetumpka will require that lithozones in the two drill cores first be interpreted as clasts or matrix of dissociated target material. See the corresponding subsection of the *Interpretations* for more details on this aspect of the comparison of these two structures.

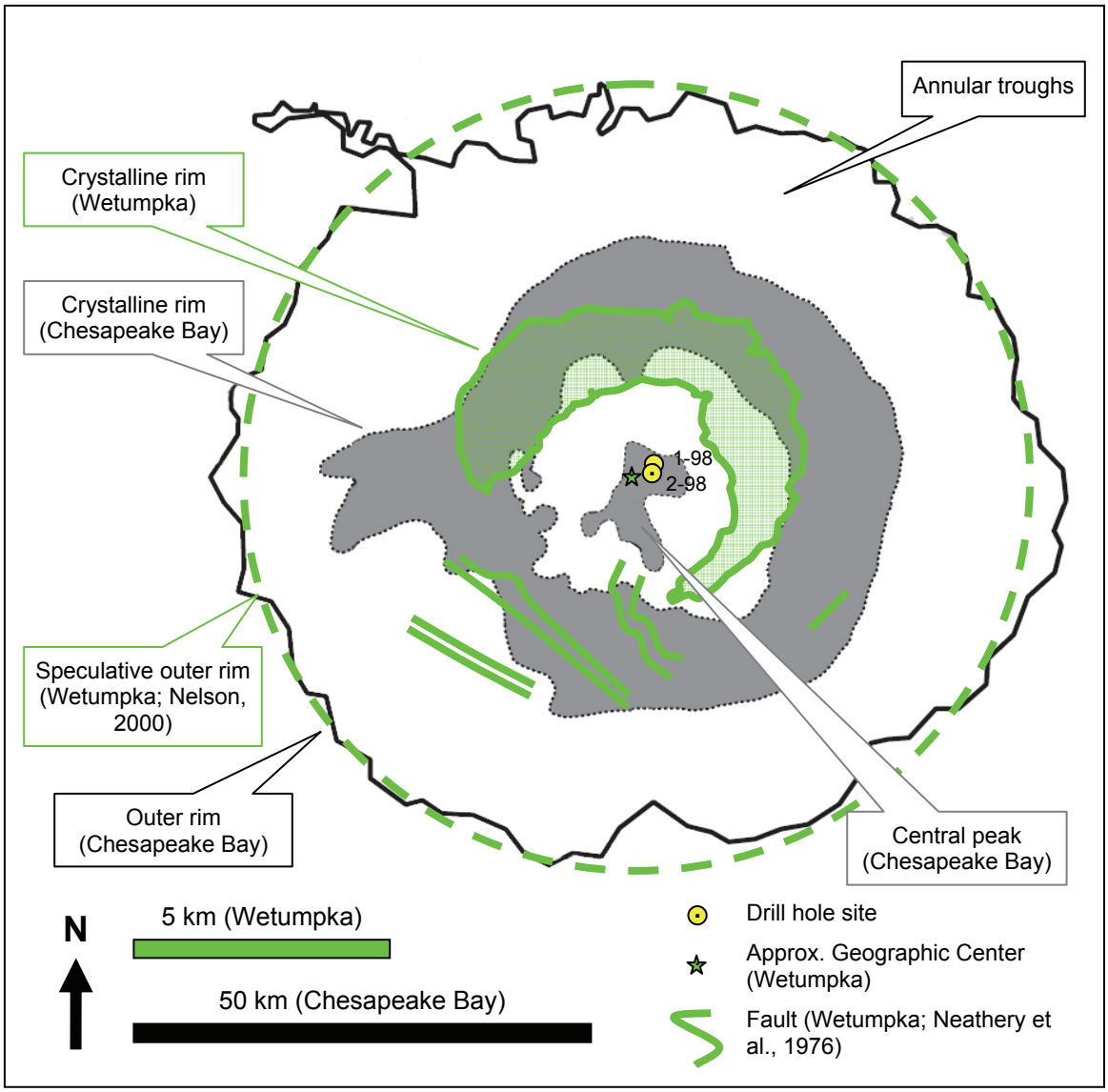

Figure 94. Comparative map of Wetumpka impact structure (green) and Chesapeake Bay impact structure (black and gray) scaled to the speculative outer rim at Wetumpka. Diameter of the speculative outer rim at Wetumpka is based on calculations from Nelson (2000). Outline of Chesapeake Bay structure modified from Poag et al. (2004). Although the Chesapeake Bay impact structure has numerous concentric ring grabens and normal faults within its annular trough (Figure 7.11 in Poag et al., 2004), they have been omitted here for clarity.

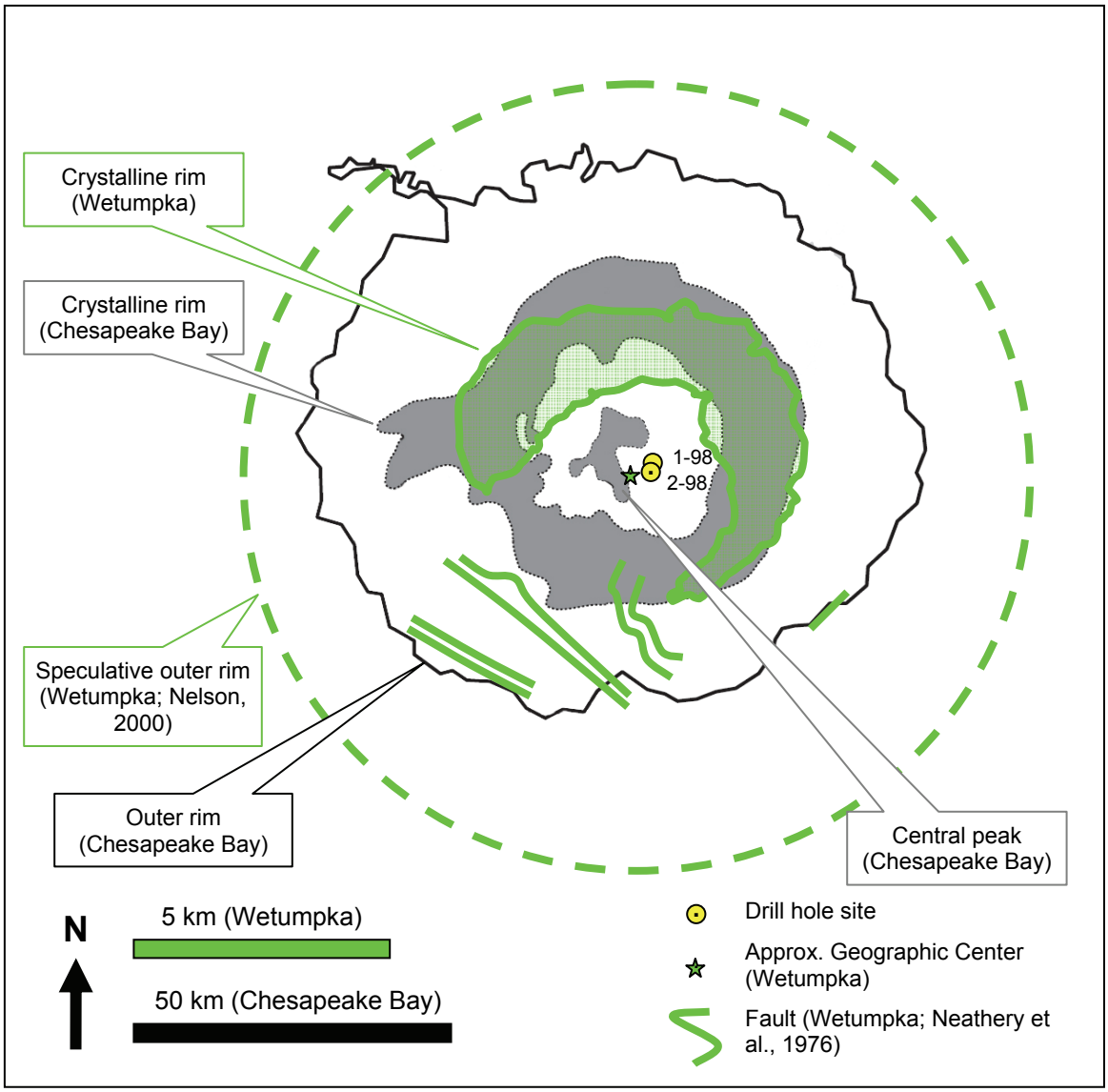

Figure 95. Comparative map of Wetumpka impact structure (green) and Chesapeake Bay impact structure (black and gray) scaled to the crystalline rim at Wetumpka. Note the excellent correlation of faults at Wetumpka with the outer rim of the Chesapeake Bay impact structure at this scale. Diameter of the speculative outer rim at Wetumpka is based on calculations from Nelson (2000). Outline of Chesapeake Bay structure modified from Poag et al. (2004). Although the Chesapeake Bay impact structure has numerous concentric ring grabens and normal faults within its annular trough (Figure 7.11 in Poag et al., 2004), they have been omitted here for clarity.

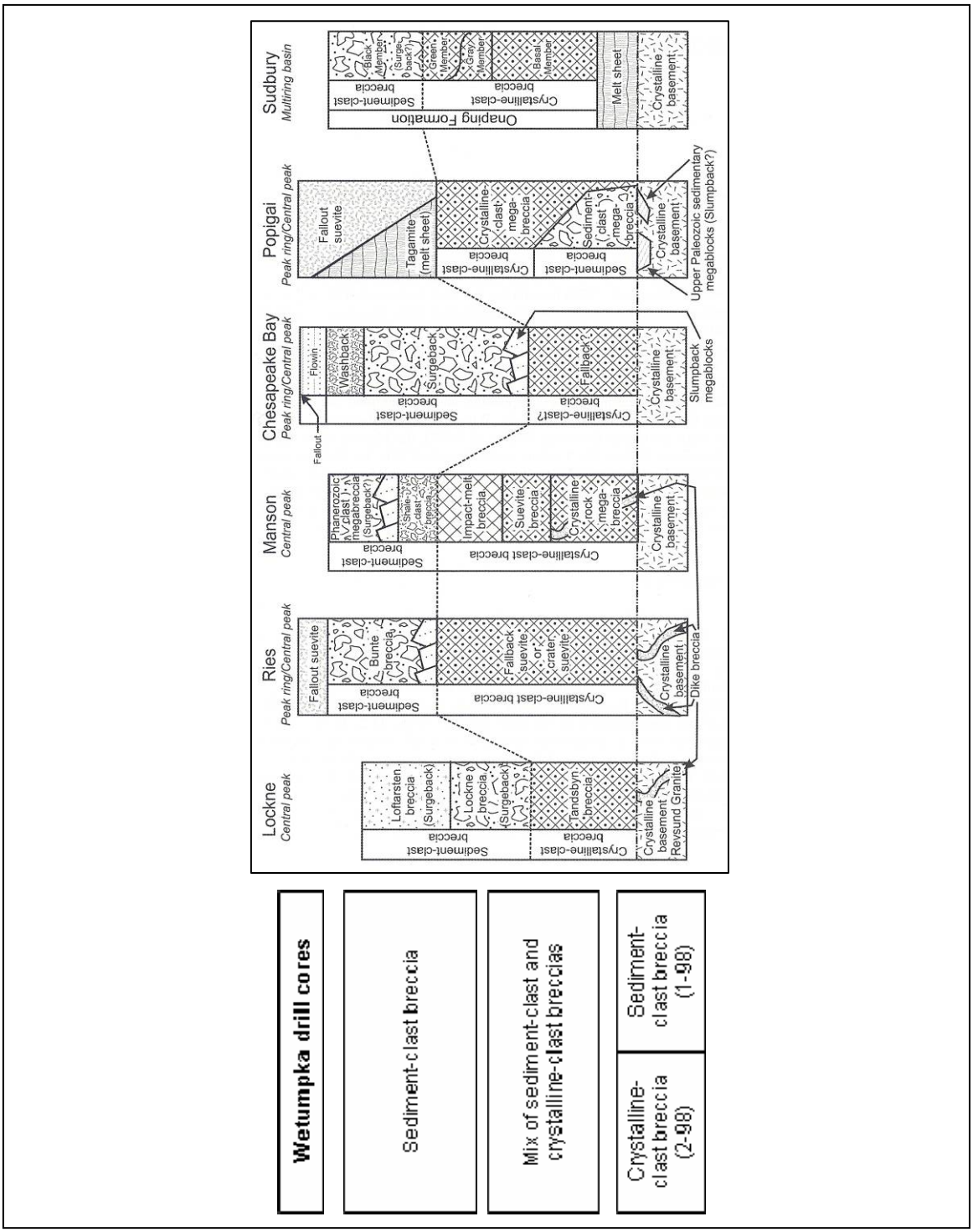

Figure 96. Schematic of Wetumpka drill core stratigraphy as compared to breccia stratigraphies, general compositions, and depositional origins for crater-filling materials at other impact structures. Note the stratigraphic similarities between the Wetumpka drill cores and Lockne and Chesapeake Bay impact structures. Modified from Poag et al. (2004)

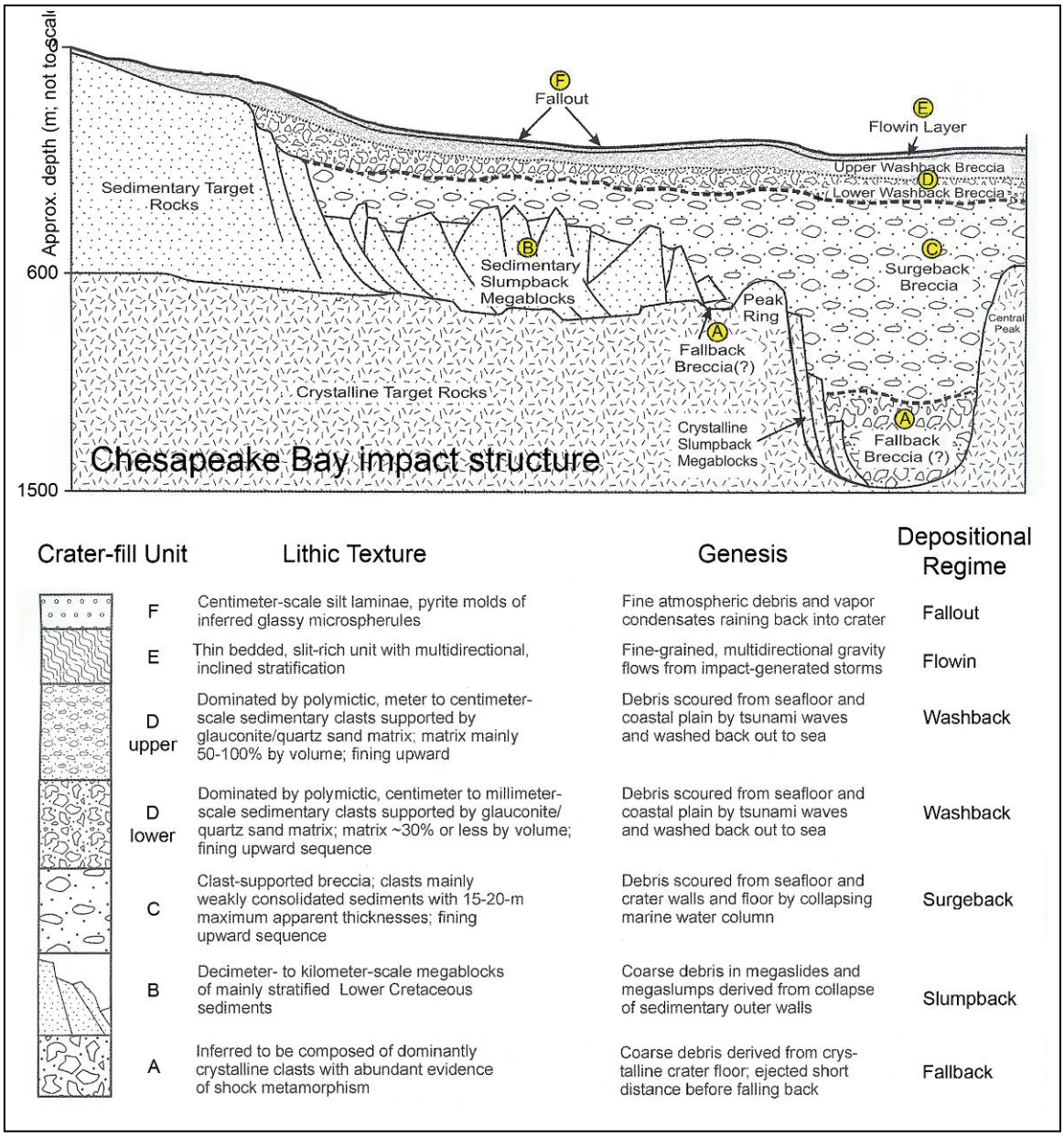

Figure 97. Geologic cross section of Chesapeake Bay impact structure and model of relationships between the lithic texture, origin, and depositional regime for each crater-filling unit. Modified from Poag et al. (2004)

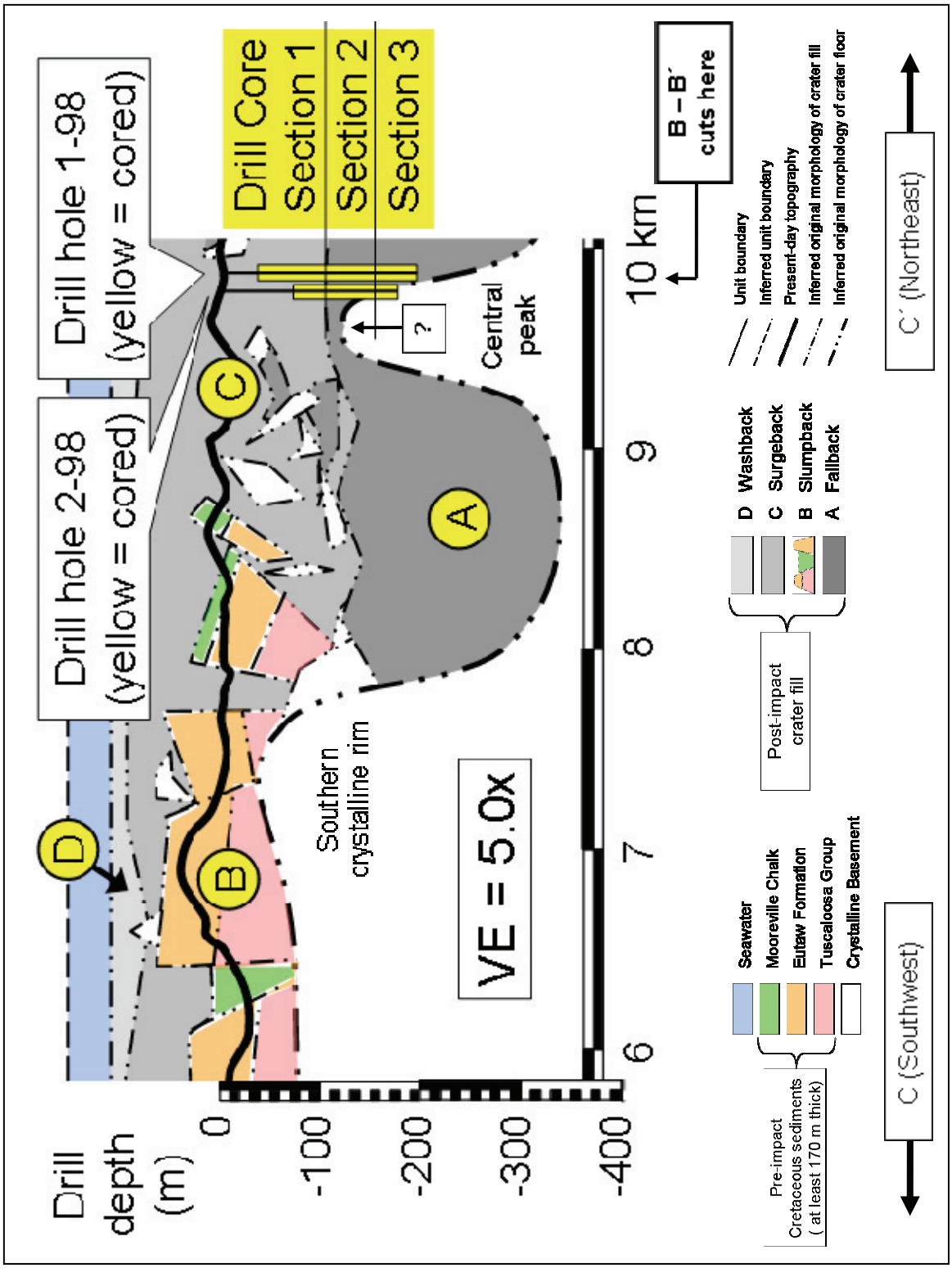

Figure 98. Chesapeake Bay model from Poag et al. (2004) applied to Wetumpka. Width of drill holes and width of cored sections not to scale.

INTERPRETATIONS

Because the preparatory objectives were non-interpretive, there will be no commentary on their results here. Although the *main objective* was also non-interpretive in nature, its results do require interpretation to understand fully their implications with regard to the Wetumpka impact structure as a whole. Similarly, the *ancillary objectives* require interpretation for the same reasons. The interpretations will overlap to some extent because aspects of one interpretation may depend partly on aspects of others.

Interpretations of Data from the Main Objective

In this first section, the results stemming from the *main objective* will be interpreted and discussed in preparation for interpretation of results stemming from the six *ancillary objectives*.

1. Interpretation of the Graphical (.pdf) Files

Interpretations appearing within the *drill core geological descriptions* (.pdf files) are present only in columns 7 and 8 of the *drill core geological descriptions* (Figure 43 and Figure 56). These columns include interpretive sketches and notes on various characteristics of the drill core. Additionally, there is a schematic diagram illustrating the drill core's lithozones, which are interpreted as clasts, matrix, or impact breccia. Further

information on these interpretations is provided below and in the last two subsections, which discusses interpretations of the results from the *ancillary objectives*.

2. Interpretation of the Lithofacies and Lithozones in the Drill Cores

In the first six columns of each *drill core geological description*, no attempt was made to assign a formal lithostratigraphic unit of origin for each lithozone of the twelve lithofacies categories. Doing so would not have been logical because different lithozones of bedded sandstone throughout the drill cores each could have come from any of the original Upper Cretaceous target units containing bedded sand.

However, in columns 7 and 8, attempts were made, where feasible, to assign a unit of origin to the various lithozones in the two drill cores. Based on lithofacies petrology, particular lithozones could be interpreted as to their probable unit of origin. The easiest to pick out were the pre-Cretaceous crystalline lithozones, which were lumped together as *pK Crystalline Basement* (or *pK* where abbreviation was necessary).

For the lithozones of sedimentary origin, no attempt was made to differentiate the Coker Formation from the Gordo Formation. Rather, these target units were both interpreted simply as *Tuscaloosa* (or *Kt* where abbreviation was necessary). Lithozones identified as being of probable Eutaw origin were labeled as *Eutaw* (*Ke*). No lithozone in either drill core could reasonably be interpreted as Mooreville Chalk.

Mooreville Chalk is absent within the drill core probably because, as the unlithified surficial unit on the seafloor at time of impact, it was largely ablated as is typical of marine-target impact processes (Poag et al., 2004). Additionally, the

Mooreville Chalk was probably not very thick at the time of impact, so it could not have contributed large quantities of crater-filling material to begin with (Figure 24).

3. Interpretation of the Quantitative Lithozone Data

In drilling and coring operations that penetrate undisturbed sedimentary, igneous, and/or metamorphic lithologies, Steno's principles, and the principles of uniformitarianism and gradualism, commonly apply. For example, one may safely assume that a 10-m-thick section of limestone in a drill core pulled from a sedimentary basin is indeed representative of that unit's actual thickness at the drill depth indicated for that particular drill hole. Further, one may also safely assume the limestone is laterally continuous (at depth) for a reasonable extent across the portion of the basin being drilled. But when drilling and coring megabreccias, Steno's principles must be applied with great care because the principles of catastrophism govern the processes involved, especially with regard to impact structures.

When interpreting the quantitative data from the two drill cores examined in this study, it is important to remember that all of the thicknesses and percentages described for the lithozones in the *Results* section are representative only of the portions cored in each lithozone's source material. As such, the quantitative values are not necessarily representative of the true thicknesses and percentages of clasts and matrix material filling the central region of the Wetumpka impact structure. Figure 99 illustrates this concept. With that in mind, the lithozones in the drill cores must be interpreted as *representative portions* of clasts or matrix material. A rigorous mathematical analysis of clast-size probability based on the thicknesses of lithozones in the drill core might lend insight into

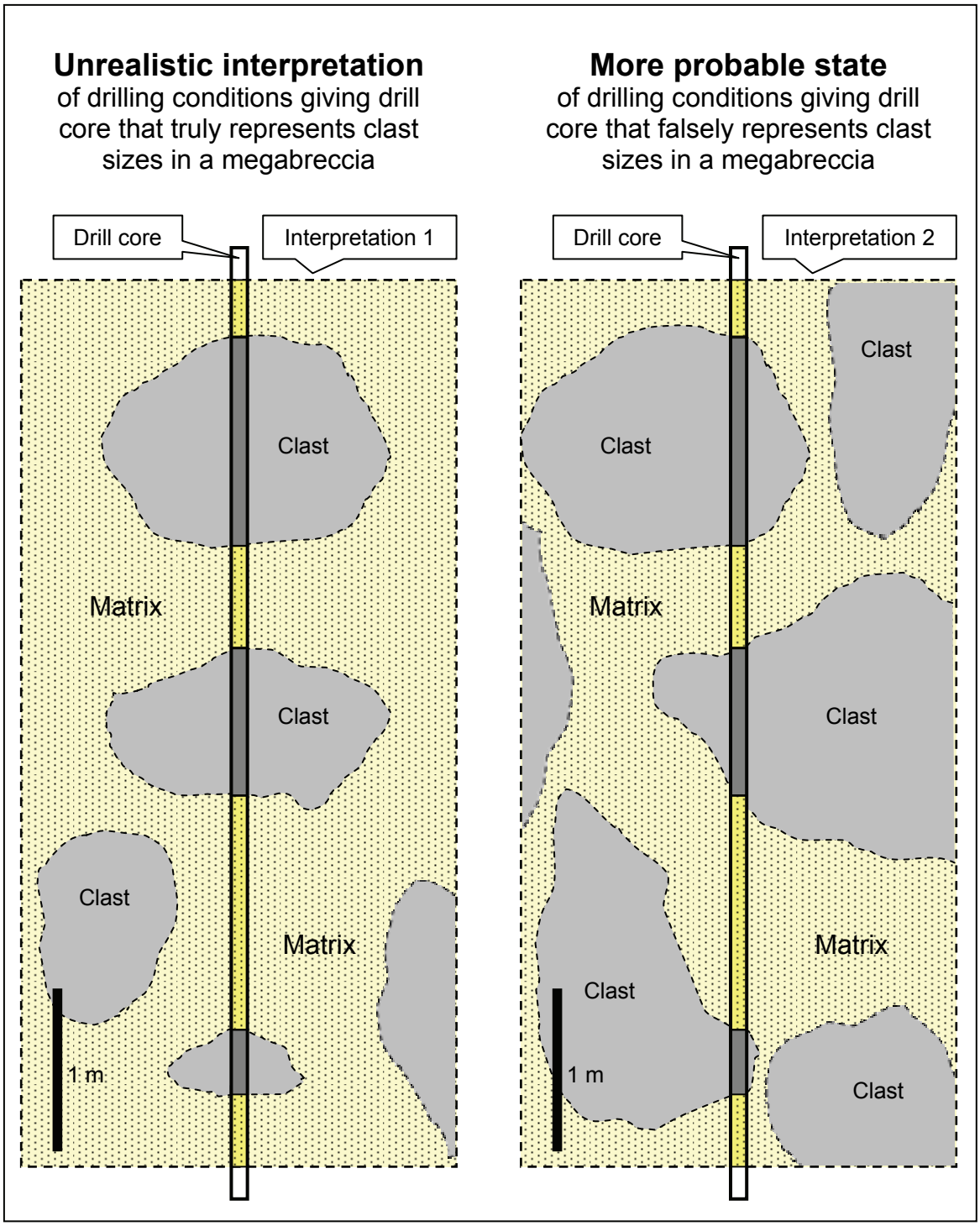

Figure 99. Differing interpretations of the same length of hypothetical drill core.

the actual sizes of clasts cored, but doing so was beyond the present study because two drill cores would not have provided sufficiently large datasets. Instead, the present author sought general trends in the thicknesses and percentages of lithozones, and rendered interpretations from these.

The graph in Figure 73 illustrates that the thicknesses represented by lithozones in the drill core generally fall into the decimeter to meter size range. The consistency of thickness and excellent recovery percentages indicate the lithozones in the drill cores probably offer a valid representation of the material drilled. Even so, those raw thicknesses are not representative of clast size and matrix thickness because some of these individual lithozones were later interpreted as lithologically different portions of the same intact clast of target strata (Figure 100A). Naturally, interpretations of this sort required that the two or more adjacent lithozones under consideration were not only in contact with each other, but could also be reasonably interpreted as having been deposited one atop the other in the pre-impact target region. Similarly, breccia lithozones were identified based on whether they had a matrix-supported or clast-supported lithofacies. Many individual though adjacent breccia lithozones in the drill cores have been subsequently lumped together during interpretation as one breccia body (Figure 100B). Still other lithozones were interpreted as fluidized sands forming the matrix between clasts (Figure 100C).

All of the material in each drill core was interpreted as above and the results of this effort are documented in the subsection comparing one drill core to the other, as well as the subsection comparing the Wetumpka impact structure to the Chesapeake Bay impact structure.

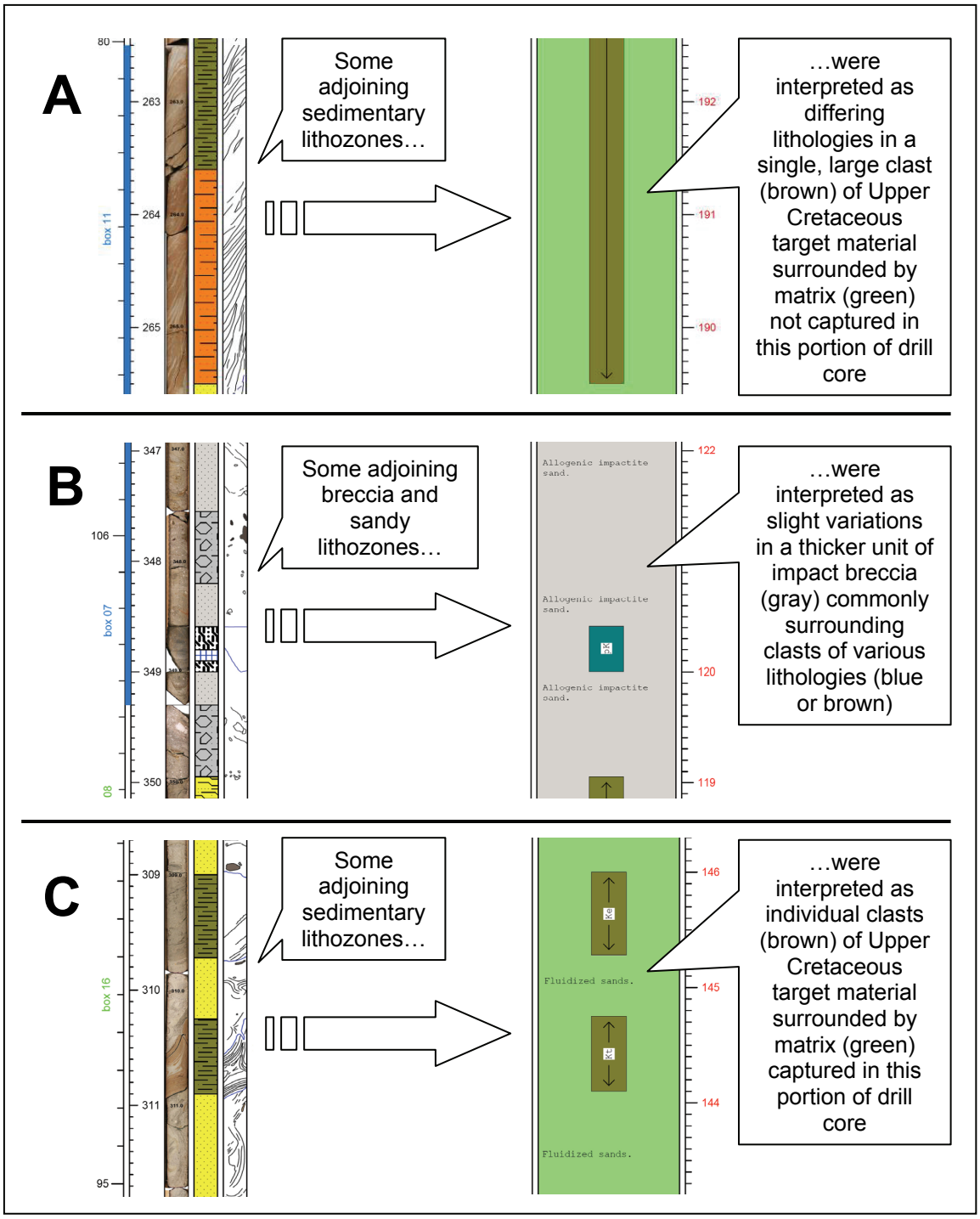

Figure 100. Examples of interpretation of lithozones based on lithofacies. A: Two lithozones interpreted as belonging to the same intact clast. B: Six lithozones interpreted as impact breccia with one large crystalline clast. C: Lithozones interpreted as two clasts within a matrix of fluidized sands.

Interpretations of Data from the Ancillary Objectives

The ancillary objectives were intended to place the drill core in a broader context than it otherwise would have been placed through description and follow-on interpretation alone. Each objective gave clear results, which are interpreted below.

1. Interpretations of Structures and Patterns Found in the Drill Core

The results of taking simulated drill core from the computer-rendered 3-D structural models were used to make interpretations and draw conclusions about the patterns and structures observed in the actual drill cores. The outcome was that some characteristics in the actual drill cores that were initially difficult to comprehend were rendered easy to interpret as, for example, simple folds, vertically oriented bedding, or simple faults. Some examples of some interpreted structures appear in the following figures: Figure 101 – inclined bedding may be misinterpreted as cross-bedding; Figure 102 – bull's-eye patterns interpreted as folds; Figure 103 – strongly disturbed bedding in vertically-oriented block; Figure 104 – enigmatic dovetail pattern interpreted as a reverse fault; and Figure 105 – a flat-faced clast appears to be a rounded clast.

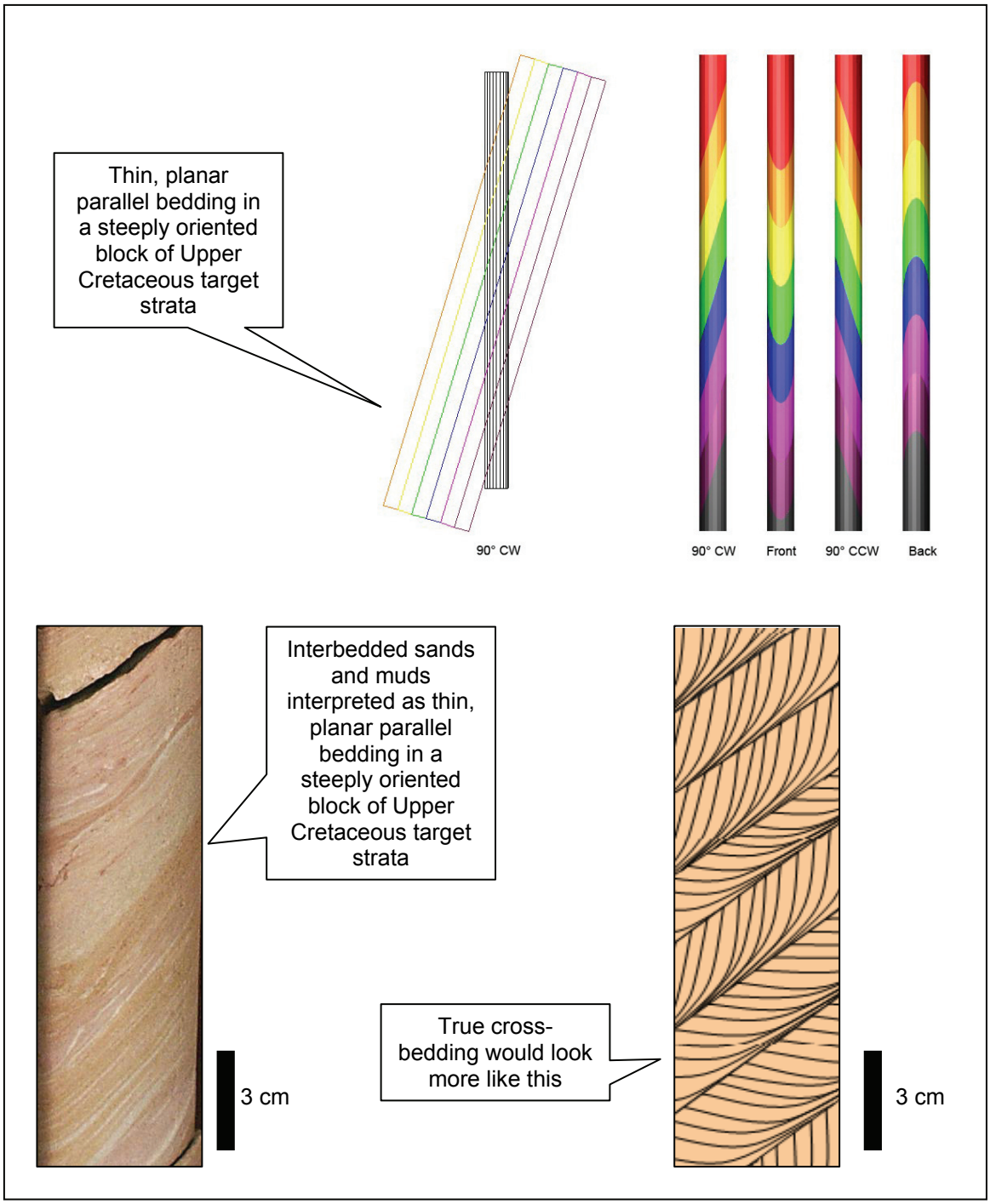

Figure 101. Inclined Bedding may be misinterpreted as cross-bedding in a thicker unit if the laminations are thin. Obviously, this is scale-dependent. Nonetheless, no cross-bedding of any scale was observed in either drill core.

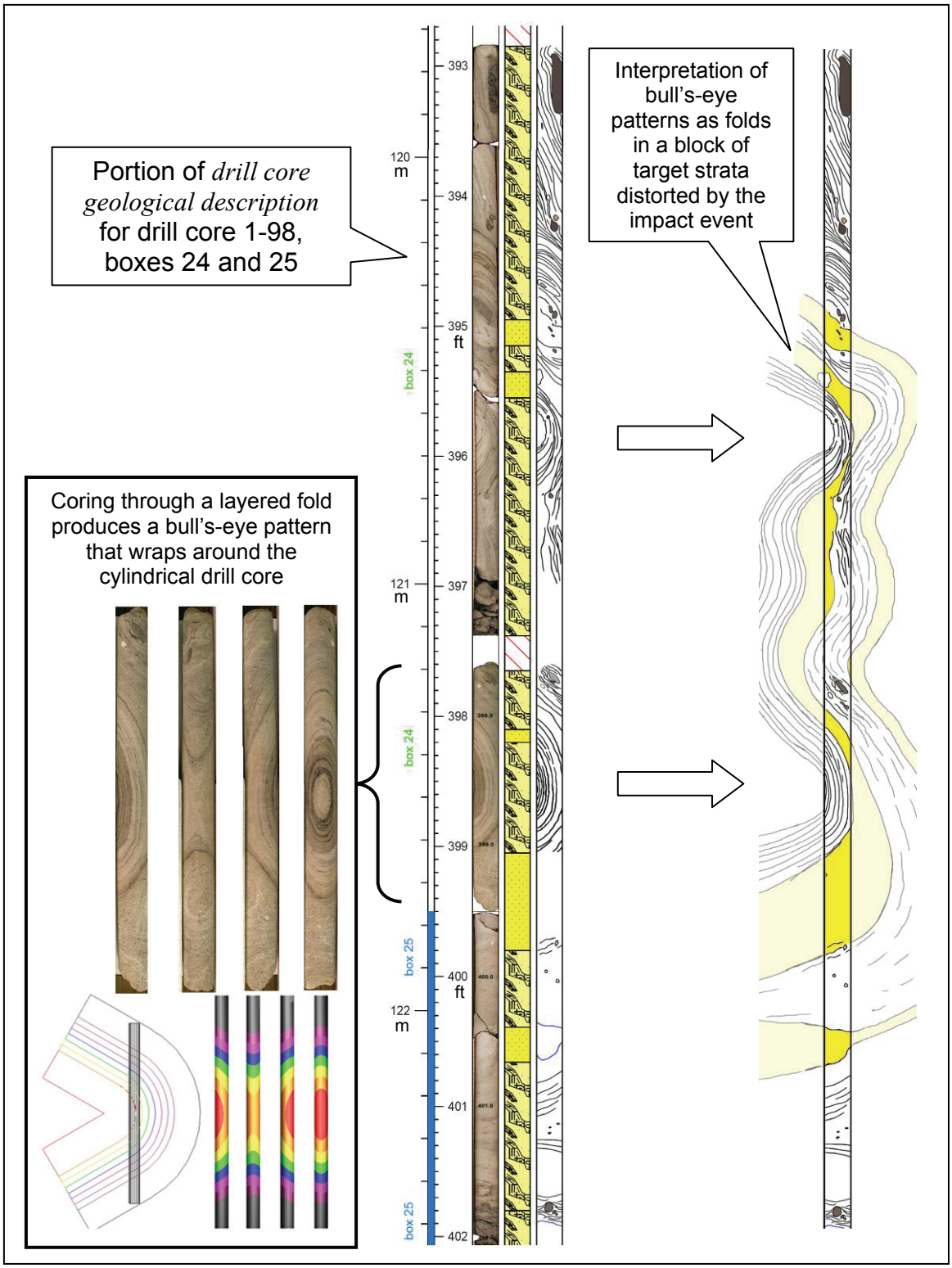

Figure 102. Although one may find these bull's-eye patterns tempting to interpret as fluidized sand that has been swirled, the present author interprets bull's-eye patterns as folding in disturbed blocks of originally layered Upper Cretaceous target strata.

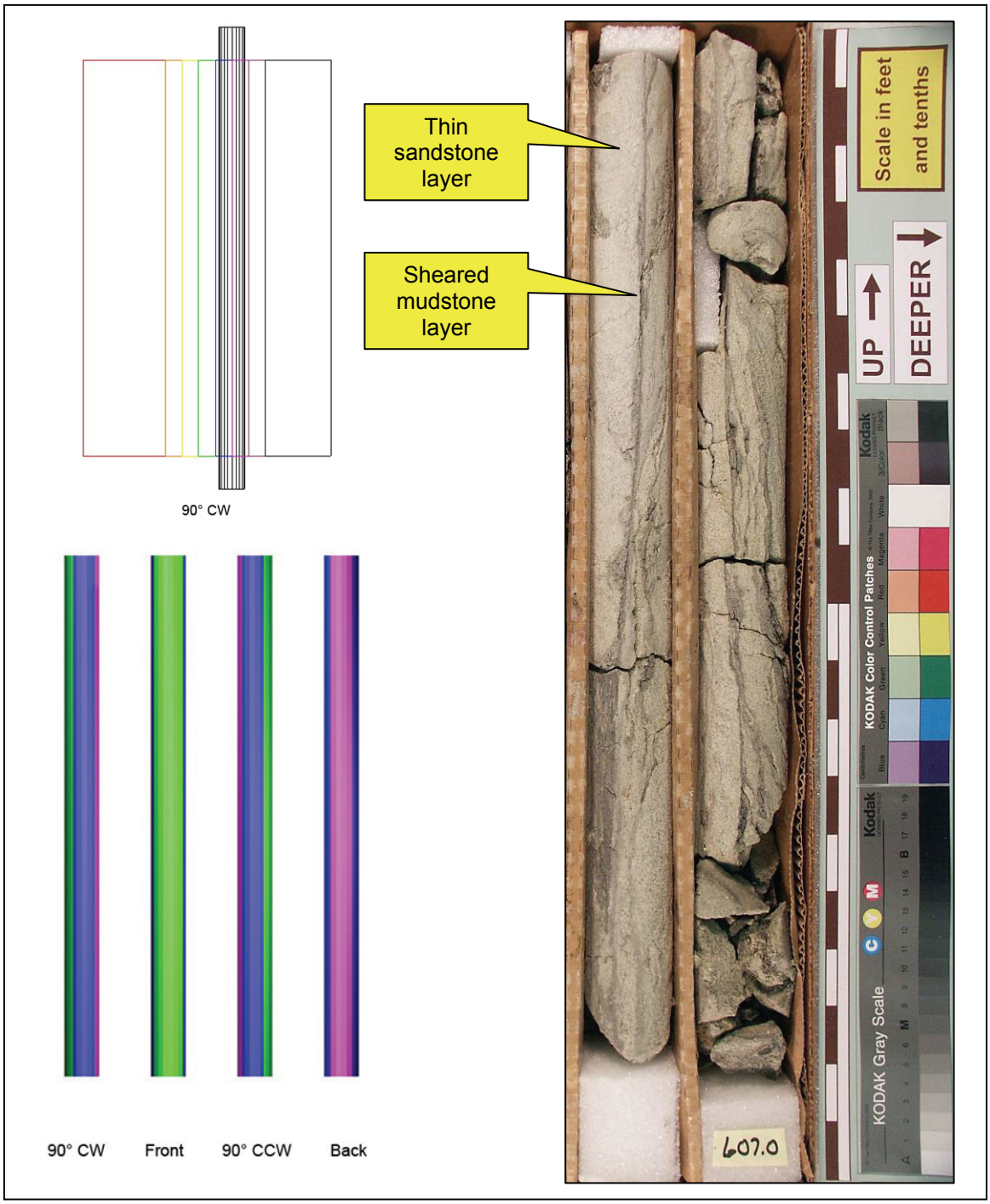

Figure 103. This chaotic-looking portion of drill core is interpreted as strongly disturbed bedding in a vertically oriented block of Upper Cretaceous target strata. The block appears to have been sheared along its original millimeter-scale mud-rich beds. Drill core 1-98, box 46. Each 0.1-foot mark is ~3 cm.

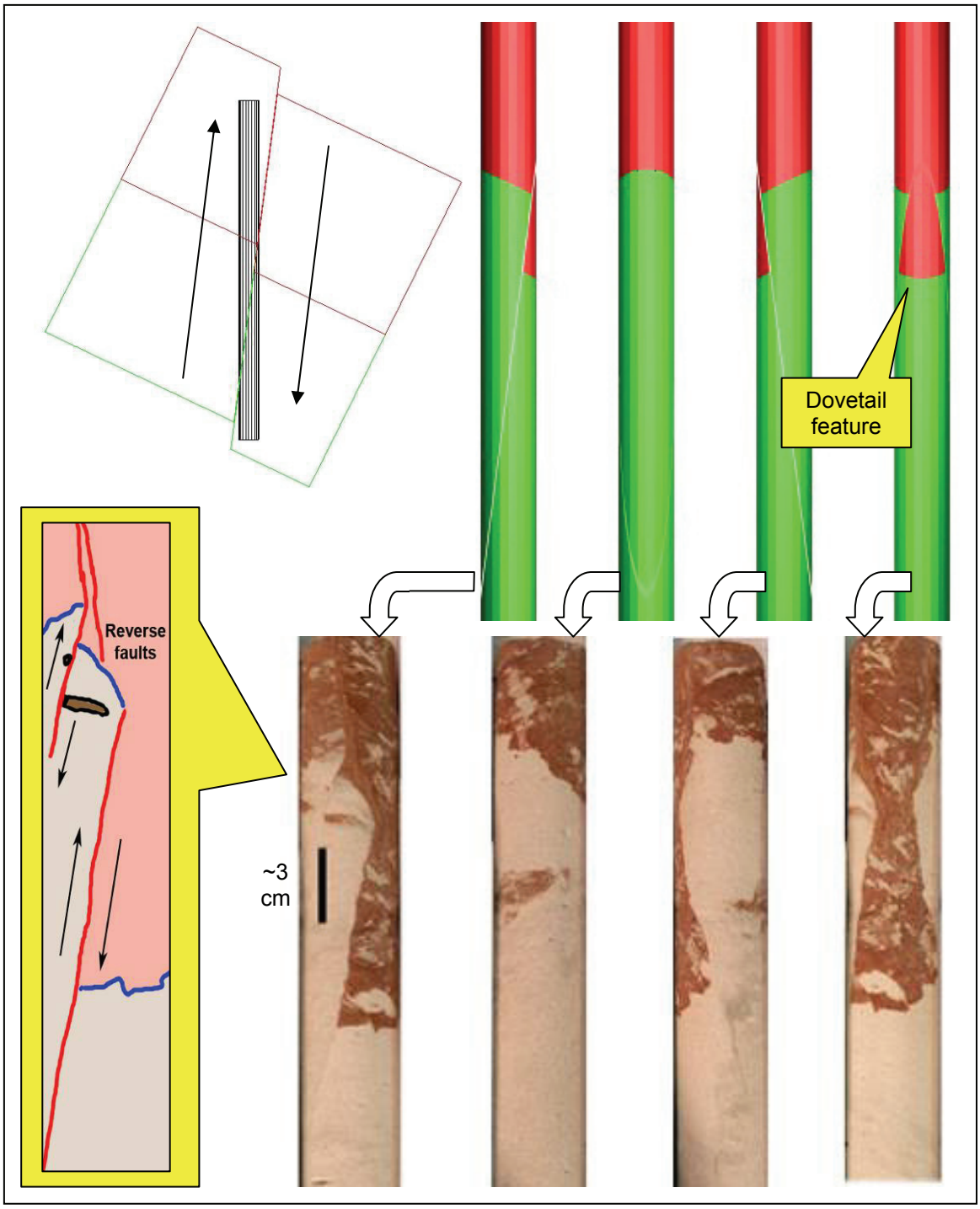

Figure 104. An enigmatic dovetail-shaped feature defining the boundary between oxidized and/or reduced zones of a sandstone is interpreted as a steeply dipping reverse fault intersecting the dipping boundary dividing the two zones. Drill core 1-98, box 40.

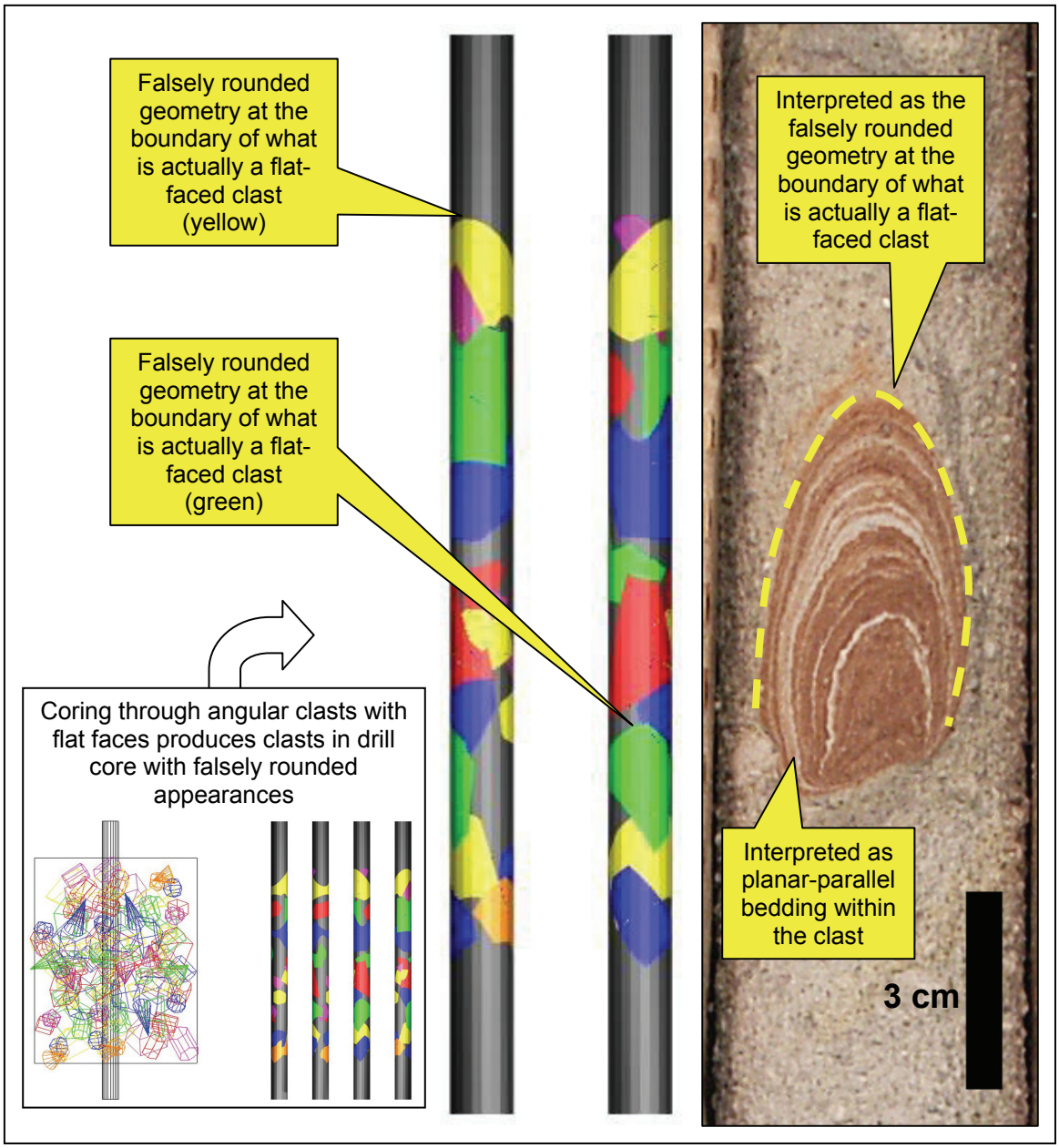

Figure 105. What appears to be either a rounded clast of layered mud, or an accretionary lapillus of silt-size material, is instead interpreted as a mud clast having a flat face that was given a falsely rounded appearance because of its exposure on the drill-core's positively curved surface. The apparently concentric layers within the mud clast are also interpreted as being planar (flat) in spite of their falsely rounded appearance. Clast found in box 36 of drill core 1-98.

2. Interpretations of the Position of Drill Core versus the Central Peak

Re-graphing and remapping the original elevation and gravity data from the 1994 survey made clear five points that have gone overlooked until now.

First, the data are interpreted to indicate that highest topographic point remaining in Wetumpka's central region is not the exposed central peak. Not only is the lithology of the wrong type, but the central peak's distinctive gravity signature is misaligned with the high point by ~0.5 km to the west (Figure 106).

Second, Neathery et al. (1976b) questioned whether the fault systems in the structurally disturbed crater-flanking terrain cut down into the crystalline basement. If the two normal faults bounding the outermost graben extended down into the crystalline basement, then there is a good chance that those two faults would have intersected the western end of the 1994 gravity survey. Given the thickness of target strata, roughly 200 m of down-throw in the graben would be required to preserve Mooreville Chalk. A down-throw of this nature in the crystalline basement would probably have left a gravity signature of reduced magnitude at one or two of the field stations (assuming the faults crossed the gravity transect). Because no reduced signature is present in the data, the present author believes the fault systems in the structurally disturbed crater-flanking terrain do not cut into the crystalline basement. Additionally, this is consistent with the marine-target impact structure model of Wetumpka wherein disturbed Upper Cretaceous target material moves in the impact structure's annular trough along a décollement.

Third, the small portion of gravity data taken at five field stations off of the pipeline transect show a markedly increased magnitude that is inconsistent with the expected structural (crystalline) floor of the impact structure (dashed blue lines, Figure

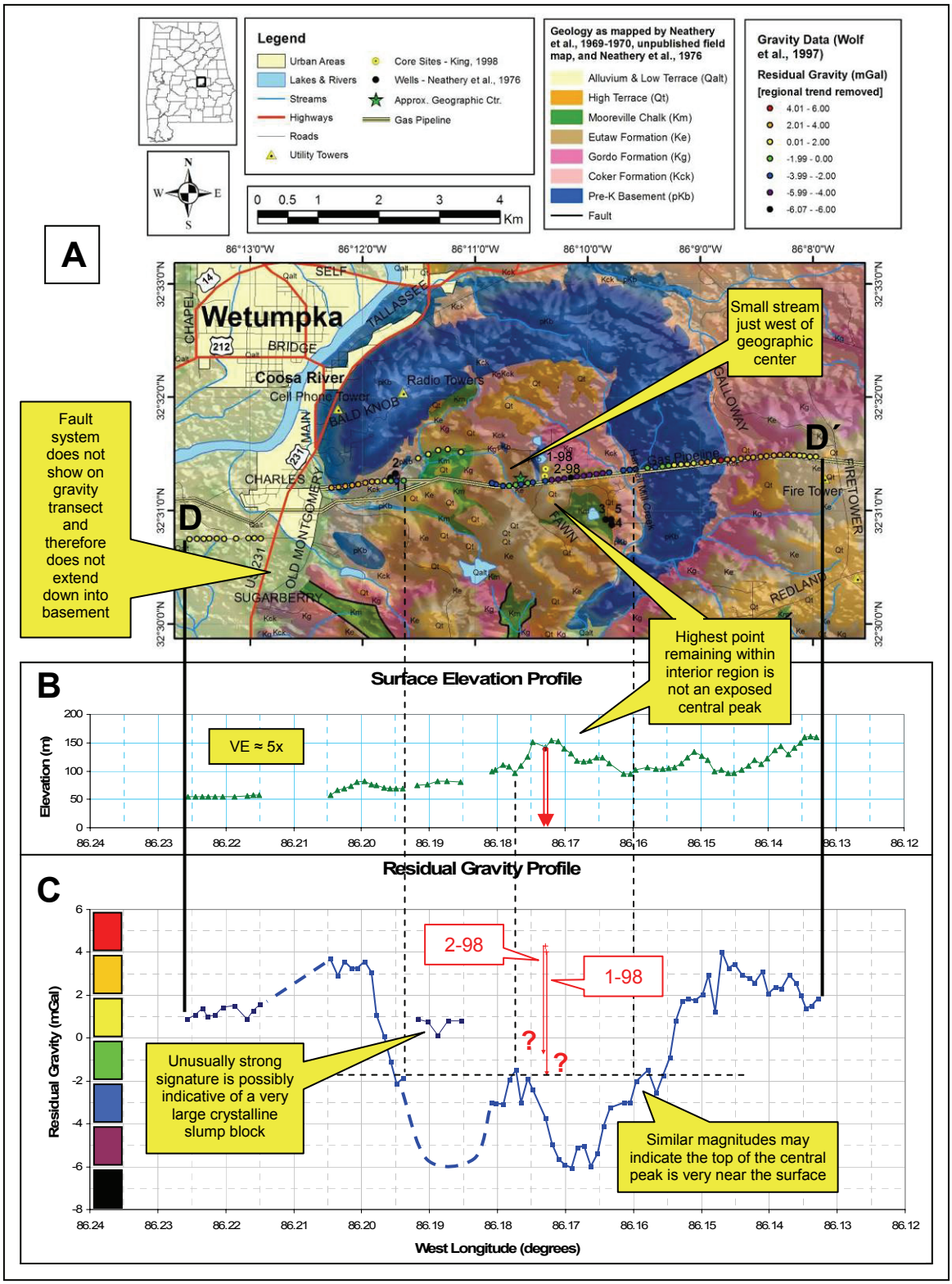

Figure 106. The present author's interpretation of original elevation and gravity data from the 1994 survey described by Wolf et al. (1997).

106C). Given their geographic position and increased magnitude, these data are interpreted by the present author as the signature of what may be a very large, buried crystalline megablock that either 1) slumped off the interior edge of the western crystalline rim; or 2) broke away from the southern crystalline rim and was moved into Wetumpka's central region during the surgeback event.

Fourth, the gravitational magnitude at the top of the central peak is essentially equal to that at the two points where the gravity transect intersects the interior edges of the crystalline rim (dashed lines, Figure 106A and C). This may indicate that the top of the central peak is very near the surface. However, the present author predicts that if the central peak is exposed, it will be so down in the small stream valley just west of Wetumpka's approximate geographic center, which is indicated by a green star on the maps in this report. This stream valley not only lies directly above the central peak, but it also provides one of the deepest cuts into Wetumpka's central region. As such, there is a good chance the stream cuts the central peak if the central peak reaches that high.

Fifth, Figure 32 shows there are small regions of enigmatic crystalline-clast breccia material cropping out immediately to the northeast of where the central peak may be exposed of just beneath the surface. King et al. (2005) interpret this material as fragments of the southwest crystalline rim deposited in their present locations during the surgeback event. However, it is also possible that this material is indeed large fragments of the central peak that were ripped away from the top of the central peak by the marine surgeback and deposited down-flow, to the northeast of the central peak. Nonetheless, this scenario is not depicted on any cross section of this report.

Sixth, considering the lateral alignment of the drill cores and the central peak's gravity signature, it is possible that drilling penetrated into the flank of the buried central peak. Further interpretation of data related to this issue will be made in subsequent portions of this report, which bring into consideration the geological features of the two drill cores.

Finally, a point worthy of mention is that when standing on the pipeline near the interior region's high point, Wetumpka's eastern crystalline rim will be visible as a low ridge within a broad valley beneath, and to the east of the observer (Figure 106B).

3. Interpretations of Palynology from the Ostensible Intra-crater Paleosol

This portion of the investigation of drill core from Wetumpka was based on the premise that the enigmatic mudstone in drill core 1-98 was either 1) a true intra-crater paleosol and/or lacustrine deposit that formed within the crater after the impact but before a catastrophic rim collapse event; or 2) a clast of Cretaceous target material at the base of the surgeback breccia. The rationale behind investigating palynomorphs from this lithozone was that palynological data could indicate the deposit's age and depositional history are consistent with one of the following scenarios:

A) If the age of palynomorphs in the mudstone was Campanian or younger, then the mudstone would have been thought to represent a terrestrial, lacustrine, and/or possibly marine lagoon deposit unique to the impact structure's inner basin. This would have indicated a long time lapse before deposition of the surgeback material.

B) If the age of palynomorphs in the mudstone was an *unusual mix* of Cenomanian and/or Santonian (and possibly Campanian too), then the mudstone would have been interpreted as a deposit of impact-pulverized mixed materials from the target units. Original, unmixed target materials would have contained the different palynomorphs in their initially separate units which became thoroughly mixed during the impact event and subsequently deposited in the crater some time between fallback deposition and surgeback thereby indicating a noteworthy (though probably brief, geologically speaking) time lapse between these two events.

C) If the age of palynomorphs in the mudstone predated the impact event, then the mudstone would probably be just a clast of target strata at the base of the

surgeback deposit, and it would not be possible to judge precisely the time lapse between deposition of the fallback breccia and the surgeback material.

Given that the palynomorphs in the deposit predate the impact event by roughly 20 million years, the present author interprets the deposit as a clast of Upper Cretaceous target material from the Tuscaloosa Group, probably the Coker Formation. Dark mudstone facies such as this are rare for the Upper Cretaceous sediments of the Wetumpka region.

4. Interpretations of $^{40}Ar/^{39}Ar$ Dating Results

Initial laser fusion analyses of individual, shock-deformed muscovite crystals yielded ages approximately coeval with regional Appalachian (crystalline) basement deformation (c. 300 Ma) suggesting little loss of accumulated radiogenic ^{40}Ar during shock deformation (Johnson et al., 2006). In essence, for the samples examined, shock pressures were high, but temperatures were not high enough to reset the age. Nonetheless, other samples dated under similar methods may yield results thought to be more consistent with the currently accepted stratigraphic age of the impact event. For such future investigations, Bottomley et al. (1990) indicate that when examining impact structures, $^{40}Ar/^{39}Ar$ dating is indeed the preferable dating method, but multiple samples need to be dated from each site. The present author would also recommend very careful selection of samples from the most shock-metamorphosed materials available.

5. Interpretations of Drill Core 1-98 and Drill Core 2-98

As indicated in the *Results* of this report, both drill cores have three sections, each with a general trend as to the variety of lithofacies present (Figure 92). Moreover, the data indicate that the drill cores share common traits with regard to these sections. Specifically, sedimentary-type lithofacies clearly dominate *section 1* in both drill cores; normalized percentages in this first section are similar between the two drill cores. *Section 2* in both drill cores contains a mix of sedimentary-type and impactoclastic-type (Stöffler and Grieve, 2006) lithofacies. Interestingly, the normalized percentages for this second section are also similar between the two drill cores. To summarize, *sections 1 and 2* can be correlated from one drill core to the next. However, the data graphed in Figure 92 also show that *section 3* in drill core 2-98 does not correlate well with *section 3* in drill core 1-98 because these lowermost sections contain diametrically opposed assemblages of lithofacies (Figure 92) that clearly dominate one drill core or the other. Figure 107 illustrates the present author's interpretation of how the three sections may or may not correlate across the distance between the two drill cores. Bear in mind that some aspects of this interpretation stem from application of data and models to be more fully interpreted in the subsection following the current subsection. But first, data from the two drill cores need further interpretation.

As explained earlier, various lithozones in the drill cores were interpreted as either a clast, a portion of a clast, or matrix depending on the geological characteristics of each lithozone (Figure 100). Taking this interpretive process to completion, the present author now proffers an interpretation of drill core data as clasts surrounded by matrix within various laterally extensive units of crater-filling material in the Wetumpka impact

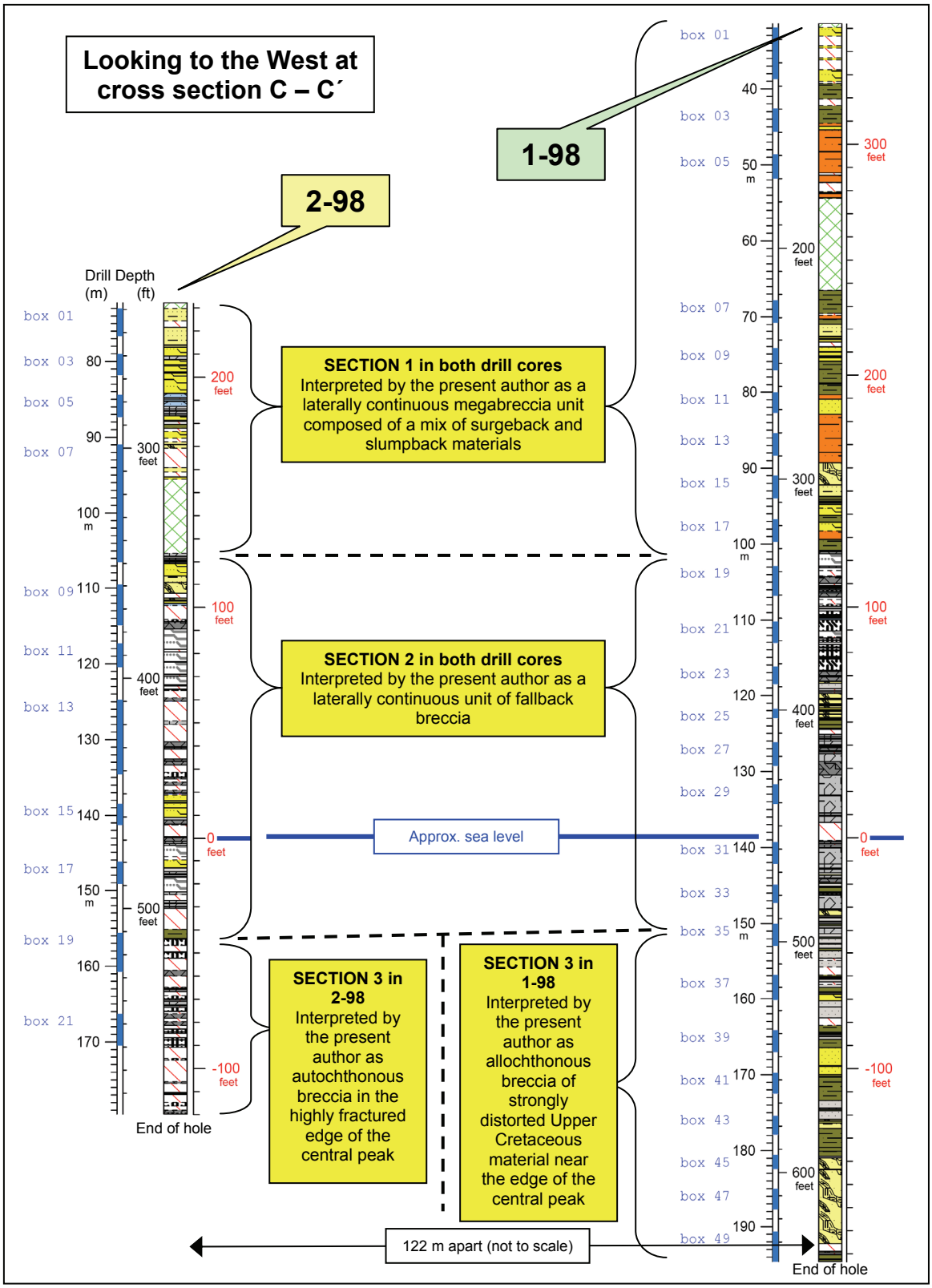

Figure 107. Interpretation of sections as crater-filling units according to impact models.

structure (Figure 108). The sizes (thicknesses) of interpreted clasts and/or clast portions are shown to the correct vertical scale, as are thicknesses of the matrix material above and/or below the clasts. The next subsection of this report places this interpretation in the context of Wetumpka as modeled according to the Chesapeake Bay impact structure.

As for the interpreted clasts themselves, Figure 109 illustrates changes in interpreted clast thickness where cored versus drill depth. Sections 1 and 2 in both drill cores exhibit matching trends between the two drill cores. These matching trends are taken as evidence that both section 1 and 2 are laterally continuous. Additionally, the upward changes in interpreted clast size may also indicate possible mega-sorting within the depositional regime responsible for each of these two sections. Conversely, section 3 in drill core 1-98 does not match with section 3 in 2-98. Both the clast sizes and their trends are dramatically different between the two drill cores. This is interpreted by the present author to be further evidence that the lower portions of both drill cores (section 3) each penetrated fundamentally different geologies. As before, the next subsection of this report will also place this interpretation in the context of Wetumpka as modeled according to the Chesapeake Bay impact structure.

Histograms showing the distribution of interpreted clast-sizes are provided in Figure 110 for thoroughness, but the author stresses that the graphs are valid only to the extent that they speak to the clasts as interpretations of lithozones in the drill cores. Everything smaller than -3.5 ϕ (medium pebble gravel) was considered to be matrix. In every section, matrix has the most common frequency of occurrence, but this is not to be confused with the thickness (or thinness) of these lithozones in the drill cores. Overall,

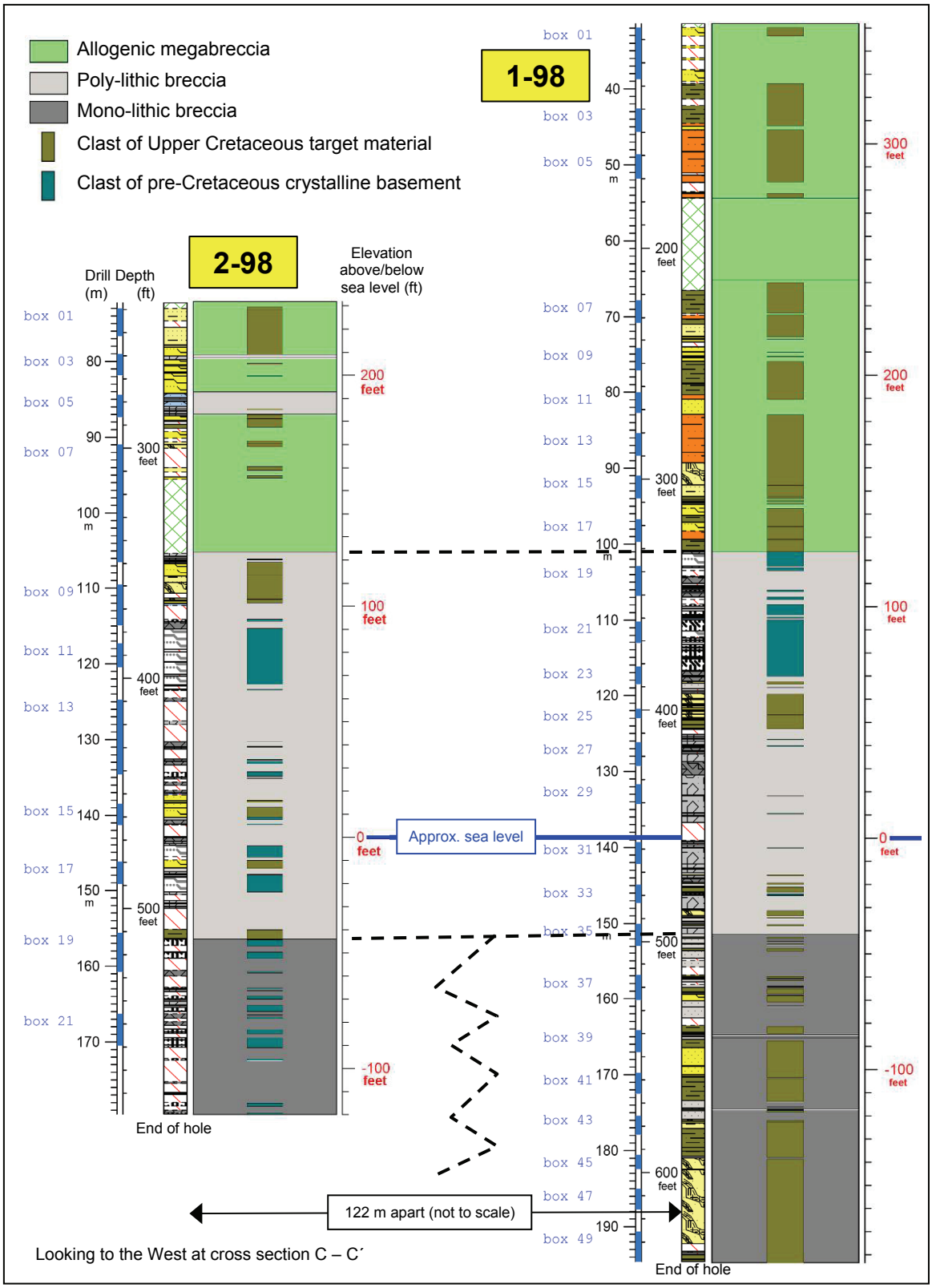

Figure 108. Interpretation of lithozones as clast portions or matrix in sections 1 to 3.

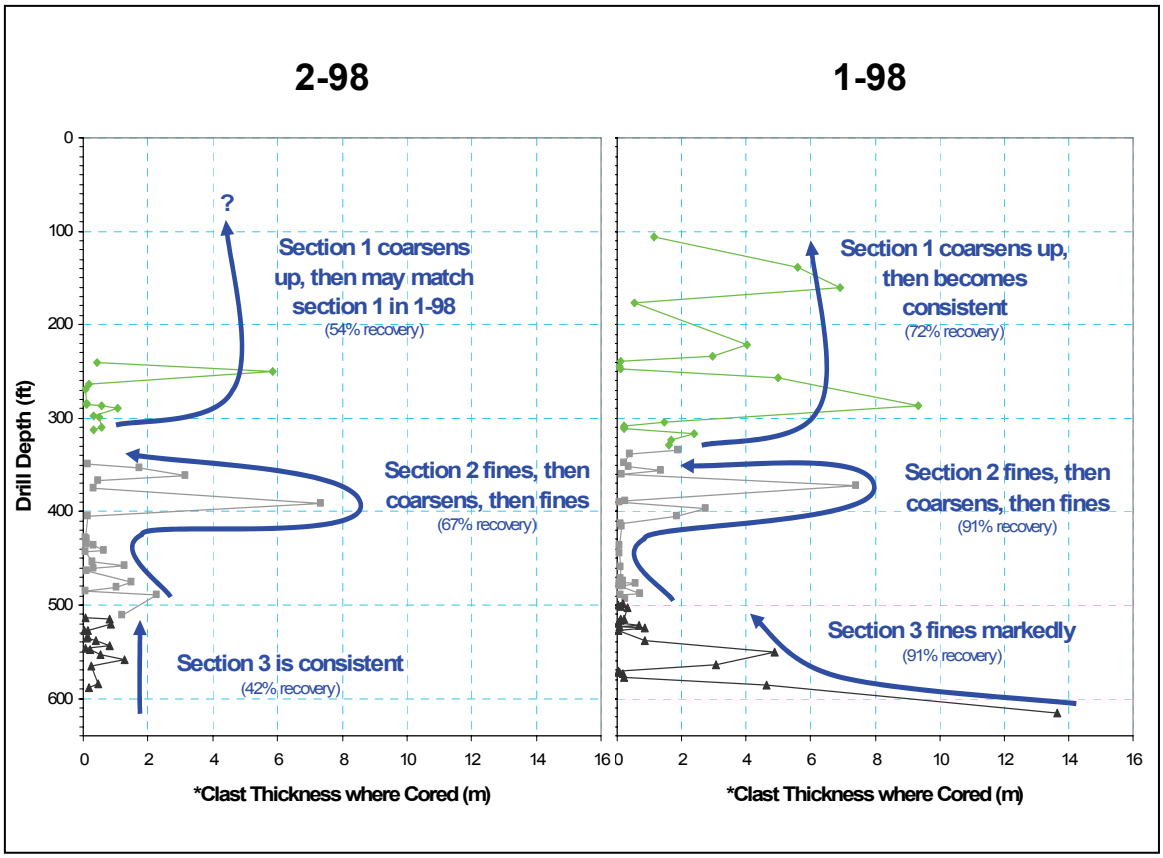

Figure 109. Comparative graphs of interpreted clast thickness where cored versus drill depth. Note the matching trends in sections 1 and 2 in both drill cores, and the mismatching trends in section 3. Changes in interpreted clast size indicate possible mega-sorting within the depositional regime responsible for each of the three sections.

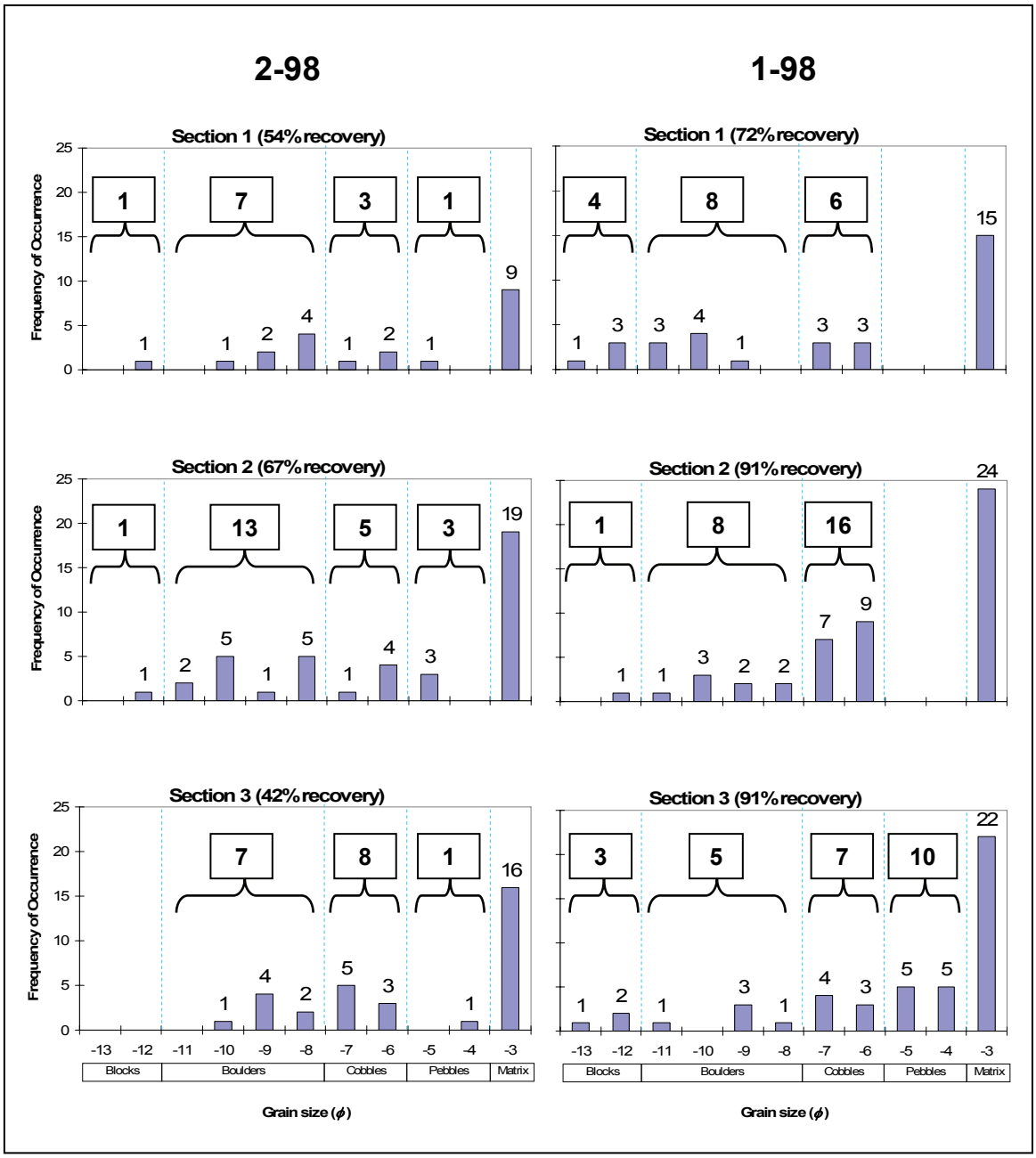

Figure 110. Histograms showing size distribution and frequency of occurrence for interpreted clasts and matrix in each section of the drill cores.

interpreted clast sizes show an even distribution with cobble- and boulder-sized portions being the most common.

6. Interpretations from Comparing Wetumpka to Chesapeake Bay

Comparing the Wetumpka impact structure to the Chesapeake Bay impact structure as described in Poag et al. (2004) helped produce refined cross sections of Wetumpka in its current state of preservation (Figure 111). Whereas much of the material in what was probably Wetumpka's annular trough has been eroded away, the crater-filling materials within Wetumpka's inner basin have been largely sequestered from regional erosion. This is probably a consequence of the raised crystalline rim, and to a lesser extent the general topographic slope away from the Appalachians, preventing the region's two major rivers from entering the inner basin once their waters cut below the flanks of the crystalline rim. While a great deal of surgeback breccia remains within Wetumpka's interior, all of the washback, flowin, and fallout materials (indicated on the Chesapeake Bay model, Figure 97) have long since been eroded away.

Figure 112 illustrates the present author's interpretive sketch of the crater-filling materials from which the two 1998 drill cores were taken. The figure ties together data from the two drill cores as well as interpretations from the gravity profile, and puts them in the context of the model developed by Poag et al. (2004) for the crater-filling material at the Chesapeake Bay impact structure. Although there are three sections in each drill core, there remain only two known main units of crater-filling material. Descriptions of the crater-filling units represented by each section follow.

Section 1, both drill cores – Surgeback and Slumpback Megabreccia

Section 1 of both drill cores was drawn from a laterally continuous megabreccia that has been eroded down to roughly 100 m thick. This topmost unit is found at the

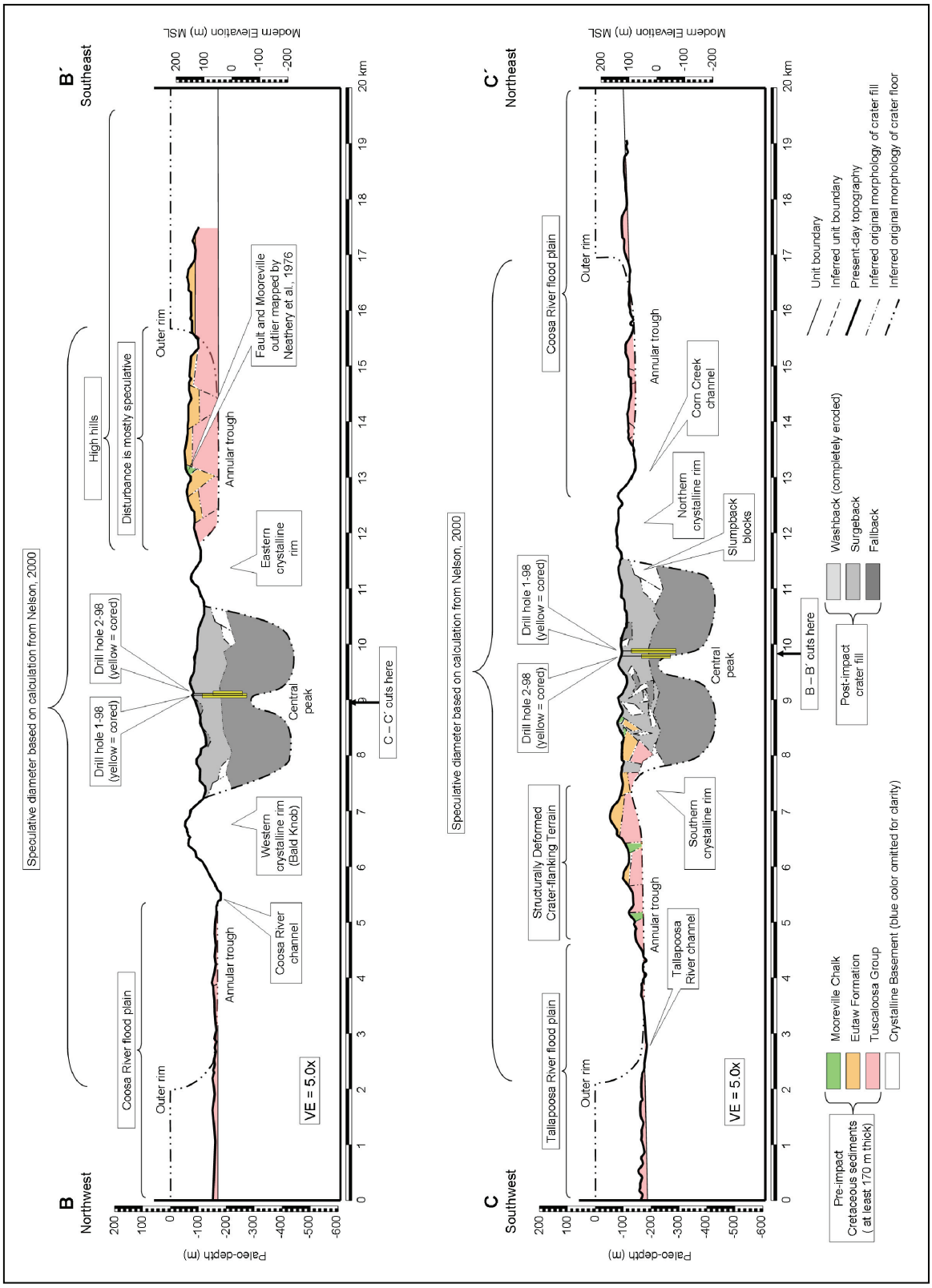

Figure 111. Current state of preservation at the Wetumpka impact structure.

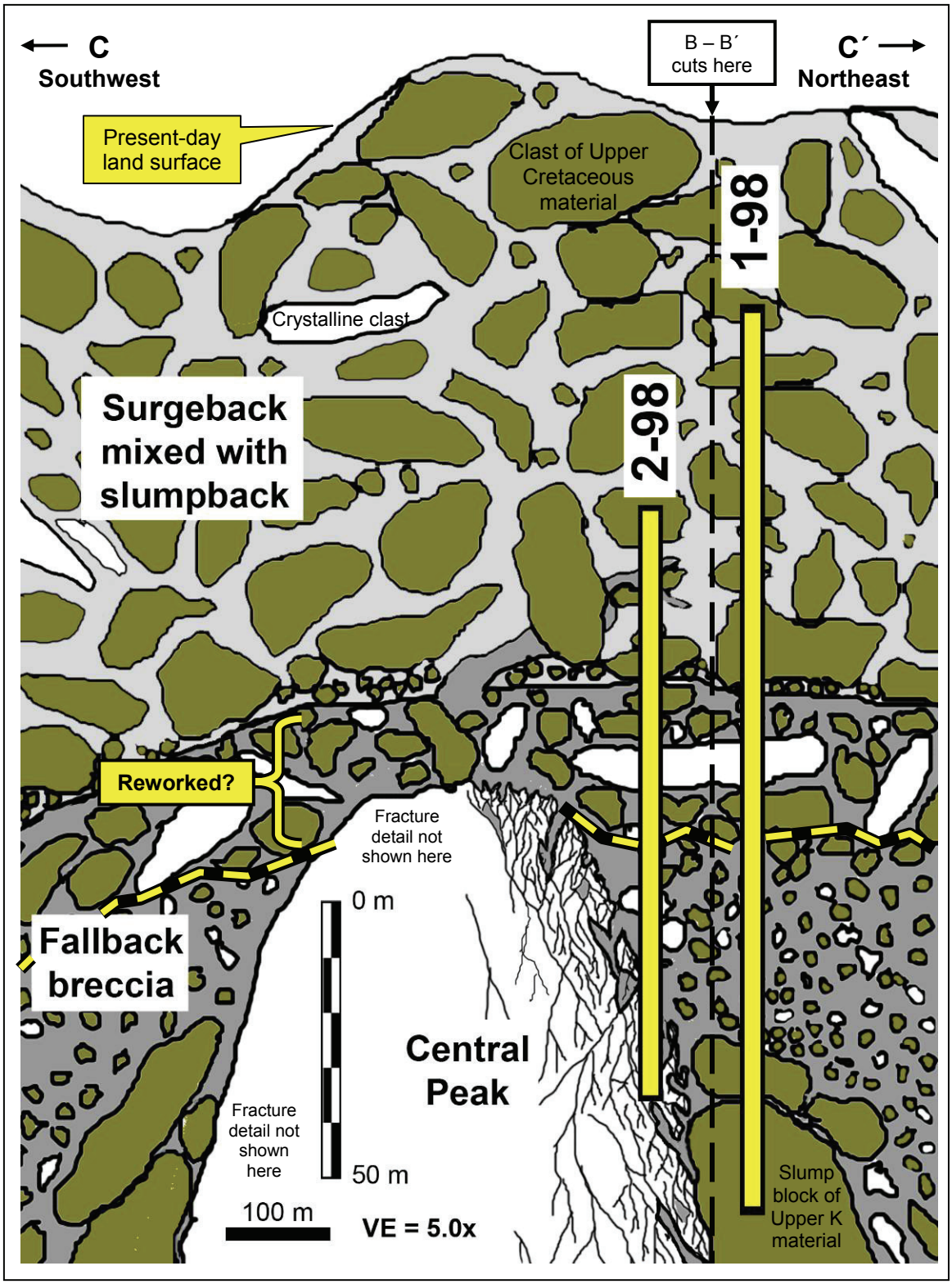

Figure 112. Interpretive sketch of drill core penetration. Width of drill cores not to scale.

surface across most (if not all) of the central interior region surrounded by Wetumpka's crystalline rim. Overall, this megabreccia is comprised of a mix of surgeback and slumpback materials composed mainly of clasts of upper Cretaceous target units within a matrix of fluidized sand, itself derived from pulverized Upper Cretaceous target units. Large crystalline clasts are known to be present at some locations on the surface of this unit, although no such clasts were observed in section 1 of either drill core. Breccia bodies (dikes?) are present but seem to be uncommon. This megabreccia appears to be primarily clast-supported. As graphed in Figure 109, and illustrated in Figure 112, this unit also appears to have at its base a ~15-m-thick region of fine to coarse boulders (0.25 to 4.1 m diameter) of Upper Cretaceous target materials that sharply coarsen to fine and medium blocks with interpreted diameters of roughly 4 to 16 m, sized according to Blair and McPherson's (1999) scale. Interpreted clasts seem to have distorted edges and undistorted interior regions.

Section 2, both drill cores – Fallback Megabreccia

Section 2 in both drill cores is interpreted to represent a laterally continuous megabreccia unit of fallback material, which apparently is not exposed anywhere at the surface. Total thickness of this unit may only be guessed at by comparative analysis with better-known impact structures of marine-impact origin because the crystalline basement at Wetumpka has yet to be drilled. Conservative estimates of this unit's total thickness put it at ~250 m. Overall, this unit contains a mix of clasts originating from both the Upper Cretaceous target units and the crystalline basement. A matrix of fluidized sands

and distinct breccia bodies (dikes?) surrounds the clasts, which are primarily matrix-supported.

As graphed in Figure 109, and illustrated in Figure 112, this fallback unit is interpreted to have a middle region at least 25 m thick defined by a slight fining upwards of interpreted clast size. Note that although this region is found at the base of section 2 in both drill cores, it is not the base of the fallback unit itself. Sizes of interpreted clasts in this region are interpreted to be coarse boulders (~2 m) at the lowest portion, and fine upwards to medium pebbles. At a drill depth of approximately 125 m in both drill cores, interpreted clast sizes, sized according to Blair and McPherson's (1999) scale sharply increase to fine block (~8 m) before dropping back to very coarse boulder (~3 m). All together, this curious pattern of apparent sorting in section 2 (Figure 109) may be an indication of normal grading in the fallback breccia, with the uppermost portion having possibly been reworked by the overlying marine surgeback as was first speculated on by King et al. (2004b).

The breccia bodies (dikes?) within the fallback unit vary from clast-supported to matrix-supported, and were observed to have clast sizes ranging downward from medium pebble to granule (~16 to 2 mm). Clasts in these breccia bodies (dikes?) are also both Upper Cretaceous and crystalline, and range from very angular to well rounded. Some sedimentary clasts are strongly sheared. Matrix material in the breccia bodies ranges from very fine and silty to medium sand-size grains.

Section 3 in 1-98 – Slump Block(s) of Upper Cretaceous Target Strata

Unlike the previous two sections, section 3 in drill core 1-98 does not correlate with section 3 in 2-98. In drill core 1-98, section 3 seems to have penetrated an unusually thick, mass of Upper Cretaceous target strata. This material is an interbedded sandstone and mudstone with its strongly distorted bedding commonly at a near vertical orientation in the drill core. Unlike other interpreted clasts, this clast not only gave exceptionally continuous recovery of drill core, but it is also over two times thicker than any other interpreted clast (Figure 109). Furthermore, this mass of Upper Cretaceous material is distorted throughout its length – not just on its edges. Therefore, as illustrated in Figure 112, this mass is interpreted to be a strongly sheared megablock of Upper Cretaceous target strata on the northeastern flank of the central peak. This presumed megablock is though to have slumped off the central peak during the peak's rise and/or rebound in the modification stage of crater formation (Figure 4). The slumped megablock is illustrated as having rounded edges owing to both the abrasive actions of the central peak's dynamic ascent and collapse, as well as the coarse nature of the fallback breccia, which would have ground against the slumping megablock.

Section 3 in 2-98 – Brecciated Edge of Central Peak

Section 3 in 2-98 is strikingly different from all other sections in either drill core. The data show that its lithology of breccia bodies and crystalline clasts is unlike anything else cored (Figure 92) and it gave the lowest percentage of recovery (42%). Such poor recovery may be due in part to the small size range of interpreted clasts in this section. Additionally, these interpreted clasts are unusually consistent in size (Figure 109) and

appear as though part of an autobreccia in the crystalline basement rock. Significantly, many lithozones of crystalline material in this section of drill core 2-98 exhibit a distinct foliation having a vertical orientation. Most other lithozones of crystalline material in the drill cores have foliations that are randomly oriented. Taking these points into consideration, and giving careful weight to the 1994 gravity data from Wolf et al. (1997), section 3 in drill core 2-98 is interpreted to represent the highly brecciated edge of the central peak (Figure 112). Apparently, drill core 2-98 penetrated ~25 m into the central peak's edge before all drilling was stopped. Figure 113 illustrates a schematic of Wetumpka's central peak with no vertical exaggeration.

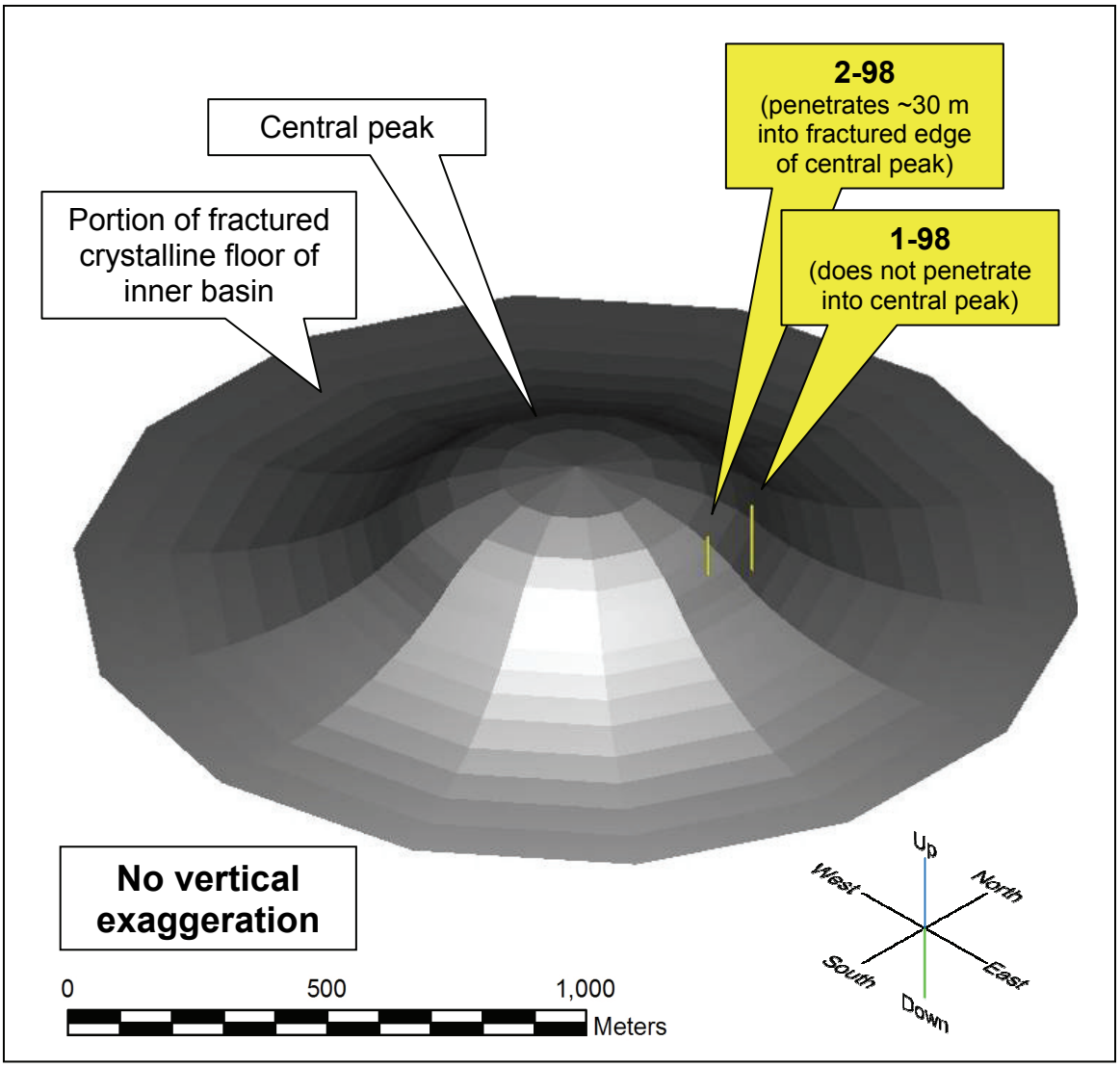

Figure 113. TurboCAD® 3-D schematic of central peak and surrounding portion of fractured crystalline floor of Wetumpka's inner basin. No vertical exaggeration is applied. Without the vertical exaggeration of 5.0x used in the cross sections, the central peak assumes a broad, subdued topology. As drawn, the central peak is centered on the impact structure's approximate geographic center (green star) shown on most maps in this report. Both drill cores are depicted in their correct geographic positions and depths. Drill core widths are enlarged to 2 meters so that they may be visible at this scale.

CONCLUSIONS

Overall, the data and illustrative figures presented in this report together demonstrate that Wetumpka models very well as a large, but strongly eroded marine-target impact structure. In essence, Wetumpka is not very different from a small version of the Chesapeake Bay impact structure. As such, by studying Wetumpka, we may gain insight into other, less-well-preserved marine impact structures and some features rendered inaccessible at the Chesapeake Bay structure by its overburden of water and sedimentary material. Based on the data compiled, examined, and modeled, the present author draws the following conclusions:

- At time of impact, the Eutaw Formation in Wetumpka's target region was at least 30 m thicker than previously recognized. As such, the Eutaw's thickness at time of impact was probably over 60 m, which means the total thickness of Upper Cretaceous target sediments would have been in excess of 170 m.
- All currently known geological features at Wetumpka fit well with the generic models for shallow, near-shore, marine-target impact structures, which have as their general morphology a central peak, a catastrophically-filled inner basin with a crystalline rim, an annular trough containing structurally disturbed slumped megablocks, and an indistinct outer rim in sedimentary strata (Higgins and Butkovich, 1967; Melosh,

1982; Nelson, 2000; Ormö and Lindström, 2000; Poag et al., 2004). This is a strong indication that the extant Wetumpka impact structure was originally a much larger impact crater that was filled during the *surgeback*, *washback*, *flowin*, and *fallout* events, further buried by post-impact normal marine deposition, then later exhumed and deeply eroded by sea level changes and fluvial action.

- The Mooreville Chalk Formation (a hemipelagic ooze topping the seafloor target strata at time of impact) was probably vaporized and/or disintegrated in the target area (Kieffer and Simonds, 1980) thus explaining 1) the overall non-calcareous nature of both drill cores; 2) the Mooreville's complete absence in the two drill cores; and 3) the Mooreville's rarity at the surface of the crater-filling material. Additionally, the Mooreville is also nearly absent from the Wetumpka impact structure because, as Stöeffler et al. (1980) demonstrated, fast-moving ejecta formed in a bolide impact is comprised mostly of the upper target strata. That is, whatever portion of the Mooreville Chalk escaped vaporization was instead ejected from the forming crater. The outliers of Mooreville Chalk at the tops of the grabens in what was originally Wetumpka's annular trough were preserved from these processes by the simple fact that the material exposed today was, at time of impact, completely buried by semi-intact overlying Mooreville.
- There are twelve recognizable facies comprising three distinct units within both drill cores. These units correlate from one drill core to the next.
- The present author's new interpretation of the 1994 gravity survey (Wolf et al., 1997) indicates the central peak may rise to near-surface levels as indicated by its similar gravitational magnitude with the inner edges of the exposed crystalline rim. As such,

Wetumpka's central peak is probably not fully exposed at the surface, but the enigmatic outcrops of crystalline clast breccias northeast of the impact structure's geographic center may have originated on the central peak. Given the outcrops' down-flow positions relative to the top of the central peak, and the direction of surgeback described by King et al. (2005), this is a distinct possibility worthy of further study. Until then, the best surface location to explore for exposure of the central peak is in a small stream valley ~0.5 km west of the 1998 drill sites.

- Five unusually strong readings of gravity magnitude recorded off-transect in the 1994 survey near the inside edge of the western crystalline rim probably indicate the presence of a buried crystalline megablock that either slumped off the crystalline rim into Wetumpka's inner basin, or was washed into the inner basin during the surgeback event. If the latter is correct, then the clast may have originated on the southwestern crystalline rim.
- The normal faults within the *structurally disturbed crater-flanking terrain* probably do not cut into the crystalline basement because there is no indication of these faults where their basement-cutting traces would be expected to intersect the 1994 gravity survey transect.
- The eastern crystalline rim at Wetumpka may be observed from the location where the gas pipeline right-of-way intersects the topographic high point within Wetumpka's central region. From this vantage point, the eastern crystalline rim sits as a low ridge at the bottom of a broad valley below and to the east of the observer.

- *Washback*, *flowin*, and *fallout* units, as described at the Chesapeake bay impact structure by Poag et al. (2004), are not presently observed at Wetumpka because they have been completely eroded away.
- Two main crater-filling units are all that remain preserved within Wetumpka's inner basin. These laterally extensive units are the fallback breccia, and the overlying mix of surgeback/slumpback breccias. Both units are consistent with similar units observed in drill cores from the Chesapeake Bay impact structure (Poag et al., 2004).
- No intra-crater paleosol unit of any kind divides the two main crater-filling units. The enigmatic lithozone thought to have been potentially indicative of a possible intra-crater paleosol (King et al., 2004b) has been shown instead to be a clast of pre-impact paleosol material from the lowermost strata of the Upper Cretaceous Tuscaloosa Group. By chance, this clast sits at the boundary between the two main crater-filling units, and its bedding is in a horizontal orientation. The clast is not indicative of a unique ecosystem within the Wetumpka structure.
- The top of the fallback breccia may show evidence of having been reworked by the marine surgeback. Interpreted clast sizes within the fallback unit seem to show two upward-fining sequences in each drill core.
- The Reeves drill core (2-98) penetrated the edge of Wetumpka's central peak. This conclusion is based on comparison of Wetumpka with the Kärdla and Chesapeake Bay impact structures, the new interpretation of the gravity transect taken at Wetumpka in 1994 (Wolf et al., 1997), and the broad morphological variations of central-peak structures in several well-documented marine-target impacts (Puura and Suuroja, 1992; Poag et al., 2004).

- The $^{40}Ar/^{39}Ar$ dating attempt is interpreted as only partly successful because it gave an age of ~326 Ma. This age is comparable to Alleghenian muscovite ages of the regional crystalline basement. What could be inferred is that the impact event was not hot enough to cause much loss of accumulated radiogenic ^{40}Ar from the shock-metamorphosed muscovite crystals that were dated (Johnson et al., 2006).
- Several enigmatic structures and/or patterns observed in the two 1998 drill cores have been modeled successfully and explained as faults, folds, sheared bedding, angular clasts, etc. These interpretations may help explain similar features found in other drill cores.

REFERENCES

Alvarez, L.W., Claeys, P., and Kieffer, S.W., 1995, Emplacement of Cretaceous-Tertiary boundary shocked quartz from Chicxulub crater: Science, v. 269, p. 930-935.

Alvarez, W., Claeys, P., and Burns, E., 1993, A candidate KT boundary impact crater in Alabama [abs.]: Eos, (Transactions, American Geophysical Union), v. 74, p. 387.

Baksi, A.K., Archibald, D.A., and Farrar, E., 1996, Intercalibration of $^{40}Ar/^{39}Ar$ dating standards: Chemical Geology, v. 129, p. 307-324.

Bentley, R.D., and Neathery, T.L., 1970, Geology of the Brevard fault zone and related rocks of the inner Piedmont of Alabama, Alabama Geological Society, 8th Annual Field Trip Guidebook: Tuscaloosa, Alabama Geological Society, 119 p.

Bentley, R.D., Neathery, T.L., and Lines, G.C., 1970, A probable impact-type structure near Wetumpka, Alabama [abs.]: Eos, (Transactions, American Geophysical Union), v. 51, p. 342.

Bentley, R.D., Neathery, T.L., and Lines, G.C., 1971, A probable impact structure near Wetumpka, Alabama [abs.]: The Journal of the Alabama Academy of Science, v. 42, p. 158-159.

Bieler, D.B., and Deininger, R.W., 1987, Geologic setting of the Kowaliga Augen Gneiss and the Zana Granite, northern Alabama Piedmont, *in* Drummond, M.S., and Green, N.L., eds., Granites of Alabama: Tuscaloosa, Alabama Geological Survey, p. 57-72.

Blair, T.C., and McPherson, J.G., 1999, Grain-size and textural classification of coarse sedimentary particles: Journal of Sedimentary Research, v. 69, p. 6-19.

Bottomley, R.J., York, D., and Grieve, R.A.F., 1990, $^{40}Argon$-$^{39}Argon$ dating of impact craters, *in* Sharpton, V.L., and Ryder, G., eds., Proceedings of the Lunar and Planetary Science Conference, vol.20, p. 421-431.

Chesley, S.R., and Ward, S.N., 2006, A Quantitative Assessment of the Human and Economic Hazard from Impact-generated Tsunami: Natural Hazards, v. 38, p. 355-374.

Cockell, C.S., and Lee, P., 2002, The biology of impact craters-a review: Biology Review, v. 77, p. 279-310.

Compton, R.R., 1985, Geology in the Field: New York, NY, United States, John Wiley & Sons, 398 p.

Copeland, C.W., 1972, Upper Cretaceous series in central Alabama, *in* Tolson, J.S., ed., Guide to Alabama Geology, Southeastern Section 21st Annual Field Trip Guidebook, Volume 72, no. 21: Tuscaloosa, Alabama Geological Society, p. 2.1-2.45.

Croft, S.K., 1982, A first-order estimate of shock heating and vaporization in oceanic impacts, *in* Silver, L.T., and Schultz, P.H., eds., Geological Society of America Special Paper 190, p. 143-152.

Dazé, A., Lee, J.K.W., and Villeneuve, M., 2003, An intercalibration study of the Fish Canyon sanidine and biotite $^{40}Ar/^{39}Ar$ standards and some comments on the age of the Fish Canyon Tuff: Chemical Geology, v. 199, p. 111-127.

de Pater, I., and Lissauer, J.J., 2001, Planetary Sciences: Cambridge, United Kingdom, Cambridge University Press, 528 p.

Dietrich, R.V., Dutro, J.T., Jr., and Foose, R.M., 1989, AGI data sheets for geology in the field, laboratory, and office: Falls Church, VA, United States, American Geological Institute, 210 p.

Dypvik, H., and Jansa, L.F., 2003, Sedimentary signatures and processes during marine bolide impacts; a review: Sedimentary Geology, v. 161, p. 309-337.

Faure, G., 1986, Principles of isotope geology: New York, NY, John Wiley & Sons, 589 p.

Frazier, W.J., and Taylor, R.S., 1980, Facies changes and paleogeographic interpretations of the Eutaw Formation (Upper Cretaceous) from western Georgia to central Alabama, *in* Tull, J.F., ed., Field trips for the Southeastern Section of the Geological Society of America: Tuscaloosa, Alabama Geological Society, p. 1-27.

French, B.M., 1998, Traces of catastrophe, a handbook of shock-metamorphic effects in terrestrial meteorite impact structures: Houston, TX, United States (USA), Lunar and Planetary Institute, 120 p.

Gault, D.E., and Sonett, C.P., 1982, Laboratory simulation of pelagic asteroidal impact; atmospheric injection, benthic topography, and the surface wave radiation field, *in* Silver, L.T., and Schultz, P.H., eds., Geological Society of America Special Paper 190, p. 69-92.

Gisler, G., Weaver, R., Mader, C., and Gittings, M., 2003, Two- and three-dimensional simulations of asteroid ocean impacts: Science of Tsunami Hazards, v. 21, p. 119-134.

Glasstone, S., and Dolan, P.J., 1977, The Effects of Nuclear Weapons, United States Department of Defense and the Energy Research and Development Administration, p. 653.

Hall, J.C., 1996, Ground zero - the Wetumpka astrobleme, Alabama Heritage, Volume 42, Fall issue, p. 6-12.

Higgins, G.H., and Butkovich, T.R., 1967, Effect of water content, yield, medium, and depth of burst on cavity radii: Lawrence Radiation Labratory Report UCRL-50203, p. 24.

Horton, J.W., Jr., Powars, D.S., and Gohn, G.S., editors, 2005, Studies of the Chesapeake Bay impact structure -- the USGS-NASA Langley corehole, Hampton, Virginia, and related coreholes and geophysical surveys, U. S. Geological Survey Professional Paper 1688, A-K, variously paginated, p. 453.

Johnson, R.C., Petruny, L.M., Hames, W., and King, D.T., Jr., 2006, Shock metamorphic characteristics and age of the Wetumpka impact structure, Alabama, Abstracts with Programs - Geological Society of America, Volume 38, p. 82.

Jones, D.E., 1967, The Selma Group in west Alabama, *in* Jones, D.E., ed., Geology of the coastal plain of Alabama, Field Trip #1 Guidebook for the 80th Annual Geological Society of America Meeting: Tuscaloosa, Alabama Geological Society, p. 26-32.

Kieffer, S.W., and Simonds, C.H., 1980, The role of volatiles and lithology in the impact cratering process: Reviews of Geophysics and Space Physics, v. 18, p. 143-181.

King, D.T., Jr., 1987, Sedimentary facies, depositional environments, and sea-level history -- Mooreville Chalk, Lower Campanian of east-central Alabama: Southeastern Geology, v. 27, p. 141-154.

King, D.T., Jr., 1994, Upper Cretaceous depositional sequences in the Alabama Gulf Coastal Plain; their characteristics, origin, and constituent clastic aquifers: Journal of Sedimentary Research, Section B: Stratigraphy and Global Studies, v. 64, p. 258-265.

King, D.T., Jr., 1997, The Wetumpka impact crater and the Late Cretaceous impact record, *in* Neathery, T.L., King, D.T., Jr., and Wolf, L.W., eds., The Wetumpka impact structure and related features, Alabama Geological Society Guidebook 34c: Tuscaloosa, Alabama Geological Society, p. 25-56.

King, D.T., Jr., 1998, Wetumpka Melange, a new stratigraphic unit in Alabama: American Association of Petroleum Geologists Bulletin, v. 82, p. 1784.

King, D.T., Jr., and Neathery, T.L., 1998, The Wetumpka asteroid impact structure in Alabama, U.S.A., American Association of Petroleum Geologists abstracts with programs, v. 7, p. 358 a-f.

King, D.T., Jr., Neathery, T.L., and Petruny, L.W., 1999a, Impactite facies within the Wetumpka impact-crater fill, Alabama, *in* Proceedings, 30th Lunar and Planetary Science Conference: Houston, LPI, Houston, Texas, p. 1634.

King, D.T., Jr., Neathery, T.L., and Petruny, L.W., 2004a, Structure-filling sediments of the Wetumpka marine-target impact structure (Alabama, USA), *in* Dypvik, H., Burchell, M., and Claeys, P., eds.: Berlin, Springer-Verlag, p. 97-113.

King, D.T., Jr., Neathery, T.L., Petruny, L.W., Koeberl, C., and Hames, W.E., 1999b, Evidence confirming meteoritic impact at *Wetumpka* Crater, Alabama, USA, Meteoritics and Planetary Science Supplement, Volume 34, no. 4: Fayetteville, AR, Meteoritical Society, p. 63-64.

King, D.T., Jr., Neathery, T.L., Petruny, L.W., Koeberl, C., and Hames, W.E., 2000, Evidence confirming meteoritic impact at Wetumpka Crater, Alabama, USA, LPI Contribution, Report: 1053: Houston, Lunar and Planetary Institute, p. 97.

King, D.T., Jr., Neathery, T.L., Petruny, L.W., Koeberl, C., and Hames, W.E., 2002, Shallow-marine impact origin of the Wetumpka Structure (Alabama, USA): Earth and Planetary Science Letters, v. 202, p. 541-549.

King, D.T., Jr., Ormö, J., Morrow, J.R., Petruny, L.W., Johnson, R.C., and Neathery, T.L., 2005, The role of water in development of the Late Cretaceous Wetumpka impact crater, coastal plain of Alabama, USA, LPI Contribution No. 1273, p.61-62.

King, D.T., Jr., Petruny, L.W., and Neathery, T.L., 2004b, Structure-filling stratigraphy of the marine-target Wetumpka impact structure, Alabama, USA, Open-File Report - U. S. Geological Survey, Report: OF 2004-1016, p. 32-33.

King, D.T., Jr., Petruny, L.W., and Neathery, T.L., 2006, Paleobiologic effects of the Late Cretaceous Wetumpka Marine Impact, a 7.6-km diameter impact structure, Gulf coastal plain, USA, *in* Cockell, C., Koeberl, C., and Gilmour, I., eds., Biological processes associated with impact events. [Impact Studies.], Springer-Verlag, Berlin, Heidelberg & New York, p. i-xvi, 1-376. Chapter pagination 121-142.

King, E.A., 1976, Space Geology; an introduction: New York, N.Y., United States, John Wiley & Sons, Inc., 349 p.

Kodak, 2000, Kodak Color Separation Guide with Grey Scale, 8" Size, #Q-13, Manufacturer Part # 1527654, The Tiffen Company.

Koeberl, C., and Anderson, R.R., 1996, Manson and Company: Impact Structures in the United States, *in* Koeberl, C., and Anderson, R.R., eds., The Manson Impact Structure, Iowa: Anatomy of an Impact Crater, Geological Society of America Special Paper 302, p. 1-29.

Lacefield, J., 2000, Lost Worlds in Alabama Rocks; A Guide to the State's Ancient Life and Landscapes, Alabama Geological Society, Tuscaloosa, AL, United States (USA), 124 p.

Mallincrodt, 2003, Material Safety Data Sheet-Sand, Washed and Dried, Mallincrodt Baker Inc., 222 Red School Lane, Phillisberg, New Jersey, 08865, MSDS No. S0722, p. 7.

McGowin, W., 1996, Discovery of the Wetumpka astrobleme, Alabama Heritage, Volume 42, Fall issue, p. 12-13.

McKinnon, W.B., and Goetz, P., 1981, Impact into the Earth's ocean floor during the last billion years; preliminary experiments, theoretical models, and possibilities for geological detection, LPI Contribution, no.449: Houston, Lunar and Planetary Institute, p. 1-34.

Melosh, H.J., 1982, The mechanics of large meteoroid impacts in the Earth's oceans, *in* Silver, L.T., and Schultz, P.H., eds., Geological implications of impacts of large asteroids and comets on the Earth: Geological Society of America Special Paper 190, p. 121-127.

Melosh, H.J., 1989, Impact Cratering: A Geologic Process: New York, Oxford University Press, 245 p.

Melosh, H.J., 2003, Impact-generated tsunamis: An over-rated hazard, 34th Annual Lunar and Planetary Science Conference, Abstract 2013: League City, Texas, Lunar and Planetary Institute.

Merriam-Webster, 1984, Webster's Ninth New Collegiate Dictionary: Springfield, MA., Merriam-Webster Inc., 1563 p.

Merrihue, C., and Turner, G., 1966, Potassium-argon dating by activation with fast neutrons: Journal of Geophysical Research, v. 71, p. 2852-2859.

Monroe, W.H., 1941, Notes on deposits of Selma and Ripley age in Alabama, Geological Survey of Alabama Bulletin 48, 150 p.

Neathery, T.L., 1975, Rock units in the high-rank belt of the northern Alabama Piedmont, *in* Neathery, T.L., and Tull, J.F., eds., Geologic profiles of the northern Alabama Piedmont: Tuscaloosa, Alabama Geological Society 13th Annual Field Trip Guidebook, p. 9-48.

Neathery, T.L., Bentley, R.D., Higgins, M.W., and Zietz, I., 1976a, Preliminary interpretation of aeromagnetic and aeroradioactivity maps of the Alabama Piedmont: Geology, v. 4, p. 375-381.

Neathery, T.L., Bentley, R.D., and Lines, G.C., 1976b, Cryptoexplosive structure near Wetumpka, Alabama: Geological Society of America Bulletin, v. 87, p. 567-573.

Neathery, T.L., King, D.T., Jr., and Wolf, L.W., 1997, The Wetumpka impact structure and related features, Alabama Geological Society Guidebook 34c, Alabama Geological Society, Tuscaloosa, AL, United States (USA).

Nelson, A.I., 2000, Geologic mapping of Wetumpka impact crater area, Elmore County, Alabama [Masters thesis]: Auburn, Auburn University, 187 p.

Neuendorf, K.K.E., Mehl, J.P., Jr., and Jackson, J.A., editors, 2005, Glossary of geology, Fifth ed.: Alexandria, VA, United States, American Geological Institute, p. 779.

Oberbeck, V.R., Marshall, J.R., and Aggarwal, H., 1993, Impacts, tillites, and the breakup of Gondwanaland: Journal of Geology, v. 101, p. 1-19.

Ormö, J., and Lindström, M., 2000, When a cosmic impact strikes the sea bed: Geological Magazine, v. 137, p. 67-80.

Ormö, J., Lindström, M., Lepinette, A., Martinez-Frias, J., and Diaz-Martinez, E., 2006, Cratering and modification of wet target craters: projectile impact experiments and field observations of the Lockne marine-target crater (Sweden): Meteoritics and Planetary Science, (accepted).

Ormö, J., Shuvalov, V.V., and Lindström, M., 2002, Numerical modeling for target water depth estimation of marine-target impact craters: Journal of Geophysical Research - Planets, v. 107 (E12), 5120, p. 3-1 - 3-9.

Palmer, A.R., and Geissman, J., compilers, 1999, 1999 Geologic Time Scale, The Geological Society of America, 1 sheet.

Poag, C.W., Koeberl, C., and Reimold, W.U., 2004, The Chesapeake Bay Crater; geology and geophysics of a late Eocene submarine impact structure: Berlin, Federal Republic of Germany (DEU), Springer-Verlag, 522 p.

Pope, K.O., Ocampo, A.C., Fischer, A.G., Alvarez, W., Fouke, B.W., Webster, C.L., Vega, F.J., Smit, J., Fritsche, A.E., and Claeys, P., 1999, Chicxulub impact ejecta from Albion Island, Belize: Earth and Planetary Science Letters, v. 170, p. 351-364.

Puura, V., and Suuroja, K., 1992, Ordovician impact crater at Kärdla, Hiiumaa Island, Estonia, *in* Pesonen, L.J., and Henkel, H., eds., Tectonophysics, Volume 216, p. 143-156.

Rajmon, D., compiler, 2006, Suspected Earth Impact Sites (SEIS) Database, http://web.eps.utk.edu/ifsg.htm, Impact Field Studies Group, University of Tennessee.

Raymond, D.E., Osborne, W.E., Copeland, C.W., and Neathery, T.L., 1988, Alabama stratigraphy, Circular - Geological Survey of Alabama, Report: 140, p. 97.

Reinhardt, J., Smith, L.W., and King, D.T., Jr., 1986, Sedimentary facies of the Upper Cretaceous Tuscaloosa Group in eastern Alabama, *in* Neathery, T.L., ed., Southeastern section of the Geological Society of America centennial field trip guidebook, Volume 6: Boulder, Colorado, Geological Society of America, p. 363-367.

Schwimmer, D.R., 2002, King of the crocodylians; the paleobiology of Deinosuchus: Bloomington, IN, Indiana University Press, 220 p.

Shoemaker, E.M., 1977, Why study impact craters? *in* Roddy, D.J., Pepin, R.O., and Merrill, R.B., eds., Impact and explosion cratering: Planetary and terrestrial implications; Proceedings of the Symposium on Planetary Cratering Mechanics: New York, Pergamon Press, p. 1-10.

Smith, E.A., 1904, A Geological Map of Alabama, Special Map 3: Baltimore, A. Hoen and Company, scale 1:2,375,000, 1 sheet.

Smith, E.A., Johnson, L.C., and Langdon, D.W., Jr., 1894, Report on the geology of the Coastal Plain of Alabama, Geological Survey of Alabama, Special Report 6, 759 p.

Smith, L.W., and King, D.T., Jr., 1983, The Tuscaloosa Formation: fluvial facies and their relationship to the basement topography and changes in paleoslope, *in* Carrington, T.J., ed., Current studies of Cretaceous formations in eastern Alabama and Columbus, Georgia: Tuscaloosa, Alabama Geological Society 20th Annual Field Trip Guidebook, p. 11-16.

Stöeffler, D., Gault, D.E., and Reimold, W.U., 1980, Experimental hypervelocity impact into quartz sand; pre-impact location of ejecta, *in* Moore, C.B., ed., Meteoritics, Volume 15, p. 371-372.

Stöffler, D., and Grieve, R.A.F., 2006, Towards a unified nomenclature of metamorphic petrology, Chapter 11: Impactites, A proposal on behalf of the IUGS Subcommission on the systematics of metamorphic rocks, International Union of Geological Sciences (IUGS) Blackwell Publishers (in press).

Stose, G.W., ed., 1926, Geologic map of Alabama, Geological Survey of Alabama Special Map 7, 1:500,000, 6 sheets.

Swanson, R.G., 1981, Sample examination manual: Tulsa, OK, American Association of Petroleum Geologists, ca 200 p.

Szabo, M.W., Osborne, W.E., Copeland, C.W., Jr., and Neathery, T.L., compilers, 1988, Geologic map of Alabama, Geological Survey of Alabama Special Map 220, scale 1:250,000, 5 sheets.

Taylor, R.S., 1973, Differentiation of the Coker and Gordo formations in east central Alabama: The Journal of the Alabama Academy of Science, v. 44, p. 189-190.

The Joint Photographic Experts Group, 2006, About JPEG, The Joint Photographic Experts Group, http://www.jpeg.org.

The Rock-Color Chart Committee, 1991, The Geological Society of America rock-color chart, 7th printing, with revised text: Boulder, Colorado, Geological Society of America.

TOPO! 2002, Alabama, Disc 2 of 4: Montgomery, National Geographic Holdings, Inc.

Tull, J.F., 1978, Structural development of the Alabama Piedmont northwest of the Brevard Zone: American Journal of Science, v. 278, p. 442-460.

U.S. Code, Title 17, Chapter 1, Section 107, 2006, http://www.law.cornell.edu/uscode/html/uscode17/usc_sec_17_00000107----000-.html.

U.S. Silica, 1997, Material Safety Data Sheet (MSDS) - Silica Sand, U.S. Silica Company, P.O. Box 187, Berkeley Springs, WV. 25411, p. 8.

von Dalwigk, I., and Ormö, J., 2001, Formation of resurge gullies at impacts at sea; the Lockne Crater, Sweden: Meteoritics & Planetary Science, v. 36, p. 359-369.

Whitehead, J., and Spray, J., compilers, 2005, Earth Impact Database, http://www.unb.ca/passc/ImpactDatabase/, Planetary and Space Science Centre, Department of Geology, University of Nouveau-Brunswick.

Wolf, L.W., Plescia, J., and Steltenpohl, M.G., 1997, Geophysical investigation of a "suspect" impact crater in Wetumpka, Alabama, *in* Neathery, T.L., King, D.T., Jr., and Wolf, L.W., eds., The Wetumpka impact structure and related features, Alabama Geological Society Guidebook 34c: Tuscaloosa, Alabama Geological Society, p. 57-68.

APPENDICES

Appendix 1. Explanatory Notes about Impact-related Nomenclature

At the time of this writing, the International Union of Geological Sciences (IUGS) was preparing a unified nomenclature of metamorphic petrology that contains a chapter by Stöffler and Grieve (2006) detailing proper application of the special terminology related to impact studies. Where practical, the present author will attempt to follow the recommendations of that work because that is what most editors are now doing (D. King, pers. comm., 2006).

However, there are *always* exceptions to *every* guiding principle. For example, when referring to the inner basin of a marine-target impact structure, it is generally recommended that an author avoid the word *crater* in descriptive terms such as *central crater*, *inner crater*, *basement crater*, etc. if the impact structure is filled. The same preference for avoiding *crater* holds true when referring to the material filling the inner basin of a marine impact structure, which might be described in a general way as *crater fill*, *crater-filling*, *basin filling*, and so on.

Nonetheless, as will be established shortly, it is sometimes preferable to use *crater* in these terms for the sake of clarity. But there is a problem in doing so. One of the terms defined below is *impact crater*. A crater is a bowl-shaped pit or depression (Neuendorf et al., 2005). No statement is made in the definition about the extent to which that pit or depression is filled, but strictly speaking, if an impact crater has been completely filled in or buried, it is no longer an actual crater. The term *impact structure* should be used instead. The present author agrees completely with this guiding principle,

so long as this is done with discretion because an overzealous adherence to this guideline only brings about new problems.

In essence, a strict adherence to the term *impact structure* (or any other term) is not entirely feasible because such a dogmatic approach simply does not always convey to the reader the specific information the author needs to communicate. Consider, for example, a sentence referring to the *structurally disturbed crater-filling material within the inner basin of a marine-target impact structure*. The author's subject is clear, and the reader may easily picture in mind what is being explained. To the contrary, an identical sentence referring to the *structurally disturbed structure-filling material within the structural basin of a marine-target impact structure* is hopelessly mired in nomenclature, and requires a great deal of mental calisthenics from the reader.

Granted, the above example is extreme for illustrative purposes, but to drive the point home consider the term *crater fill*, which is used regularly by the impact community to document material within genuine craters on the Moon, for example. *Crater fill* is actually defined by Neuendorf et al. (2005) in the *Glossary of Geology* as "solidified lava at the bottom of a volcanic crater, with associated cinders and weathering debris." Importantly, that is the *only* definition provided for *crater fill*. An overly strict adherence to the guiding principles of nomenclature would require that no geologist ever use the term *crater fill* when referring to any material within a fresh crater of impact origin because the definition of *crater fill* limits its use exclusively to a volcanic context. But what if there were a second definition for the same word – that is, a definition of *crater fill* for use in an impact-related context?

One may predict that scientists studying impact structures will have to accept multiple definitions for single words and terms as is already common in all languages and other scientific fields. As such, a particular word's definition will be understood by context. For example, if a biologist refers to a tiger as a *cat*, the reader never confuses the author's meaning to be a housecat, a malicious woman, or a player or devotee of jazz; yet these are all longstanding definitions of the word *cat* when used as a noun (Merriam-Webster, 1984). When *cat* is used as a verb, there are other meanings to contend with, such as, to search for a sexual mate (Merriam-Webster, 1984). Without recognizing context, one might be tempted to ask how biologists ever understand each other. What is interesting is that they do understand each other, and they do so without specifying the definition of *cat* in their work. Rather, the meaning is simply understood because the audience is already familiar with the various definitions, and can do the filtering on their own. The present author believes the same holds true when *carefully* using terms like *inner crater* or *crater fill* to refer, for example, to the inner basin of a marine-target impact structure. The nature of the structure will be understood by the context of the words used to describe it.

An alternate solution to the problem might be to change the spelling of a particular word according to how it is used. Examples include *whether* and *weather*; *there*, *their*, and *they're*; *to*, *too*, and *two*; *hole* and *whole*; *discrete* and *discreet*; *inn* and *in*; etc. Could *krater*, *chrater* and *endocrater* be the answer?

The present author strongly agrees that there needs to be an established and well-thought-out nomenclature that is widely agreed upon and just as widely used. But that nomenclature has to be fluid enough to not restrict or totally confound the flow of

information, even when its guiding principles are rigidly applied. As history shows, the two tools of context and spelling variation have served the human race well in numerous languages throughout time simply because they work. Why should the language of science be exempt? After all, scientists are no less intelligent than any other group who write, read, speak, and listen.

Complicating the issue of impact nomenclature is the rapid acceptance, metamorphosis, and/or rejection of terms and definitions used in recent published studies of impact structures. The problem is illustrated in work by Poag et al. (2004) versus work by Horton et al. (2005). Both works document the Chesapeake Bay impact structure, but in one publication as compared to the other, various features of the structure are labeled differently. Examples include, respectively, *central peak* versus *central uplift*; *central basin* versus *central crater* or *inner basin*; *peak ring* versus *margin of central crater*; and *crater rim* versus *outer margin*.

Clearly, the field of impact studies is struggling with overcoming the obstacles presented by established geologic nomenclature developed at a time before impact events, processes, morphologies, and structures were recognized by the scientific community. Moreover, this field is also struggling to develop its own nomenclature as evidenced by the problematic definitions proposed for the below-listed terms. These definitions were developed with an impact-related context in mind, and still, they are awkward. All of the terms and definitions below are quoted from Stöffler and Grieve (2006), and are provided to assist the reader. However, for a complete list, the reader is referred to the work of those authors. The reader should also be aware that many of the terms and definitions in Stöffler and Grieve (2006) are nearly identical to those *already*

given in Neuendorf et al. (2005). To help clarify the definitions below and explain how the term may apply to the Wetumpka impact structure, a comment from the present author follows most definitions. Finally, the present author cautions the reader against a rigid application of the terms because 1) doing so obstructs understanding; 2) they are a work in progress; and 3) they are rather narrow as worded. See the comments below for explanations.

> IMPACT STRUCTURE = geological structure caused by impact irrespective of its state of preservation

Comment from present author: In essence, an impact structure is the whole of all impact-related geological structures in a given locale that were formed by a specific impact event, regardless of how eroded, filled in, and/or buried the overall structure may be. Every impact crater is, by default, an impact structure. This term is not to be confused with the terms, *impact crater* and *impact formation*, the definitions of which are quoted below.

> IMPACT CRATER = generally circular crater formed either by impact of an interplanetary body (projectile) on a planetary surface or by an experimental hypervelocity impact of a projectile into solid matter; craters formed by very oblique impacts may be elliptical

Comment from present author: As a cautionary note, this definition listed by Stöffler and Grieve (2006) is too narrow because, for example, impact craters are readily found on more than just *planetary* surfaces – they are found on virtually all solid objects in the solar system as previously outlined.

> MULTI-RING CRATER = impact crater with relatively low depth / diameter ratio and with at least two concentric rings inside the crater; synonymous with MULTI-RING BASIN

Comment from present author: Because this term is synonymous with a very specific class of large impact structure, it cannot be applied to the Wetumpka impact structure.

IMPACT FORMATION = geological formation produced by impact; includes various lithological and structural units inside and beneath an impact crater (inner impact formations), the continuous ejecta blanket (outer impact formations) and distal ejecta such as tektites and impactoclastic air fall beds

Comment from present author: Presumably, this definition also applies to *impact structures*, not just *impact craters* as worded. This term is not to be confused with the processes of impact structure formation, nor the terms, *impact structure*/*crater*.

IMPACTOCLASTIC DEPOSIT = Consolidated [*sic*] or unconsolidated sediment resulting from ballistic excavation, transport, and deposition of rocks at impact craters; may contain particles of impact melt rock

Comment from present author: Presumably, this definition also applies to impact structures, not just impact craters as worded.

IMPACT BRECCIA = monomict or polymict breccia, which occurs around, inside and below impact craters

Comment from present author: Presumably, this definition also applies to impact structures, not just impact craters as worded.

MONOMICT IMPACT BRECCIA = cataclasite produced by impact and generally displaying weak or no shock metamorphism; occurs in the (par)autochthonous floor of an impact crater or as clast (up to the size of blocks and megablocks) within allochthonous breccias

Comment from present author: Presumably, this definition also applies to impact structures, not just impact craters as worded.

POLYMICT IMPACT BRECCIA = breccia with clastic matrix or crystalline matrix (derived from the crystallization of impact melt) containing lithic and mineral clasts of different degree of shock metamorphism excavated by an impact from different regions of the target rock section, transported, mixed, and deposited inside or around an impact crater or injected into the target rocks as dikes

Comment from present author: Presumably, this definition also applies to impact structures, not just impact craters as worded.

ALLOCHTHONOUS (ALLOGENIC) IMPACT BRECCIA = impact breccia in which component materials have been displaced from their point of origin; includes clastic matrix breccias (lithic breccias, suevite breccias), and dike breccias

The present author offers no comment.

AUTOCHTHONOUS (AUTHIGENIC) IMPACT BRECCIA = cataclastic (monomict) impact breccia in which component materials have not been displaced any significant distance from their point of origin

The present author offers no comment.

Appendix 2. Master Photos of Drill Core 1-98

The following figures depict scaled-down versions of the master photos used in this investigation of two drill cores from the Wetumpka impact structure. Each box may be read as though it were text, except one must read backwards from top to bottom because of the order in which the pieces were boxed (Figure A - 1).

There are 49 *master photos* for drill core 1-98, and 22 *master photos* for drill core 2-98. The photographs are shown two-per-page, beginning with drill core 1-98. The warped appearance of each photograph's edges is a consequence of digitally correcting (using Adobe® Photoshop®) for fish-eye distortion caused by the camera's lens. Without such a correction, the straight lengths of drill core would have appeared bowed. The shadow in each corner of every photograph is vignetting caused by a protective lens filter.

The full size of each image is approximately 35 inches wide, by 26 inches tall (~ 90 x 70 cm). Despite this large size, the resolution is only 72 pixels per inch. However, using photo processing software such as Adobe® Photoshop®, the resolution may be boosted (200 to 300 is usually a sufficient value, although larger values such as 1200 may be used), and the size reduced to fit standard letter-sized sheets of paper. This procedure will result in genuine, high-resolution images of manageable size.

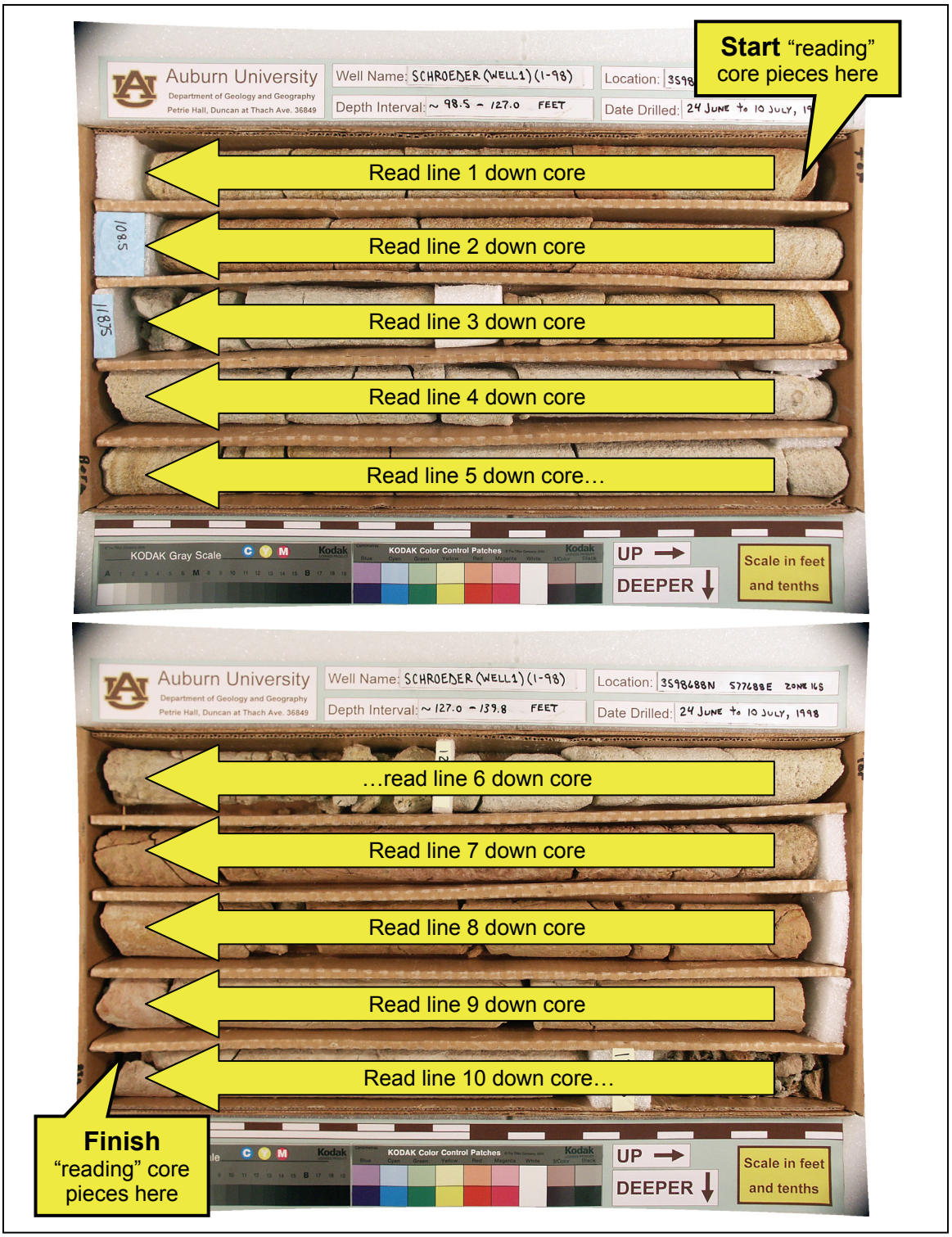

Figure A - 1. Illustration of how to "read" the boxed pieces of drill-core in the following figures as though they were lines of text on a page.

Figure A - 2. Boxes 1 (top) and 2 (bottom) of drill core 1-98.

Figure A - 3. Boxes 3 (top) and 4 (bottom) of drill core 1-98.

Figure A - 4. Boxes 5 (top) and 6 (bottom) of drill core 1-98.

Figure A - 5. Boxes 7 (top) and 8 (bottom) of drill core 1-98.

Figure A - 6. Boxes 9 (top) and 10 (bottom) of drill core 1-98.

Figure A - 7. Boxes 11 (top) and 12 (bottom) of drill core 1-98.

Figure A - 8. Boxes 13 (top) and 14 (bottom) of drill core 1-98.

Figure A - 9. Boxes 15 (top) and 16 (bottom) of drill core 1-98.

Figure A - 10. Boxes 17 (top) and 18 (bottom) of drill core 1-98.

Figure A - 11. Boxes 19 (top) and 20 (bottom) of drill core 1-98.

Figure A - 12. Boxes 21 (top) and 22 (bottom) of drill core 1-98.

Figure A - 13. Boxes 23 (top) and 24 (bottom) of drill core 1-98.

Figure A - 14. Boxes 25 (top) and 26 (bottom) of drill core 1-98.

Figure A - 15. Boxes 27 (top) and 28 (bottom) of drill core 1-98.

Figure A - 16. Boxes 29 (top) and 30 (bottom) of drill core 1-98.

Figure A - 17. Boxes 31 (top) and 32 (bottom) of drill core 1-98.

Figure A - 18. Boxes 33 (top) and 34 (bottom) of drill core 1-98.

Figure A - 19. Boxes 35 (top) and 36 (bottom) of drill core 1-98.

Figure A - 20. Boxes 37 (top) and 38 (bottom) of drill core 1-98.

Figure A - 21. Boxes 39 (top) and 40 (bottom) of drill core 1-98.

Figure A - 22. Boxes 41 (top) and 42 (bottom) of drill core 1-98.

Figure A - 23. Boxes 43 (top) and 44 (bottom) of drill core 1-98.

Figure A - 24. Boxes 45 (top) and 46 (bottom) of drill core 1-98.

Figure A - 25. Boxes 47 (top) and 48 (bottom) of drill core 1-98.

Figure A - 26. Box 49, drill core 1-98. End of this drill hole.

Appendix 3. Master Photos of Drill Core 2-98

The following figures depict the 22 master photos for drill core 2-98. For detailed instructions on how to "read" the master photos of boxed drill core, see the beginning of Appendix 2. Also there are details about the photographs themselves.

Figure A - 27. Boxes 1 (top) and 2 (bottom) of drill core 2-98.

Figure A - 28. Boxes 3 (top) and 4 (bottom) of drill core 2-98.

Figure A - 29. Boxes 5 (top) and 6 (bottom) of drill core 2-98.

Figure A - 30. Boxes 7 (top) and 8 (bottom) of drill core 2-98.

Figure A - 31. Boxes 9 (top) and 10 (bottom) of drill core 2-98.

Figure A - 32. Boxes 11 (top) and 12 (bottom) of drill core 2-98.

Figure A - 33. Boxes 13 (top) and 14 (bottom) of drill core 2-98.

Figure A - 34. Boxes 15 (top) and 16 (bottom) of drill core 2-98.

Figure A - 35. Boxes 17 (top) and 18 (bottom) of drill core 2-98.

Figure A - 36. Boxes 19 (top) and 20 (bottom) of drill core 2-98.

Figure A - 37. Boxes 21 (top) and 22 (bottom) of drill core 2-98. End of this drill hole.

Appendix 4. CD-ROM File Tree

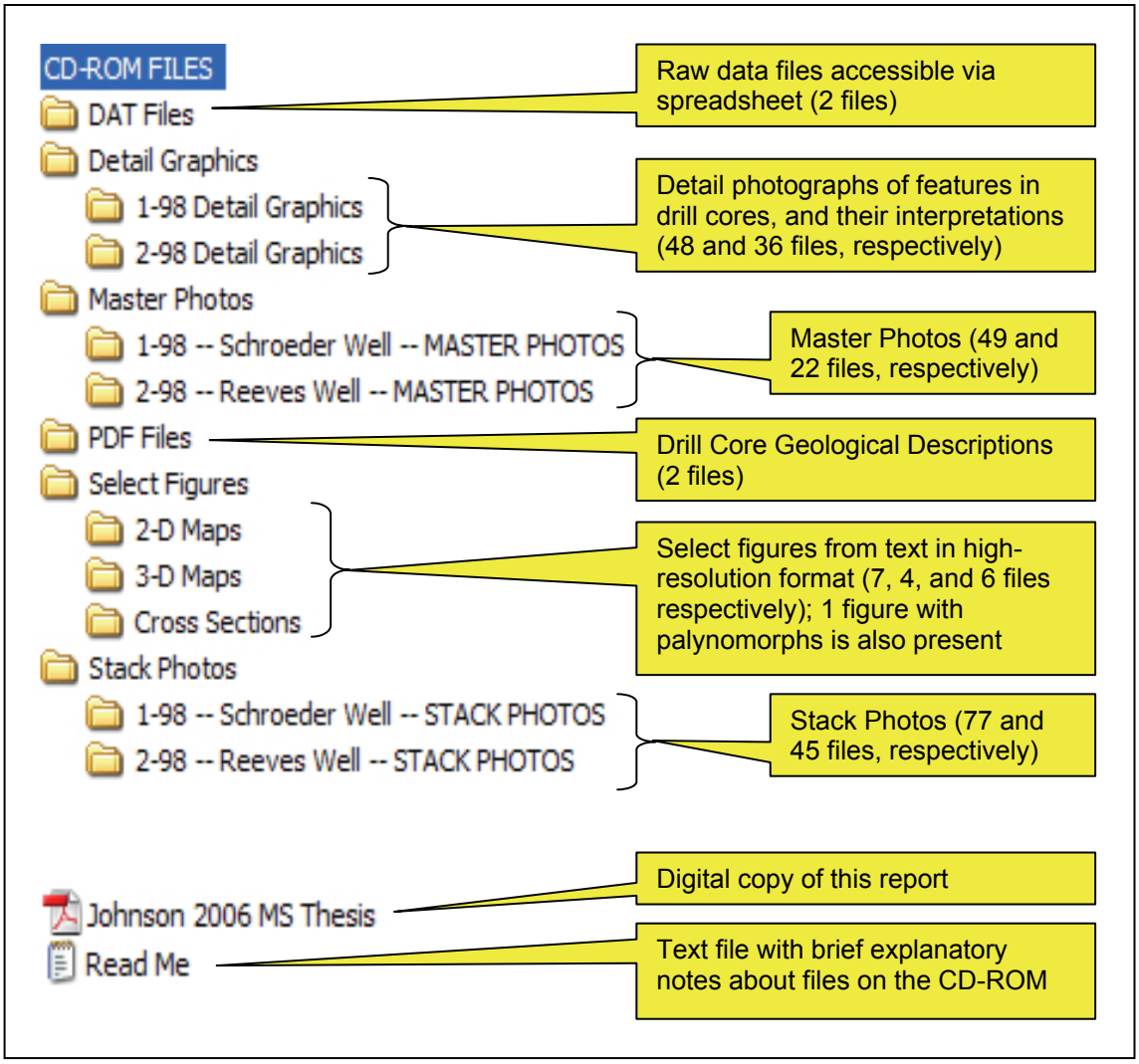

Figure A - 38. Index of files on the CD-ROM. There are a total of 301 files, not counting hidden and/or system files.